

PREDICTION OF LOW-TEMPERATURE AND THERMAL-FATIGUE
CRACKING IN FLEXIBLE PAVEMENTS

by

Mohamed Y. Shahin
B. Frank McCullough

Research Report Number 123-14

A System Analysis of Pavement Design
and Research Implementation
Research Project 1-8-69-123

conducted for

The Texas Highway Department

in cooperation with the
U. S. Department of Transportation
Federal Highway Administration

by the

Highway Design Division
Texas Highway Department
Texas Transportation Institute
Texas A&M University
Center for Highway Research
The University of Texas at Austin

August 1972

The contents of this report reflect the views of the authors, who are responsible for the facts and the accuracy of the data presented herein. The contents do not necessarily reflect the official views or policies of the Federal Highway Administration. This report does not constitute a standard, specification, or regulation.

PREFACE

This report describes a design system for predicting temperature cracking in asphalt concrete surfaces. Included herein are the system development, verification, and important variables in the system with respect to temperature cracking. This is one of a series of reports emanating from the project entitled "A System Analysis of Pavement Design and Research Implementation." The project, sponsored by the Texas Highway Department in cooperation with the Federal Highway Administration, is a long range comprehensive research program to develop a pavement design and feedback system.

Special appreciation is extended to Mr. Michael Darter and the rest of the Center for Highway Research personnel for their cooperation.

Mohamed Y. Shahin
B. Frank McCullough

August 1972

This page replaces an intentionally blank page in the original.

-- CTR Library Digitization Team

LIST OF REPORTS

Report No. 123-1, "A Systems Approach Applied to Pavement Design and Research," by W. Ronald Hudson, B. Frank McCullough, F. H. Scrivner, and James L. Brown, describes a long-range comprehensive research program to develop a pavement systems analysis and presents a working systems model for the design of flexible pavements.

Report No. 123-2, "A Recommended Texas Highway Department Pavement Design System Users Manual," by James L. Brown, Larry J. Buttler, and Hugo E. Orellana, is a manual of instructions to Texas Highway Department personnel for obtaining and processing data for flexible pavement design system.

Report No. 123-3, "Characterization of the Swelling Clay Parameter Used in the Pavement Design System," by Arthur W. Witt, III, and B. Frank McCullough, describes the results of a study of the swelling clay parameter used in pavement design system.

Report No. 123-4, "Developing A Pavement Feedback Data System," by R. C. G. Haas, describes the initial planning and development of a pavement feedback data system.

Report No. 123-5, "A Systems Analysis of Rigid Pavement Design," by Ramesh K. Kher, W. R. Hudson, and B. F. McCullough, describes the development of a working systems model for the design of rigid pavements.

Report No. 123-6, "Calculation of the Elastic Moduli of a Two Layer Pavement System from Measured Surface Deflections," by F. H. Scrivner, C. H. Michalak, and W. M. Moore, describes a computer program which will serve as a subsystem of a future Flexible Pavement System founded on linear elastic theory.

Report No. 123-6A, "Calculation of the Elastic Moduli of a Two Layer Pavement System from Measured Surface Deflections, Part II," by Frank H. Scrivner, Chester H. Michalak, and William M. Moore, is a supplement to Report No. 123-6 and describes the effect of a change in the specified location of one of the deflection points.

Report No. 123-7, "Annual Report on Important 1970-71 Pavement Research Needs," by B. Frank McCullough, James L. Brown, W. Ronald Hudson, and F. H. Scrivner, describes a list of priority research items based on findings from use of the pavement design system.

Report No. 123-8, "A Sensitivity Analysis of Flexible Pavement System FPS2," by Ramesh K. Kher, B. Frank McCullough, and W. Ronald Hudson, describes the overall importance of this system, the relative importance of the variables of the system and recommendations for efficient use of the computer program.

Report No. 123-9, "Skid Resistance Considerations in the Flexible Pavement Design System," by David C. Steitle and B. Frank McCullough, describes skid resistance consideration in the Flexible Pavement System based on the testing of aggregates in the laboratory to predict field performance and presents a nomograph for the field engineer to use to eliminate aggregates which would not provide adequate skid resistance performance.

Report No. 123-10, "Flexible Pavement System - Second Generation, Incorporating Fatigue and Stochastic Concepts," by Surendra Prakash Jain, B. Frank McCullough, and W. Ronald Hudson, describes the development of new structural design models for the design of flexible pavement which will replace the empirical relationship used at present in flexible pavement systems to simulate the transformation between the input variables and performance of a pavement.

Report No. 123-11, "Flexible Pavement System Computer Program Documentation," by Dale L. Schafer, provides documentation and an easily updated documentation system for the computer program FPS-9.

Report No. 123-12, "A Pavement Feedback Data System," by Oren G. Strom, W. Ronald Hudson, and James L. Brown, defines a data system to acquire, store, and analyze performance feedback data from in-service flexible pavements.

Report No. 123-13, "Benefit Analysis for Pavement Design System," by W. Frank McFarland, presents a method for relating motorist's costs to the pavement serviceability index and a discussion of several different methods of economic analysis.

Report No. 123-14, "Prediction of Low-Temperature and Thermal-Fatigue Cracking in Flexible Pavements," by Mohamed Y. Shahin and B. Frank McCullough, describes a design system for predicting temperature cracking in asphalt concrete surfaces.

ABSTRACT

Temperature cracking is a severe problem for flexible pavements in northern parts of the United States and Canada and in cold areas in general. Although the State of Texas is known for its warm climate, severe temperature cracking has been reported in the western parts of the state.

In this research effort, a system was developed to predict the amount of temperature cracking in asphalt concrete surfaces throughout their service lives using laboratory materials data and available weather information. Basically, four models were developed to form the system. In brief, the models are as follows:

- Model I - Simulation of bituminous pavement temperatures
- Model II - (i) Estimation of asphalt concrete stiffness as a function of temperature and loading time
 - (ii) Prediction of in-service aging of asphalt
 - (iii) Estimation of thermal stresses
- Model III - Prediction of low-temperature cracking
- Model IV - Prediction of thermal-fatigue cracking

The consideration of thermal-fatigue cracking (Model IV) due to daily temperature cycling makes the system an improvement over other available techniques in this field.

In a comparison of the amount of temperature cracking predicted from the system and that measured in the Ontario Test Roads and Ste. Anne Test Road, the system has been shown to be reasonable and reliable. In analyzing the system, the most important weather parameters with respect to temperature cracking were found to be solar radiation and air temperature. Meanwhile, the most important asphalt concrete properties were found to be the thermal coefficient of contraction and asphalt penetration and temperature-susceptibility. Data from the Ontario Test Roads and computations from the system showed that the percent of original penetration after the thin-film oven test can be a good guide for differentiating among asphalt sources when the rest of the asphalt properties are the same.

The adoption of the system by the highway agencies who are concerned with temperature cracking seems warranted, particularly because the system is made available in the form of a single computer program. Another factor that makes the system easy to adopt is that most of the necessary information for using the computer program needs to be collected only one time. For example, the environmental variables for a specific area need to be collected only once. The system can be a decision-maker to accept or reject an asphalt supplier; it can also help the engineer in designing an asphalt concrete mixture that will best fit the surrounding environmental conditions. Above all, the use of the proposed system will reduce the maintenance cost, especially for those locations that suffer from flexible pavement temperature cracking.

KEY WORDS: low-temperature cracking, thermal-fatigue cracking, temperature cracking, solar radiation, conductivity, diffusivity, specific heat, rheology penetration, softening-point, stochastic.

SUMMARY

A computerized system for predicting temperature cracking in asphalt concrete surfaces has been developed. The models and submodels forming the system are simulation of pavement temperatures, estimation of asphalt concrete stiffness, prediction of in-service aging of asphalts and consideration of stochastic variations and thermal fatigue distresses. Temperature cracking as predicted from the developed system is the appropriate addition of two forms of cracking, which are briefly defined below:

- (1) low-temperature cracking, which occurs when the thermal tensile stress exceeds the asphalt concrete tensile strength, and
- (2) thermal-fatigue cracking which occurs when the thermal fatigue distress, due to daily temperature cycling, exceeds the asphalt concrete fatigue resistance.

This page replaces an intentionally blank page in the original.

-- CTR Library Digitization Team

IMPLEMENTATION STATEMENT

The developed system predicts the amount of temperature cracking that may develop in a particular asphalt concrete road under specific environmental conditions. Most of the necessary information about the asphalt concrete mixture can be determined through routine laboratory tests; the environmental data can be easily obtained from regular weather service reports. The model is, in itself, an excellent tool that will help the highway design engineer in selecting the asphalt concrete mixture design that will best eliminate or reduce temperature cracking in a road to be located in a particular area. The model can also be used to differentiate among asphalt suppliers and select the best in regard to temperature cracking, and, above all, it will help reduce the maintenance cost. Besides the independent usefulness of the system, it can be combined with either the current flexible pavement design system (FPS) (Ref 32) or the second generation FPS (Ref 36) to give a complete flexible pavement design system that takes into account both traffic and environmental variables.

This page replaces an intentionally blank page in the original.

-- CTR Library Digitization Team

TABLE OF CONTENTS

PREFACE	iii
LIST OF REPORTS	v
ABSTRACT	vii
SUMMARY	ix
IMPLEMENTATION STATEMENT	xi
CHAPTER 1. INTRODUCTION	1
CHAPTER 2. THE NEED AND THE APPROACH	
The Need	5
The Approach	5
CHAPTER 3. SIMULATION OF PAVEMENT TEMPERATURES	
Theory	11
Developed Model	17
Verification of the Model	19
Sensitivity Analysis of the Model	25
Summary	32
CHAPTER 4. ASPHALT CONCRETE RHEOLOGY	
Introduction	33
Methods of Characterizing Viscoelastic Materials	33
Time-Temperature Equivalency Concept	38
Van der Poel Stiffness Theory	43
Summary	49
CHAPTER 5. APPLICATION TECHNIQUES FOR VAN DER POEL'S THEORY	
Converting Van der Poel's Nomograph to a Computer Form	51
Development of the Regression Equations	55
Summary	61
CHAPTER 6. IN-SERVICE AGING OF ASPHALTS	
Sources of Data Used in Developing the Asphalt Aging Models	63
Penetration Aging Model	64
Softening-point Aging Model	66

Factors Considered but not Used in the Final Models	74
Summary and Conclusions	77
CHAPTER 7. ESTIMATION OF THERMAL STRESSES	
The Stress Model	79
Thermal Loading Time for Estimating Asphalt Stiffness	83
Summary	90
CHAPTER 8. LOW-TEMPERATURE CRACKING	
Introduction	91
Theory	91
Stress Variability	95
Strength Variability	98
Example	100
Transformation from Area to Linear Cracking	102
Summary and Conclusions	102
CHAPTER 9. THERMAL-FATIGUE CRACKING	
Introduction	107
Temperature System for Fatigue Analysis	107
Daily Mean Air Temperature Model	108
Daily Mean Solar Radiation Model	108
Thermal-Fatigue Theory	112
Summary and Conclusions	118
CHAPTER 10. COMPUTERIZED SYSTEM, IMPORTANT VARIABLES AND SYSTEM VERIFICATION	
System Behavior	126
Important Variables	126
System Verification	132
Summary	143
CHAPTER 11. SUMMARY, CONCLUSIONS, AND RECOMMENDATIONS	
Summary	145
Conclusions	145
Recommendations	146
REFERENCES	149
APPENDIX 1. TEMPERATURE PREDICTION PROGRAM LISTING AND INPUT	159
APPENDIX 2. ESTIMATION OF ASPHALT CONCRETE STIFFNESS (AFTER VAN DER POEL'S NOMOGRAPH) PROGRAM LIST AND INPUT GUIDE	165
APPENDIX 3. DATA USED FOR THE PREDICTION OF THE PENETRATION AND SOFTENING-POINT AGING MODELS	179

APPENDIX 4.	ESTIMATION OF THERMAL STRESSES PROGRAM LIST, INPUT GUIDE, AND EXAMPLE OUTPUT	187
APPENDIX 5.	TEMPERATURE-CRACKING SYSTEM PROGRAM LIST AND INPUT GUIDE . .	195
APPENDIX 6.	ONTARIO TEST ROADS AND STE. ANNE TEST ROAD DATA, USED FOR THE VERIFICATION OF THE TEMPERATURE-CRACKING SYSTEM	219
THE AUTHORS		225

CHAPTER 1. INTRODUCTION

The purpose of this research was to develop a system for predicting temperature cracking in asphalt concrete surfaces throughout the service life based on material's laboratory data and available weather information. Temperature cracking as predicted from the developed system occurs in two forms:

- (1) low-temperature cracking, which occurs when the thermal tensile stress exceeds the asphalt concrete tensile strength, and
- (2) thermal-fatigue cracking, which occurs when the thermal fatigue distress, due to daily temperature cycling, exceeds the asphalt concrete fatigue resistance.

Temperature cracking usually takes the form of transverse cracking perpendicular to the direction of traffic (Fig 1.1). The need for investigating this problem and the approach to attack it are explained in detail in Chapter 2. The models and submodels that were developed and are discussed herein are

- (1) simulation of pavement temperatures (Chapter 3),
- (2) estimation of asphalt concrete stiffness from laboratory measurements (Chapters 4 and 5),
- (3) prediction of in-service aging of asphalts (Chapter 6),
- (4) estimation of thermal stresses (Chapter 7),
- (5) probability of low-temperature cracking (Chapter 8), and
- (6) probability of thermal-fatigue cracking (Chapter 9).

All of these were included in a computer program to form a complete system for predicting temperature cracking (Chapter 10). In comparing the predicted cracking with that which is actually measured in some projects, the system has been shown to be reliable. The information required to use the program is easy to obtain. Most information about the asphalt concrete mixture can be determined through routine laboratory tests; environmental data can be easily obtained from regular Weather Service reports. The model is, in itself, an excellent tool that will help the highway design engineer in selecting appropriate asphalt concrete mixture design, the one that will eliminate or substantially reduce temperature cracking. The model can also be used to differentiate among asphalt sources and to select the best with regard to temperature



Fig 1.1. Temperature cracking in Southern Utah highways.

cracking and thus to reduce the maintenance cost. Besides the independent usefulness of the system, it can be combined with either the current flexible pavement design system (FPS) (Ref 32) or the second-generation FPS (Ref 36) to result in a complete flexible pavement design system that considers both traffic and environmental variables.

This page replaces an intentionally blank page in the original.

-- CTR Library Digitization Team

CHAPTER 2. THE NEED AND THE APPROACH

THE NEED

Temperature cracking is one of the severe problems of flexible pavements in the northern parts of the United States, Canada, and cold areas in general. Although the State of Texas is known for its warm weather, severe temperature cracking has been reported in the areas of West Texas. Investigations have been carried out by many capable engineers in an attempt to define the causes(s) and establish methods of eliminating or reducing such cracking and thus increase a pavement's service life. Nobody has yet developed a complete system approach that enables the design engineer to design a pavement that is free of temperature cracking, although the attempts to do so have provided a rather comprehensive background to the problem. The purpose of this research is to assimilate and interpret the findings of different researchers and, equally important, to develop the necessary models to result in a complete system approach to the problem.

Temperature cracks usually take the form of transverse cracks, with spacing ranging from 4 or 5 feet to several hundred feet. The problem is not only the effect that these cracks have on the highway user, but also the major distresses that occur later in the pavement. The type of distress will depend upon the type of the subgrade, loss of support or swelling, and, above all, the result will be a loss in the rideability (PSR) and increase in the frequency and cost of maintenance. These distresses have been noticed by several investigators, among whom are Anderson et al (Fig 2.1), Kelly (Ref 39), and Hajek (Ref 26).

THE APPROACH

In order to achieve the correct approach to solving any problem, causes have to be known. There are two main causes of temperature cracking:

- (1) Thermal tensile stresses exceed the resisting capability of the surface layer (asphalt concrete strength), which results in low temperature cracking.
- (2) Daily temperature cycles cause thermal fatigue distress, and if it exceeds the asphalt concrete fatigue resistance, thermal fatigue cracks will occur.

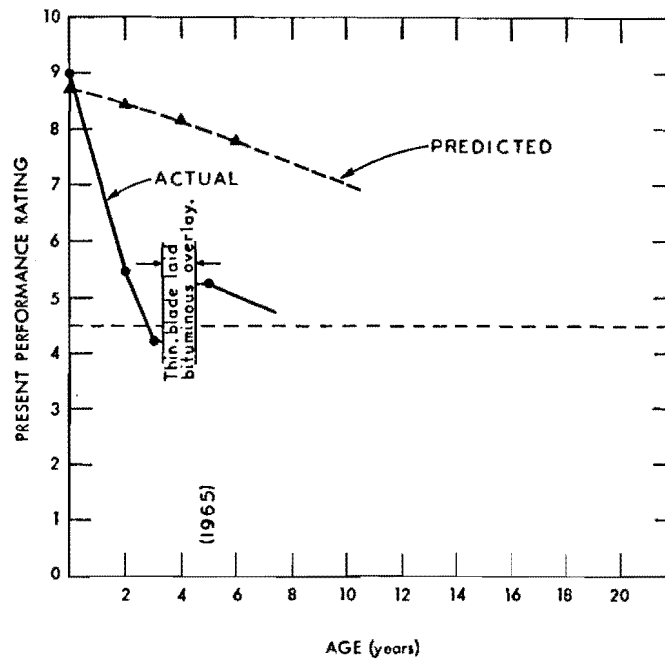


Fig 2.1. Comparison of predicted and actual performance losses in pavements exhibiting transverse cracking (after Anderson, et al, Ref 1).

Temperature cracking, as described above, is one of the principal forms of nontraffic-associated cracking, especially in the cold regions. Other forms of nontraffic-associated cracking may be due to moisture loss in the subgrade, differential swelling of the subgrade, etc. However, these forms of cracking are beyond the scope of this research.

Once the causes of the problem are known, the next step is to develop a complete system that enables the highway engineer to predict the amount of cracks that would occur with a certain material and mixture design.

Figure 2.2 shows a general system approach to pavement design, which includes:

- (1) inputs - material characteristics, load frequency and intensity, environmental conditions, variations associated with the inputs, etc.;
- (2) model(s) - techniques developed to handle the problem under consideration, which can be based on theory or empirical axioms or both;
- (3) outputs - stresses, strains, strength, etc.;
- (4) distress - cracks, roughness, rutting, etc.; and
- (5) performance - a history of distress manifestations which consider the user.

The utilization of such a system for the temperature cracking problem is shown in Fig 2.3. In developing the temperature cracking models, four basic items were kept in mind: prediction of pavement temperatures; prediction of thermal stresses, strains, and strengths; fatigue considerations; and finally but certainly not the least important, stochastic variations. A summary flow chart of the developed system is shown in Fig 2.4, which shows four models, each of which has its own function and serves as an input to the next model. The whole system was computerized to provide a quick and efficient tool for the design engineer. In the following chapters, the development and use of each model is discussed in detail.

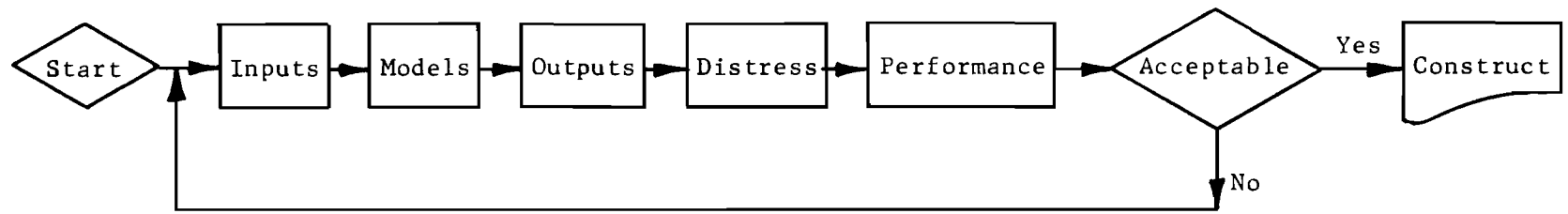


Fig 2.2. General system approach to pavement design.

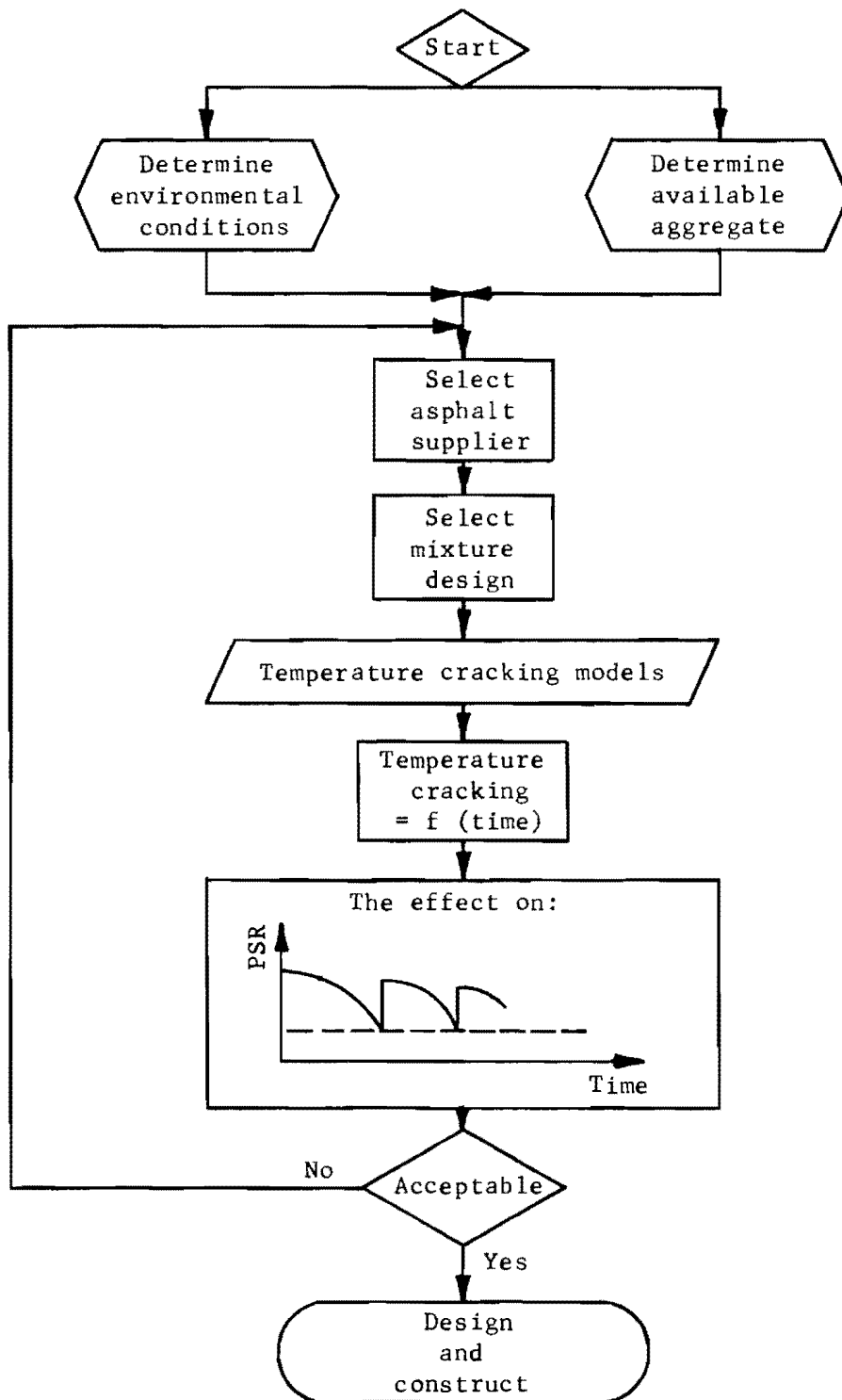


Fig 2.3. Flow chart of a temperature cracking design system.

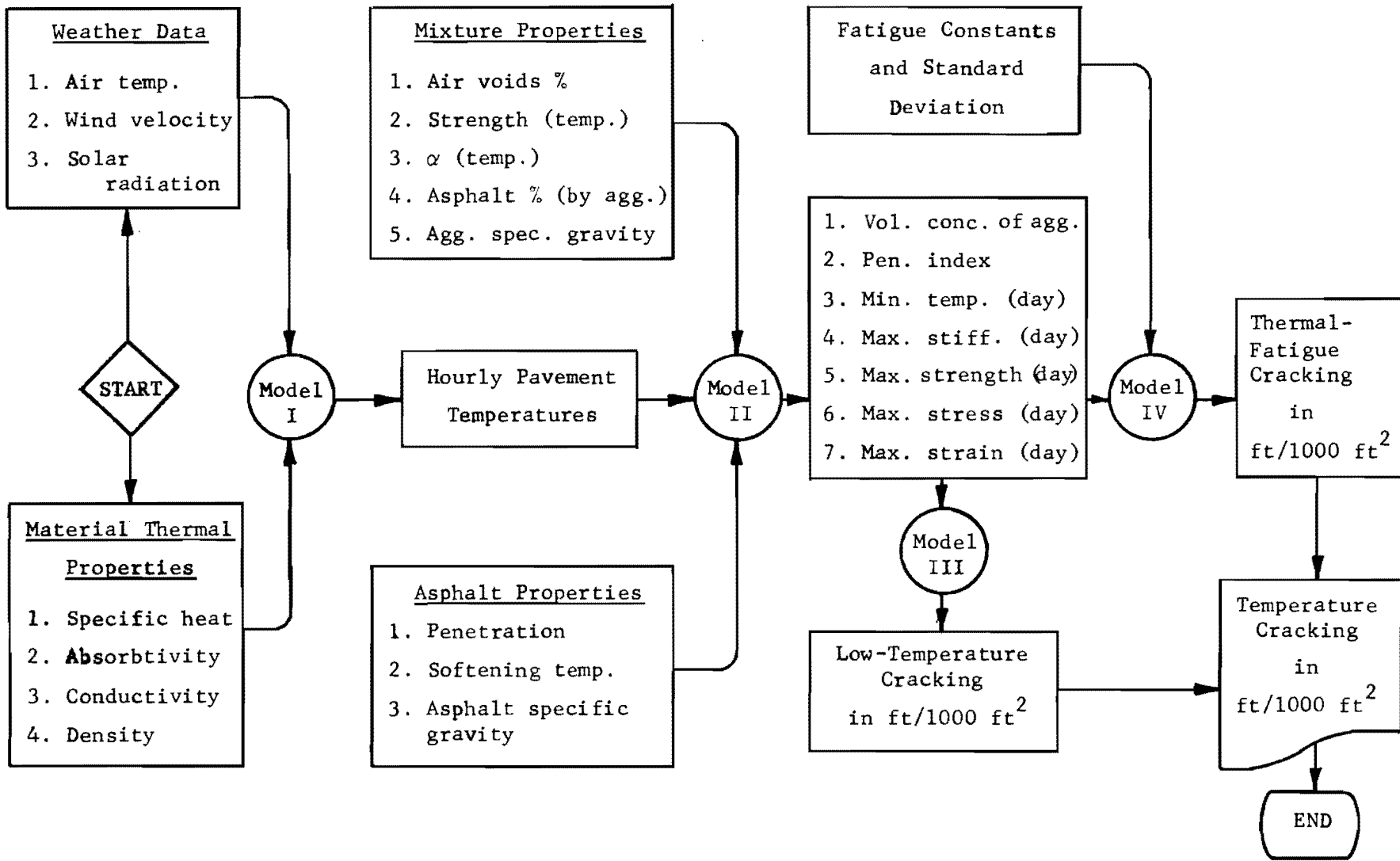


Fig 2.4. Summary flow chart of the developed temperature cracking system.

CHAPTER 3. SIMULATION OF PAVEMENT TEMPERATURES

Experience has indicated that temperature changes have a pronounced effect on pavement structures. In flexible pavements, high temperatures cause instability and excessive deflections, and yet low temperatures cause pavement fracture, which is considered to be a severe distress manifestation. In rigid pavements, the main problem is curling, which occurs due to temperature differences between the top and the bottom of the concrete slab. Therefore, in both flexible and rigid pavements, it is quite important to be able to simulate pavement temperatures at any time and depth.

To date, most of the available models for forecasting daily pavement temperatures, utilizing the available weather records, can simulate the maximum, but not the minimum pavement temperatures. One of the better models was presented by Barber (Ref 2), and it is discussed in the next section. However, Straub et al (Ref 67) presented a model by which daily pavement temperatures could be simulated, but one of the limitations was that the initial pavement temperatures had to be provided. This chapter presents a model that has been developed for simulating bituminous pavement temperatures, as related to air temperature, wind velocity, solar radiation, and the thermal properties of the pavement materials. The model has the advantage of simulating both maximum and minimum pavement temperatures and can be easily computerized.

THEORY

The differential equation of conduction of heat in a homogeneous isotropic solid (Ref 7) is as follows:

$$\frac{\partial T}{\partial t} = c \left(\frac{\partial^2 T}{\partial x^2} + \frac{\partial^2 T}{\partial y^2} + \frac{\partial^2 T}{\partial z^2} \right) \quad (3.1)$$

where

T = temperature of mass as a function of t , x , y , and z ;

t = time;

x, y, z = directions in rectangular coordinate, e.g., x is the depth coordinate;

c = diffusivity.

When the heat flow is assumed to be unidirectional, i.e., the temperature is a function of t and x only, Eq 3.1 reduces to

$$\frac{\partial T}{\partial t} = c \frac{\partial^2 T}{\partial x^2} \quad (3.2)$$

The solution of the above equation for estimating the 24-hour periodic temperature of a semi-infinite mass T in contact with air at a temperature which is equal to $T_M + T_V \sin 0.262t$, was given by Barber (Ref 2) as follows:

$$T = T_M + T_V \frac{H e^{-xC}}{\sqrt{(H+C)^2 + C^2}} \sin \left(0.262t - xC - \arctan \frac{C}{H+C} \right) \quad (3.3)$$

where

T = temperature of mass, $^{\circ}F$;

T_M = mean effective air temperature, $^{\circ}F$;

T_V = maximum variation in temperature from the effective mean, $^{\circ}F$;

t = time from beginning of cycle (one cycle = 24 hours), hours;

x = depth below surface, feet;

H = h/k ;

h = surface coefficient, BTU per square foot per hour, $^{\circ}F$;

- k = conductivity, BTU per square foot per hour, $^{\circ}$ F per foot;
 c = diffusivity, square foot per hour = $\frac{k}{sw}$;
 s = specific heat, BTU per pound, $^{\circ}$ F;
 w = density, pounds per cubic foot; and
 C = $0.131/c$.

Before proceeding, a physical definition of some of the above terms is needed:

- (1) thermal conductivity - the capacity of material for transferring heat,
- (2) specific heat - amount of heat which must be supplied to a unit mass of material to increase its temperature one degree,
- (3) solar radiation - amount of heat from the sun per unit area and time, and
- (4) absorbtivity - ability of the surface to absorb heat.

The temperature of a semi-infinite mass sheltered from solar radiation as compared to the temperature of the air is shown in Fig 3.1. In order to include the effect of solar radiation and wind velocity in estimating the effective air temperature, i.e., T_M and T_V in Eq 3.3, Barber (Ref 2) made use of the following statements:

- (1) For a forced convection, including average reradiation, the surface coefficient h can be estimated as follows:

$$h = 1.3 + 0.62V^{3/4} \quad (3.4)$$

where

$$V = \text{wind velocity, mph.}$$

- (2) There is an average net loss of about one-third of the solar radiation (by longwave reradiation), so that the average contribution of the solar radiation to the effective air temperature can be expressed as follows:

$$R = \frac{2}{3} \times b \times \text{solar radiation} \times \frac{1}{h} \quad (3.5)$$

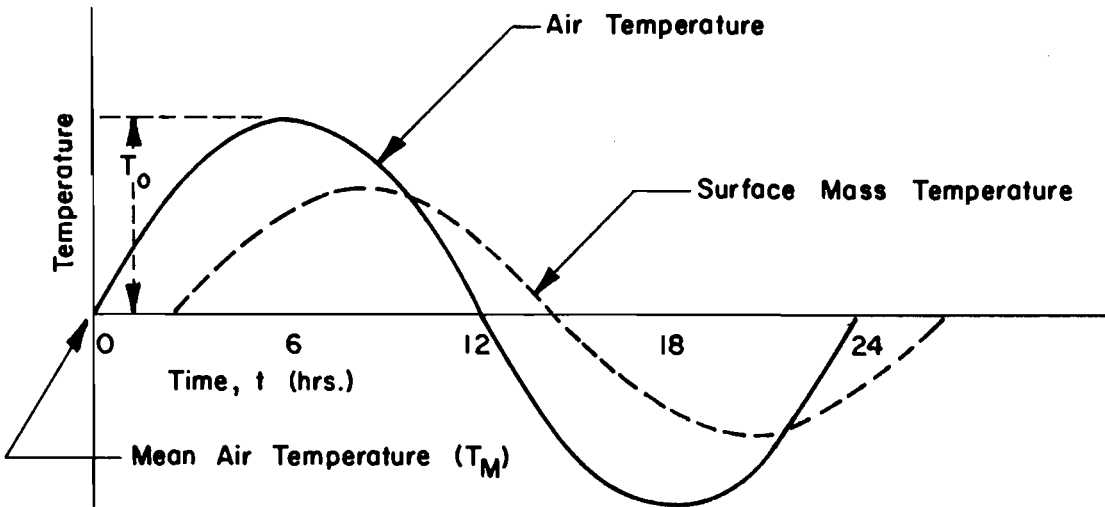


Fig 3.1. Surface temperature as a function of time without radiation and wind (Ref 2).

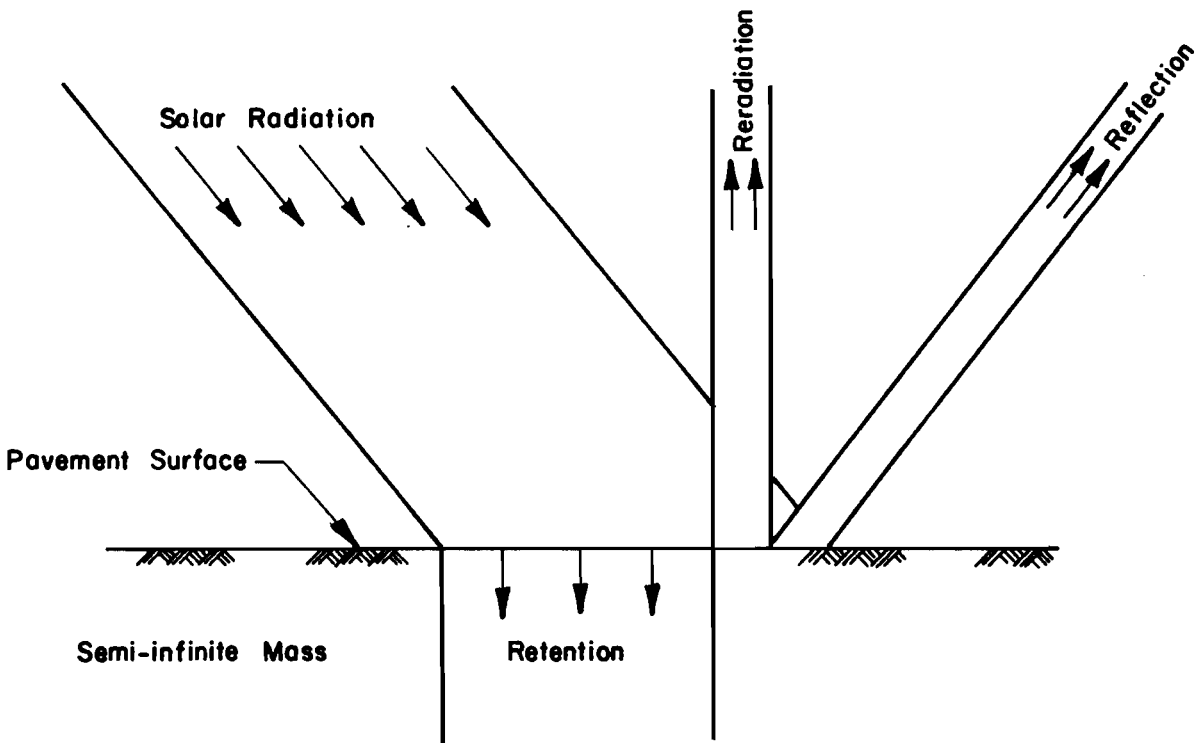


Fig 3.2. Illustration of the effect of solar radiation on pavements (Ref 2).

where

b = surface absorbtivity to the solar radiation.

Since the solar radiation is usually reported in Langleys per day, which is 3.69 BTU per square foot per day, Eq 3.5 can be rewritten as follows:

$$R = \left(\frac{2}{3}\right) \times b \times \left(\frac{3.69 \times L}{24}\right) \times \frac{1}{h} \quad (3.6)$$

where

L = solar radiation in Langleys per day.

Figure 3.2 illustrates the effect of solar radiation on pavement temperatures.

- (3) The deviation of the radiation from R can be approximated by a sine wave with a half-amplitude of $3R$.
- (4) From the above three statements, Eqs 3.7 and 3.8 can be used in conjunction with Eq 3.3 to estimate the maximum pavement temperature.

$$T_M = T_A + R \quad (3.7)$$

$$T_V = 0.5T_R + 3R \quad (3.8)$$

where

T_M = mean effective air temperature, $^{\circ}$ F;

T_A = mean air temperature, $^{\circ}$ F;

T_V = the half-amplitude of the effective air temperature, $^{\circ}$ F;

T_R = daily air temperature range, $^{\circ}$ F.

Figure 3.3 shows a comparison between the air temperature and the effective air temperature. As previously noted, the above technique estimates the maximum pavement temperatures only, and a different curve is required for minimum temperature (Ref 2).

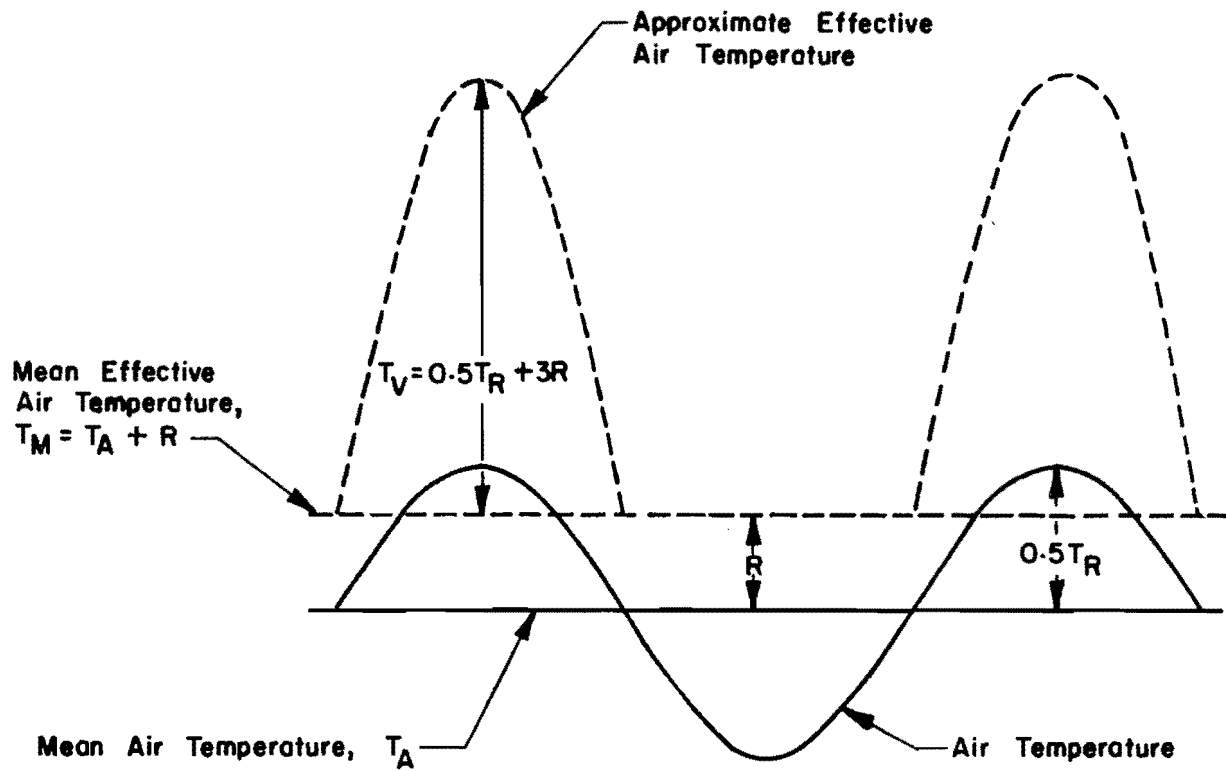


Fig 3.3. A comparison between air temperature and effective air temperature.

DEVELOPED MODEL

The developed model is a justified practical improvement to Barber's model, the purpose of which was to simulate the minimum pavement temperatures as well as the maximum. Straub (Ref 67) stated that: "It should be noted that minimum temperatures of the surface seldom drop below the lowest air temperature, barring an unusually clear night producing a so-called radiation frost. Thus, local weather records are immediately usable for predicting 'worst minimum'." Hence, the effective air temperature parameters T_M and T_V for simulating minimum temperatures were assumed to be as follows:

$$T_M = T_A + (B \times R)$$

$$T_V = 0.5T_R$$

where

B = constant to be determined;

T_A , R , T_R are as defined before.

Using the data presented by Kallas (Ref 37), the constant B was estimated through trial and error to be 0.5. In addition, for better simulation, weighted coefficients for the temperature sinusoidal function were developed. In doing so, Eq 3.3 was rewritten as follows:

$$T = T_M + T_V \frac{He^{-xC}}{\sqrt{(H+C)^2 + C^2}} \sin(S_i) \quad (3.9)$$

where

$\sin(S_i)$ = a sinusoidal function composed of three differently weighted sine curves ($i = 1$ to 3);

$$S_i = A_{i1}(A_{i2}t - A_{i3}xc - A_o) ;$$

A_{i1} , A_{i2} , A_{i3} , A_o = forecasting constants;

and the rest of the variables are the same as defined before.

In solving for the above constants, the following two axioms were utilized:

- (1) on the average, the minimum surface temperature occurs at 6:00 A.M.; and
- (2) on the average, the maximum surface temperature occurs at 2:00 P.M.

The three different sine curves were selected to represent different times of the day; that is

Curve 1, for $t = 2$ to 9 (7:00 A.M. to 2:00 P.M.)

Curve 2, for $t = 10$ to 14 (3:00 P.M. to 7:00 P.M.)

Curve 3, for $t = 15$ to 25 (8:00 P.M. to 6:00 A.M.)

Therefore, it was necessary to satisfy the following boundary conditions:

- (1) the temperature estimated from curve 1 at 3:00 P.M. matches that estimated from curve 2,
- (2) the temperature estimated from curve 2 at 8:00 P.M. matches that from curve 3, and
- (3) the temperature estimated from curve 3 at 7:00 A.M. matches that from curve 1.

Using the above assumptions and boundary conditions, the constants were estimated by iteration. The developed model is given below:

$$T = T_M + T_V \frac{He^{-xC}}{\sqrt{(H+C)^2 + C^2}} \sin(S) \quad (3.10)$$

where

$$S_1 = 6.81768 (.0576t - .075xc - .288) \text{ for } t = 2 \text{ to } 9 \text{ (7:00 A.M. to 2:00 P.M.)};$$

$$S_2 = 14.7534 (.02057t - .075xc - .288) \text{ for } t = 10 \text{ to } 14 \text{ (3:00 P.M. to 7:00 P.M.)};$$

$$S_3 = -6.94274 (.02057t - .12xc - .288) \text{ for } t = 15 \text{ to } 25 \text{ (8:00 P.M. to 6:00 A.M.)};$$

$$T_V = 0.5T_R + 3R \text{ if } \sin(s) \geq 0 ;$$

$$T_M = T_A + R \text{ if } \sin(s) \geq 0 ;$$

$$T_V = .5T_R \text{ if } \sin(s) < 0 ;$$

$$T_M = T_A + .5R \text{ if } \sin(s) < 0 ; \text{ and}$$

H, x, C, and c are the same as defined before (Eq 3.3).

All the weather information necessary for the calculations is available in weather reports. Table 3.1 gives conventional values for the thermal properties of asphalt concrete mixtures.

TABLE 3.1 AVERAGE VALUES OF THE THERMAL PROPERTIES OF ASPHALT CONCRETE MIXTURES (Ref 2)

(1) Absorbitivity of surface to solar radiation	=	.95
(2) Thermal conductivity (BTU/ft ² /hr, ° F)	=	0.7
(3) Specific heat (BTU/lb, ° F)	=	0.22

Limitations of the Model

- (1) The effect of rain, snow, and clouds on pavement temperatures is not included.
- (2) The model assumes a semi-infinite mass; however, Kallas (Ref 37) measured the pavement temperatures at several depths for 6 and 12-inch asphalt concrete slabs and concluded the following:

"The temperatures at depths of 2, 4, and 6 inches in a 6-inch-thick asphalt concrete pavement were essentially the same as temperatures at the same depths in a 12-inch-thick asphalt concrete pavement."

Therefore, it is believed that the error due to the assumption of a semi-infinite mass is practically negligible.

VERIFICATION OF THE MODEL

In order to see how well the developed model simulates the measured pavement temperatures, the model was computerized to operate on a CDC 6600 electronic computer (see Appendix 1). A comparison between the predicted and measured pavement temperatures at College Park, Maryland, (Ref 37) was then performed. The comparison was performed for two days on which the highest and lowest pavement temperatures were recorded, June 30, 1964, and January 19, 1965, respectively. The asphalt concrete thermal properties and the weather data are given in Tables 3.2 and 3.3. Table 3.4 is an example output of the computer program used to perform the calculations. Figure 3.4 shows the comparison at

TABLE 3.2. ASPHALT CONCRETE THERMAL PROPERTIES,
COLLEGE PARK, MARYLAND

Unit weight	142.0 PCF
Thermal conductivity	0.7 BTU/FT ² /HR, °F/FT
Specific heat	0.22 BTU/LB, °F
Surface Absorptivity	0.95

TABLE 3.3. WEATHER DATA, COLLEGE PARK, MARYLAND

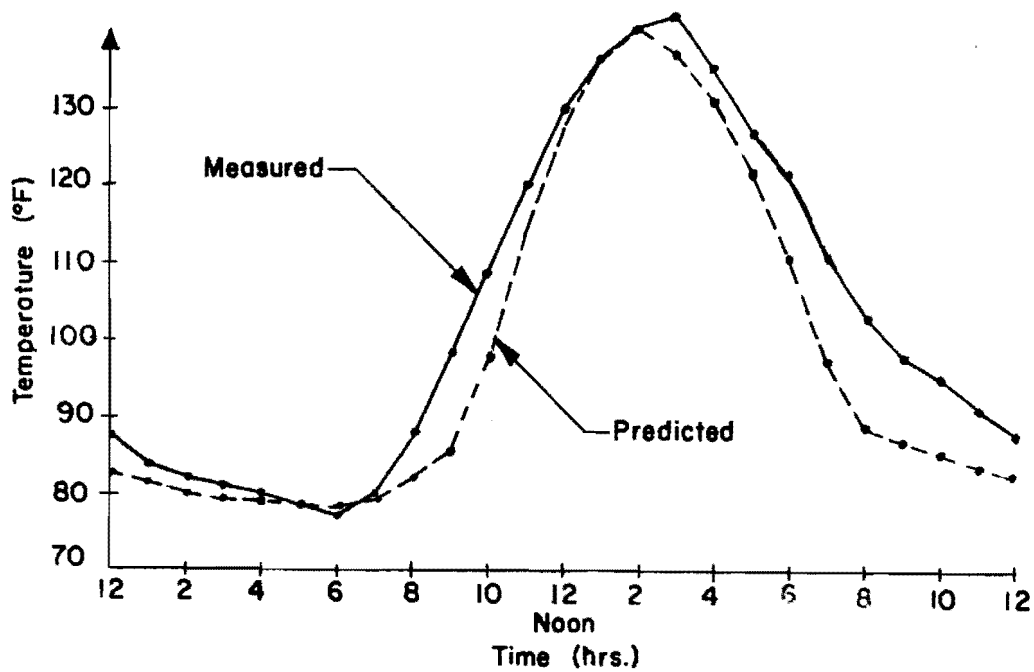
	<u>June 30, 1964</u>	<u>January 19, 1965</u>
Mean air temperature, °F	83.4	17.3
Air temperature range, °F	35.0	28.0
Mean wind velocity*	9.0	10.4
Solar radiation**	660.0	270.0

* Ref 65

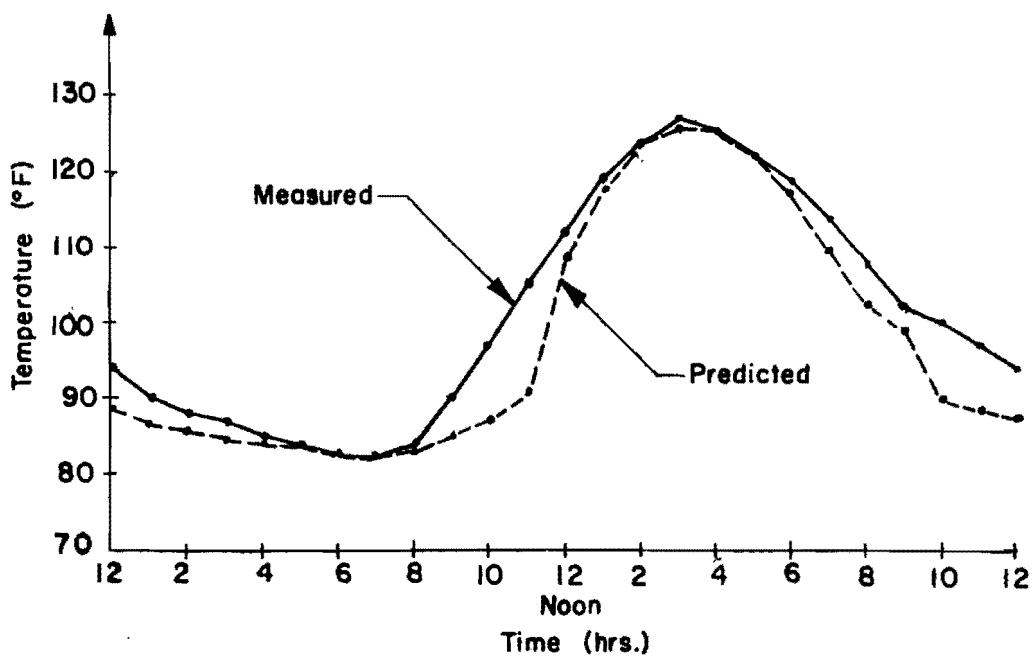
** Ref 38

TABLE 3.4 EXAMPLE OUTPUT OF THE PROGRAMMED MODEL FOR PREDICTING PAVEMENT TEMPERATURES

PROB. NO.	1	EXAMPLE OUTPUT- COLLEGE PARK - JAN,19,1965	
AVE. AIR TEMP.	=	17.300	DEG.F
TEMP. RANGE	=	28.000	DEG.F
WIND VELOCITY	=	10.400	MPH.
MATL. DENSITY	=	142.000	PCI.
SPEC. HEAT	=	.220	BTU. PER POUND DEG.F
CONDUCTIVITY	=	.700	(BTU., HOUR, FT., DEG.F)
ABSORBTIVITY	=	.950	
SOLAR RAD.	=	270.000	LANGELYS PER DAY
DEPTH	=	0.000	INCHES
HOUR OF DAY		TEMP.=DEG.F	
	7A.M	10.7	
	8A.M	12.9	
	9A.M	16.1	
	10A.M	22.7	
	11A.M	31.0	
	12NOON	38.1	
	1P.M	42.8	
	2P.M	44.4	
	3P.M	43.1	
	4P.M	39.9	
	5P.M	35.1	
	6P.M	29.2	
	7P.M	22.7	
	8P.M	18.6	
	9P.M	17.2	
	10P.M	15.8	
	11P.M	14.6	
	12MID NIGHT	13.4	
	1A.M	12.4	
	2A.M	11.5	
	3A.M	10.8	
	4A.M	10.3	
	5A.M	10.0	
	6A.M	9.9	

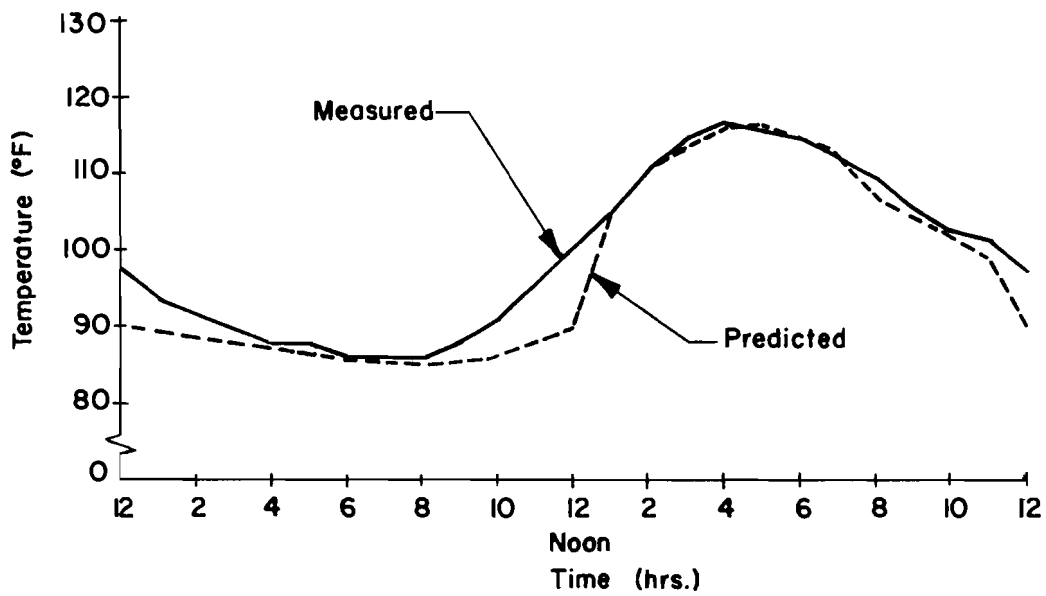


(a) Depth = 0"

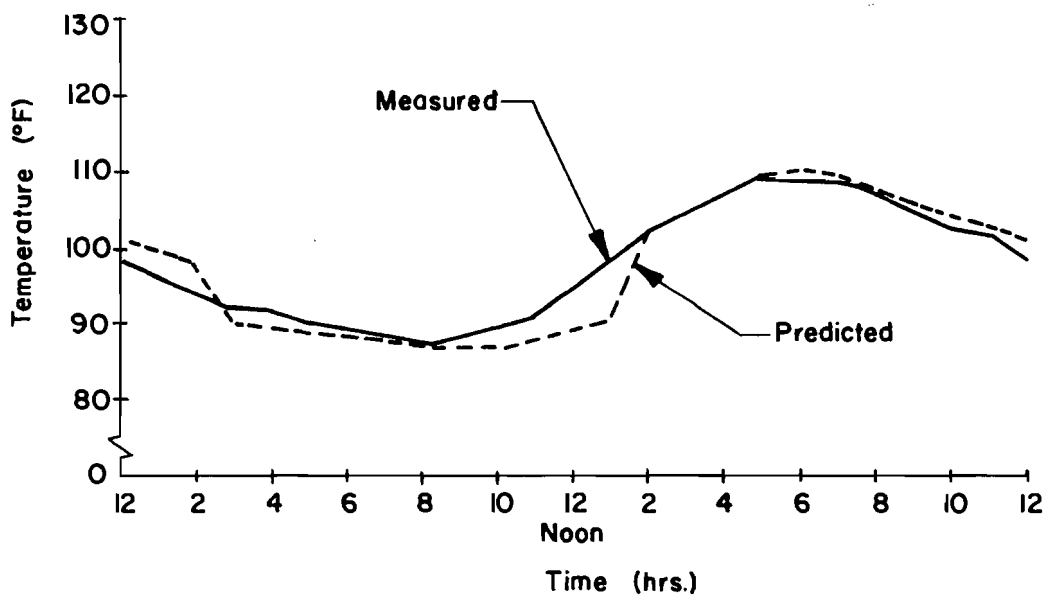


(b) Depth = 2"

Fig 3.4. Comparison between predicted and measured pavement temperatures on June 30, 1964.

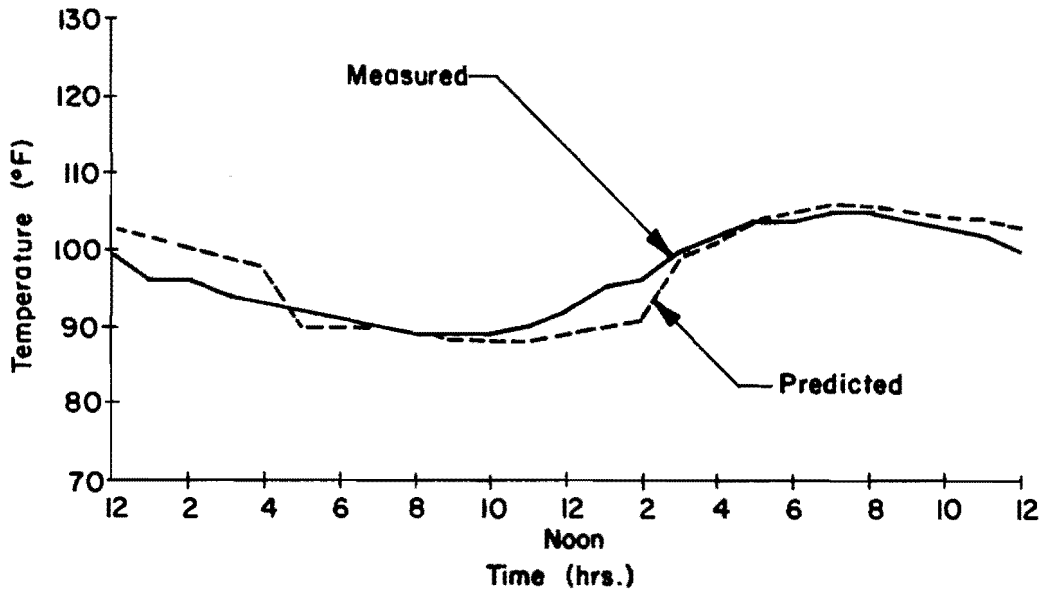


(c) Depth = 4"

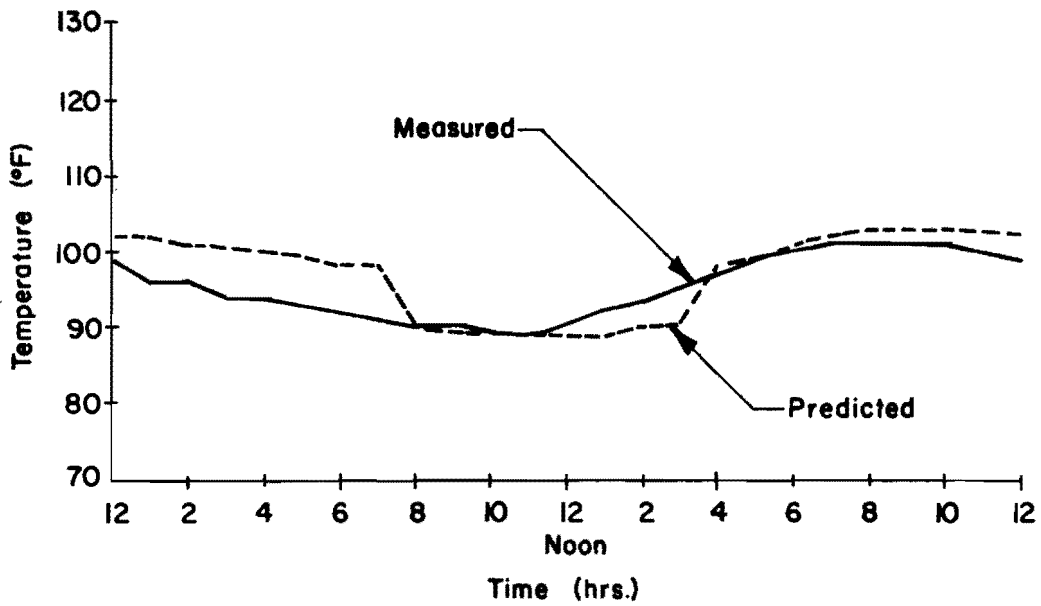


(d) Depth = 6"

Fig 3.4. Continued.



(e) Depth = 8"



(f) Depth = 10"

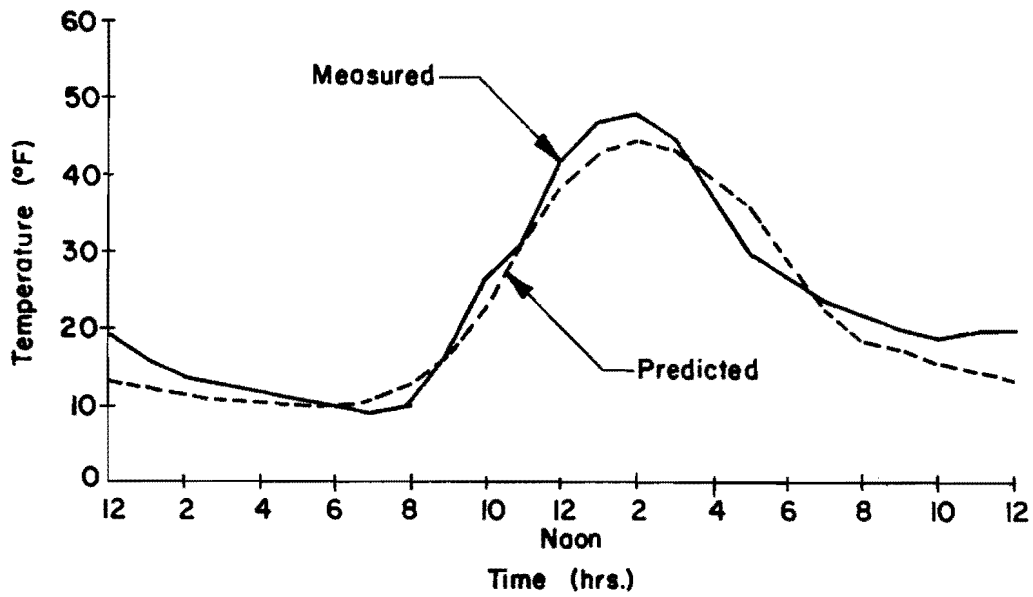
Fig 3.4. Continued.

different depths for June 30, 1964, while Fig 3.5 shows the comparison for January 19, 1965. The figures indicate that the predicted and measured pavement temperatures are in good agreement and that the model can be reliably used for engineering purposes.

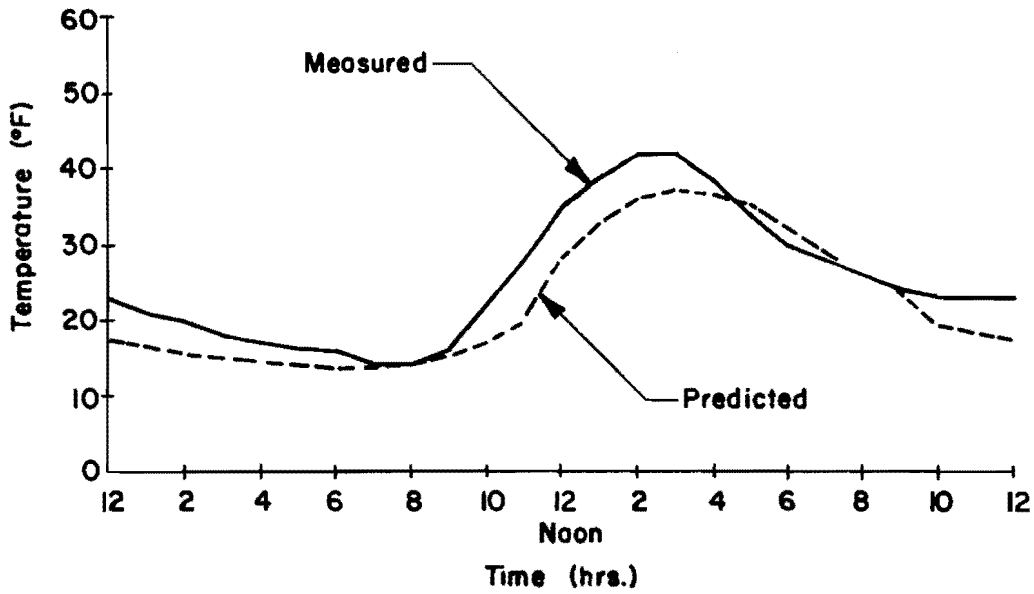
SENSITIVITY ANALYSIS OF THE MODEL

The purpose of such an analysis is to detect the significant factors that affect pavement temperatures. In doing so, eight variables were considered: average daily air temperature, daily air temperature range, wind velocity, solar radiation, surface absorbtivity, thermal conductivity, specific heat, and unit weight. Weather variables were selected to represent the average weather conditions in Texas, except that the average daily air temperature was on the low side. Material thermal properties were selected to represent asphalt concrete mixtures (Table 3.5). Using these values, the maximum and minimum pavement temperatures were estimated. Keeping the rest of the variables at their average values, one variable at a time was increased by 10 percent and the effect on the maximum and minimum pavement temperatures was calculated. Similarly, one variable at a time was decreased by 10 percent and again the effect on the maximum and minimum pavement temperatures was calculated. The results of the calculations are shown in Figs 3.6 and 3.7. The following conclusions were drawn from the above analysis:

- (1) The increase, or decrease, of the average air temperature will shift the pavement temperature curve up, or down.
- (2) The increase in the daily air temperature range causes an equal increase and decrease in the maximum and minimum pavement temperatures, respectively. However, a decrease in the air temperature range will cause the reverse.
- (3) Solar radiation shows a relatively significant effect on the maximum pavement temperature.
- (4) An increase of wind velocity will decrease both the maximum and minimum pavement temperatures.
- (5) The most significant factor of the material's thermal properties is its surface absorbtivity to the solar radiation.
- (6) Surface absorbtivity and solar radiation have approximately equal effects.
- (7) The effects of thermal conductivity, specific heat, and unit weight are relatively insignificant.

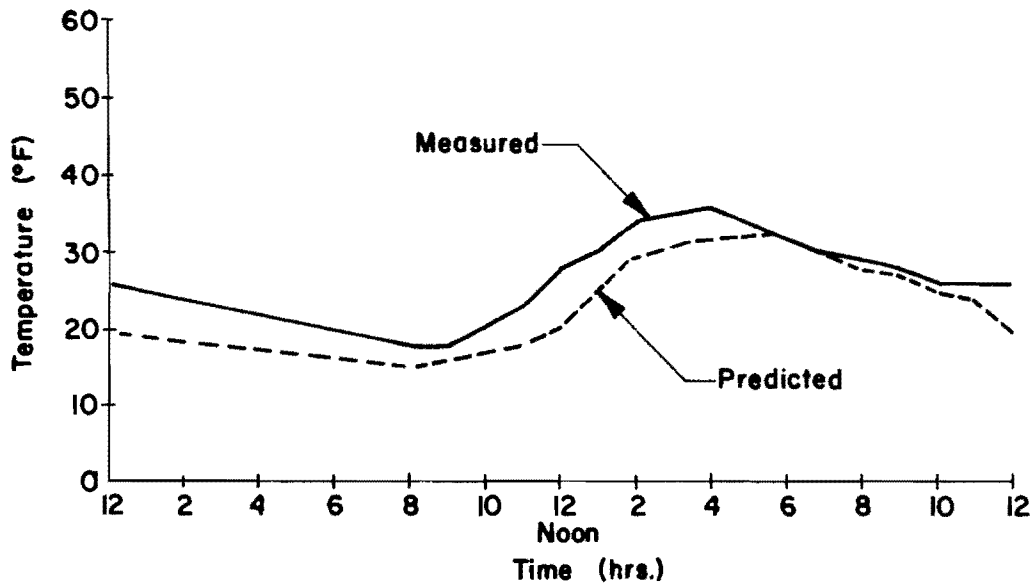


(a) Depth = 0"

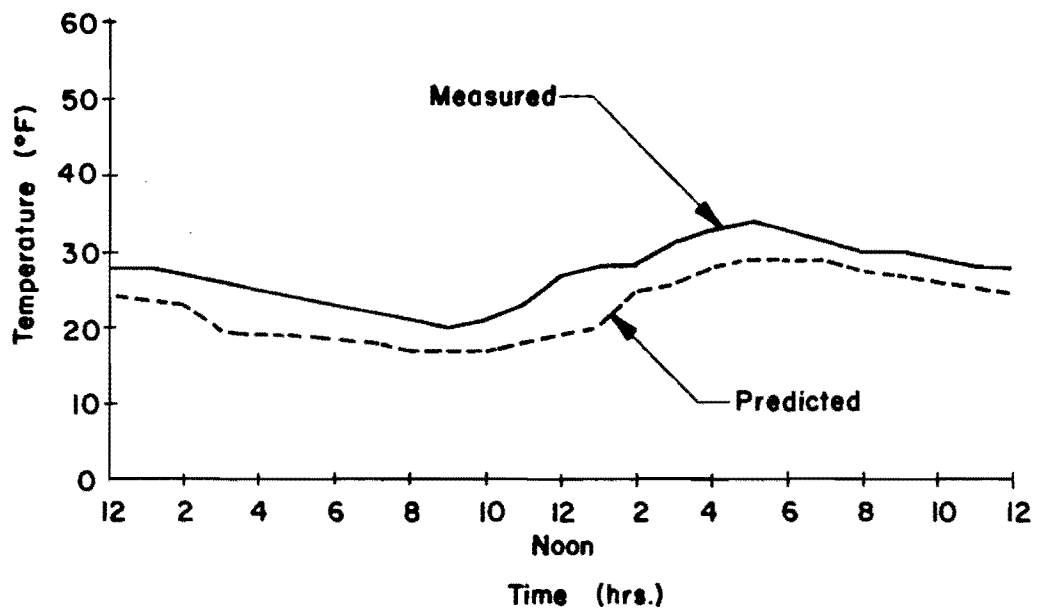


(b) Depth = 2"

Fig 3.5. Comparison between predicted and measured pavement temperatures on January 19, 1965.

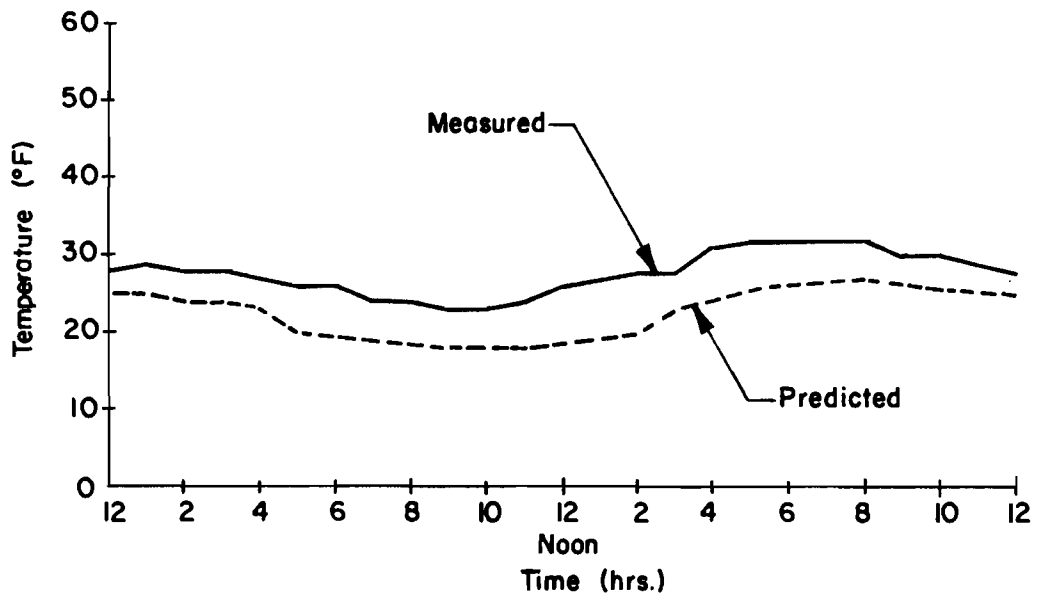


(c) Depth = 4"

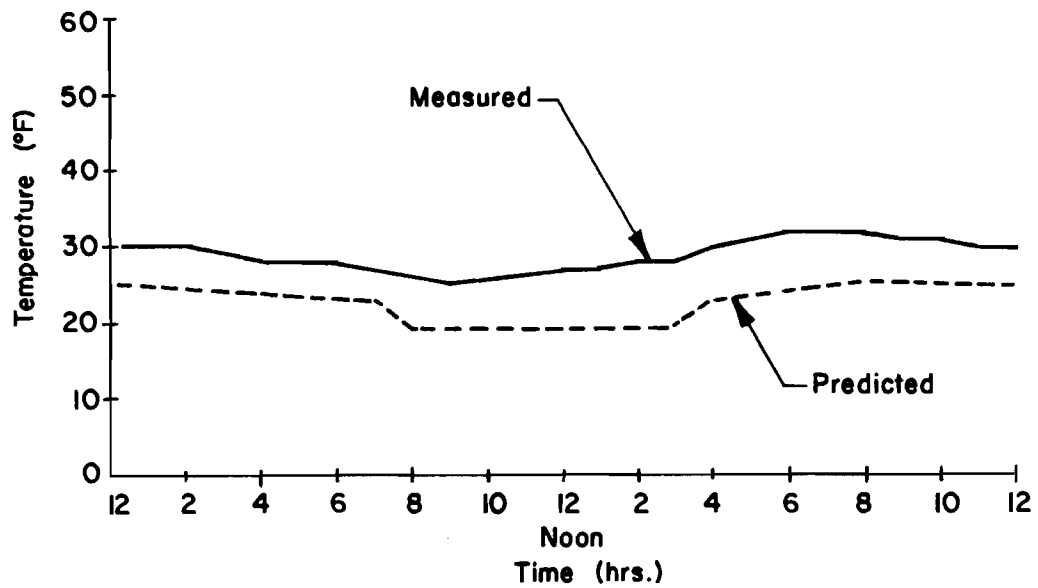


(d) Depth = 6"

Fig 3.5. Continued.



(e) Depth = 8"



(f) Depth = 10"

TABLE 3.5. SELECTED (AVERAGE) VALUES FOR THE SENSITIVITY ANALYSIS

Average air temperature	50, °F
Air temperature range	25, °F
Wind velocity	10, mph
Solar radiation	500, Langleys/Day
Surface absorptivity	0.9
Thermal conductivity	0.7, BTU/FT ² /HR, °F/FT
Specific heat	0.22, BTU/LB, °F
Unit weight	150, PCF

RESULTING PAVEMENT TEMPERATURES

Maximum pavement temperature = 89.1 °F

Minimum pavement temperature = 46.0 °F

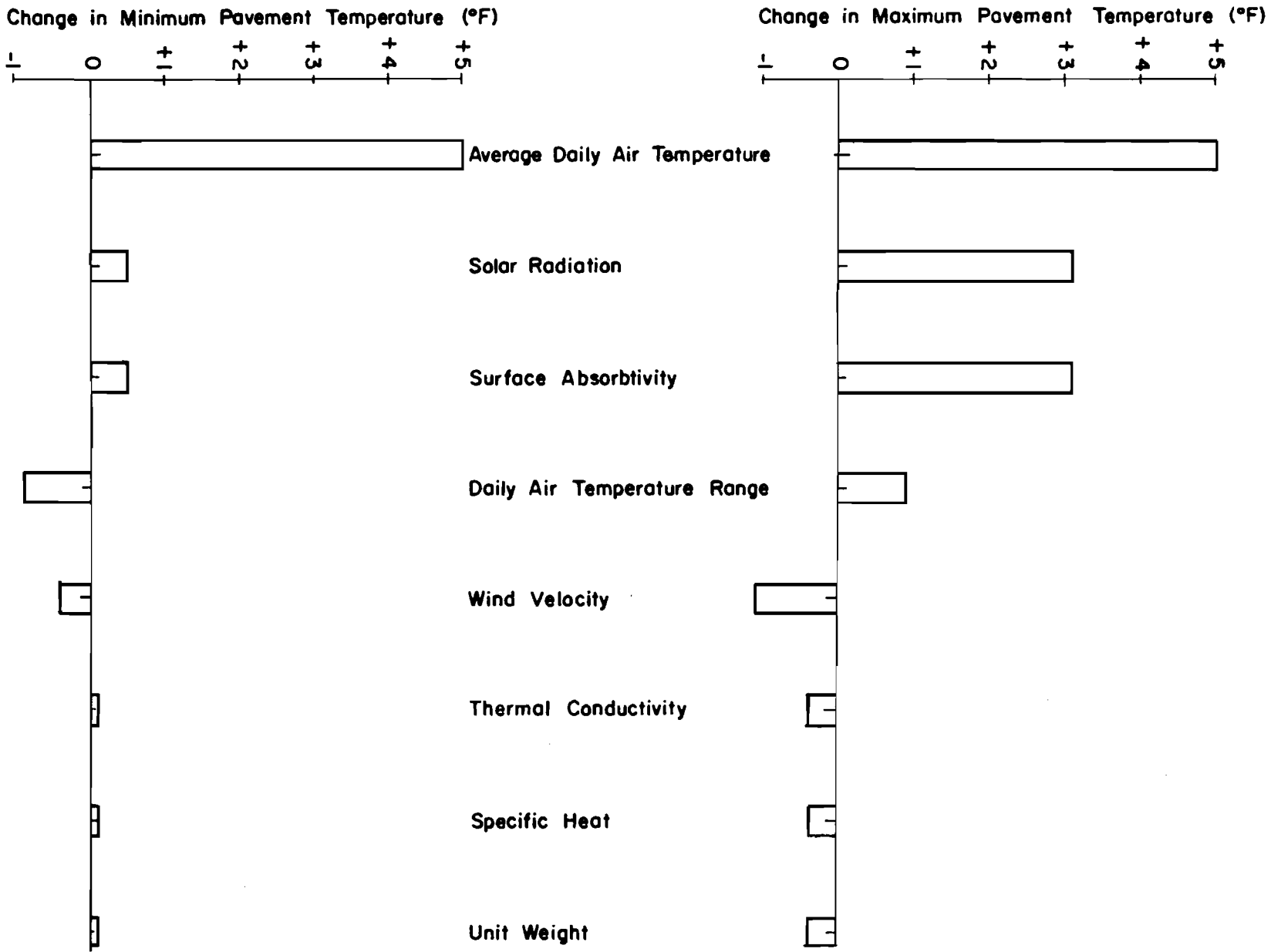


Fig 3.6. The effect of 10% increase in one variable at a time on maximum and minimum pavement temperatures (surface).

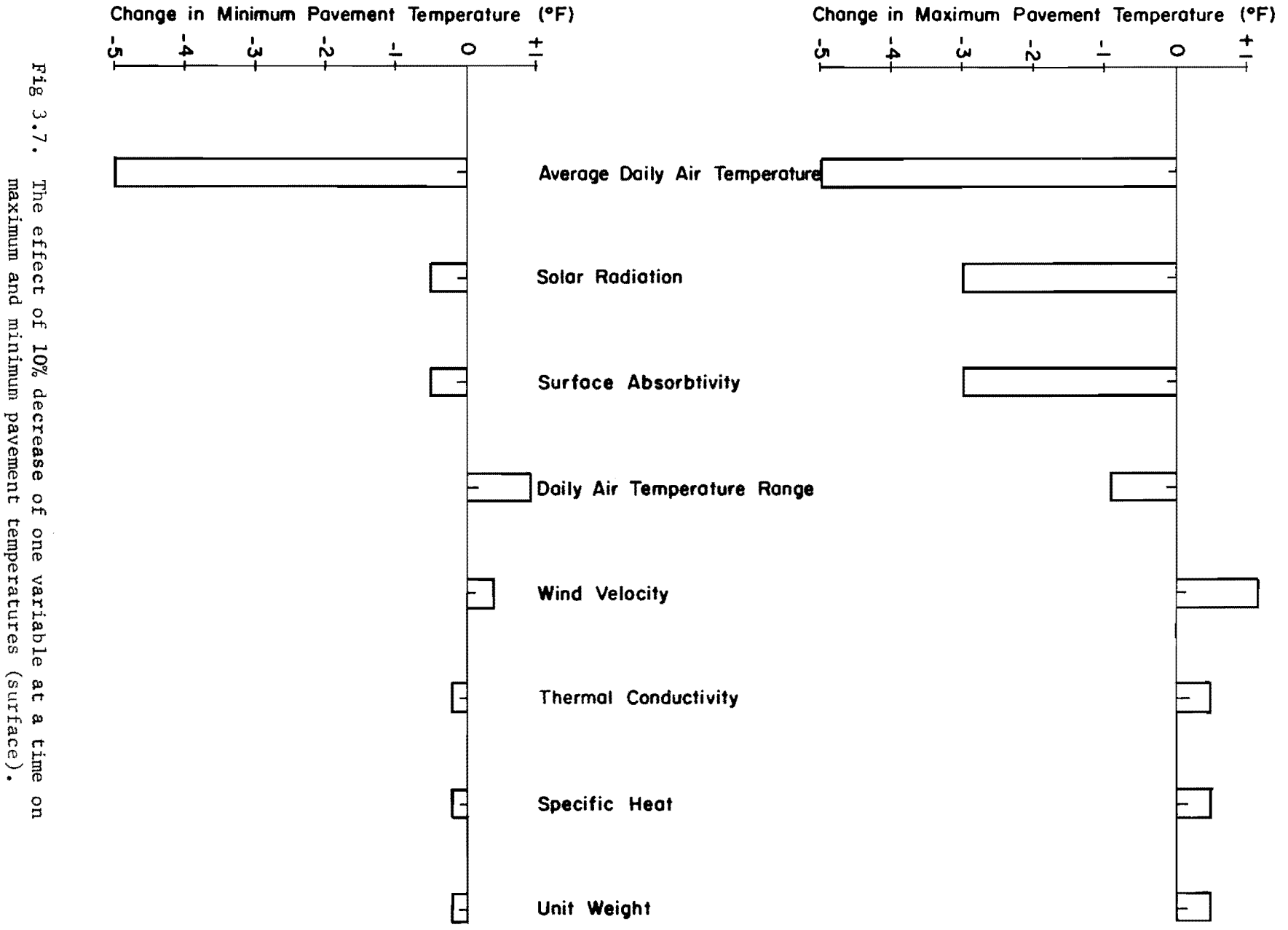


Fig 3.7. The effect of 10% decrease of one variable at a time on maximum and minimum pavement temperatures (surface).

SUMMARY

A model for predicting bituminous pavement temperatures has been developed. All the necessary weather information to use the model can be obtained from regular Weather Service reports. The model is an essential element in the overall system for predicting temperature cracking in asphalt concrete surfaces.

CHAPTER 4. ASPHALT CONCRETE RHEOLOGY

INTRODUCTION

This chapter is directed primarily toward the characterization of the behavior of asphalt concrete. The behavior of asphalt concrete as a function of time and temperature has been studied by several investigators; among these are Monismith (Ref 49), Heukelom and Klomp (Ref 29), and Van Der Poel (Ref 74), who agreed that asphalt concrete mixtures are neither elastic nor viscous, but are viscoelastic in nature.

Briefly, elastic materials are those which obey the law of conservation of energy; deformations are recovered when the load is removed. An elastic material can be represented by a spring, the coefficient of which is the modulus of elasticity of the material (Fig 4.1(a)). On the other hand, viscous materials are those in which the energy is completely dissipated, and there is unrecoverable permanent deformation. A viscous material can be represented by a dashpot whose coefficient is about three times the coefficient of viscosity of the material (Fig 4.1(b)). Only a few methods are available for the characterization of viscoelastic materials.

METHODS OF CHARACTERIZING VISCOELASTIC MATERIALS

Models

Mathematical expressions describing the behavior of different combinations of springs and dashpots can be written and it is often assumed that these expressions also describe the behavior of the viscoelastic material. Mathematical expressions are sometimes very complicated, and engineers have often found that models do not represent material behavior in a satisfactory manner under all load conditions. The two basic types of models are shown in Fig 4.2, but it has been found (Ref 49) that these simple models do not adequately represent the behavior of asphalt concrete.

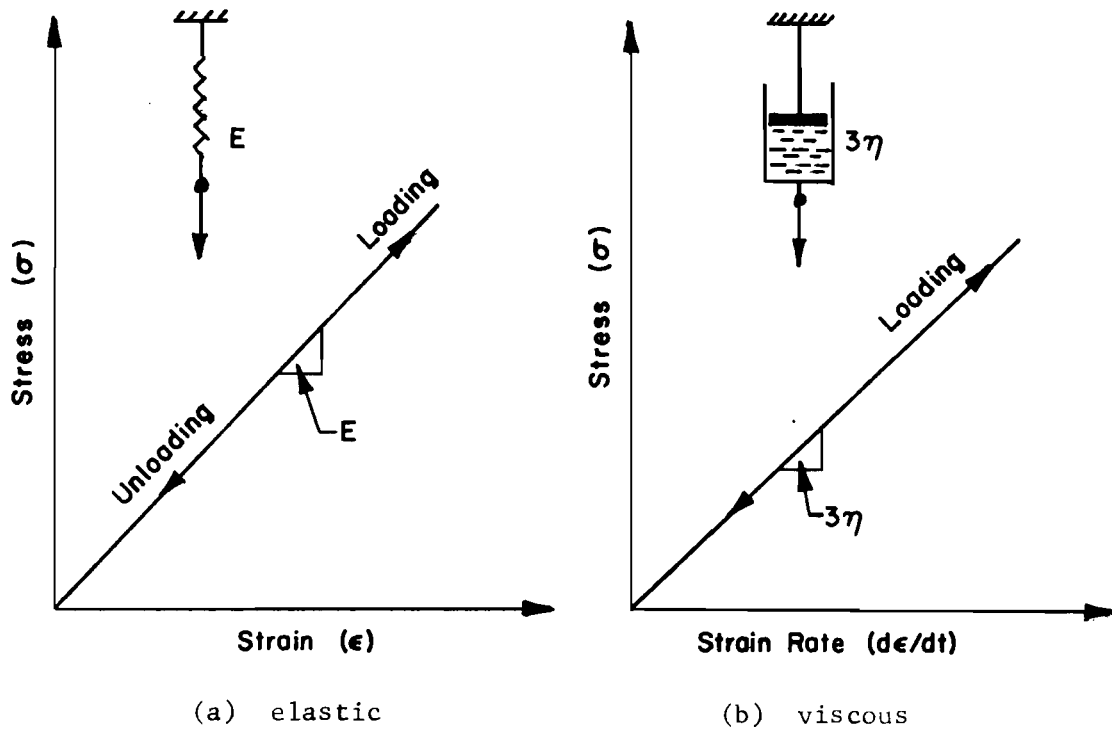


Fig 4.1. Stress-strain diagram for (a) spring, elastic; (b) dashpot, viscous.

Maxwell Model		Kelvin Model	
$\left(E \frac{d}{dt}\right) \epsilon_t = \left(\frac{d}{dt} + \frac{E}{\lambda}\right) \sigma_t$	OPERATOR EQUATION	$\left(\frac{d}{dt} + \frac{E}{\lambda}\right) \epsilon_t = \frac{1}{\lambda} \sigma_t$	
$\epsilon_t = \sigma_o \left[\frac{t}{\lambda} + \frac{1}{E} \right]$	CREEP ($\sigma = \sigma_o$)	$\epsilon_t = \frac{\sigma_o}{E} \left[1 - e^{-\frac{Et}{\lambda}} \right]$	
$\sigma_t = \epsilon_o E e^{-\frac{Et}{\lambda}}$	RELAXATION ($\epsilon = \epsilon_o$)	$\sigma_t = E \epsilon_o$	

Fig 4.2. Basic rheological elements and their time-displacement relationships, viscoelastic.

Direct Measurements

Some of the tests that can be used for direct measurements are listed below:

(1) Creep

$$J(t) = \frac{\epsilon(t)}{\sigma_0}$$

where

- σ_0 = applied constant stress,
- $\epsilon(t)$ = strain as a function of time,
- $J(t)$ = creep compliance.

Monismith et al (Ref 49) showed that for engineering purposes the stiffness modulus or the relaxation modulus can be approximated as $(1/J(t))$. Figure 4.3 is a schematic diagram of a creep test results.

(2) Relaxation

$$E_r(t) = \frac{\sigma(t)}{\epsilon_0}$$

where

- $\sigma(t)$ = stress as a function of time,
- ϵ_0 = applied constant strain,
- $E_r(t)$ = stress relaxation modulus.

Practically speaking, the engineer is interested in the relaxation modulus when dealing with viscoelastic material. Figure 4.4 is a schematic diagram of a relaxation test results.

(3) Dynamic loading

In such a test, a sinusoidal stress or strain is applied to the specimen and the corresponding strain or stress is measured (Fig 4.5):

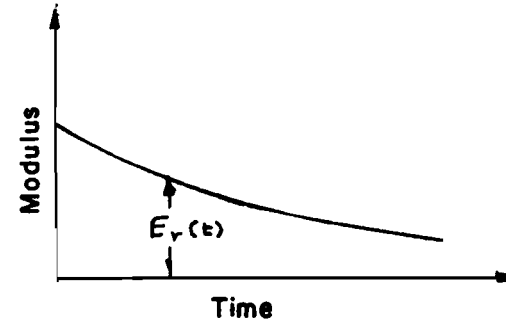
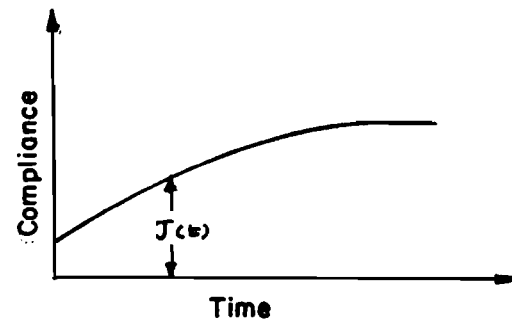
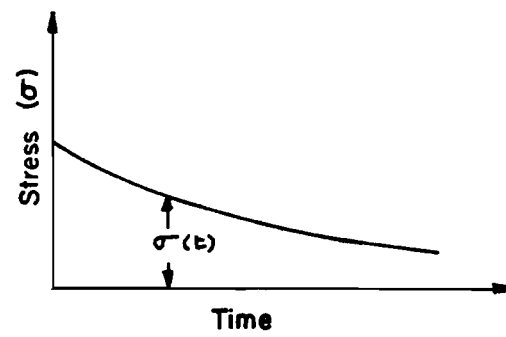
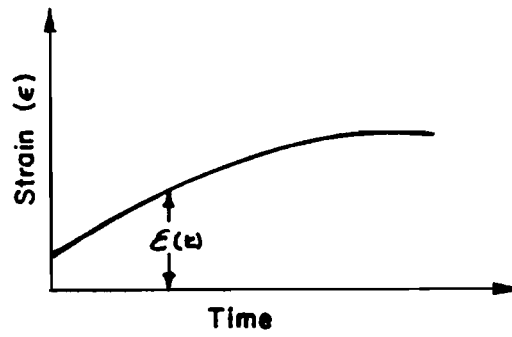
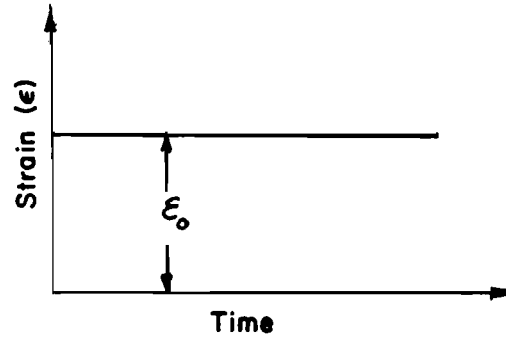
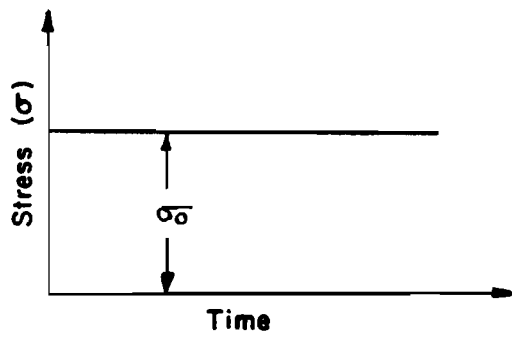
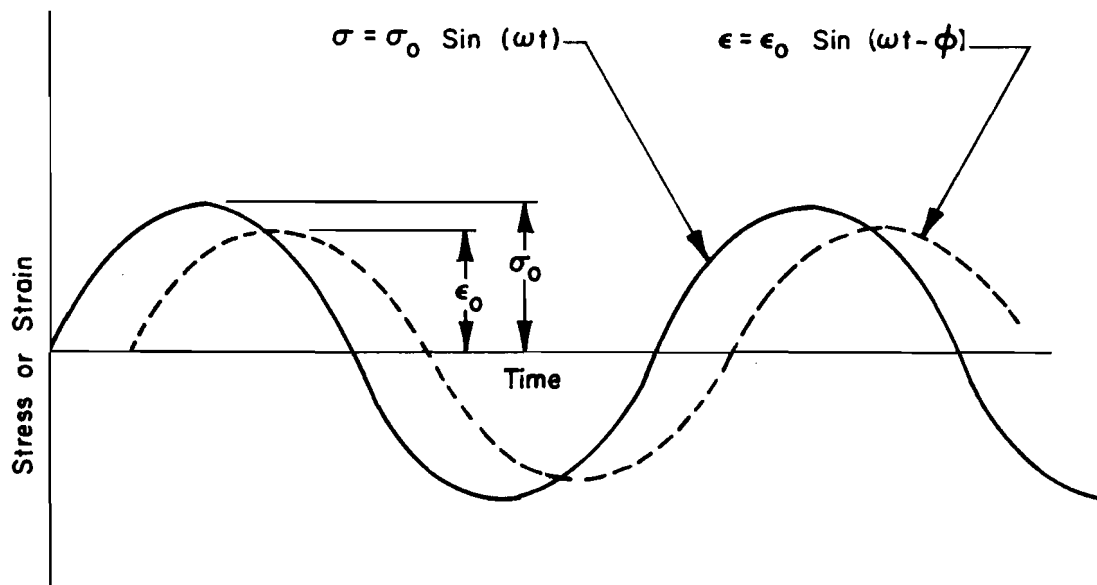


Fig 4.3. A schematic diagram of a creep test result.

Fig 4.4. A schematic diagram of a relaxation test result.



where

ω = frequency of loading,

ϕ = the phase angle, the values of which range from 0° for a pure elastic material to 90° for a pure viscous material.

Figure 4.5. A schematic diagram of a dynamic test result.

$$|E^*| = \frac{\sigma_0}{\epsilon_0}$$

where

$|E^*|$ = absolute value of the complex modulus (psi),

σ_0 = peak amplitude of stress, and

ϵ_0 = peak amplitude of strain.

Indirect Methods

There are many different ways to measure stiffness indirectly; however, this discussion is based on the original work by Van der Poel (Ref 74). Van der Poel defined the stiffness of asphalt as follows:

$$S_{(t,T)} = \left(\frac{\sigma}{\epsilon} \right)_{t,T} = \left(\frac{\text{tensile stress}}{\text{total strain}} \right)_{t,T}$$

where

t = time of loading,

T = temperature,

$S_{(t,T)}$ = stiffness as a function of time and temperature.

Using the above equation and the time-temperature equivalency concept, which is discussed in the next section, Van der Poel constructed a nomograph to determine the stiffness of asphalt. His theory and its utilization for estimating the asphalt concrete stiffness are presented in detail in a later section.

TIME-TEMPERATURE EQUIVALENCY CONCEPT

Although the relaxation modulus decreases with time of loading and temperature, it is possible to obtain the same material characterization while varying both time of loading and temperature by appropriately decreasing time for an increase in temperature and vice-versa.

Figure 4.6 depicts the basis for this concept. The notation in this figure can be explained as follows:

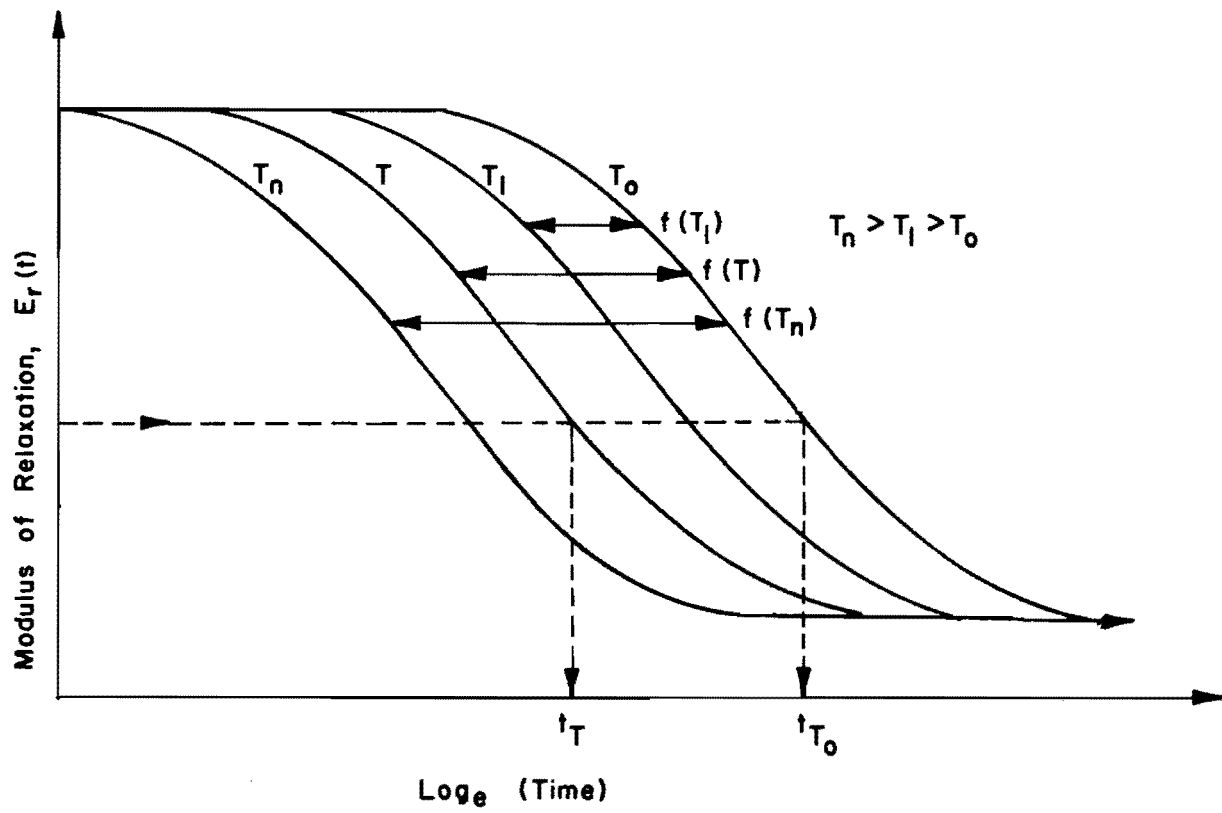


Fig 4.6. Relationship of time and temperature (after Monismith, Ref 49).

t_{T_0} = relaxation time at a reference temperature T_0 , or the reduced time;

t_T = relaxation time at any temperature T ;

$f(T)$ = a function of temperature.

From the figure,

$$\text{Log}_e t_{T_0} = \text{Log}_e t_T + f(T)$$

$$\therefore \text{Log}_e \frac{t_{T_0}}{t_T} = f(T)$$

or

$$\text{Log}_e \frac{t_{T_0}}{t_T} = \text{Log}_e e^{f(T)}$$

$$\therefore t_{T_0} = t_T e^{f(T)} \quad (4.1)$$

putting:

$$a_T = \frac{1}{e^{f(T)}}$$

where

a_T = the shift factor.

$$\therefore t_{T_0} = \frac{t_T}{a_T} \quad (4.2)$$

One method for estimating the shift factor a_T in the laboratory uses the following approximation:

$$a_T \approx \frac{\eta_T}{\eta_{T_0}}$$

where

η_{T_0} = the coefficient of viscosity at the reference temperature T_0 ,

η_T = the coefficient of viscosity at a temperature T .

Figure 4.7 is a schematic diagram that shows the values of the shift factor for a given asphalt at different temperatures, based on a reference temperature T_0 .

From Eq 4.2, if the shift factor is known, the corresponding time of loading for a given temperature can be estimated in order to give the relaxation modulus corresponding to a certain time of loading at the reference temperature.

The following example explains the use of the time-temperature interchangeability concept.

Example

For a given pavement section subjected to load for 30 minutes under a field temperature of 10° F, the loading time in the laboratory at a temperature of 70° F which will yield the same relaxation modulus as in the field can be calculated as follows:

$$a_T = \text{shift factor} = \frac{\eta_T}{\eta_{T_0}} = \frac{\text{coeff. of viscosity at temp. } 70^{\circ} \text{ F}}{\text{coeff. of viscosity at temp. } 10^{\circ} \text{ F}}$$

$$\text{Assume } a_T = 1 \times 10^{-3}$$

$$\therefore t_{70} = t_{10} \times a_T$$

where

t_{70} = time of loading at 70° F,

t_{10} = time of loading at 10° F = 30 minutes.

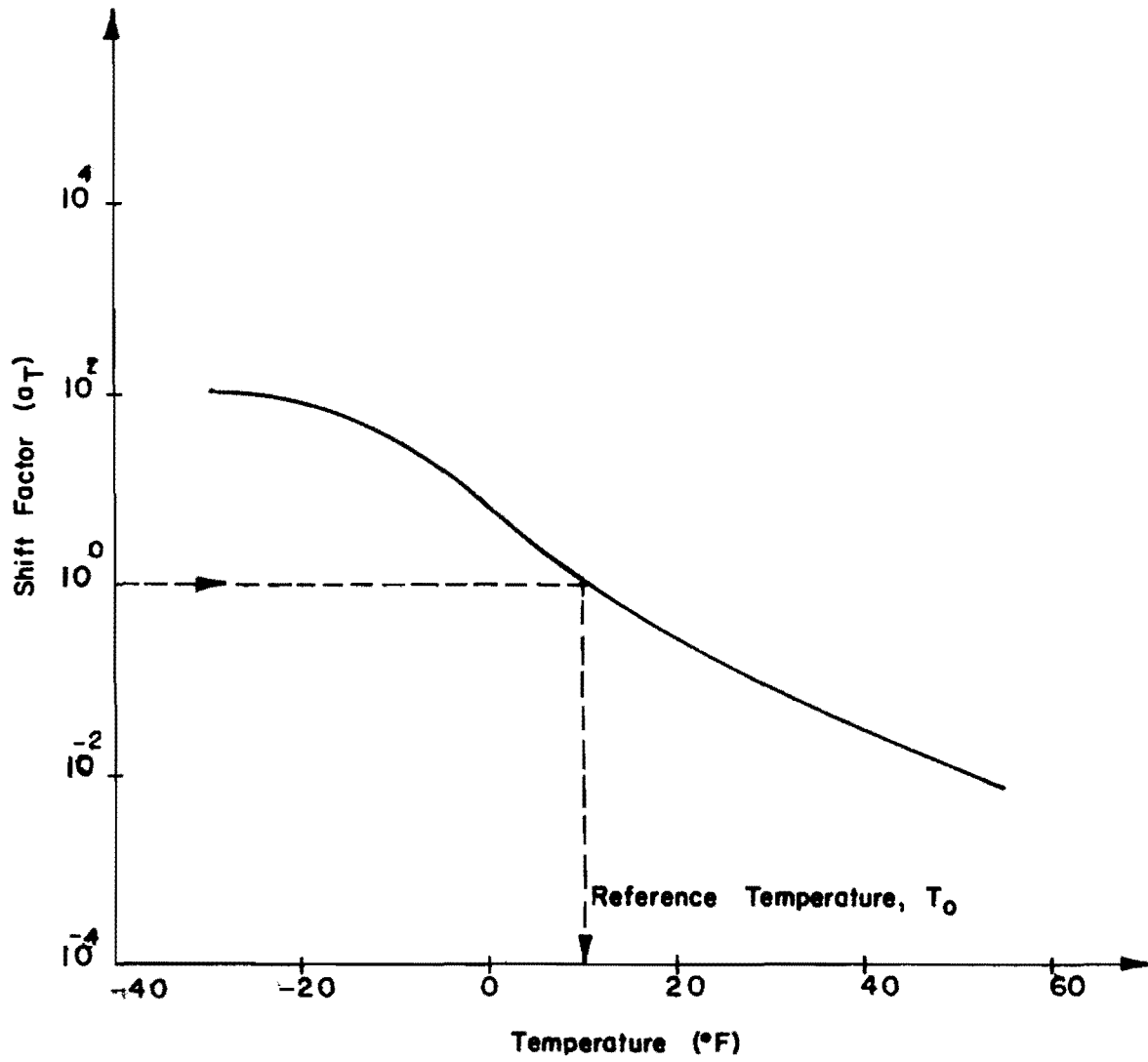


Fig 4.7. A schematic diagram showing the variation of the shift factor with temperature for a given reference temperature t_0 .

$$\begin{aligned}
 t_{70} &= (30 \times 60) \times 1 \times 10^{-3} \\
 &= 1.8 \text{ seconds}
 \end{aligned}$$

Figure 4.8 graphically illustrates the calculations relationships.

VAN DER POEL STIFFNESS THEORY

Asphalt Cement

The concept of stiffness was introduced by Van der Poel as follows (Ref 74):

$$\text{Stiffness modulus (S)} = \frac{\text{tensile stress}}{\text{total strain}} \quad (4.3)$$

The stiffness modulus is an extension of Young's Modulus of Elasticity for a purely elastic solid. However, asphalt is a viscoelastic material and the stress-strain relationship is dependent upon time of loading and temperature.

A nomograph (Fig 4.9) was derived by Van der Poel from experimental data from two types of tests:

- (1) constant-stress test (static creep test in tension), and
- (2) dynamic test with an alternating stress of constant amplitude and frequency.

Two physical tests of a given asphalt cement are required to determine its stiffness modulus (S) from the nomograph. These tests are the penetration (ASTM Designation D5-65) and the softening point ring and ball test (ASTM Designation D36-66T). From the penetration test and softening point temperature, the penetration index for the asphalt can be calculated. The penetration index PI is an index introduced by Pfeiffer and Van Doormall (Ref 56) to indicate the temperature susceptibility of the penetration of the asphalt. This concept is based on the assumption that the penetration of an asphalt at the softening point temperature is about 800. The penetration-temperature susceptible PTS is then calculated from the slope of a line where the logarithm of the penetration is plotted against the temperature:

$$\text{PTS} = \frac{\log 800 - \log(\text{Pen})}{(\text{R\&B softening point, } ^\circ\text{C}) - \text{TPT}} \quad (4.4)$$

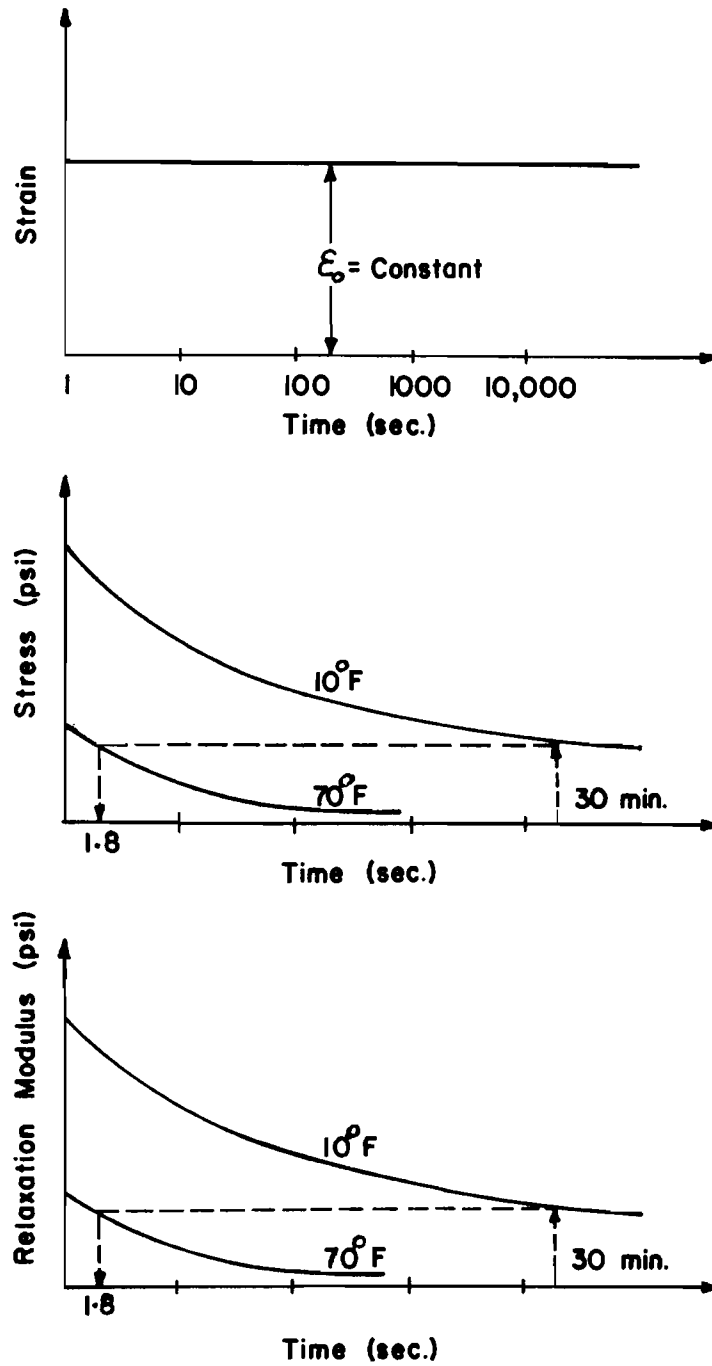
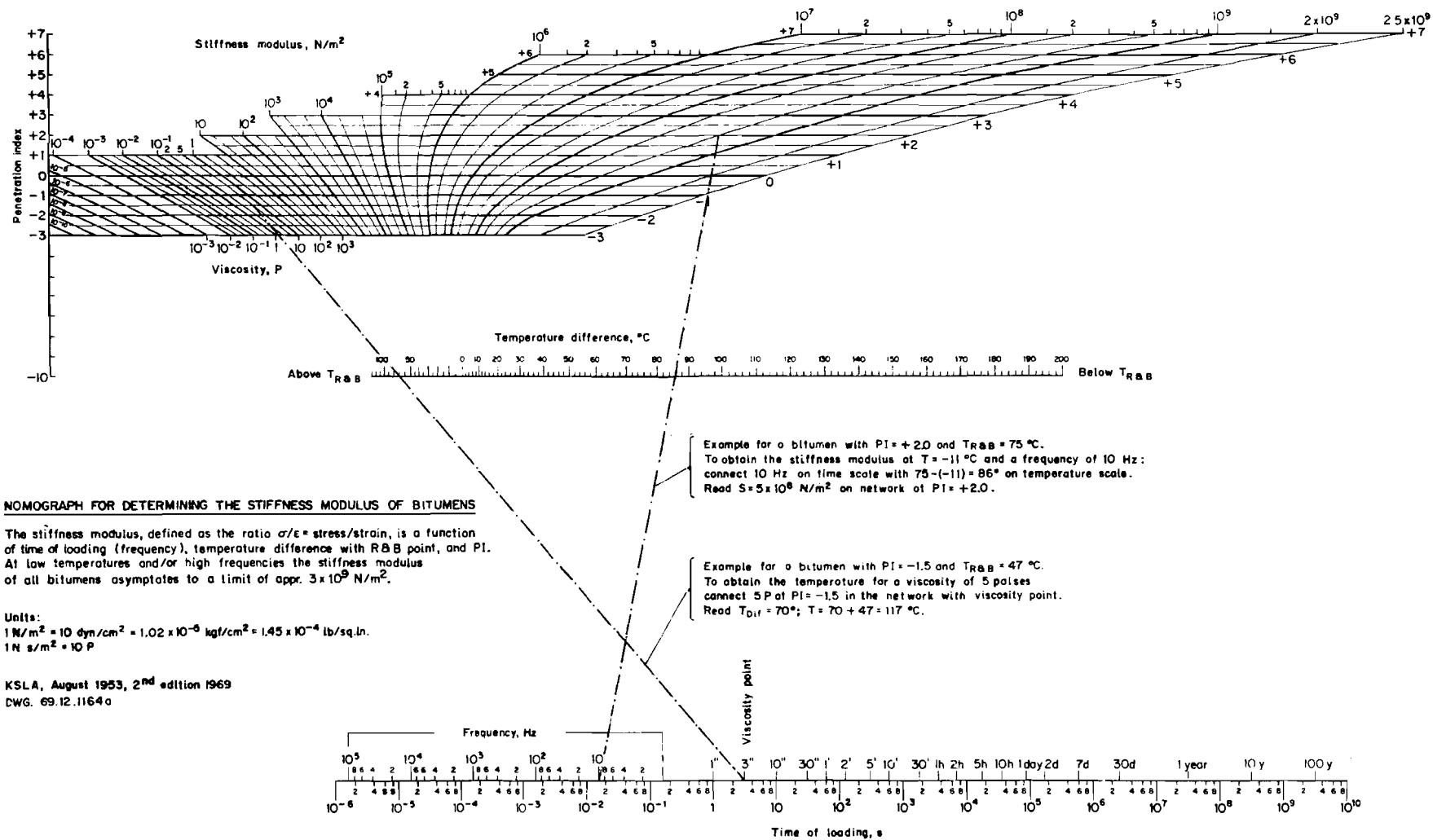


Fig 4.8. A schematic diagram showing the effect of time and temperature on viscoelastic materials.



NOMOGRAPH FOR DETERMINING THE STIFFNESS MODULUS OF BITUMENS

The stiffness modulus, defined as the ratio σ/ϵ = stress/strain, is a function of time of loading (frequency), temperature difference with R&B point, and PI. At low temperatures and/or high frequencies the stiffness modulus of all bitumens asymptotes to a limit of appr. 3×10^9 N/m².

Units:
 $1 \text{ N/m}^2 = 10 \text{ dyn/cm}^2 = 1.02 \times 10^{-6} \text{ kgf/cm}^2 = 1.45 \times 10^{-4} \text{ lb/sq.in.}$
 $1 \text{ N s/m}^2 = 10 \text{ P}$

KSLA, August 1953, 2nd edition 1969
 DWG. 69.12.11640

Fig 4.9. Nomograph for determining the stiffness modulus of bitumens (after Van der Poel, Ref 74).

where

Pen = penetration at 100 gm and 5 seconds,

TPT = temperature in ° C at which the penetration test is carried out.

The value of PTS is then used to obtain the penetration index PI of the asphalt:

$$PI = \frac{20 - 500PTS}{1 + 50 PTS} \quad (4.5)$$

The penetration index PI of most asphalts varies from -2.6 to +8.0 (Ref 74). The lower the PI, the higher the temperature susceptibility.

The original nomograph developed by Van der Poel was developed from a functional relationship between stiffness, time of loading, temperature of test, and rheological types of asphalt, as follows:

$$S = f[-\log t[t_0 + cg(T_{R\&B} - T)]] \quad (4.6)$$

where

t_0 = constant,

c = constant,

f = function depending on rheological character of asphalt,

g = function depending on rheological character of asphalt.

Van der Poel, however, did not evaluate the exact mathematical forms of f and g , but expressed the functional relationship shown in Eq 4.6 in graphical form. His nomograph was modified slightly by Heukelom and Klomp (Ref 29); the stiffness is determined in kg/cm^2 instead of Newtons per square meter, and the lines for negative penetration indices are in a different location. This modified nomograph is shown in Fig 4.10. The determination of stiffness from the nomographs published by Van der Poel and by Heukelom and Klomp requires three parameters:

- (1) time of loading,
- (2) softening-point temperature minus test temperature, and
- (3) penetration index of the asphalt.

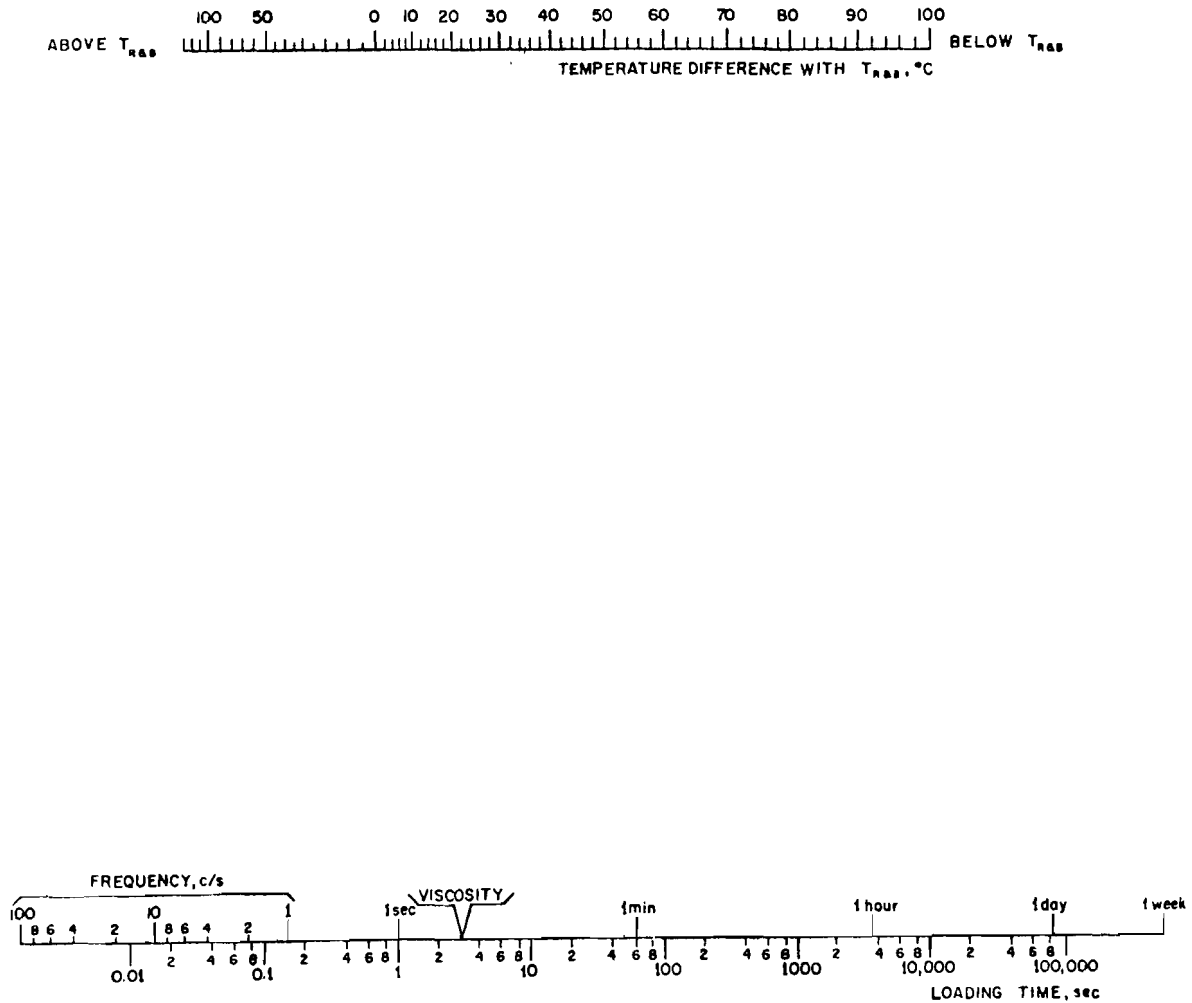
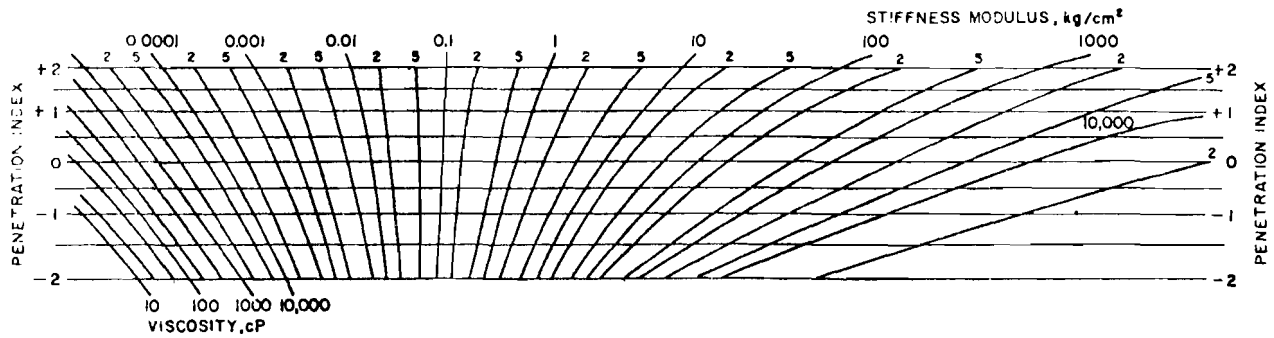


Fig 4.10. Nomograph for predicting the stiffness modulus of asphaltic bitumens (after Heukelom and Klomp, Ref 29).

Asphalt Concrete

Using the stiffness modulus of the asphalt cement, it is possible to determine the stiffness of the asphalt concrete mixture from the following relationship, also developed by Van der Poel (Ref 75) and later modified by Heukelom and Klomp (Ref 29):

$$S_{\text{mix}} = S_{\text{ac}} \left[1.0 + \left(\frac{2.5}{n} \right) \left(\frac{C_v}{1.0 - C_v} \right) \right]^n \quad (4.7)$$

where

$$n = 0.83 \log_{10} \left[\frac{4 \times 10^5}{S_{\text{ac}}} \right]$$

S_{mix} = stiffness of asphalt concrete mixture, in kg/cm^2 ,

S_{ac} = stiffness of asphalt cement, in kg/cm^2 .

The volume concentration of the aggregate in a mixture is defined as follows:

$$C_v = \frac{\text{volume of compacted aggregate}}{\text{volume of (asphalt + aggregate)}} \quad (4.8)$$

This equation can be replaced by an equivalent equation (4.9) by replacing the terms with values which can be measured in an asphaltic concrete core cut from a pavement or a compacted laboratory sample:

$$C_v = \frac{1}{1 + C} \quad (4.9)$$

where

$$C = \left(\frac{w_s}{w_g} \right) \times \left(\frac{G_g}{G_s} \right) = (\% \text{ asphalt by weight aggregate}/100) \left(\frac{G_g}{G_s} \right),$$

w_s = weight of asphalt,

w_g = weight of aggregate,

G_s = specific gravity of asphalt,

G_g = specific gravity of aggregate.

Equation 4.7 is applicable to well-compacted mixtures with about 3 percent air voids. For mixtures with air voids greater than 3 percent, Draat and Sommer (Ref 73) derived a correction to be applied to the C_v :

$$C'_v = \frac{C_v}{1 + H} \quad (4.10)$$

where

$$H = \text{actual air voids} - 0.03.$$

Several investigators have investigated the accuracy of the Van der Poel and Heukelom and Klomp nomographs. Pell and McCarty (Ref 55) reported that in the majority of cases stiffnesses computed by Van der Poel compared reasonably well with those measured on actual samples. Monismith (Ref 50) also checked laboratory determined stiffness values with both laboratory compacted samples and samples cut from in-service pavements. The results showed reasonable agreement with those determined from Heukelom and Klomp.

Van der Poel (Ref 74) also independently checked the accuracy of his nomograph and concluded that the difference in measured stiffness values of an asphalt and the stiffness obtained from the nomograph seldom exceeded a factor of 2.

SUMMARY

In this chapter, a summary of the methods available for characterizing the behavior of asphalt concrete mixtures has been presented. Out of the three methods presented, i.e., models, direct measurements, and indirect methods, Van der Poel's theory of indirectly estimating asphalt concrete stiffness will be utilized in the overall computerized system for predicting temperature cracking. This choice is based on the fact that Van der Poel's method can be fitted into the overall computerized system better than any of the other methods.

This page replaces an intentionally blank page in the original.

-- CTR Library Digitization Team

CHAPTER 5. APPLICATION TECHNIQUES FOR VAN DER POEL'S THEORY

The calculation of thermal stresses and fatigue distress in flexible pavements demands the estimation of many values of asphalt concrete stiffness at many temperatures, e.g., calculations of thermal stresses on an hourly basis for a single year will require the estimation of $360 \times 24 = 8640$ stiffness values. Therefore, the estimation of asphalt concrete stiffness should be in a form that can be solved using electronic computers. After a review of the literature and also personal contact with Van der Poel, it was found that no equation had been developed since the nomograph was first published in 1954. As a result, two techniques to estimate the asphalt concrete stiffness by using electronic computers were developed:

- (1) converting the nomograph to a computerized form, and
- (2) developing a predictive model through the use of regression techniques.

The details of development and use of each of the above techniques are discussed in the following two subsections.

CONVERTING VAN DER POEL'S NOMOGRAPH TO A COMPUTER FORM

Van der Poel's nomograph was converted to a computer form to provide a more rapid means of calculating asphalt stiffness. The nomograph is four-dimensional, i.e., it includes asphalt stiffness as the response plus three independent factors: time of loading, test temperature minus the asphalt softening point, and the penetration index. In order to simplify the problem, to make it three-dimensional instead of four, fixed levels of time of loading were selected. For each level of loading time, a similar mathematical form for predicting the asphalt stiffness was developed (Fig 5.1). The mathematical procedure can be expressed in the following steps.

Step A - Inputs

- (1) loading time levels;
- (2) temperatures at which stiffness is to be calculated;

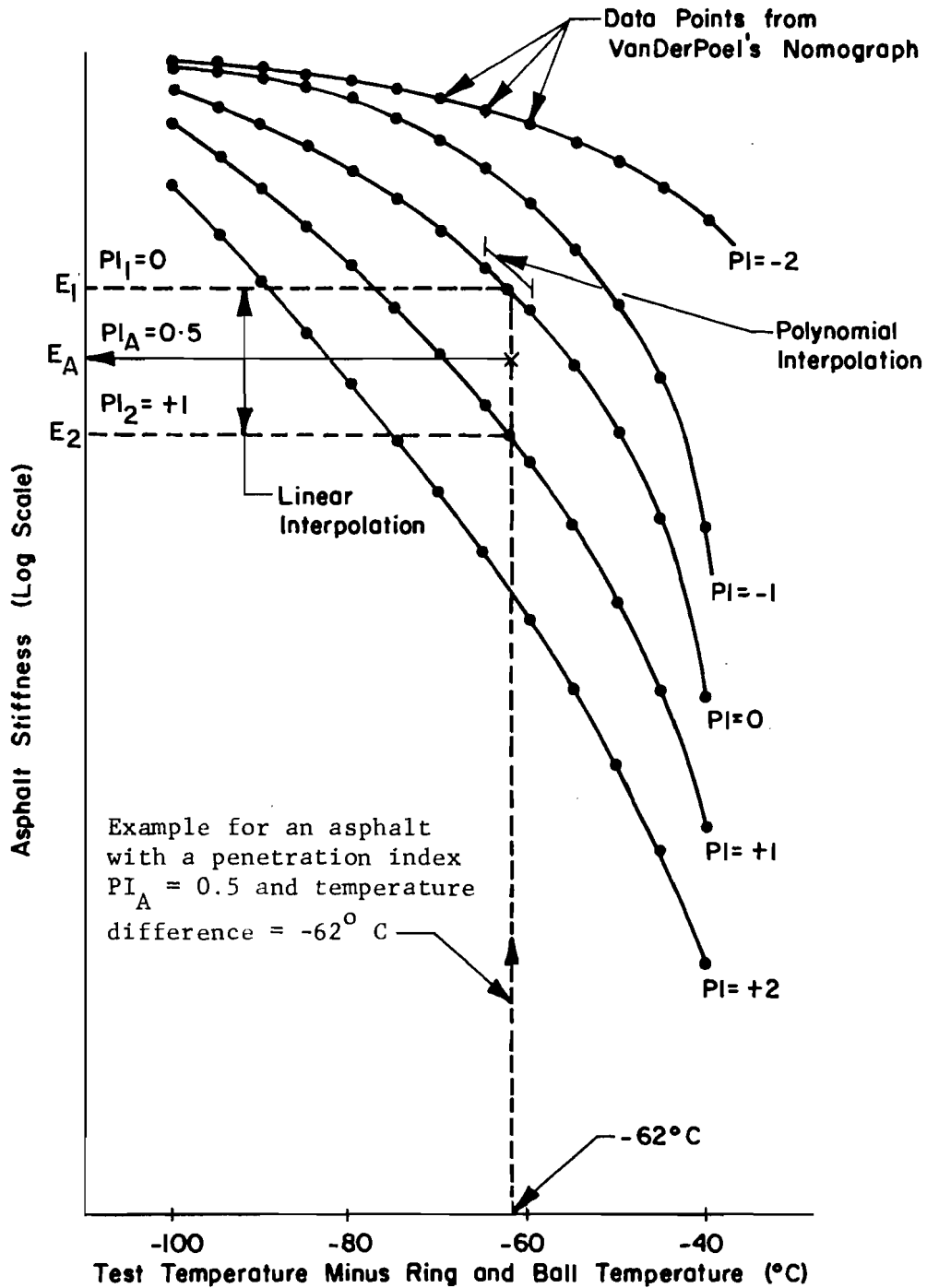


Fig 5.1. A schematic diagram showing the mathematical procedure for each time of loading, in converting Van der Poel's nomograph to a computer form.

- (3) asphalt penetration and softening point; and
- (4) volume concentration of the aggregate in the asphalt concrete mixture.

Step B - Mathematical Process

- (1) calculate the penetration index of the asphalt (PI_A);
- (2) find the closest two integer values of penetration indices to the calculated asphalt penetration index (PI_1, PI_2);
- (3) using each integer penetration index and the given temperature, polynomially interpolate the corresponding asphalt stiffness (E_1, E_2);
- (4) between the two stiffness values (E_1, E_2) linearly interpolate the asphalt stiffness corresponding to PI_A , (E_A);
- (5) from the asphalt stiffness (E_A), and the volume concentration of the aggregate estimate the asphalt concrete stiffness;
- (6) repeat 3, 4, 5 for each given temperature; and
- (7) repeat 2, 3, 4, 5, 6 for each level of time of loading.

Step C - Output

- (1) loading time,
- (2) asphalt penetration and softening point,
- (3) asphalt penetration index,
- (4) volume concentration of the aggregate, and
- (5) each temperature and the corresponding asphalt stiffness and asphalt concrete stiffness.

Using the above mathematical procedure, a computer program was developed to operate on the CDC 6600 computer, which is available at The University of Texas at Austin. Table 5.1 is an example output of the program.

Limitations to Using the Program

- (1) Only three levels of time of loading are available in the program: .01 sec, one hour, and a frequency of 8 cycles/sec (Dynalect). However, the program is written such that any other level of time of loading can be incorporated.
- (2) The range of temperature at which the stiffness can be estimated using the program is 70° C below to 70° C above ring and ball softening-point temperature.
- (3) If the penetration index is more than +2 or less than -2 (practical values), the program will give the stiffness for $PI = +2$ or -2 , respectively.

The program list and input guide are given in Appendix 2.

TABLE 5.1 TYPICAL COMPUTER OUTPUT OF THE PROGRAM DEVELOPED FOR ESTIMATING ASPHALT CONCRETE STIFFNESS, UTILIZING VAN DER POEL'S NOMOGRAPH.

TIME= 0.01 SECOND

PENETRATION= 91.000 PENT TEMP= 25.000 TEMP RING BALL= 47.200

PENT INDEX= -.40379 CV= .87000

TEMPERATURE DEG C	SBIT PSI	SMIX PSI
-6.7	7.2776E+04	3.4452E+06
-5.0	6.1027E+04	3.1825E+06
-1.7	4.3600E+04	2.7198E+06
11.1	1.0858E+04	1.3282E+06
18.9	3.3125E+03	6.7148E+05
21.7	2.1116E+03	5.1129E+05
23.3	1.6338E+03	4.3641E+05
23.9	1.4830E+03	4.1086E+05
19.4	3.0562E+03	6.3986E+05
12.2	9.3132E+03	1.2201E+06
5.0	2.3215E+04	1.9899E+06
-2.2	4.5795E+04	2.7842E+06

DEVELOPMENT OF THE REGRESSION EQUATIONS

There are several procedures available for selecting the variables of a regression model (Ref 16). The one selected was the stepwise regression method, since it was felt that this method provides the best selection of independent variables. The dependent variable was chosen as the \log_{10} of stiffness since the stiffness varies over many orders of magnitude. The independent variables that were selected were time of loading t , temperature of test - softening point temperature T , penetration index PI , $\log t$, $\log T + 101$, $\log PI + 3$, t^2 , T^2 , PI^2 , t^3 , T^3 , PI^3 , all two-way interactions of these variables, and other combinations of these factors which seemed theoretically reasonable.

As explained in Draper and Smith (Ref 16), the stepwise regression procedure starts with the simple correlation matrix and enters into regression the X independent variable most highly correlated with the dependent variable Y , \log_{10} (stiffness). Using partial correlation coefficients it then selects as the next variable to enter regression that X variable whose partial correlation with the response Y is highest, and so on. The procedure re-examines at every stage of the regression the variables incorporated into the model in previous stages (Ref 16). The program does this by testing every variable at each stage as if it entered last and checks its contribution by means of the partial F test.

The overall goals for the prediction equation were as follows:

- (1) The final equation should explain a high percentage of the total variation ($R^2 \geq 0.98$).
- (2) The standard error of the estimate should be less than 0.20 (this value being a log), to assure a small coefficient of variation.
- (3) All estimated coefficients should be statistically significant with $\alpha \leq .05$.
- (4) There should be no discernable patterns in the residuals.

Mathematical Models:

An attempt to characterize the entire nomograph with a single regression equation was first made. A large factorial grouping of data as shown in Table 5.2 was taken from the nomograph in Fig 4.10. The data represent time of loading from 10^{-2} to 10^5 seconds, PI from -2 to +2, and $T_{\text{test}} - T_{\text{R\&B}}$ from +50 to -100° C. After many attempts to obtain a suitable prediction equation which met the goals listed without being able to reduce the standard error of

TABLE 5.2 SUMMARY OF FACTORIAL DATA OBTAINED FROM HEUKELOM AND KLOMP'S NOMOGRAPH USED TO DERIVE REGRESSION EQUATIONS 5.1 AND 5.2 (VALUES IN KG/CM²)

Loading Time, seconds Penetration Index T test - TRB, °C		10 ⁻²	10 ⁻¹	10 ⁰	10 ¹	10 ²	10 ³	10 ⁴	10 ⁵
+50	-2	3.3E-3	4.0E-4	4.2E-5	5.0E-6	4.0E-7	7.0E-8	1.0E-8	1.0E-9
	-1	7.2E-3	9.5E-4	1.0E-4	1.1E-5	9.5E-7	1.0E-7	1.8E-8	2.0E-9
	0	1.3E-2	1.7E-3	2.0E-4	2.1E-5	2.0E-6	2.3E-7	3.0E-8	5.1E-9
	+1	2.0E-2	2.8E-3	4.0E-4	4.4E-5	4.0E-6	5.0E-7	5.1E-8	7.1E-9
	+2	2.7E-2	4.2E-3	5.7E-4	7.7E-5	5.5E-6	1.0E-6	6.1E-8	1.0E-8
+20	-2	1.3E-1	1.6E-2	1.8E-3	1.8E-4	1.8E-5	1.9E-6	1.9E-7	4.1E-8
	-1	2.0E-1	2.3E-2	2.9E-3	2.9E-4	3.0E-5	2.9E-6	2.9E-7	5.1E-8
	0	2.3E-1	3.0E-2	3.8E-3	4.1E-4	4.6E-5	5.0E-6	4.7E-7	7.1E-8
	+1	2.4E-1	3.5E-2	4.9E-3	5.7E-4	7.2E-5	7.0E-6	6.5E-7	1.0E-7
	+2	2.4E-1	4.1E-2	6.0E-3	8.5E-4	1.1E-4	1.1E-5	1.0E-6	2.0E-7
-10	-2	3.0E1	3.7E0	4.0E-1	4.4E-2	3.9E-3	4.6E-4	5.0E-5	5.0E-6
	-1	1.4E1	2.0E0	2.8E-1	3.4E-2	3.4E-3	4.0E-4	4.2E-5	4.6E-6
	0	7.7E0	1.4E0	2.2E-1	3.0E-2	3.0E-3	3.8E-4	4.2E-5	4.6E-6
	+1	5.0E0	1.1E0	1.9E-1	2.6E-2	2.9E-3	4.0E-4	5.0E-5	4.7E-6
	+2	4.0E0	9.0E-1	1.6E-1	2.4E-2	3.0E-3	4.6E-4	6.0E-5	5.0E-6
-40	-2	1.2E4	5.0E3	1.4E3	2.2E2	2.2E1	2.5E0	3.5E-1	3.7E-2
	-1	1.7E3	5.7E2	1.9E2	3.8E1	4.9E0	6.0E-1	8.0E-2	8.5E-3
	0	5.7E2	2.1E2	6.0E1	1.1E1	1.9E0	2.5E-1	4.0E-2	4.5E-3
	+1	2.5E2	8.5E1	2.5E1	4.9E0	1.0E0	1.6E-1	2.3E-2	3.0E-3
	+2	1.02E2	3.9E1	1.15E1	3.2E0	6.0E-1	1.1E-1	1.7E-2	2.0E-3
-70	-2	2.6E4	2.3E4	2.0E4	1.8E4	1.7E4	1.3E4	5.6E3	1.4E3
	-1	2.0E4	1.6E4	1.2E4	6.7E3	2.4E3	1.0E3	3.0E2	7.0E1
	0	1.1E4	7.0E3	3.7E3	1.6E3	6.0E2	2.3E2	6.2E1	1.1E1
	+1	5.1E3	2.3E3	1.35E3	5.0E2	2.0E2	6.5E1	1.7E1	3.5E0
	+2	2.1E3	1.05E3	5.0E2	1.9E2	7.0E1	2.2E1	6.7E0	1.7E0
-100	-2	3.3E4	3.2E4	3.10E4	3.0E4	2.9E4	2.6E4	2.4E4	2.1E4
	-1	3.1E4	2.9E4	2.8E4	2.5E4	2.2E4	1.9E4	1.7E4	1.2E4
	0	2.7E4	2.5E4	2.1E4	1.9E4	1.4E4	1.1E4	5.5E3	2.3E3
	+1	2.2E4	1.9E4	1.3E4	9.0E3	6.0E3	3.2E3	1.6E3	7.0E2
	+2	1.5E4	1.0E4	6.1E3	4.9E3	2.4E3	1.1E3	5.0E2	1.9E2

the estimate to an acceptable level, it was decided to split the nomograph into two parts and fit a separate equation to each part. Almost all of the stiffness values of practical significance to a pavement design engineer are greater than 10 kg/cm^2 of the asphalt cement. This is approximately 400 kg/cm^2 for a mix with C_v of 0.86, which equals about 5700 psi. Therefore, a regression equation was derived using the data in Table 5.2 with stiffness values greater than 10 kg/cm^2 and another regression equation was built using all data that had stiffness values less than 10 kg/cm^2 . Acceptable prediction equations were then obtained for each portion of the data which met all of the goals set for the regression equations.

The following equations were obtained with the corresponding statistics:

- (1) Stiffness from 10^{-7} to 10^1 kg/cm^2

Prediction model:

$$\begin{aligned} \log_{10} S = & -1.35927 - 0.06743(T) - 0.90251 \log(t) + 0.00038(T^2) \\ & - 0.00138 (T \times \log t) + 0.00661 (PI \times T) \end{aligned} \quad (5.1)$$

where

T = temperature of test minus temperature R&B ($^{\circ} \text{C}$);

t = time of loading, second; and

PI = penetration index (Eq 4.5).

Corresponding statistics:

$$R^2 = 0.99$$

$$\text{Standard error of estimate} = 0.1616$$

$$n = 126 \text{ data points}$$

Range of factors:

$$PI: -2 \text{ to } +2$$

$$T: +50 \text{ to } -100^{\circ} \text{ C}$$

$$t: 10^{-2} \text{ to } 10^5 \text{ seconds}$$

(2) Stiffness from 10 to 20,000 kg/cm²

Prediction model:

$$\begin{aligned} \log_{10} S = & -1.90072 - 0.11485(T) - 0.38423(PI) - 0.94259 \log(t) \\ & - 0.00879(T \times \log t) - 0.05643(PI \times \log t) - 0.02915(\log t)^2 \\ & - 0.51837 \times 10^{-3}(T^2) + 0.00113(PI^3 \times T) \\ & - 0.01403(PI \times T^3) \times 10^{-5} \end{aligned} \quad (5.2)$$

Corresponding statistics:

$$R^2 = 0.98,$$

$$\text{Standard error of estimate} = 0.1638,$$

$$n = 79 \text{ data points.}$$

Range of factors:

$$PI: -1.5 \text{ to } +2.0$$

$$T: +50 \text{ to } -100^{\circ} \text{ C}$$

$$t: 10^{-2} \text{ to } 10^5 \text{ seconds}$$

To verify the model, stiffness values were obtained from the nomograph and plotted against the stiffness as calculated from Eqs 5.1 and 5.2. The results are shown in Figs 5.2 and 5.3, which indicate that the models are reliable.

The following guidelines are given with regard to using the prediction equations to predict asphalt stiffness:

- (1) Use Eq 5.1 to predict stiffnesses from 10^{-7} to 10 kg/cm², and use Eq 5.2 to predict stiffnesses from 10 to 2×10^4 kg/cm². The user should not employ predictions that fall outside of these limits.
- (2) The ranges given for T, t, and PI should not be exceeded. It was found that Eq 5.2 values of stiffness obtained when the PI was -2 were not accurate enough, so the equation is limited to PI of -1.5 or greater.

Equations 5.1 and 5.2 can be utilized to estimate the asphalt concrete stiffness using Eq 4.7.

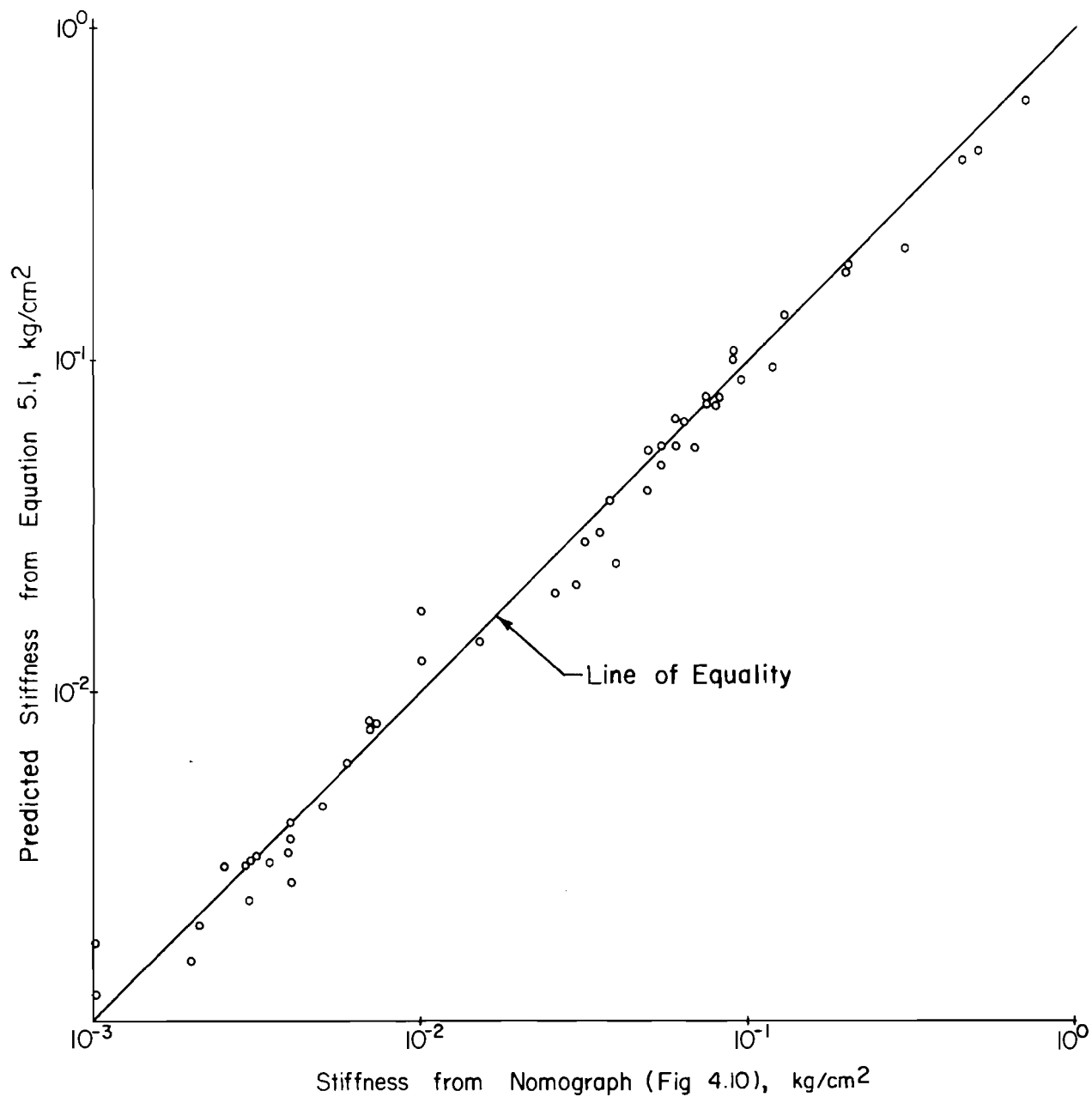


Fig 5.2. Comparison of stiffness of asphalt obtained manually from nomograph (Fig 4.10) to stiffness of asphalt predicted from regression equation 5.1 (for stiffness values from 10^{-3} to 10^0 kg/cm²).

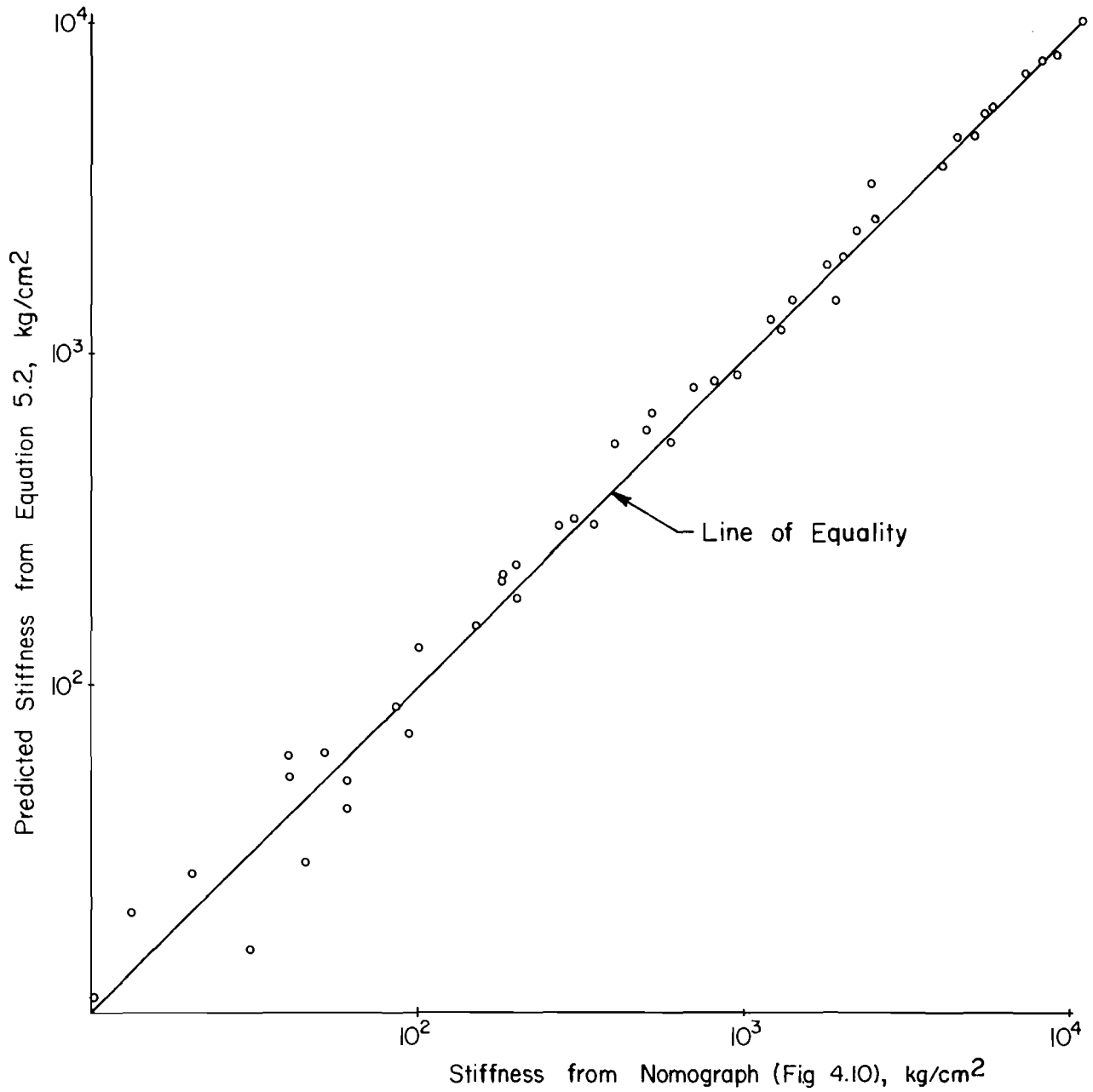


Fig 5.3. Comparison of stiffness of asphalt obtained manually from nomograph (Fig 4.10) to stiffness of asphalt predicted from regression equation 5.2 (for stiffness values from 10 to 10⁴ kg/cm²).

SUMMARY

Two techniques have been established to computerize the nomograph originally developed by Van der Poel (Ref 74):

- (1) converting the nomograph to a computerized form, and
- (2) developing predictive models through the use of regression.

The first technique is accurate (as compared with the nomograph); however, it is limited in use to three times of loading. The technique can be extended to other times of loading with little difficulty.

The second technique is more flexible than the first one since it covers the practical ranges of all the variables; however, it is less accurate (as compared with the nomograph).

Both techniques are utilized in the overall computerized system presented in Chapter 10.

This page replaces an intentionally blank page in the original.

-- CTR Library Digitization Team

CHAPTER 6. IN-SERVICE AGING OF ASPHALTS

Change in asphalt concrete mixture properties as a pavement ages is one of the important causes of flexible pavement deterioration. The ingredients of asphalt concrete mixtures are asphalt and aggregate. Since aggregate properties experience almost no variation with time, the variation of mixture properties can be reasonably attributed to the hardening and oxidation of the asphalt.

In the previous chapter, a model was developed to estimate the stiffness of asphalt, given its penetration, softening point, time of loading, and temperature.

In this chapter, the histories of penetration and softening point with time are investigated and models to estimate the aging effect are developed. The intention is to use these models in conjunction with the asphalt stiffness model to estimate asphalt stiffness of in-service, asphalt concrete mixtures as a function of temperature and age (time).

Three physical tests were used to develop the aging models:

- (1) penetration (ASTM Designation D5-65),
- (2) softening-point (ASTM Designation D36-66T), and
- (3) thin-film oven test (ASTM Designation D1754).

SOURCES OF DATA USED IN DEVELOPING THE ASPHALT AGING MODELS

In developing the models, a stepwise regression computer program (Ref 66) was used. An extensive search was conducted for projects all over the United States where asphalt hardening studies had been conducted. The data from these projects were difficult to correlate and utilize since different asphalt properties were measured on each one. Several variables were considered but not used in the final models. These variables and the reasons for not using them are discussed in a separate section at the end of this chapter. The locations and the references used in developing the penetration and the softening-point aging models are given below:

(1) penetration

California - Refs 35, 62, 63, and 80;

Delaware - Ref 40;

Utah - Refs 3 and 42; and

Pennsylvania - Ref 24.

(2) softening-point

California - Refs 35, 62, 63, and 80; and

Delaware - Ref 40.

PENETRATION AGING MODEL

The purpose of developing the model is to predict the penetration of the in-service asphalt (at any time after construction) from the ordinary laboratory measurements. An acceptable prediction equation was obtained using the stepwise regression technique. The following is the equation with the corresponding statistics:

$$\begin{aligned} \text{Pen}(\text{time}) = & -48.258 - 2.561 \sqrt{\text{Time}} + .1438(\text{OPEN}) \\ & - 8.466 (\text{VOID})(\text{XTIME}) + 1.363 (\text{TFOT}) \\ & + 0.9225 (\text{OPEN})(\text{XTIME}) \end{aligned} \quad (6.1)$$

where

time = time from placement of the asphalt concrete mixture, in months;

XTIME = $1./(\sqrt{\text{TIME}} + 1.)$;

OPEN = original penetration (100 grams, 5 seconds, 77^o F);

VOID = initial percent voids in the asphalt concrete mixture (preferably after mixture placement and compaction);

TFOT = thin-film oven test, percent of original penetration.

Corresponding statistics:

Number of cases	93
Number of variables in the model	5
Mean of the dependent variables (penetration)	49.5
Standard error for residuals	13.1
Coefficient of variation	26.51
Multiple R	.922
Multiple R ²	.85

Limitations of Model Application

This model is valid only for the following ranges of the different variables:

Time	1 - 100 months
Original penetration	60 - 240
Percent voids	3.8 - 13.6
TFOT (original penetration < 100)	55 - 70
(original penetration 100 - 175)	45 - 70
(original penetration > 175)	30 - 70

Table 1 of Appendix 3 gives the data that were used in developing the model.

Discussion of the Model

The model explains 85 percent of the variability of the dependent variable (penetration). An important point is that the variations of the dependent variable are those in the 93 cases used to predict the model. However, since the 93 cases represent different projects at different locations, it can be concluded that the model is satisfactory for practical purposes.

Also, the model shows a coefficient of variation of 26.5 percent (standard error of residuals/mean of the penetration). This value which appears to be high, resulted not only from a lack of fit but also from unexplained errors (measurement errors, human variations, replications, etc.). Welborn (Ref 78) reported that in some projects where the mean penetration was 46.7, the standard deviation reached 17.6, which gives a coefficient of variation of about 38 percent.

Figure 6.1 illustrates the relationship between estimated and measured values of penetration for the 93 cases used to develop the model. The effect of the variation of each of the independent factors in the model (Eq 6.1) is discussed in the following subsections.

Original Penetration. With both the initial voids (9 percent) and the TFOT (60 percent) as constants, the decrease of penetration with time for five different original penetration values is as shown in Fig 6.2. From the figure, the following observations can be made:

- (1) the higher the original penetration, the higher the rate of initial hardening (Fig 6.2a);
- (2) the rate of hardening decreases considerably with time for all values of original penetration (Fig 6.2a); and
- (3) the penetration at a given time is a linear function of the original penetration (Fig 6.2b).

Voids. Based on an original penetration of 100 and a TFOT of 60 percent, the effect of five levels of voids on asphalt hardening is as shown in Fig 6.3, which indicates that the amount of hardening is larger for higher percentage voids. Vallerga and Halstead (Ref 72) concluded that in pavements with less than 2 percent voids, aging appeared to be negligible, and that above this level, hardening increased with increased air voids.

Thin-Film Oven Test (TFOT). Field observations have shown a direct correlation between the percent of original penetration from the TFOT and the percent of original penetration after field mixing (Fig 6.4). In addition, laboratory results from different asphalts have shown that the higher the original penetration, the lower the percentage of original penetration after the TFOT. Therefore, the developed penetration model was used to analyze the behavior of two different asphalts having different original penetrations under different TFOT percentages (Fig 6.5). As expected, more hardening occurred during the mixing process for asphalts exhibiting a lower percentage of original penetration after the TFOT.

SOFTENING-POINT AGING MODEL

The purpose of this model is to predict the softening point of the in-service asphalt (any time after construction) from the ordinary laboratory measurements. An acceptable prediction equation was obtained using the

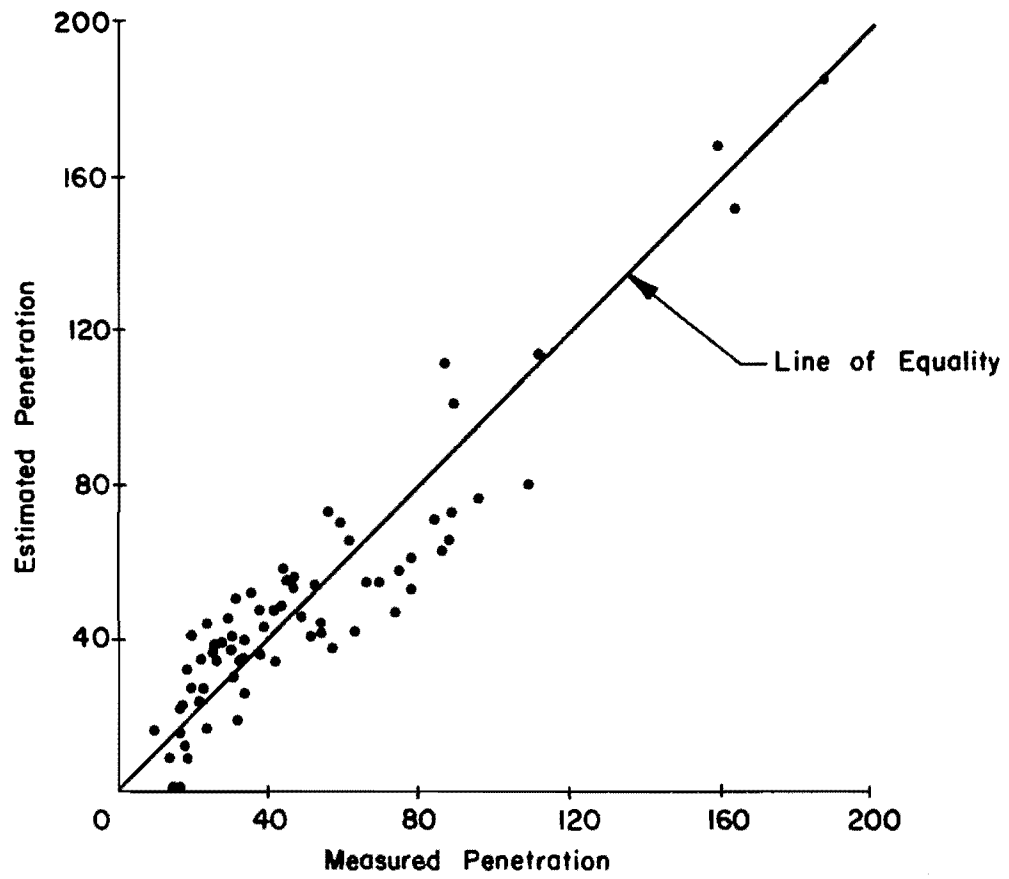
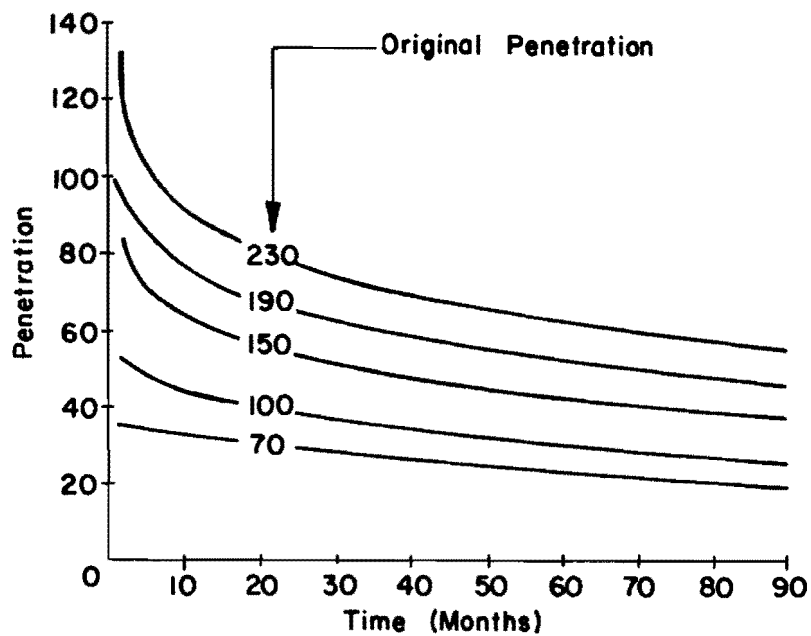
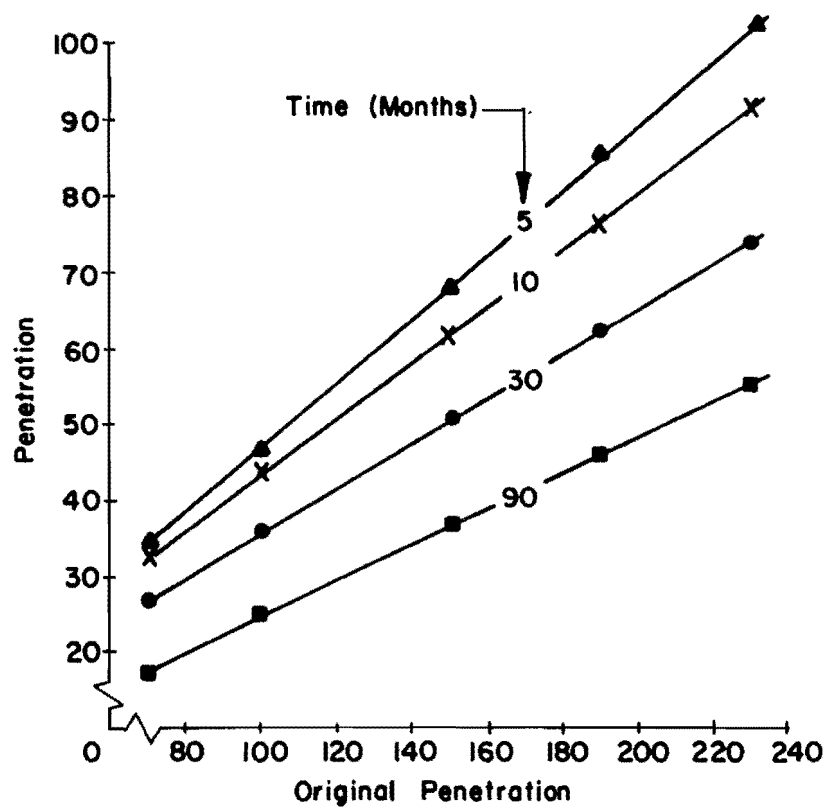


Fig 6.1. Measured in-service penetration versus predicted values from the penetration model.



(a) Penetration (time) versus time.



(b) Penetration (time) versus original penetration.

Fig 6.2. The effect of original penetration on the in-service values of penetration as predicted from the penetration model (voids = 9 percent, TFOT = 60 percent).

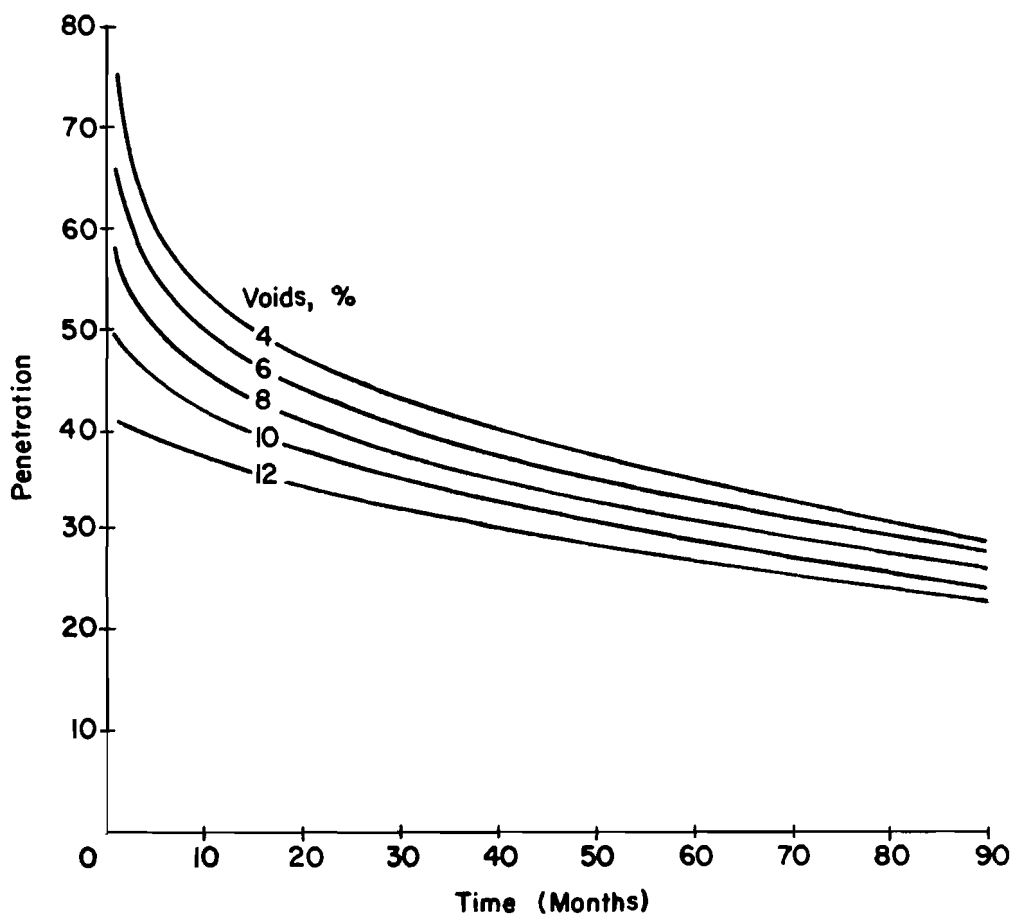


Fig 6.3. The effect of air voids on the in-service values of penetration as predicted from the penetration model (original penetration = 100, TFOT = 60 percent).

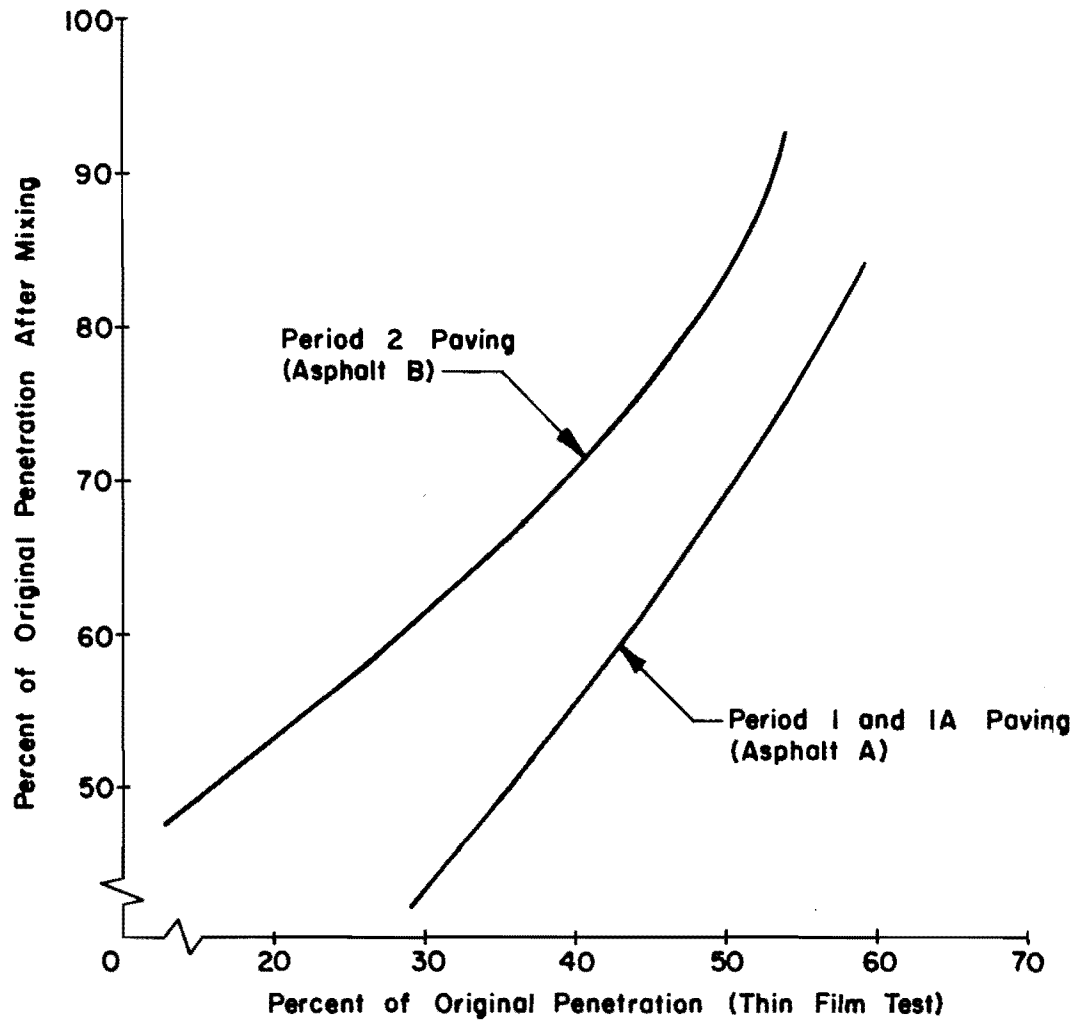
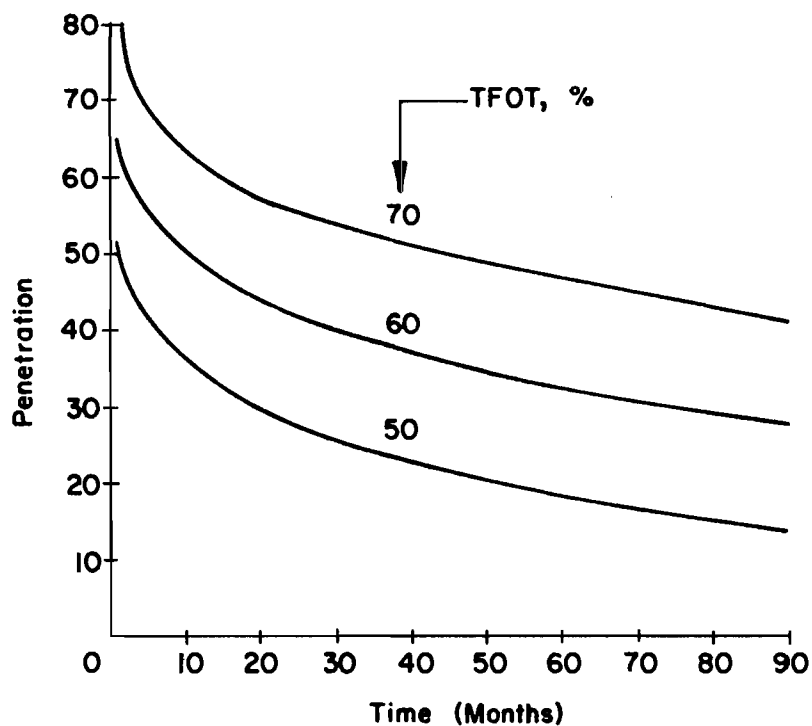
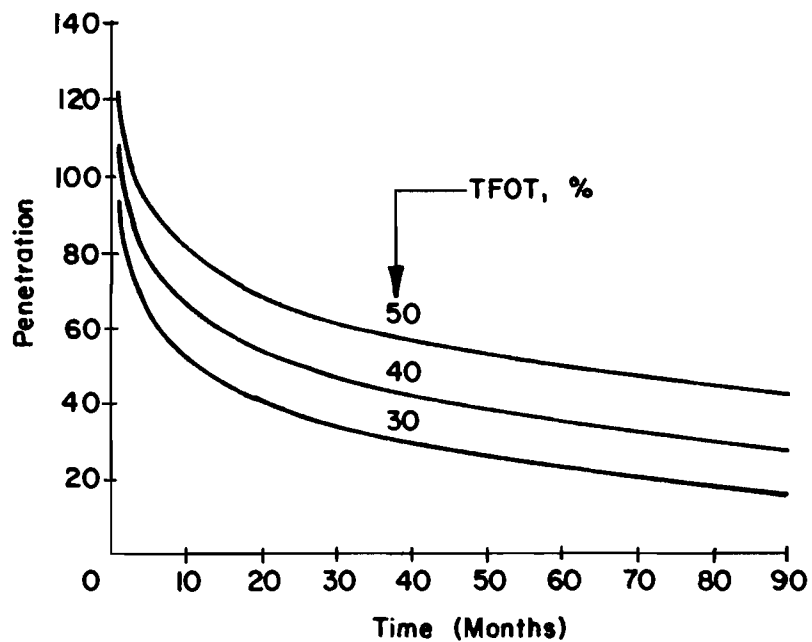


Fig 6.4. Relation between hardening in field mixer and thin film test (after Hveem et al, Ref 35).



(a) Original penetration = 100, voids = 6 percent.



(b) original penetration = 230, voids = 8 percent.

Fig 6.5. The effect of thin film oven test (percent of original penetration) on the in-service values of penetration as predicted from the penetration model.

stepwise regression technique. The following is the equation with the corresponding statistics:

$$\text{TRB}(\text{TIME}) = -4.632 + 3.162\sqrt{\text{TIME}} + 1.585(\text{ORB}) - .93(\text{TFOT}) \quad (6.2)$$

where

TIME = time from placement of the asphalt concrete mixture, in months;

ORB = original ring and ball temperature, ° F; and

TFOT = percent of original penetration, thin-film oven test.

Corresponding statistics:

Number of cases	49
Number of variables in the model	3
Mean of the dependent variable	134.4
Standard error for residuals	4.8
Coefficient of variation (percent)	3.6
Multiple R	.93
Multiple R ²	.87

Limitations of Model Application

This model is valid only for the following ranges of the different variables:

Time	1 - 100 months
Original R&B	99 - 125° F
TFOT (percent)	30 - 70

Table 2 of Appendix 3 gives the data used to predict the model.

Discussion of the Model

With only three variables in the model the multiple $R^2 = .87$ indicates that the model is satisfactory. This indicates that the model explains 87 percent of the variability of the 49 cases used to predict the model. It can be seen that the voids did not enter the final model, which can be explained by the fact that the 49 cases have percent voids that are relatively high. A plot of measured versus estimated values of the softening point for the 49 cases used to predict the model is shown in Fig 6.6.

So that the behavior of the model for different values of each factor in the mathematical equation (original softening point and TFOT) could be studied, the model was computerized and the factors were varied one at a time with the others held constant. Figure 6.7 shows the increase of softening point with time for three different original softening points (100, 110, and 120) and a constant value of TFOT (60 percent). Figure 6.8 shows the same concept for three different values of TFOT (40, 50, and 60) and a constant initial softening point (110^o F).

FACTORS CONSIDERED BUT NOT USED IN THE FINAL MODELS

For different reasons, several variables were considered but not used in the final penetration and softening-point aging models. A summary of these factors is given below.

- (1) Climatology factors -
 - (a) solar radiation on an annual basis,
 - (b) wind velocity,
 - (c) number of days with temperature > 90^o F,
 - (d) average annual temperature, and
 - (e) average annual daily range of temperatures.

The most significant environmental variable that showed a high correlation with asphalt hardening was the solar radiation. However, due to the limited number of geographical locations, it was decided not to include it in the final models, but it should be considered in future investigations.

- (2) Inverse gas-liquid chromatography (IGLC) -

IGLC is a new technique developed by Davis, Peterson, and Haines (Ref 14). In this test, the asphalt is adsorbed on the surface of an inert support and placed in a chromatography column. Different chemical test compounds are injected individually into the column. Based on the retention time for a nonreactive material of the same molecular weight as the test compound, a parameter known as the interaction coefficient (Ip) is computed. High values of Ip indicate a high reaction of the test compound with the asphalt.

An extension of this technique was introduced by Davis and Peterson (Ref 13). The extension suggests oxidation of the asphalt

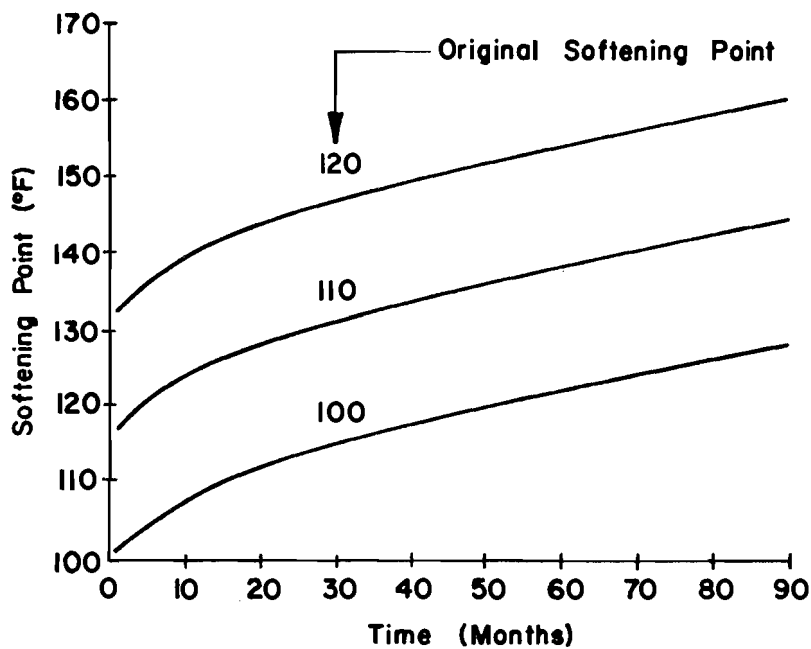


*
Fig 6.7. The effect of original softening point on the in-service values of the softening point as predicted from the softening point model (TFOT = 60 percent).

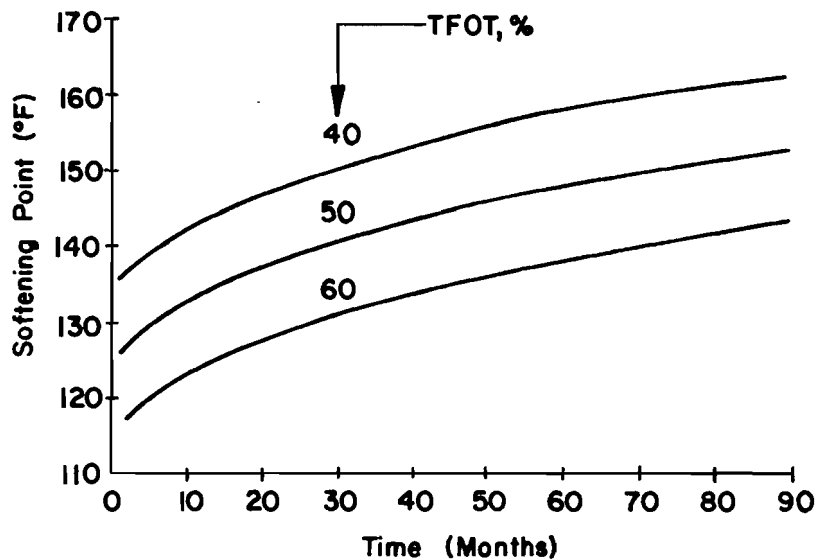


Fig 6.8. The effect of thin film oven test (percent of original penetration) on the in-service values of the softening point as predicted from the softening point model (original softening point = 110° F).

in the chromatography column before the chemical test compounds were injected.

In developing both asphalt hardening models (penetration and softening-point), I_p resulting from injecting phenol into oxidized asphalt showed extremely high correlation with asphalt hardening. Gietz and Lamb (Ref 22) concluded that in correlation with pavement performance, the most significant relationship was found in the values of I_p with the test compound phenol, when the I_p values of oxidized samples were compared with those values before oxidation. The IGLC test values were not included in the final aging models because of the shortage of test locations where the test was performed. The IGLC is believed to hold a promise for improved prediction of asphalt hardening and thus should be given attention in future research studies.

(3) Asphalt components -

The five components of asphalt are asphaltenes (A), nitrogen bases (N), first acidaffins (A1), second acidaffins (A2), and paraffins (P). The ratio $(N + A1)/(P + A2)$ was proposed by Rostler to express the ratio between the more reactive components to the less reactive ones. None of the variables showed a significant correlation with asphalt hardening (penetration and softening-point). Gotolski, Ciesielski, and Heagy (Ref 24) concluded the following about asphalt components:

"In the overall picture, the asphaltene content or that of any of the other single components does not determine the performance of asphalts."

(4) Percentage asphalt -

The percentage of asphalt in the asphalt concrete mixture showed a correlation with asphalt hardening whenever it was considered by itself, i.e., without considering the effect of the percentage of air voids in the mixture. However, whenever the percentage of voids enters the models, the percentage of asphalt loses its significance. This is logical since the percentage of voids and percentage of asphalt are known to be related to each other.

(5) Asphalt viscosity -

Viscosity is not included in final aging models because asphalt viscosities were determined under different conditions for all the projects used to develop the models, and it was difficult to match the viscosity results from all the projects. A specific viscosity test and test conditions should be established and specified for future studies.

(6) Penetration index -

The penetration index suggested by Pfeiffer and Van Doermall (Ref 56) correlated with asphalt hardening. However, due to the limited range of the penetration indices reported in the different projects, this factor was omitted from the final models.

SUMMARY AND CONCLUSIONS

In this chapter, two asphalt aging models were developed, one for penetration and the other for the softening point. Both models will be used in conjunction with the asphalt stiffness model (Chapter 5) to estimate the asphalt stiffness as a function of age (time).

The factors that were used in the aging models were the original values of each dependent factor, time from mixture placement, TFOT (percentage penetration), and percentage of voids in the asphalt concrete mixture. Several other factors were considered but not included for various reasons. One of these factors is the inverse gas-liquid chromatography test with phenol as the chemical test compound. This factor showed an excellent correlation with asphalt hardening and should be considered for further application and research.

This page replaces an intentionally blank page in the original.

-- CTR Library Digitization Team

CHAPTER 7. ESTIMATION OF THERMAL STRESSES

Temperature cracking, as described in Chapter 2, usually takes the form of transverse cracking, with spacing ranging from 5 feet to several hundred feet. Since the pavement surface is subjected to lower temperatures and greater daily temperature ranges than any other depth (Fig 7.1), it appears that temperature cracks usually start at the surface. Instrumentation at the Ste. Anne Test Road (Refs 5, 15, and 79) indicated that most of the cracks started at the surface of the pavement. The following conclusion is from the Ste. Anne Road test (Ref 5):

"Initial cracking appears to be initiated mainly at the pavement surface at a time when the surface temperature is close to the minimum on a given day."

As a result, the model for estimating the thermal stresses was developed with this conclusion in mind.

THE STRESS MODEL

Theory

The thermal stresses that develop in the surface layer of a flexible pavement, i.e., asphalt concrete, can be estimated by several different approaches. Some of these approaches are rigorous and time-consuming. However, the aim is not sophisticated mathematics but an approach that yields an acceptable estimation of the thermal stresses.

The stress-strain relationship for the asphalt concrete can be expressed by the stiffness modulus presented by Van der Poel (Ref 74):

$$S(t, \bar{T}_{\Delta}) = \frac{\Delta\sigma(t, \Delta T)}{\Delta\epsilon(\Delta T)} \quad (7.1)$$

where

$$S(t, \bar{T}_{\Delta}) = \text{asphalt concrete stiffness at a given time of loading } t \text{ and the mean value of a temperature interval } \Delta T ;$$

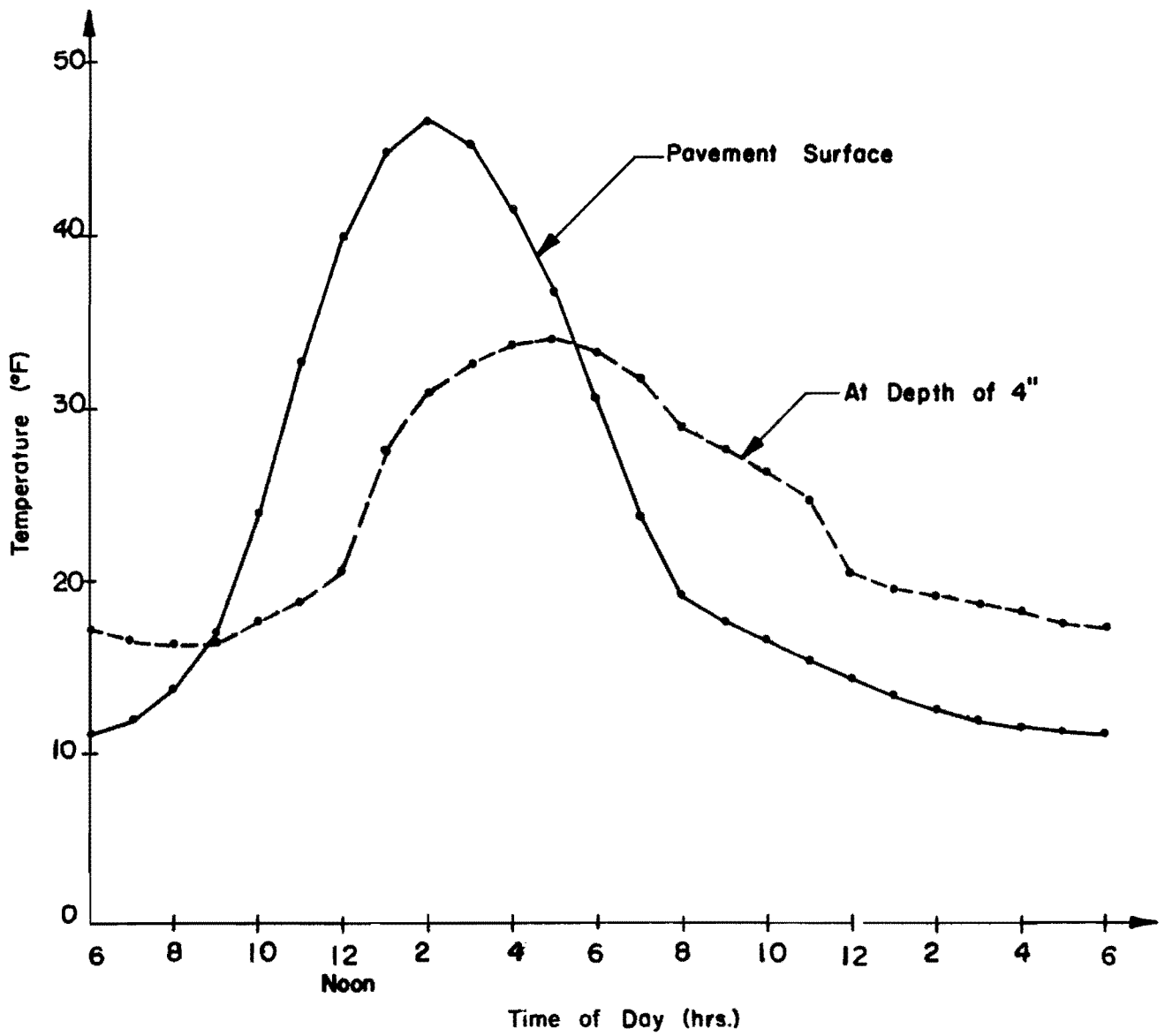


Fig 7.1. Comparison between pavement temperatures at the surface and a depth of 4 inches.

- $\Delta\sigma(t, \Delta T)$ = the increase in a thermal stress for a given time of loading t and a temperature interval of ΔT ; and
- $\Delta\epsilon(\Delta T)$ = the increase in a thermal strain in a temperature interval ΔT .

The thermal strain can be easily estimated if the thermal coefficient of contraction is known:

$$\Delta\epsilon(\Delta T) = \alpha(\bar{T}_{\Delta}) \times \Delta T \quad (7.2)$$

where

$$\alpha(\bar{T}_{\Delta}) = \text{thermal coefficient of contraction of the asphalt concrete at the mean value of the temperature interval } \Delta T .$$

From Eqs 7.1 and 7.2, the increase in thermal stress can be expressed as follows:

$$\Delta\sigma(t, \Delta T) = S(t, \bar{T}_{\Delta}) \times \alpha(\bar{T}_{\Delta}) \times \Delta T \quad (7.3)$$

Utilization of the Theory in Practice

In order to utilize the above theory in actual development of a model for use in estimating thermal stresses in the surface layer, i.e., asphalt concrete, the following assumptions were made:

- (1) The surface layer is fully restrained.
- (2) The surface slab behaves as an infinite beam.
- (3) The contribution of the lateral restraint (by the supporting layers) to the developed longitudinal thermal stresses is negligible.
- (4) At the end of each daily temperature cycle, the stress and strain are negligible (Fig 7.2). Estimation of induced thermal stresses in asphalt concrete pavements by Christison et al (Ref 9) supports the above hypothesis.
- (5) The maximum daily stress occurs at the minimum daily pavement temperature as a result of accumulation of thermal stress increments during the day.

Figure 7.2 is a schematic diagram of pavement temperatures, strains, stiffnesses, and stresses during a single day. For the calculations, the accumulation of thermal stresses can be expressed as follows:

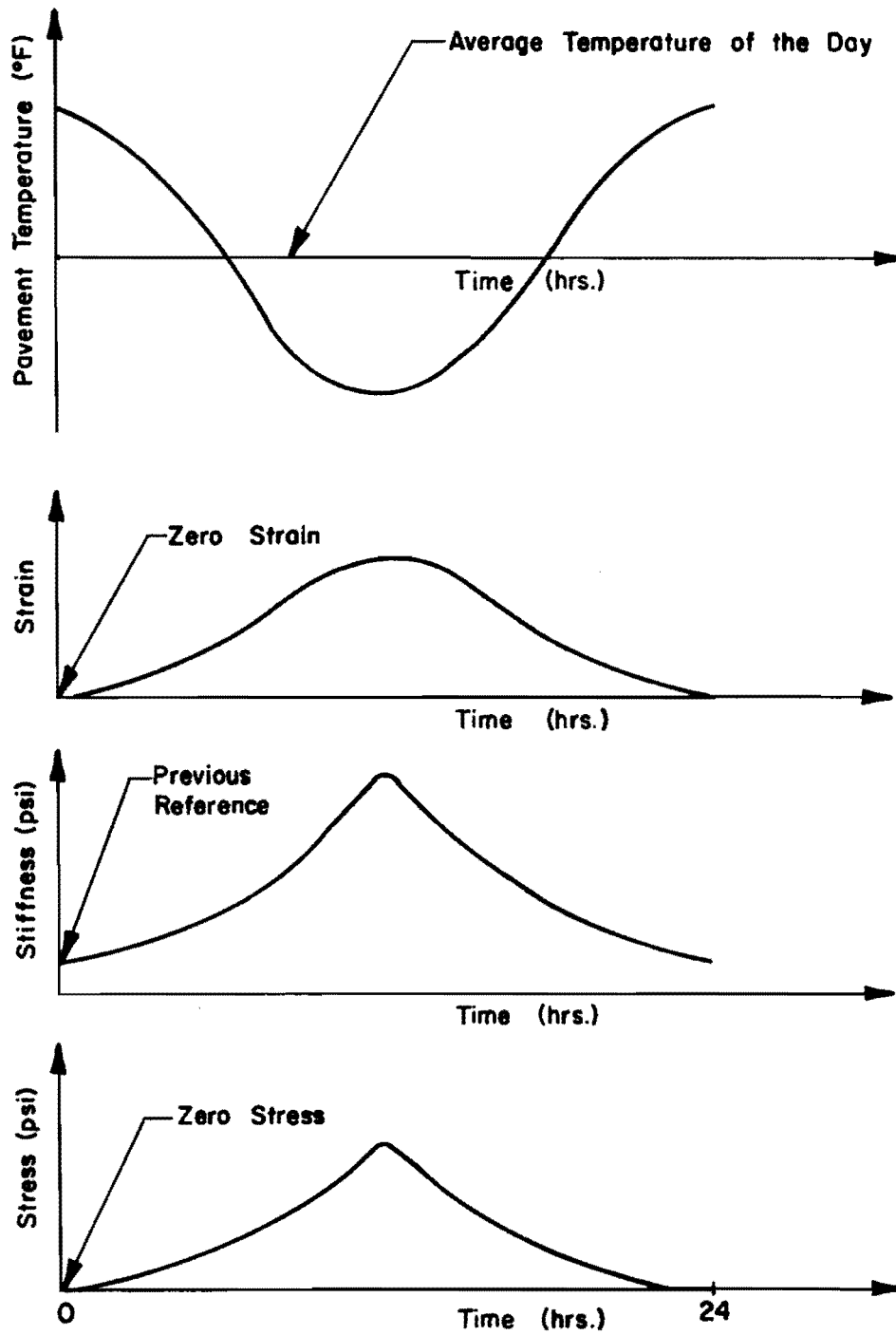


Fig 7.2. A schematic diagram showing the assumed behavior of pavement strain, stiffness, and stress during a normal day.

$$\sigma(t, T) = \sum \alpha(\bar{T}_{\Delta}) \times (\Delta T) \times S(t, \bar{T}_{\Delta}) \quad (7.4)$$

However, if α is assumed to be constant all over the temperature range, Eq 7.4 can be expressed as follows:

$$\sigma(t, T) = \bar{\alpha} \sum (\Delta T) \times S(t, \bar{T}_{\Delta}) \quad (7.5)$$

where

$\bar{\alpha}$ = average coefficient of thermal contraction of the asphalt concrete over the entire range of temperature it is subjected to.

Equation 7.5 was also presented by Hills and Brien (Ref 31) and has been used by others. Studies have shown good agreement between predicted and measured thermal stresses.

THERMAL LOADING TIME FOR ESTIMATING ASPHALT STIFFNESS

Asphalt stiffness is partly dependent on the loading time. For traffic, the loading time can be physically measured or estimated, but as far as temperature is concerned, the thermal loading time has been a question to be answered by engineering judgment. Most engineers have considered the thermal loading time as the time corresponding to the temperature interval ΔT used for calculating the thermal stresses (Eq 7.4). However, it is believed that thermal loading time depends mainly on the rate of temperature drop and the asphalt concrete mixture properties. To illustrate this hypothesis, the experimental work performed by Monismith et al (Ref 52) has been utilized. In this experiment, an asphalt concrete beam was subjected to a temperature drop and the developed thermal stresses were measured. The properties of the mixture are listed in Table 7.1. In this table, the penetration and the softening point are those of the asphalt before the mixing process.

Performing the calculations with only these values is meaningless. However, the recovered properties of asphalt were estimated to be as follows:

Penetration at 77 ^o F, 100 gm, 5 sec	31
Softening point, ring and ball, ^o F	132

TABLE 7.1. PROPERTIES OF THE ASPHALT CONCRETE MIXTURE

Penetration at 77°F, 100 gm., 5 seconds	96
Softening point, ring and ball, °F	110
Percent asphalt by weight of aggregate	5.1%
Average density of the compacted specimens	152 lb/ft ³
Average thermal coefficient of contraction	$1.35 \times 10^{-5}/^{\circ}\text{F}$

TABLE 7.2. CALCULATED THERMAL STRESSES, PSI

(Temperature drop 75-35°F,
period of 4500 seconds)

Temperature Interval, °F	10	100	1000
0.04	96.51	34.02	7.18
.4	96.43	34.08	7.25
4.0	96.67	33.55	7.42
5.0	95.72	32.94	7.91
8.0	95.95	33.19	4.91
10.0	94.61	34.06	4.81
20.0	93.16	32.54	4.11
40.0	75.73	11.06	2.37

The specimens were subjected to a temperature drop from 75 to 35° F. In order to simplify the calculations, the temperature drop was assumed to be linear (Fig 7.3). A factorial experiment was then designed for the estimation of thermal stresses under different conditions of loading time and temperature intervals (Table 7.2). A computer program was written (Appendix 4) utilizing the stiffness regression models developed in Chapter 5. Figure 7.4 is a plot of the results of the calculations. The figure seems to indicate the following conclusions:

- (1) A temperature interval as large as 20° F will result in an acceptable estimation of the thermal stresses.
- (2) The choice of the appropriate loading time is more important than the temperature interval.

With the importance of the above conclusions in mind, a more rational approach for estimating the actual thermal loading time was developed and is summarized below.

A Suggested Method for Estimating the Time of Thermal Loading

- (1) From Weather Service reports and Model I (see Chapter 3), estimate the average rate of daily pavement temperature drop.
- (2) Experimentally determine the developed thermal stresses in an asphalt concrete beam in a reasonable period of time (2 hours) by subjecting it to the rate of temperature drop estimated in Step 1. This can be performed by putting the asphalt concrete beam in an environmental chamber in the laboratory and using the technique described by Monismith et al (Ref 52) or Tuckett et al (Ref 71) or any similar technique.
- (3) Using different loading times, calculate the developed thermal stress for the same temperature conditions (Step 2).
- (4) Plot the relationship between the loading time and the corresponding thermal stress for the tested asphalt concrete mixture.
- (5) By locating the measured thermal stress (Step 2) on the graph (Step 4), find the actual thermal loading time.

The application of the method for the previous example is shown in Fig 7.5. The thermal stresses were calculated on the computer (Appendix 4) for a temperature interval of 4° F. By plotting thermal stress, 27.5 psi, on the vertical axis, the actual loading time was estimated as 155 seconds. Utilizing this value of loading time, the comparison was made between the calculated and measured thermal stresses (Fig 7.6).

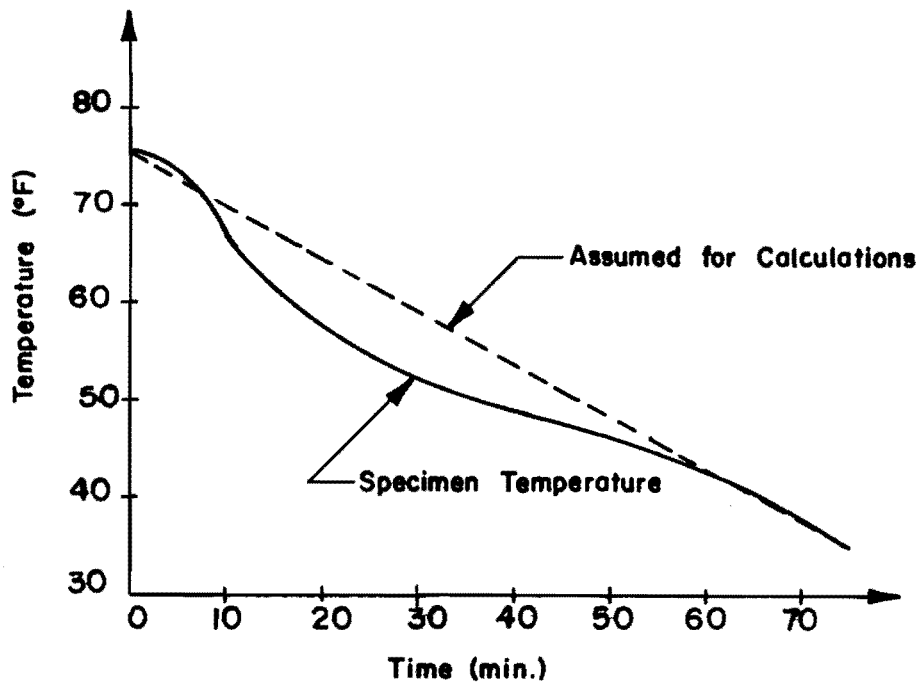


Fig 7.3. Measured and assumed asphalt concrete specimen temperatures for thermal stresses calculations.

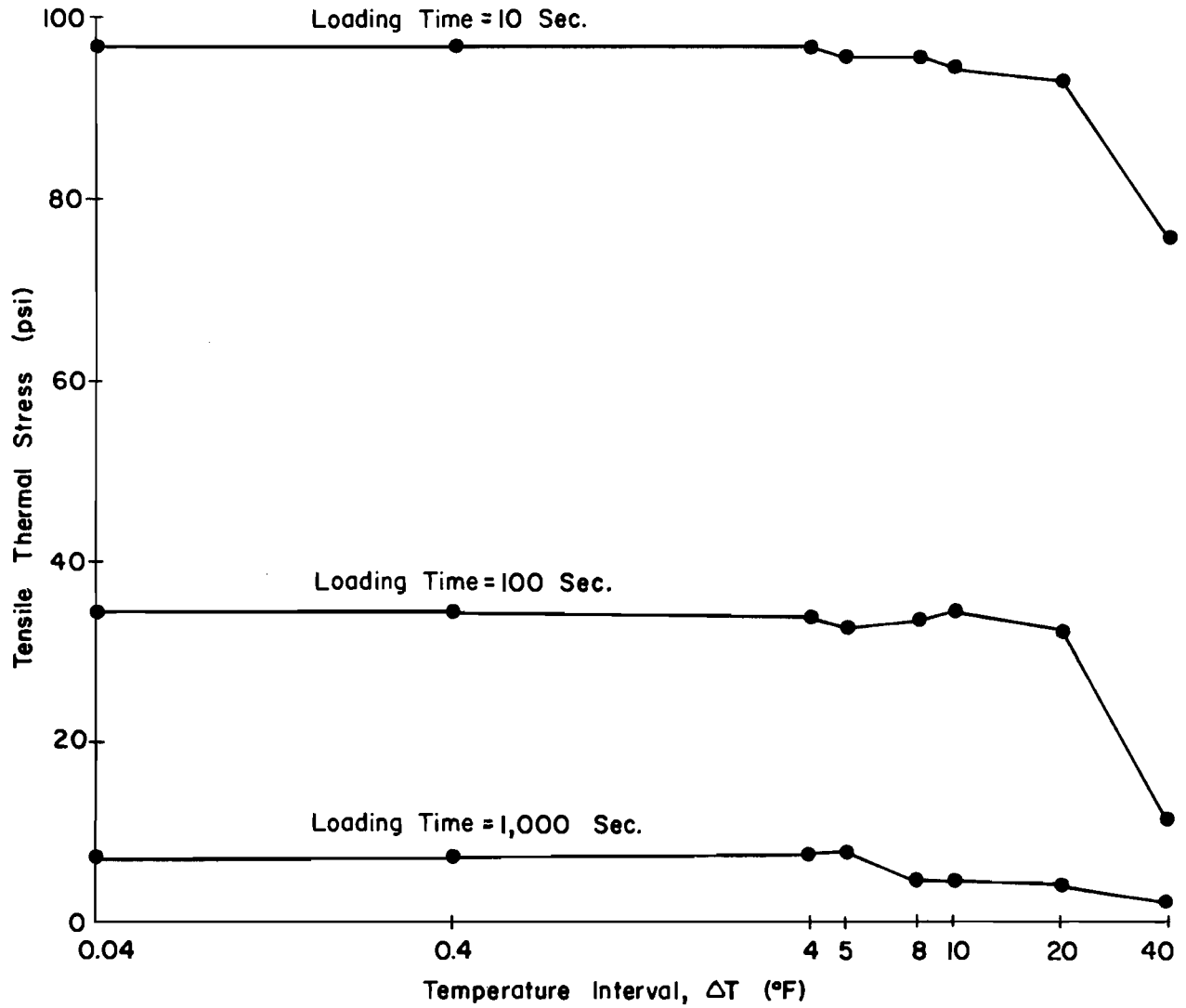


Fig 7.4. Maximum thermal stresses for a linear temperature drop from 75° F to 35° F, in a time period of 4500 seconds.

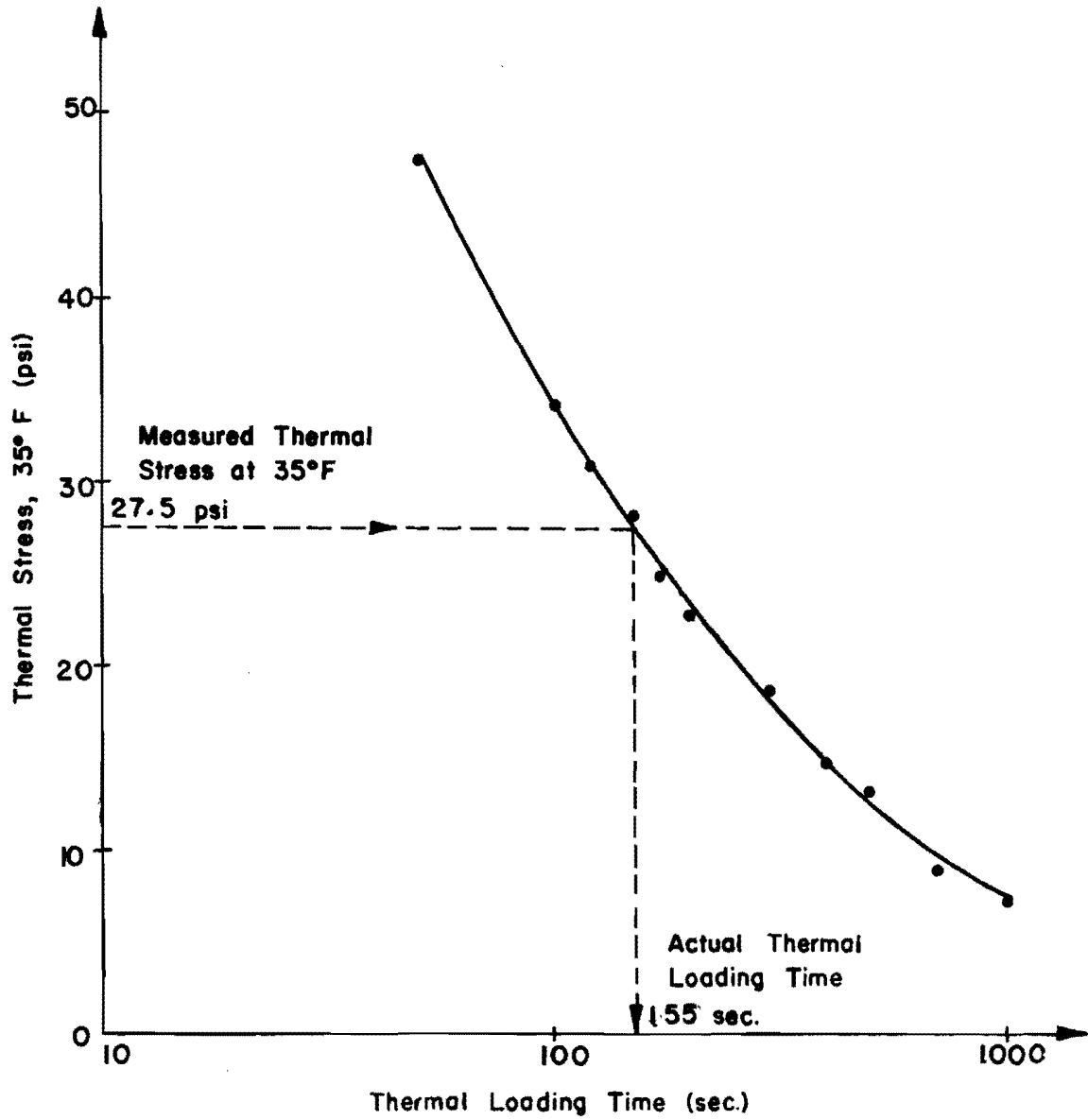


Fig 7.5. Estimation of the actual time of thermal loading.

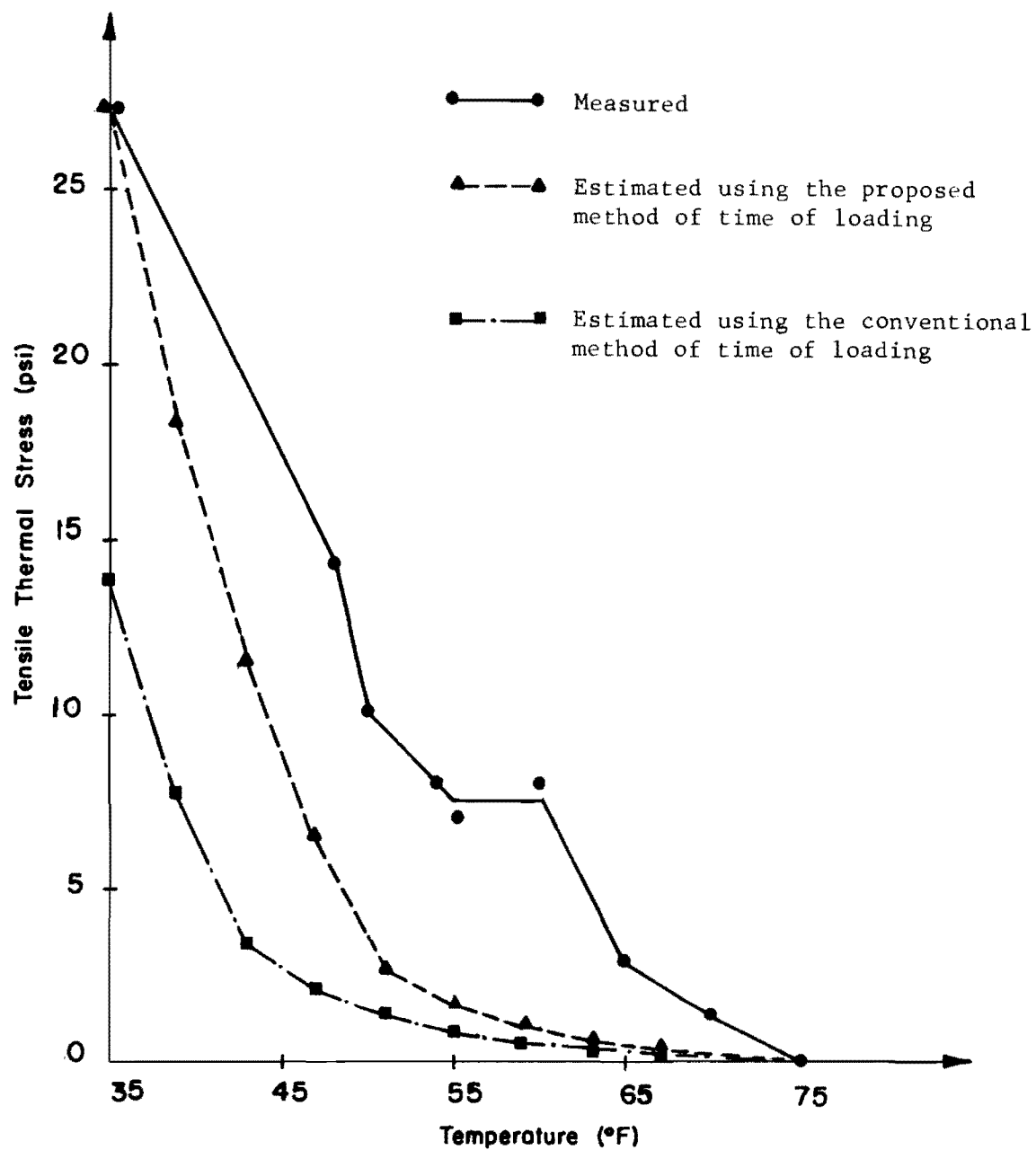


Fig 7.6. Comparison between measured and estimated tensile thermal stresses (see Fig 7.3 for the rate of temperature drop).

On the same figure, the thermal stresses calculated by the conventional method (loading time = $\frac{\text{total time}}{\text{no. of intervals}} = 450 \text{ sec}$) are shown.

Figure 7.6 depicts the following

- (1) When the difference between the assumed and the actual specimen temperatures is recognized, it is obvious that the agreement between the measured and calculated thermal stresses (based on the proposed method for estimating the thermal loading time) is good. At the beginning of the test, where the actual rate of temperature drop was higher than the assumed, the observed rate of thermal stresses build-up was also higher than the calculated. However, at the end of the test the reverse was true.
- (2) The hypothesis on which the conventional method for calculating thermal stresses (loading time = $\frac{\text{total time}}{\text{no. of intervals}}$) is based, is inaccurate. The maximum thermal stress calculated by this method is less than one-half the measured value in this example.

Generally speaking, the conventional method can predict different values of thermal stresses depending on the engineering judgment in choosing the size of the temperature interval.

SUMMARY

A model for estimating thermal stresses in the asphalt concrete surface was discussed. Studies showed that the conventional hypothesis for estimating the thermal loading time ($\frac{\text{total time of temp. drop}}{\text{number of temp. intervals for calculation}}$) is meaningless. Therefore, a more rational method for estimating the loading time was developed. As a conclusion, the discussed model for calculating thermal stresses can be used provided that the proposed method for estimating thermal loading time is utilized.

CHAPTER 8. LOW-TEMPERATURE CRACKING

INTRODUCTION

Low-temperature cracks are cracks that develop as the tensile thermal stress exceeds the asphalt concrete strength. Until now, the most common criterion in selecting the proper asphalt concrete mixture to avoid temperature cracking was the mixture fracture temperature. The fracture temperature is defined as the temperature at which the developed tensile thermal stress exceeds the tensile strength of the asphalt concrete mixture (Fig 8.1). According to the above criterion, the pavement will fail thermally as soon as its temperature drops to the fracture temperature. However, this has not been the case in most of the observations made on thermally cracked roads. Instead, it has been shown that only a few thermal cracks form first; these increase in number, year after year, until the road is considered to be failed. It is important to note that a pavement may never experience a condition in which the tensile stress exceeds the strength and yet still suffers from temperature cracking. This type of cracking is referred to as thermal-fatigue cracking and will be discussed in detail in the next chapter.

It is believed that asphalt concrete properties vary over the entire road length. Therefore, a single fracture temperature is considered to be an unsatisfactory criterion. Instead, the variability of mixture properties should be accounted for by an appropriate stochastic approach. A method for estimating low-temperature cracking has been developed and is explained in detail in this chapter.

THEORY

The two factors that control low-temperature cracking are the stress σ and the strength H . In order to account for the variability of asphalt concrete properties in a particular road, it is assumed that both the stress and the strength vary normally and randomly along that road. The probability of failure is then defined as the probability of the stress exceeding the strength at any point of the road (Eq 8.1):

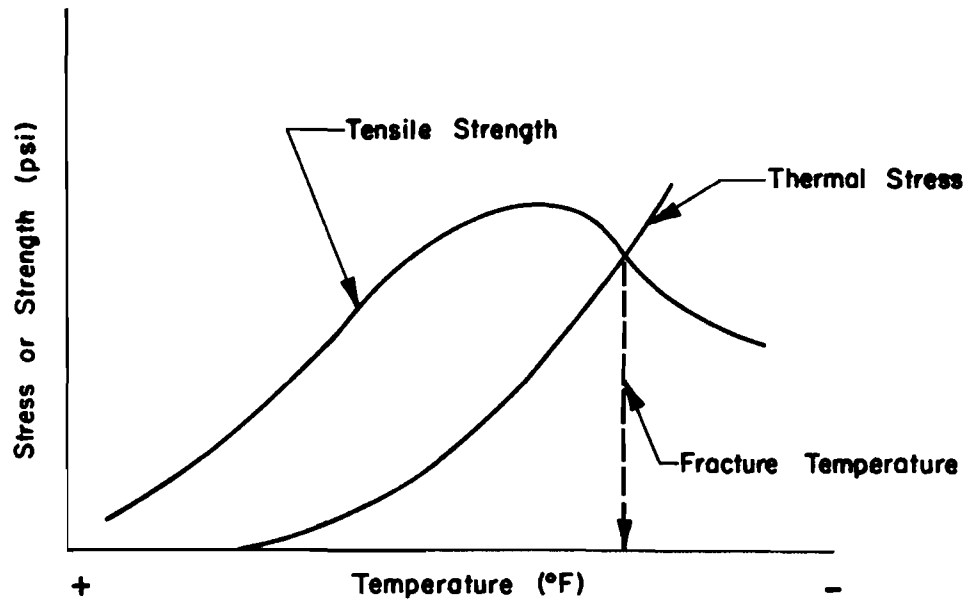


Fig 8.1. Schematic diagram of the fracture temperature concept.

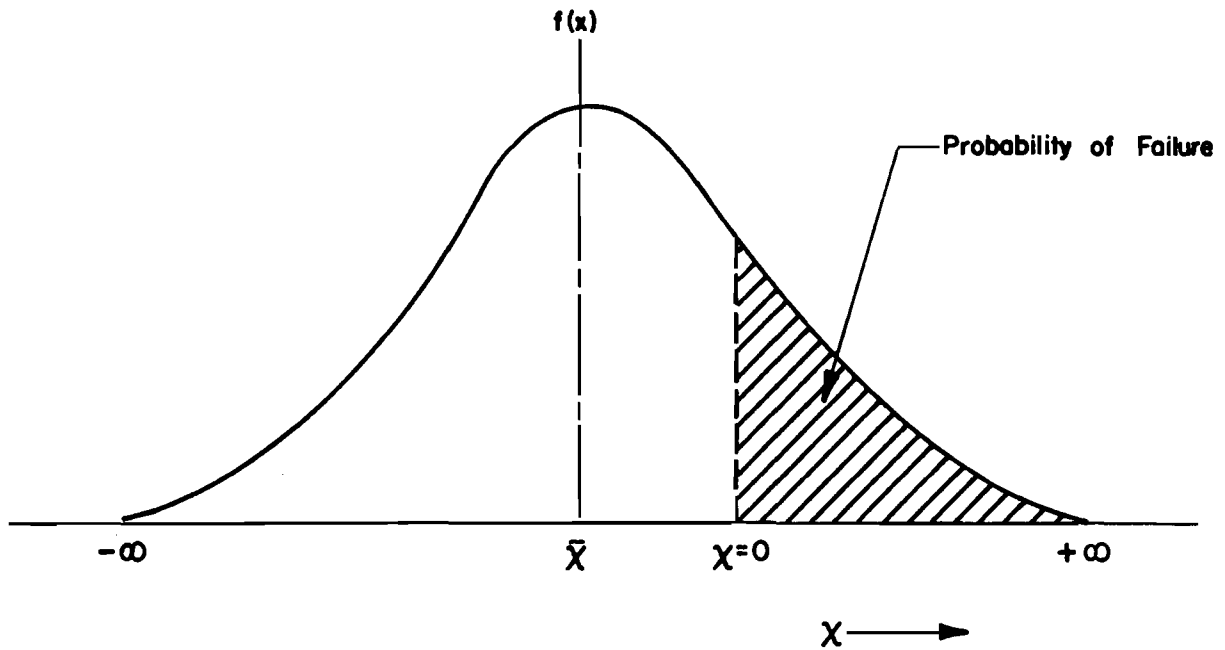


Fig 8.2. Difference distribution ($x = \text{stress} - \text{strength}$).

$$P(\text{failure}) = P(F) = P(\sigma > H) \quad (8.1)$$

Introducing $x = \sigma - H$, Eq 8.1 can be rewritten as follows:

$$P(F) = P(\sigma - H > 0) = P(x > 0) \quad (8.2)$$

Figure 8.2 is a conceptual diagram showing the probability of failure on the normal distribution of x .

Since the stress and strength are assumed to be normally distributed, then $f(x)$ is normally distributed and

$$f(x) = \frac{1}{SD_x \sqrt{2\pi}} \exp \left[-\frac{1}{2} \left(\frac{x - \bar{x}}{SD_x} \right)^2 \right] \quad (8.3)$$

where

$f(x)$ = the density function of x ,

SD_x = standard deviation of x ,

$$= \sqrt{SD_\sigma^2 + SD_H^2},$$

\bar{x} = mean value of x .

$$\therefore P(F) = P(x > 0) = \int_0^{\infty} (f(x) dx) \quad (8.4)$$

By substituting Eq 8.3 in Eq 8.4,

$$P(F) = \frac{1}{SD_x \sqrt{2\pi}} \int_0^{\infty} \text{Exp} \left[-\frac{1}{2} \left(\frac{x - \bar{x}}{SD_x} \right)^2 \right] dx \quad (8.5)$$

In order to make use of the normal tables the variable x was normalized:

$$Z_x = \frac{x - \bar{x}}{SD_x} \quad (8.6)$$

Accordingly, the limits of the integration in Eq 8.5 will be as follows:

$$(1) \quad x = 0 \quad Z_{x_{\min}} = -\frac{\bar{x}}{SD_x},$$

$$(2) \quad x = \infty \quad Z_{x_{\max}} = \infty, \text{ and}$$

$$(3) \quad dx = SD_x dZ$$

Equation 8.5 can then be rewritten in terms of z as follows:

$$P(F) = \frac{1}{\sqrt{2\pi}} \int_{Z_{x_{\min}}}^{Z_x = \infty} e^{-\frac{Z^2}{2}} dZ \quad (8.7)$$

If the lower limit of the integration of Eq 8.7 is known, then the normal tables can be used to determine the probability of failure, $P(F)$:

$$Z_{x_{\min}} = \frac{-\bar{x}}{SD_x} = -\frac{(\bar{\sigma} - \bar{H})}{\sqrt{SD_{\sigma}^2 + SD_H^2}} \quad (8.8)$$

where

$\bar{\sigma}$ = mean value of the stress,

\bar{H} = mean value of the strength,

SD_{σ} = standard deviation of the stress, and

SD_H = standard deviation of the strength.

As an example to illustrate the above concept, the following values were assumed:

$\bar{\sigma}$ = 100 psi,

SD_{σ} = 50 psi,

$$\bar{H} = 200 \text{ psi,}$$

$$SD_H = 40 \text{ psi, and}$$

$$Z_{x_{\min}} = - \frac{(100 - 200)}{50^2 + 40^2} = + 1.8$$

From the normal tables, $P(F) = 2.94$ percent, which means that 2.94 percent of the area of a road will fail if the assumed values of stress and strength occur.

In the next two sections, an estimate of the variability associated with the stress and the strength is presented.

STRESS VARIABILITY

The calculation of thermal stresses was presented in Chapter 7, and it was concluded that the following equation can be used to estimate thermal stresses, provided that the suggested method for estimating the time of loading is utilized:

$$\sigma(t, T) = \Sigma \alpha(\bar{T}_{\Delta}) \times \Delta T \times S(t, \bar{T}_{\Delta}) \quad (8.9)$$

where

$\sigma(t, T)$ = thermal stress as a function of time of loading and temperature,

$\alpha(\bar{T}_{\Delta})$ = thermal coefficient of contraction of the asphalt concrete at the mean value of a selected temperature interval ΔT ,

ΔT = a selected temperature interval,

$S(t, \bar{T}_{\Delta})$ = asphalt concrete stiffness at a given time of loading and the mean value of a selected temperature interval ΔT .

For any general function $y(x)$, in the following form

$$y = x_1 + x_2 + x_3$$

The variance of y is the summation of the variances of x_1 , x_2 , and x_3 , providing that x_1 , x_2 , and x_3 are independent. Considering the logarithm of both sides of Eq 8.9,

$$\text{Log}_{10} \sigma = \text{Log}_{10} \alpha + \text{Log}_{10} T + \text{Log}_{10} S$$

or

$$V(\text{Log}_{10} \sigma) = V(\text{Log}_{10} \alpha) + V(\text{Log}_{10} T) + V(\text{Log}_{10} S) \quad (8.10)$$

where the symbol V refers to the variance of the associated function. Going a step further, the variance of any function g_x can be approximated by Taylor Series as follows (Ref 27):

$$V(g_x) \approx \left(\frac{\partial g_x}{\partial x} \right) V(x)$$

Substituting $\text{Log}_{10} \sigma$ for g_x

$$\begin{aligned} V(\text{Log}_{10} \sigma) &\approx \left(\frac{\partial \text{Log}_{10} \sigma}{\partial \sigma} \right) V(\sigma) \\ &\approx 0.189 \frac{V(\sigma)}{\sigma^2} \end{aligned}$$

or

$$V(\text{Log}_{10} \sigma) \approx 0.189 (CV_\sigma)^2 \quad (8.11)$$

where

$CV_\sigma =$ the coefficient of variation of the stress σ .

By performing similar transformations on the right hand side of Eq 8.10, Eq 8.12 was developed:

$$0.189(CV_{\sigma})^2 \approx 0.189(CV_{\alpha})^2 + 0.189(CV_T)^2 + 0.189(CV_S)^2$$

or

$$(CV_{\sigma})^2 \approx (CV_{\alpha})^2 + (CV_T)^2 + (CV_S)^2 \quad (8.12)$$

The notation CV refers to the coefficient of variation of the subscripted function.

In the above equation, if the coefficients of variation of α , T, and S are known, the coefficient of variation of the stress can be estimated. During a flexural test of asphalt concrete beams made with the California kneading compactor, Busby and Rader (Ref 4) found that the coefficient of variation of the stiffness modulus reaches a value of 0.23. Therefore, a rough approximation of the actual coefficient of variation of the stiffness modulus along the road, may lead to a value as much as double (or more) the above value, i.e., ≈ 0.45 .

Substituting this value in Eq 8.12,

$$(CV_{\sigma})^2 = (CV_{\alpha})^2 + (CV_T)^2 + (0.45)^2$$

or

$$(CV_{\sigma})^2 = (CV_{\alpha})^2 + (CV_T)^2 + 0.2025 \quad (8.13)$$

Due to the lack of data, the coefficients of variation of α and T were difficult to estimate. However, an approximation leads to the following values:

$$CV_{\alpha} \approx 0.1$$

$$CV_T \approx 0.2$$

STRENGTH VARIABILITY

In this section, a method for estimating the asphalt concrete tensile strength along with the variability associated with it is presented. The method for estimating the asphalt concrete tensile strength is adopted after Heukelom (Ref 28). In developing his method, Heukelom made the following assumptions:

- (1) Fracture of a mix is generally caused by fracture of the asphalt cement.
- (2) M_H = Mix Factor = Mix Strength/bitumen strength.
- (3) The mix factor M_H is a function of percent asphalt, aggregate gradation, degree of compaction, and, presumably, also of the effect of the hard mineral walls.
- (4) The mix factor is likely to remain constant for a given mix under all conditions of loading time or rate of deformation, temperature, etc.

As a result, the following equation was presented:

$$H_{\text{mix}} = M_H \times H_{\text{bit}} \quad (8.14)$$

where

H_{mix} = tensile strength of the mixture,

M_H = mix factor,

H_{bit} = tensile strength of the asphalt cement.

Figure 8.3 shows the validity of the above equation. In this figure, the curve marked type I is an example of mixes with poor grading and/or compaction, whereas type II represents better grading and/or compaction. The difference between the two curves is the difference in the mix factor. In order to normalize the relationship between the bitumen stiffness and the mix tensile strength, Heukelom (Ref 28) considered the relative tensile strength, i.e., the tensile strength divided by its maximum value, so that differences in the value of M_T were eliminated. Figure 8.4 shows the normalized relationship for eight mixes. In this figure it can be noted that the maximum tensile strength corresponds to a bitumen stiffness of about 600 kg/cm^2 . The concept in Fig 8.4 was then used to introduce the following statements:

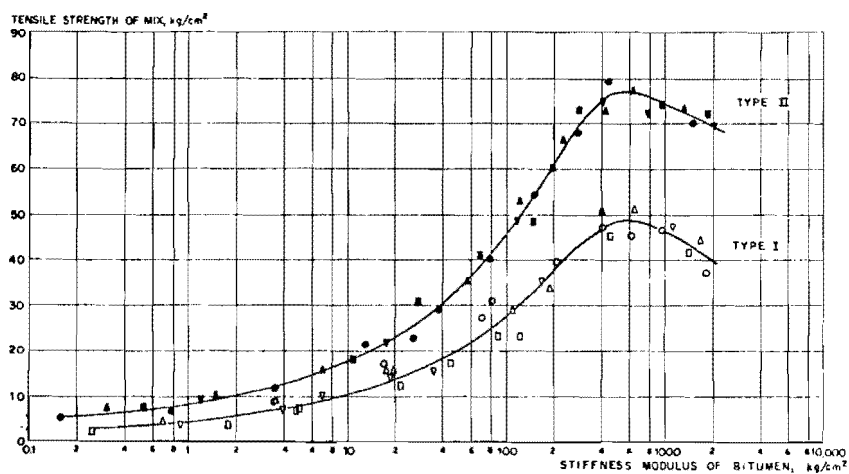


Fig 8.3. Tensile strength of mixes as a function of the stiffness modulus of the asphalt cement (Ref 28).

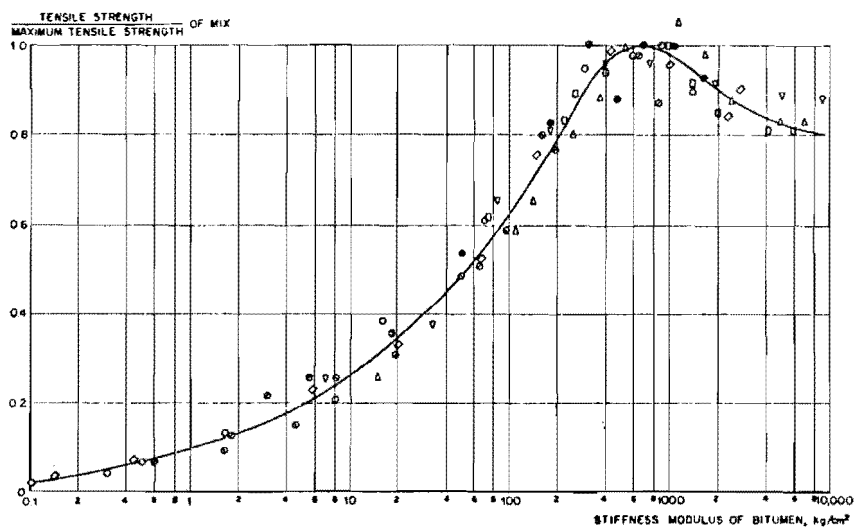


Fig 8.4. Relative tensile strength of eight mixes containing 45 to 54 percent stone (Ref 28).

$$H = R_H \times H_{MAX} \quad (8.15)$$

where

H = tensile strength of the mix;

R_H = relative tensile strength, which is a function of the bitumen stiffness;

H_{max} = maximum tensile strength of the mix.

From Eq 8.15, the only unknown for estimating the tensile strength is the maximum tensile strength of the mix.

To account for the variability associated with Eq 8.15, the same procedure as described in the preceding section (stress variability) was utilized:

$$\text{Log}_{10} H = \text{Log}_{10} R_H + \text{Log}_{10} H_{max}$$

or

$$(CV_H)^2 = (CV_{R_H})^2 + (CV_{Hmax})^2 \quad (8.16)$$

CV refers to the coefficient of variation of the subscripted function. The coefficient of variation of the relative strength CV_{R_H} was calculated from data extracted from Fig 8.4. The calculations resulted in the following value: $CV_{R_H} = 0.075$. Due to the lack of data, the coefficient of variation of the maximum tensile strength was hard to estimate. However a good approximation may lead to a value of $CV_{Hmax} \approx 0.2$.

EXAMPLE

To show the procedure for estimating low temperature cracking, the following illustrative numerical example is given. In a newly constructed flexible pavement road, the following mixture properties were determined:

- (1) maximum tensile strength $H_{max} = 500$ psi,
- (2) coefficient of variation of H_{max} $CV_{Hmax} = 0.2$,

- (3) coefficient of variation of the thermal coefficient of contraction = 0.1,
 (4) coefficient of variation of temperature = 0.2.

It is desired to predict the amount of low temperature cracking as the tensile thermal stress reaches an average value of 300 psi when the asphalt cement stiffness is estimated to be $\approx 5,700$ psi.

From Fig 8.4, the relative strength R_H corresponding to a bitumen stiffness of 5,700 psi ≈ 0.95 .

From Eq 8.15, the average tensile strength

$$\bar{H} = 0.95 \times 500 = 475 \text{ psi}$$

From Eq 8.16, the coefficient of variation of strength

$$CV_H = \sqrt{0.075^2 + 0.2^2} \approx 0.214$$

$$SD_H = CV_H \times \bar{H} = (0.214)(475) \approx 101 \text{ psi}$$

From Eq 8.13, the coefficient of variation of stress

$$CV_\sigma = \sqrt{0.1^2 + 0.2^2 + 0.2025} \approx 0.5$$

$$SD_\sigma = CV_\sigma \times \bar{\sigma} = (0.50)(300) = 150 \text{ psi}$$

From Eq 8.8

$$z_{x_{\min}} = - \frac{300 - 475}{\sqrt{150^2 + 101^2}} \approx 0.966$$

From the statistical normal tables (Ref 30), the probability of failure $P(F) \approx 0.167$; i.e., 16.7 percent of the pavement area will crack due to low temperature.

TRANSFORMATION FROM AREA TO LINEAR CRACKING

Since thermal cracks take the form of transverse cracks, they are usually reported as the average frequency per mile or, as reported in the AASHO Road Test, in linear feet, per 1000 ft². The spacing between transverse cracks ranges from 5 feet to several hundred feet. Considering this observation as a criterion, it can be assumed that if the spacing between transverse cracks reaches 5 feet, the pavement is no longer restrained. In other words, it can be assumed that the area of influence of each transverse crack is equal to its length times a width of 5 feet (Fig 8.5). Therefore, to transfer a predicted area of thermal cracking into linear cracking, the area can be divided by the width of influence, which can be approximated as 5 feet.

SUMMARY AND CONCLUSIONS

The predominate equation in the low temperature cracking model is Eq 8.8. To study the behavior of the model, the four variables in the equation were varied over a selected range. The results of the above analysis are shown in Figs 8.6, 8.7, and 8.8. The following conclusions are drawn from these figures:

- (1) When the average tensile stress is equal to the average tensile strength, the probability of failure is 50 percent, regardless of the stress and strength coefficients of variation.
- (2) For both stress and strength, the higher the coefficient of variation, the higher the low-temperature cracking up to a probability of failure of 50 percent, after which the reverse is true.

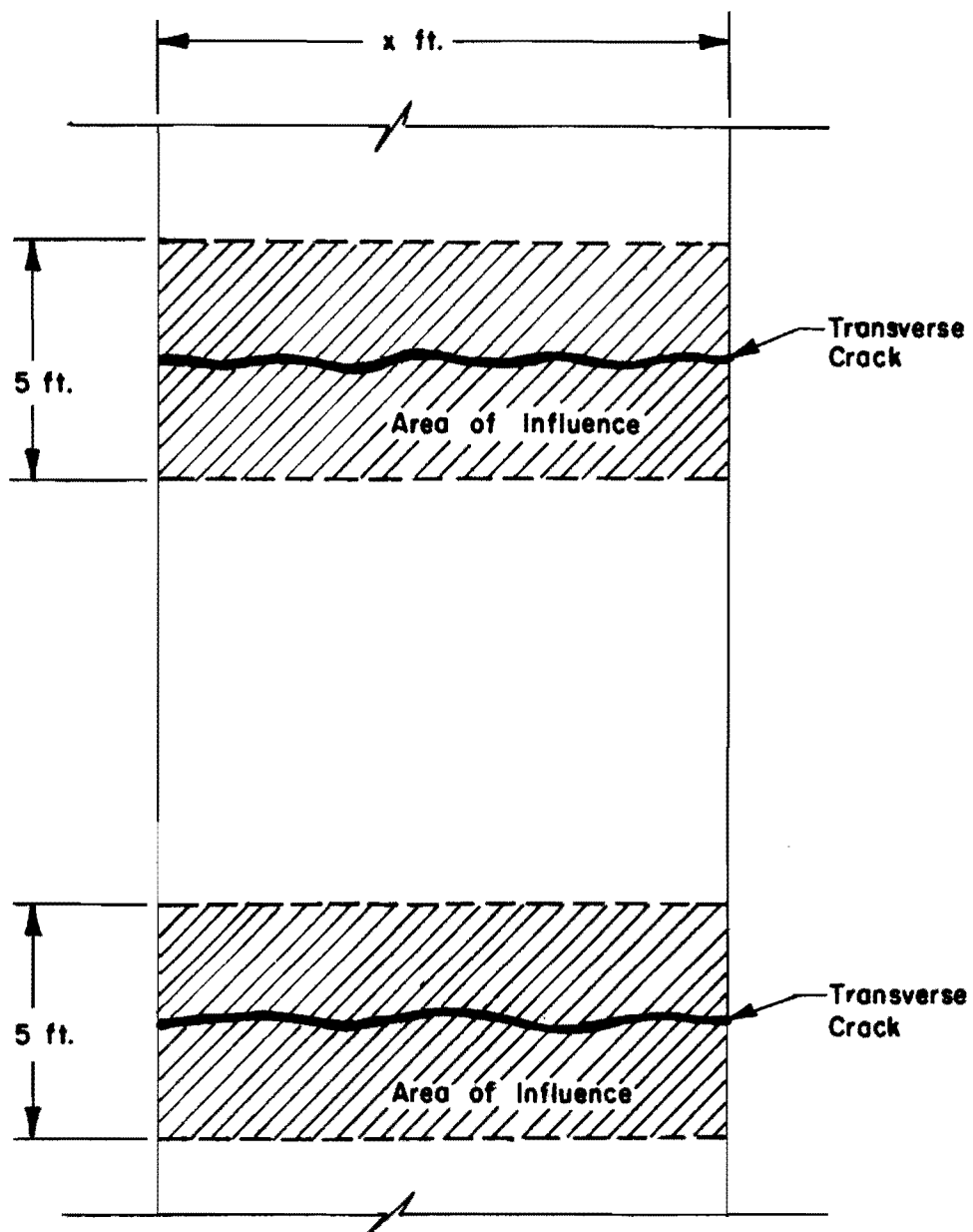
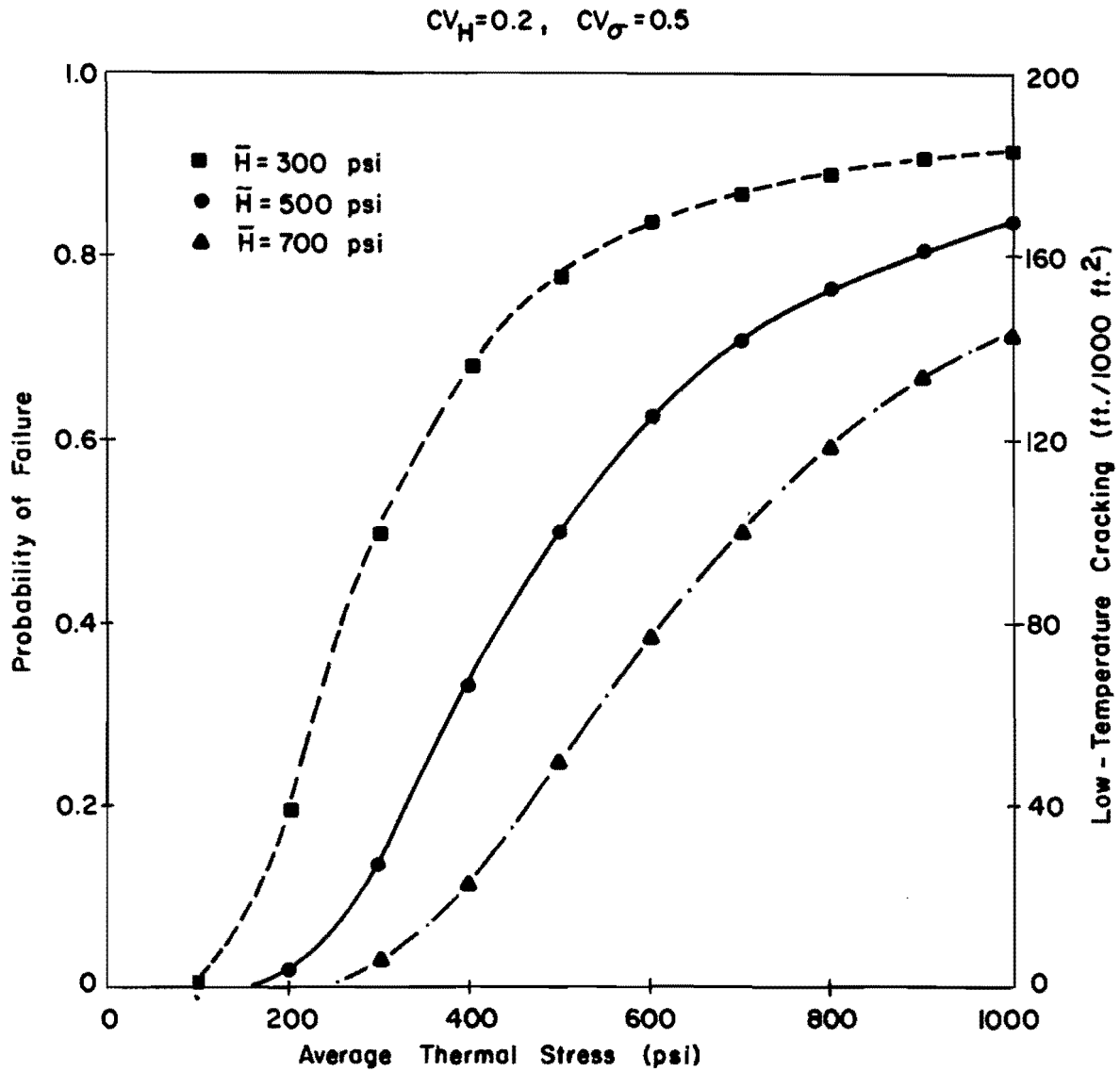
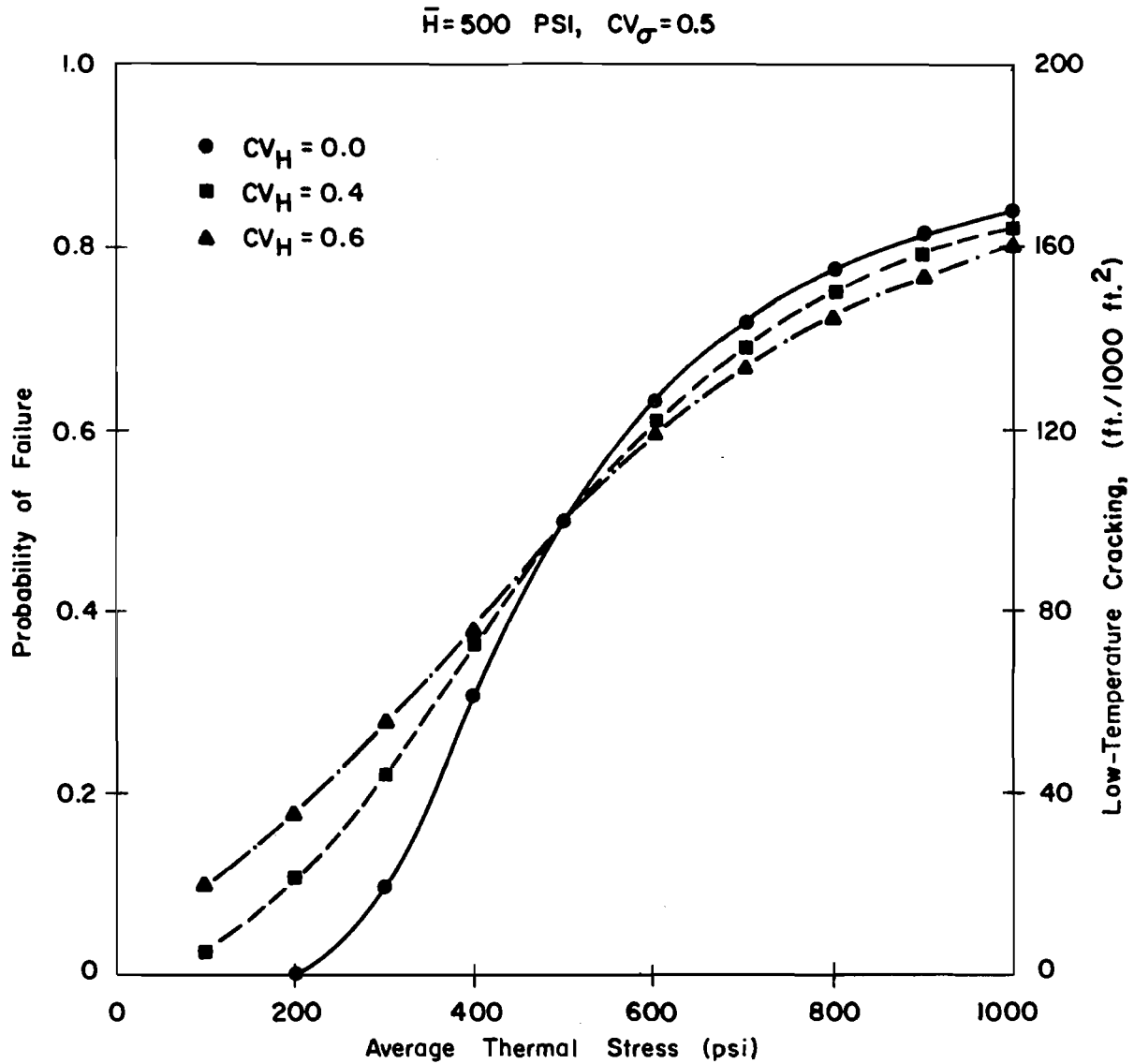


Fig 8.5. Area of influence of transverse cracks.



\bar{H} = mean value of the tensile strength,
 CV_H = coefficient of variation of the strength,
 CV_σ = coefficient of variation of the stress.

Fig 8.6. Effect of mean strength on low-temperature cracking.

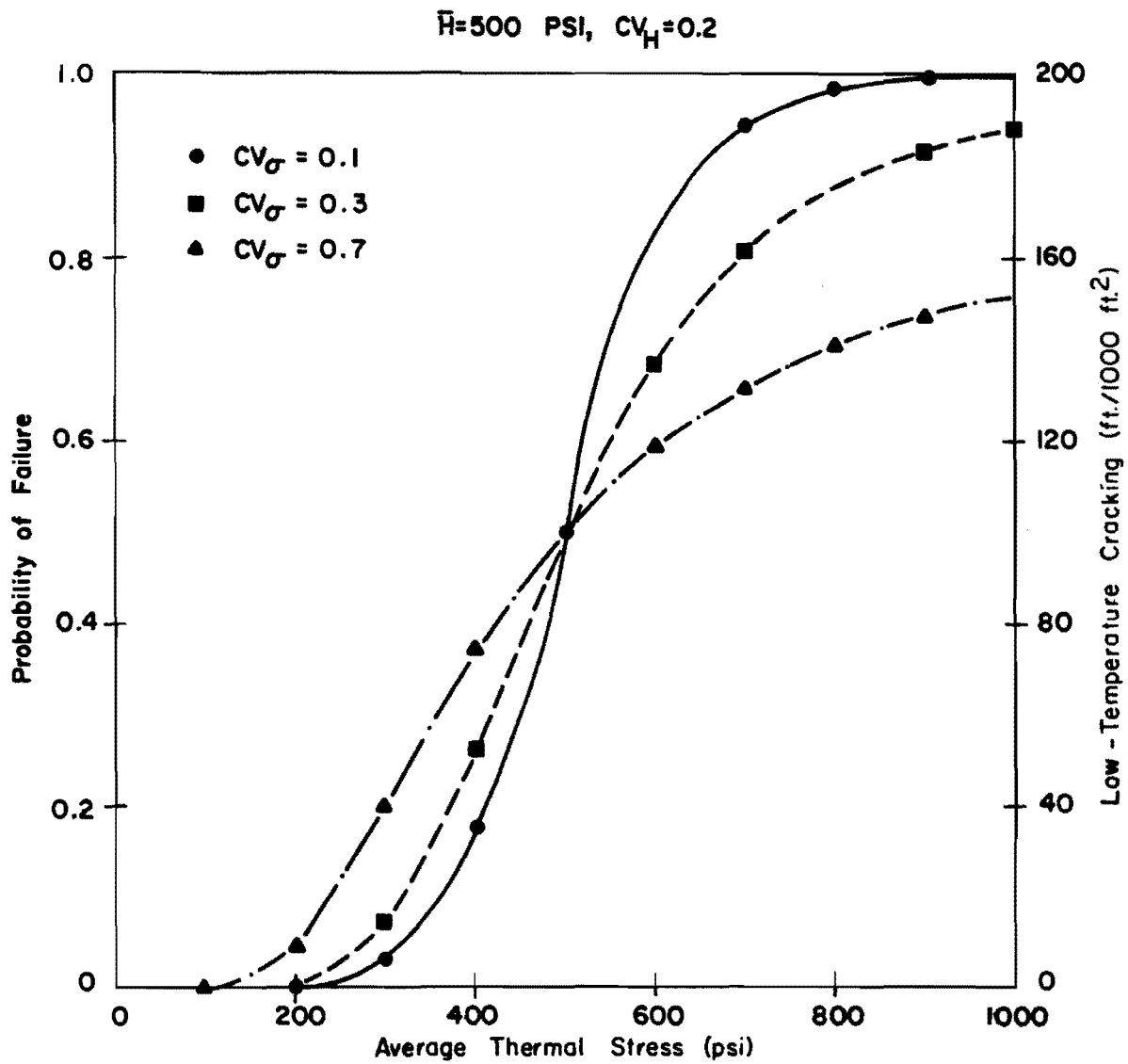


CV_H = coefficient of variation of the strength,

\bar{H} = mean value of the tensile strength,

CV_{σ} = coefficient of variation of the stress.

Fig 8.7. Effect of the coefficient of variation of strength on low-temperature cracking.



CV_σ = coefficient of variation of the stress,
 \bar{H} = mean value of the tensile strength,
 CV_H = coefficient of variation of the strength.

Fig 8.8. Effect of the coefficient of variation of stress on low-temperature cracking.

CHAPTER 9. THERMAL-FATIGUE CRACKING

INTRODUCTION

In the preceding chapter, a model for predicting low-temperature cracking was developed. Low-temperature cracking is only one form of temperature cracking; the other form of temperature cracking is called thermal-fatigue cracking and is due to daily temperature cycling. Since the air temperature cycles every day, the pavement temperature also cycles daily. Air and pavement temperature cycles not only differ in phase angle but also in size (range) and the mean temperature about which they cycle. These differences depend on the surrounding environmental conditions and the depth of pavement at which the temperature is studied.

To study the relation between temperature cycling and the fatigue concept, the pavement behavior (stress, strain, etc.) under temperature cycling was analyzed. The analysis showed that temperature cycling stimulates a constant strain rather than a constant stress fatigue distress. The development of a thermal fatigue theory is explained in detail in the next sections.

TEMPERATURE SYSTEM FOR FATIGUE ANALYSIS

In Chapter 3, a model was developed by which pavement temperatures during a single day can be predicted on an hourly basis. The inputs to this model are as follows:

- (1) daily mean air temperature,
- (2) daily air temperature range,
- (3) daily mean solar radiation,
- (4) daily average wind velocity, and
- (5) pavement thermal properties.

To utilize the model to predict thermal-fatigue cracking, it is necessary to consider the variation of its inputs during an average year. In doing this, it was assumed that the pavement thermal properties are constant; however, it was found that the daily mean air temperature and solar radiation are the most

significant factors affecting pavement temperatures; therefore, models to account for their day-to-day variation were developed.

DAILY MEAN AIR TEMPERATURE MODEL

To depict a general scheme for the annual air temperature variation, the normal monthly average air temperatures for three weather stations in Texas (Ref 65) were plotted (Fig 9.1).

From this figure one may conclude the following:

- (1) In a normal year, daily mean air temperatures vary in a sinusoidal fashion.
- (2) Minimum annual temperature occurs on the average in December or January.
- (3) Maximum annual temperature occurs on the average in June or July.

As a result the following model was developed:

$$TA(N) = ANNVE + (ANR/2)COS(N) \quad (9.1)$$

where

N = no. of day; e.g., N = 1, July 1st
 N = 360, June 30th

TA = daily mean air temperature,

ANNVE = annual average air temperature, and

ANR = annual air temperature range.

Figure 9.2 depicts the above model. To verify the model, a comparison between predicted and measured monthly mean air temperatures was performed for three weather stations selected at random (Ref 65). Figure 9.3 indicates the reliability of the model.

DAILY MEAN SOLAR RADIATION MODEL

Following the same steps as in the preceding model, the following formula for the solar radiation model was hypothesized:

$$SR(N) = A + B COS(N) \quad (9.2)$$

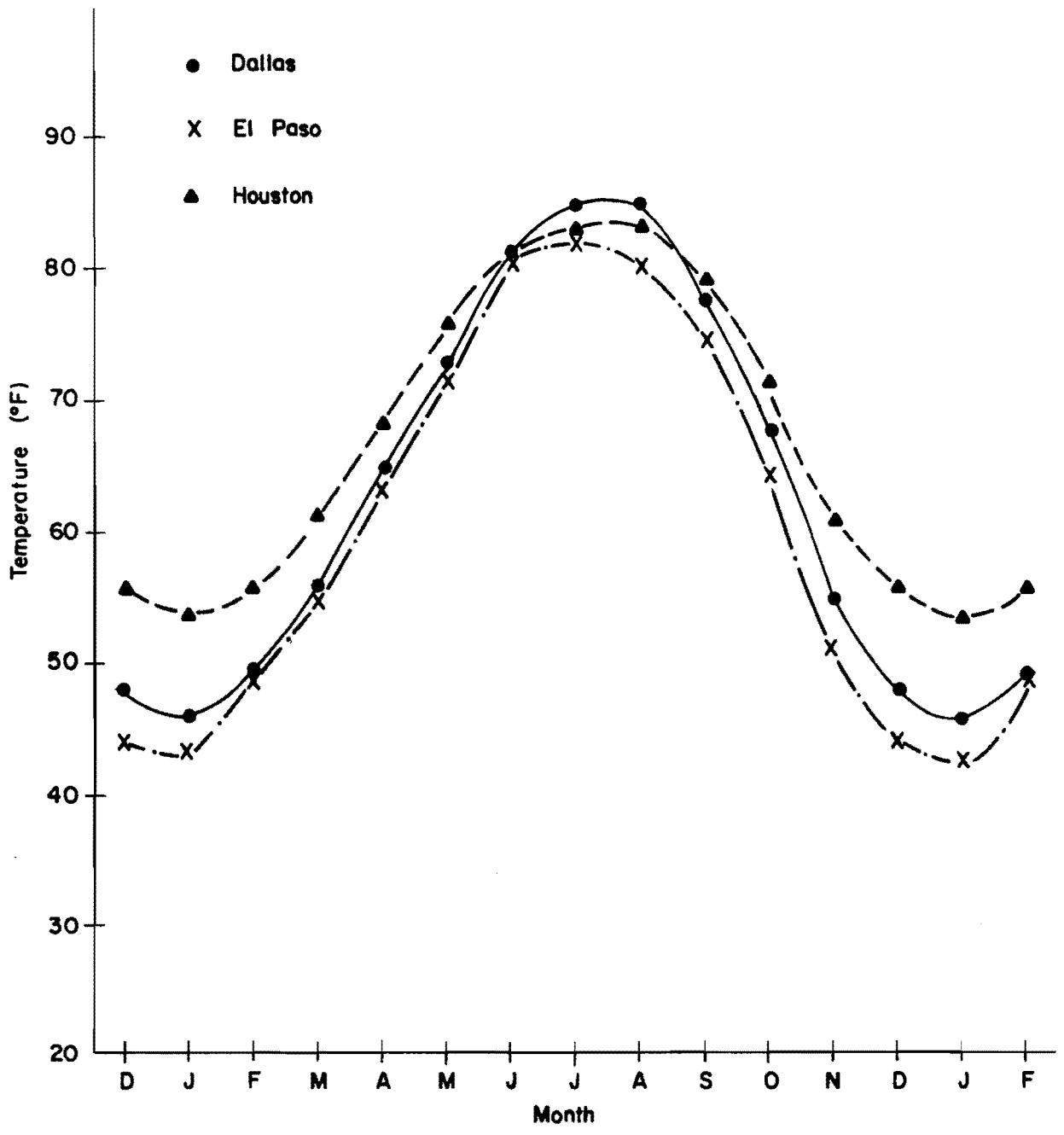


Fig 9.1. Monthly normal average temperatures.

$$TA(N) = ANNVE + (ANR/2) \cos(N)$$

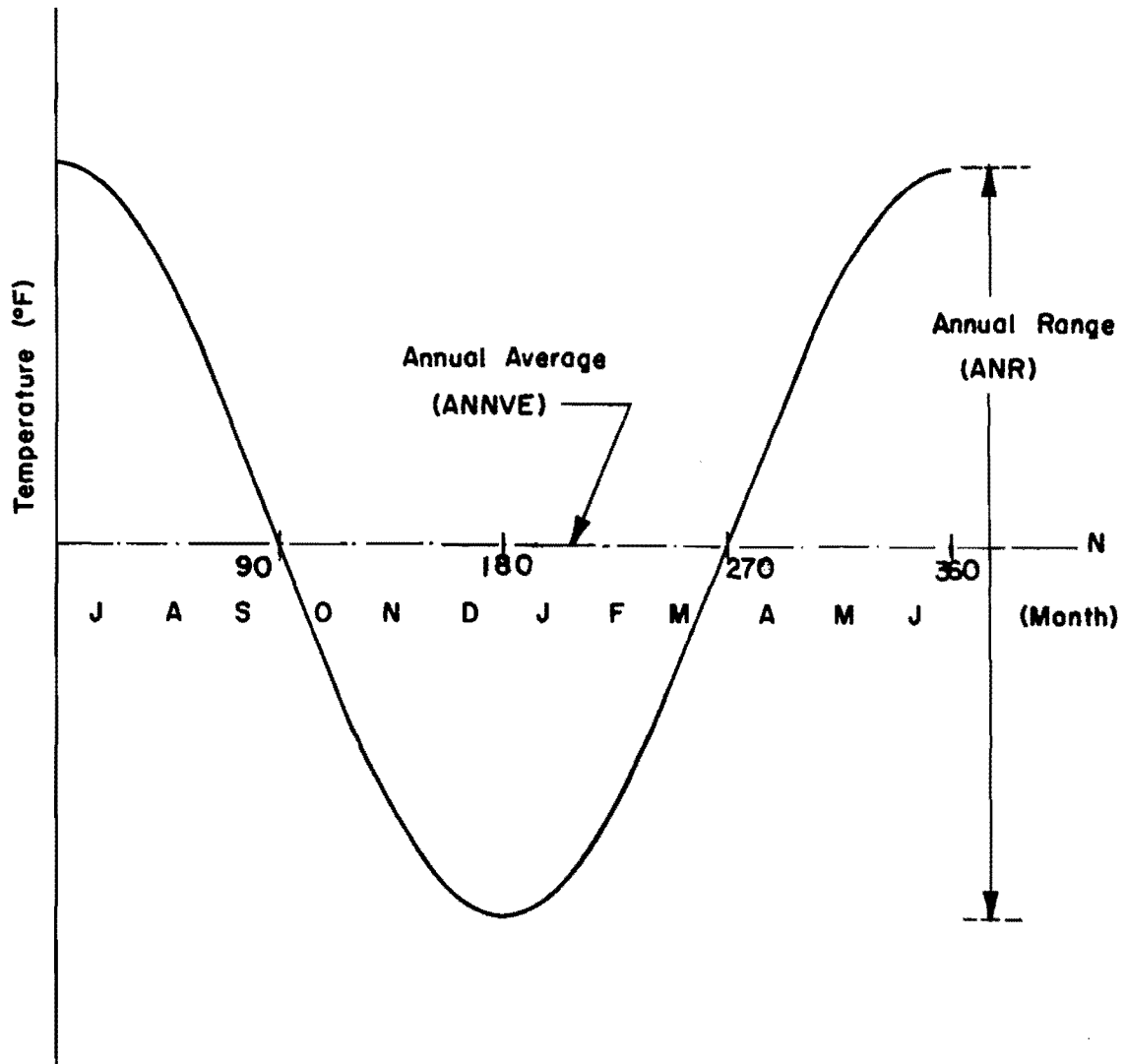


Fig 9.2. Daily mean air temperature model.

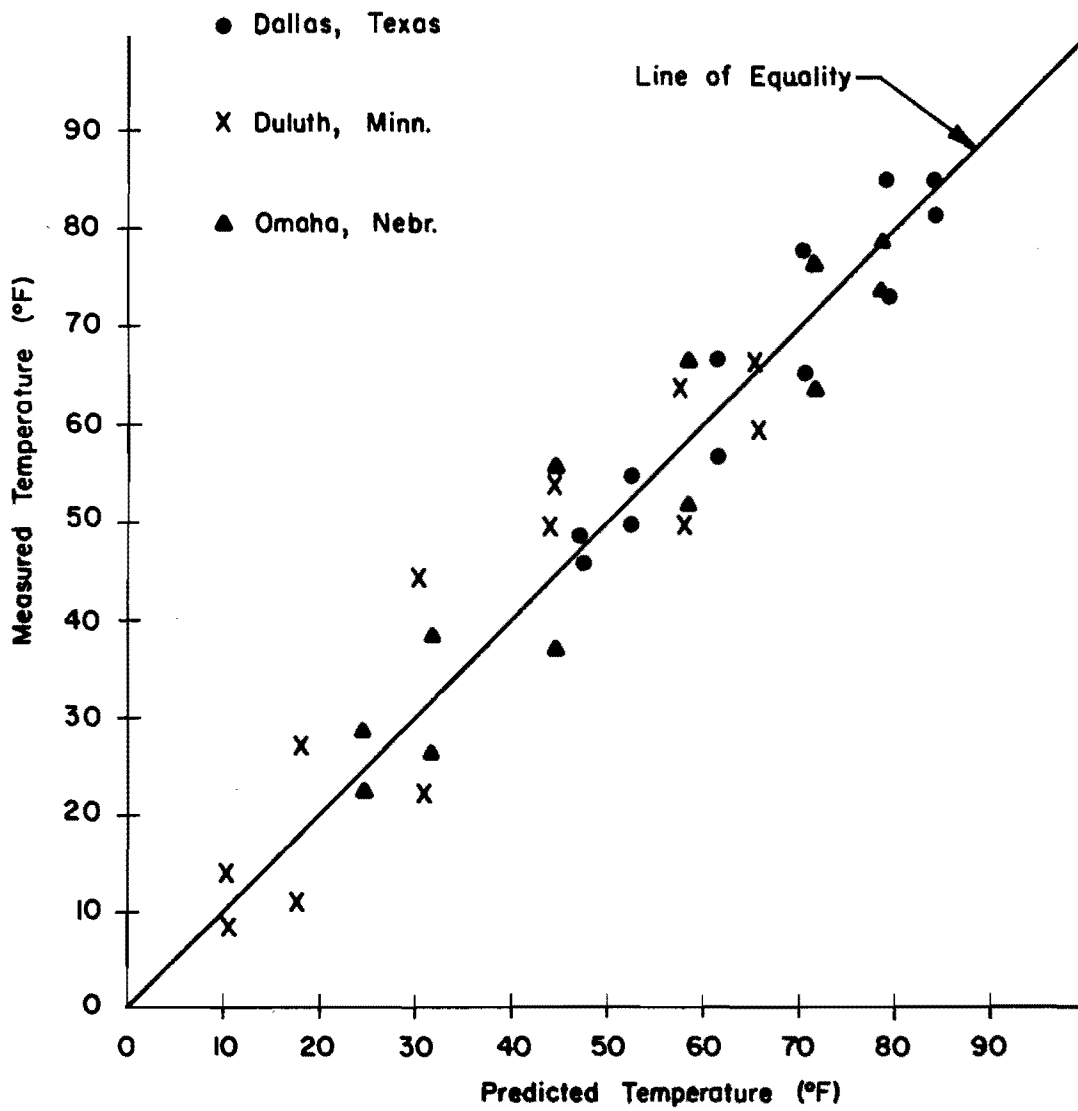


Fig 9.3. Verification of the daily mean air temperature model.

where

N is as defined for Eq 9.1,

A and B = constants.

To determine A and B , the following two boundary conditions were assumed (see Fig 9.4):

$$(1) \text{ At } N = 90 \text{ or } 270, \text{ SR}(N) = \overline{\text{SR}}$$

$$(2) \text{ At } N = 15 \text{ or } 345, \text{ SR}(N) = \text{SR}_1$$

where

$\overline{\text{SR}}$ = mean daily annual average solar radiation,

SR_1 = mean daily July average solar radiation.

Using the above two boundary conditions and solving for A and B , the solar radiation model can be expressed as follows:

$$\text{SR}(N) = \overline{\text{SR}} + \frac{(\text{SR}_1 - \overline{\text{SR}})}{0.966} \text{Cos}(N) \quad (9.3)$$

Figure 9.5 shows a comparison between predicted and measured solar radiation for 6 weather stations selected at random (Ref 10). From the figure, it is evident that the model is quite reliable for engineering purposes.

THERMAL-FATIGUE THEORY

The word fatigue is used to indicate the tendency of flexible pavements to thermally crack under repeated temperature cycling. The distress effect of each cycle depends on the maximum stiffness and strain during that day (cycle), Fig 7.2. For two cycles causing the same strain, the higher the stiffness the higher the distress. Meanwhile under the same stiffness conditions, the higher the strain the more damage to the pavement. The pavement is subjected to 30 cycles per month (360 cycles/year) with each cycle having a different distress intensity than the other. Furthermore, hardening of asphalt is an important phenomenon that should be considered. As time passes, the asphalt gets harder (Chapter 6) and hence, on the average, the asphalt concrete stiffness increases year after year. In conclusion, it is believed that

$$SR(N) = \overline{SR} + \frac{(SR_1 - \overline{SR})}{0.966} \times \cos(N)$$

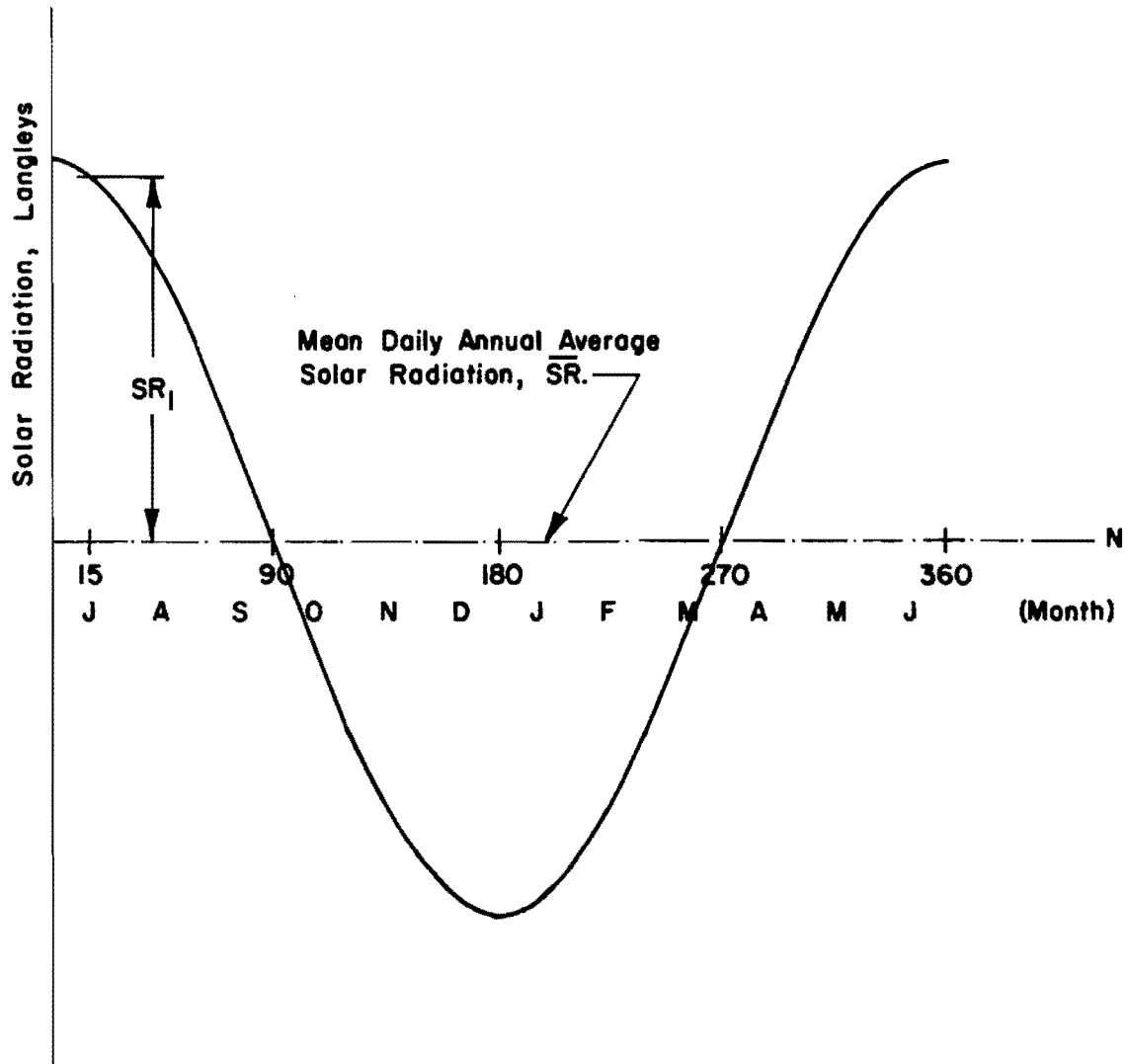


Fig 9.4. Daily mean solar radiation model.

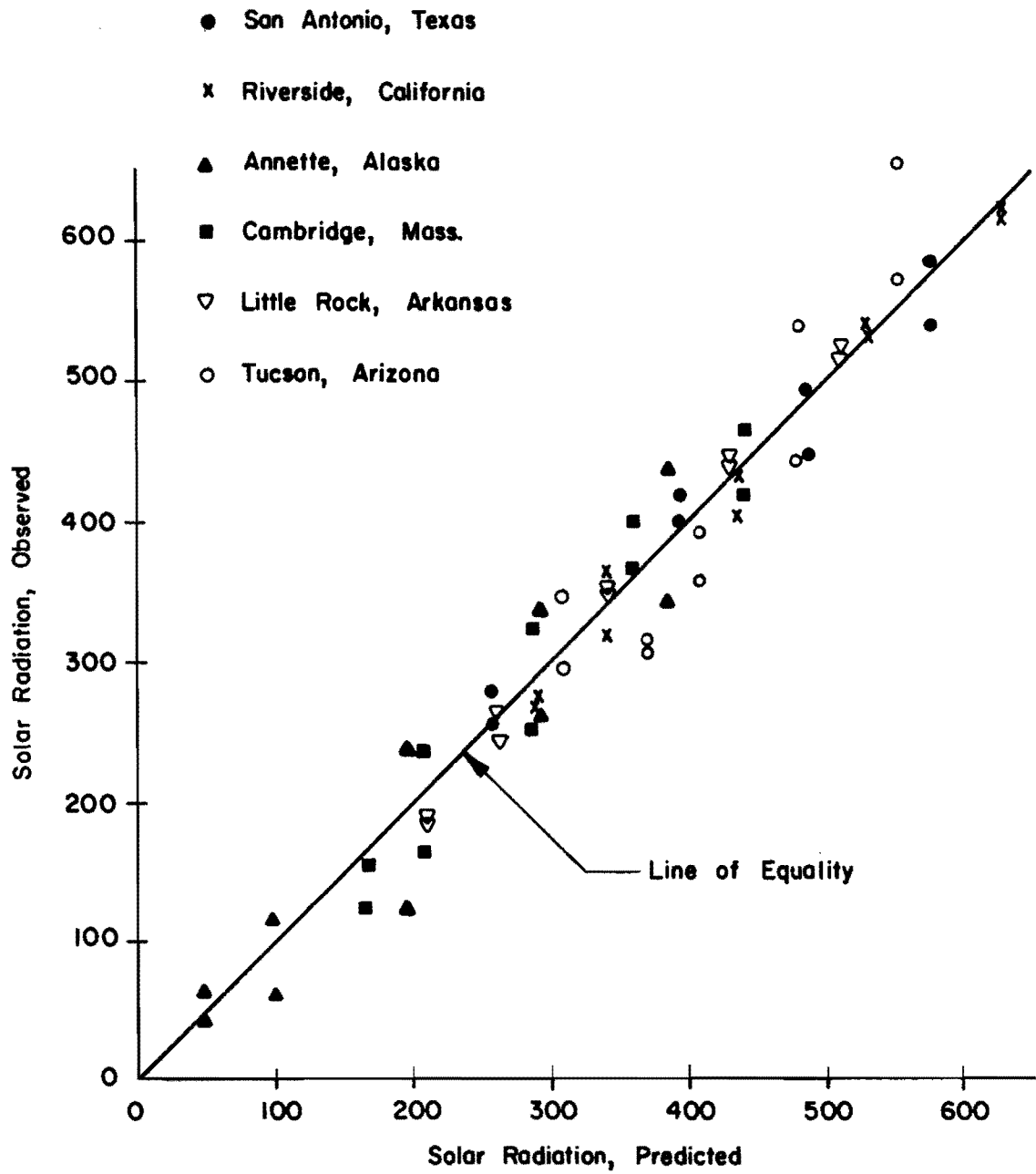


Fig 9.5. Verification of the solar radiation model.

stiffness is the major factor separating asphalt concrete mixes with reference to their ability to withstand repeated temperature cycling. Figure 9.6 depicts a conceptual relation between strain level and the number of cycle applications until failure for different stiffnesses. The general relation may be written as follows:

$$\bar{N} = A \left(\frac{1}{\epsilon} \right)^B \quad (9.4)$$

where

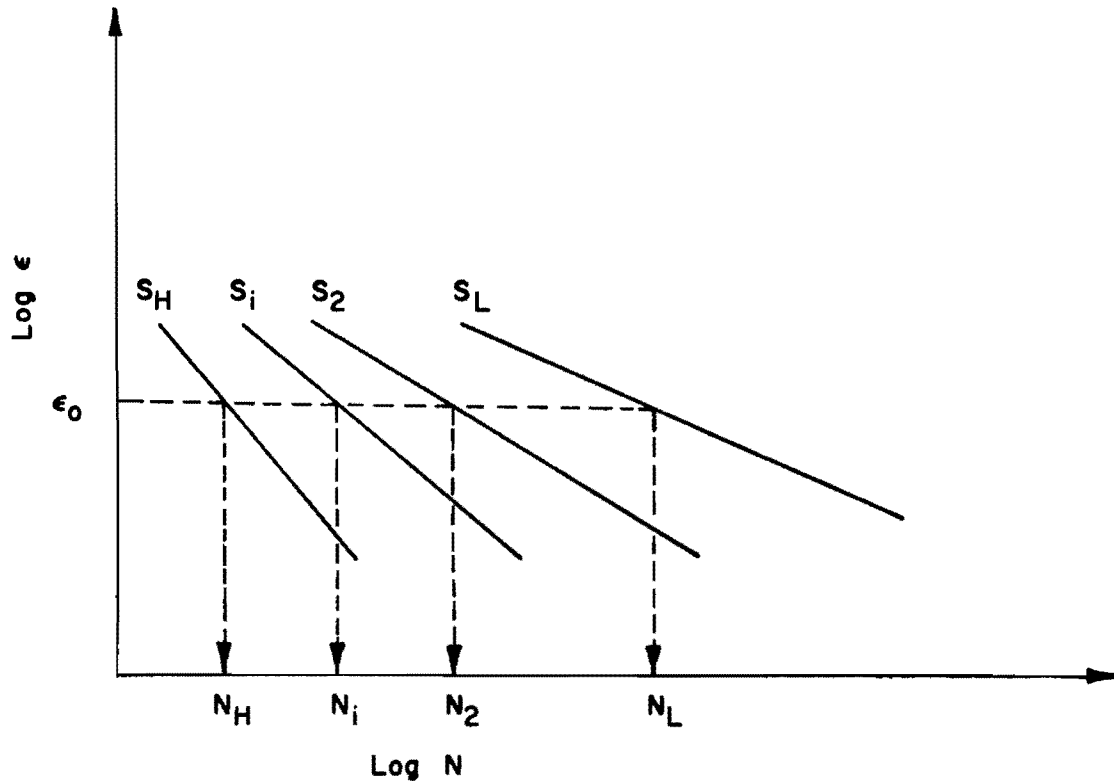
\bar{N} = average number of cycle applications till failure,

ϵ = strain level (constant strain fatigue test), and

A and B = fatigue constants.

According to the preceding concept the fatigue constants will vary with stiffness. An experiment was designed to determine these constants in the laboratory and to establish a criterion for estimating the cumulative damage. However, due to the high cost of such an experiment, it was suggested that the experiment be performed in the future. Therefore, fatigue constants were estimated from available data (Chapter 10). To estimate the cumulative damage due to temperature cycling the following formula was hypothesized:

$$\begin{aligned} D &= \sum_{i=1}^K \sum_{j=1}^M \frac{n_{ij}}{N_{ij}} \\ &= \frac{n_{11}}{N_{11}} + \frac{n_{12}}{N_{12}} + \dots + \frac{n_{1M}}{N_{1M}} \\ &+ \frac{n_{21}}{N_{21}} + \frac{n_{22}}{N_{22}} + \dots + \frac{n_{2M}}{N_{2M}} \\ &+ \dots \\ &+ \frac{n_{K1}}{N_{K1}} + \frac{n_{K2}}{N_{K2}} + \dots + \frac{n_{KM}}{N_{KM}} \end{aligned} \quad (9.5)$$



- S_L = low stiffness,
- S_H = high stiffness,
- S_i = any intermediate stiffness,
- N = number of temperature cycles until failure,
- ϵ = strain level.

Fig 9.6. A conceptual diagram showing the relation between strain and number of cycle applications until failure under a constant strain fatigue mode.

where

- D = accumulated damage,
- K = number of equal strain level groups,
- M = number of equal stiffness level groups,
- n = actual number of cycle applications, and
- N = number of cycle applications till failure.

In formulating the above hypothesis, it was assumed that the damage caused by each cycle is irrecoverable and hence the cumulative damage is a simple addition of all individual damages disregarding their sequence of occurrence.

The logarithm of the average number of cycles till failure \bar{N} has been shown to be normally distributed (Ref 46). For a particular confidence level α , the number of cycle applications until failure N_α can be expressed as follows:

$$\text{Log } N_\alpha = \text{Log } \bar{N} - Z_\alpha \text{Log } SD_N \quad (9.6)$$

where

Z_α = value from the normal tables corresponding to a confidence level α , and

SD_N = standard deviation of N .

From Eqs 9.5 and 9.6, the probability of failure $P(F)$ can be expressed as follows:

$$P(F) = \text{probability} \left(\sum_{i=1}^K \sum_{j=1}^M \frac{n_{ij}}{N_{\alpha_{ij}}} \geq 1.0 \right) \quad (9.7)$$

The best way to explain the above concept is through a numerical example.

For a particular road section under particular environmental conditions the accumulated damage $\left(\sum_{i=1}^K \sum_{j=1}^M \frac{n_{ij}}{N_{\alpha_{ij}}} \right)$ was estimated, after each month from

construction, at different confidence levels (Table 9.1). The relationship between the accumulated damage and the confidence levels after x month from construction is shown in Fig 9.7. The probability of failure after x month can be interpolated from Fig 9.7 as follows:

$$P(F) = 1.0 - \text{the confidence level associated with accumulated damage of } 1.0$$

$$P(F) = 1.0 - 0.93 = 0.07$$

To transfer the probability of failure into cracking, the procedure explained in Chapter 8 was followed:

$$\text{Cracking in } ft^2/1000 ft^2 = 0.07 \times 1000 = 70.0$$

$$\text{Cracking in linear } ft/1000 ft^2 = 70.0/5.0 = 14.0$$

SUMMARY AND CONCLUSIONS

- (1) Cracking estimated from the above model is referred to as thermal fatigue cracking.
- (2) The developed system for predicting thermal-fatigue cracking is unique in nature, considering that this is the first time that both fatigue and stochastic variations are being utilized to predict the distress resulting from temperature cycling.
- (3) The usefulness and the behavior of the model are disclosed in Chapter 10.
- (4) As both thermal-fatigue cracking and low-temperature cracking (see Chapter 8) are functions of time, they may be appropriately added to estimate the total temperature cracking after a specified time from construction.

TABLE 9.1. ACCUMULATED DAMAGE

$$\left[\sum_{i=1}^{i=k} \sum_{j=1}^{j=M} \frac{n_{ij}}{N_{\alpha_{ij}}} \right]$$

Time (months) Confidence Level (percent)	1	2	3	--	--	x	--	--	--
	99	0.1	--				1.2		
95	0.05	--				1.05			
90	0.02	--				.95			
85	0.01	--				.9			
80	--	--				.8			
--						--			

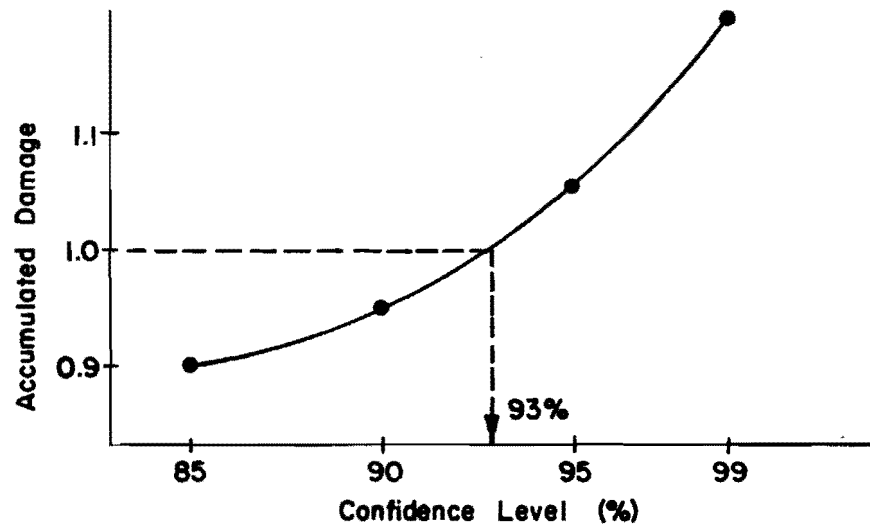


Fig 9.7. Relationship between accumulated damage and confidence level after x month.

This page replaces an intentionally blank page in the original.

-- CTR Library Digitization Team

CHAPTER 10. COMPUTERIZED SYSTEM, IMPORTANT VARIABLES
AND SYSTEM VERIFICATION

In this chapter, a computerized system for predicting low-temperature and thermal-fatigue cracking is developed. The theories upon which the system is developed are those presented and discussed in Chapters 3 and 5-9. Figure 10.1 shows a summary flow chart of the system, in which the calculations may be expressed in steps as follows:

- (1) From the temperature system (Chapter 9) calculate the daily mean air temperature and solar radiation.
- (2) Calculate hourly pavement temperature for each day (Chapter 3).
- (3) Locate the maximum and minimum pavement temperatures for each day.
- (4) Starting from the maximum temperature and going down on an hourly basis to the minimum temperature, estimate the stiffness at the middle of the temperature intervals (Chapter 5), and the increments of strain and stress (Chapter 7).
- (5) Accumulate the increments of strain and stress to estimate the maximum strain and stress for that day.
- (6) Estimate the strength corresponding to the maximum stress.
- (7) Predict low-temperature cracking (Chapter 8).
- (8) Predict thermal-fatigue cracking (Chapter 9).
- (9) Total temperature cracking is the appropriate addition of low-temperature and thermal-fatigue cracking.

In Chapter 5, two mathematical models for estimating asphalt stiffness were developed for: (1) converting Van der Poel's nomograph to a computer form, in which the loading time is limited to a few selected levels, (2) regression equations for Heukelom and Klomps' nomograph, in which the time of loading is a variable. However in examining the behavior of the regression equations, it was found that at high stiffnesses, the predicted values are somewhat lower than the measured. Therefore, both models were included in the system if the thermal loading time is one hour, which represents average conditions, the first model is utilized; otherwise, when thermal loading time is not one hour, the second model is utilized.

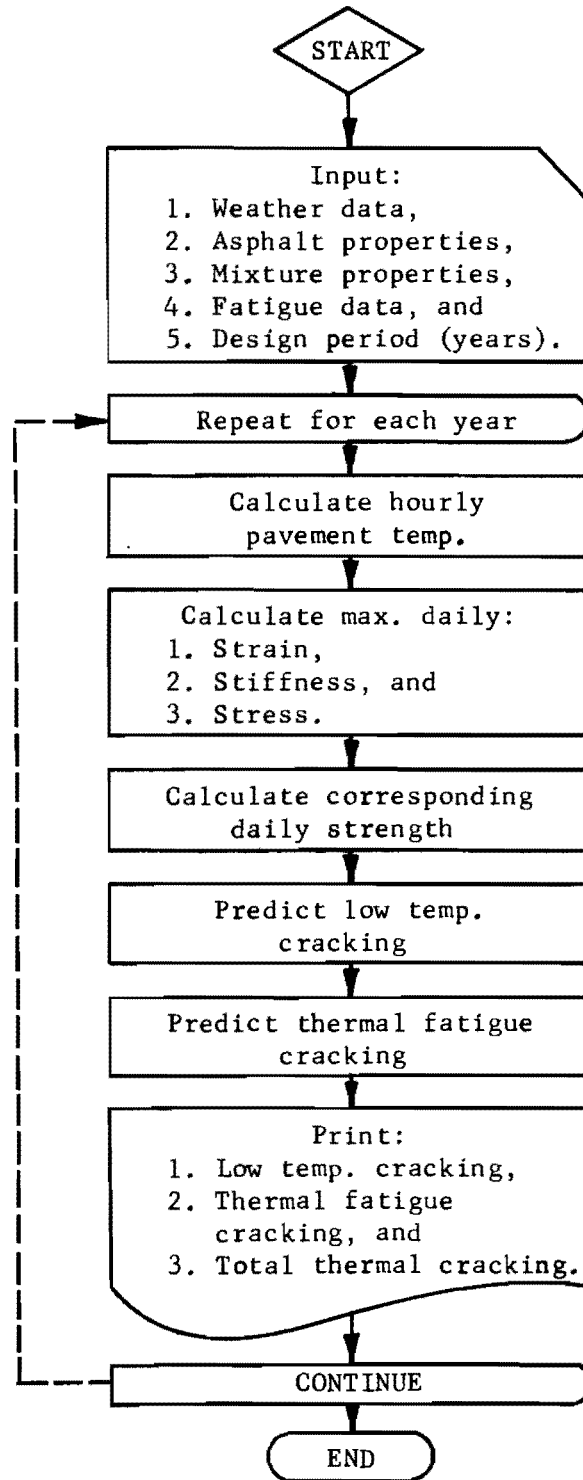


Fig 10.1. Summary flow chart of the system.

As shown in Chapter 9, the general expression for estimating the fatigue life can be written as follows:

$$N = A \left(\frac{1}{\epsilon} \right)^B \quad (9.4)$$

where the fatigue constants A , and B vary with the stiffness of the asphalt concrete. To incorporate this concept into the computerized system, the fatigue constants were estimated at two stiffness levels between which the constants at any other stiffness can be interpolated.

The two stiffness levels chosen were 10.0 and 5.0 times $(10)^6$ psi, since they represent the lowest and highest stiffness values for asphalt concrete mixtures. The four fatigue constants, two for each stiffness level, were estimated so as to result in the amount of temperature cracking reported after the eighth year in Road No. 1, asphalt supplier No. 2 (Ref 47) (see Fig 10.8). Other factors that are considered in estimating the four fatigue constants are the following:

- (1) At high stiffness, the number of temperature cycles until failure is less than that at low stiffness for the same strain level.
- (2) The slope of the logarithmic relationship between the strain level and the number of temperature cycles until failure is steeper for high stiffness than for low stiffness (Fig 9.6).

The fatigue constants are shown in Table 10.1.

At this stage, it should be emphasized that the four fatigue constants were estimated to fit one data point and were kept the same for all the other data from different projects that were used for the verification. Therefore, if the verification (conducted in a later section) showed the system to be reliable, that would be in essence a proof of the thermal fatigue theory presented in Chapter 9. To estimate the fatigue constants at any other stiffness level between the selected two levels, linear interpolation among the logarithmic transformation of the stiffness and the fatigue constants was utilized, since it was shown to be the most rational.

Table 10.1 shows the input data for the developed program as printed out on the first page of the computer output; Table 10.2 is a typical print out of the temperature cracking calculations for each year after construction. The input guide and the program listing are given in Appendix 5.

TABLE 10.1 TYPICAL PRINT OUT OF THE INPUT DATA - FIRST PAGE OF THE COMPUTER OUTPUT.

FAV.SEC.NO. 63 SIE ANNE - 3/23/1972

TIME OF LOADING ,SEC = 3600.000

		MONTH CODE			
JULY	AUG.	SEPT.	OCT.	NOV.	DEC.
1	2	3	4	5	6
JAN.	FEB.	MAR.	APR.	MAY.	JUNE
7	8	9	10	11	12

AIR TEMPERATURE

ANNUAL AVERAGE	,DEG.F	=	36.600
ANNUAL RANGE	,DEG.F	=	80.000
DAILY RANGE	,DEG.F	=	20.900

FACTORS AFFECTING PAV. TEMP.

ANNUAL AVE.SCLAR RAD.	,LANGLEYS	=	312.000
JULY AVE.SCLAR RAD.	,LANGLEYS	=	514.000
ANNUAL AVE.WIND VEL.	,MPH.	=	11.000
SURFACE ABSORBTIVITY		=	.950
DEPTH FOR CALCULATION,IN.		=	0.000
MIX. CONDUCTIVITY	,BTU-FT-HR-F.	=	.700
MIX. SPECIFIC HEAT	,BTU-LB-F.	=	.220
MIX. DENSITY	,LB/FT3	=	148.000

ASPHALT PROPERTIES

ORIG. PENETRATION	,DMM-5SEC.	=	192.000
PEN. TEST TEMP.	,DEG.F	=	77.000
ORIG. SOFTENING POINT	,DEG.F	=	95.000
THIN FILM CVEN TEST	,PCT.ORIG.PEN.	=	44.100

MIXTURE PROPERTIES

PCT. ASPHALT	,BY WT.OF AGG.	=	4.800
ASPH. SPECIFIC GRAV.		=	1.000
AGG. SPECIFIC GRAV.		=	2.650
MIX. AIR VOIDS	,PERCENT	=	4.900
AGG. VOL. CONCENTRATION	-CALCULATED	=	.871
COEF. OF CONTRACTION	TEMP (F)	ALPH(10**5)	
	70		1.000
	210		1.800
COEF. OF VARIATION OF ALPH		=	.100
MAX. TEN.STRENGTH	,PSI	=	450.000
COEF. OF VARIATION OF MAX.STRENGTH		=	.200

INPUT FATIGUE DATA

FATIGUE CURVE			N=A*(1.0/STRAIN)**B
MIX.STIF.(PSI)	CONST.A		CONST.B
1.0000E+01	1.0000E-02		3.0000E+00
5.0000E+06	8.0000E-13		3.9500E+00

TABLE 10.2 TYPICAL PRINT OUT OF THE TEMPERATURE CRACKING CALCULATIONS

FAV. SEC. NO. 63 STE. ANGLE - 3/27/1972

YEAR NO. 1

DAY	MIN. PVT. TEMP., DEG. F	MAX. STIF, PSI	STRENGTH, PSI	MAX. STRESS, PSI	MAX. STRAIN	PEN	TRR	PI
30	6.8673E+01	1.5523E+02	1.1250E+01	1.7903E-02	5.8880E-04	104.72	108.06	-1.57
60	5.3289E+01	1.0795E+03	1.1250E+01	1.2010E-01	5.1314E-04	92.02	109.37	-1.69
90	3.2275E+01	1.8022E+04	4.3782E+01	1.9262E+00	4.1613E-04	84.67	110.38	-1.74
120	1.1261E+01	2.3016E+05	2.0664E+02	2.4259E+01	3.2645E-04	72.55	111.22	-1.75
150	-4.1226E+00	1.0861E+06	4.4208E+02	1.2765E+02	2.6544E-04	75.65	111.97	-1.75
180	-9.7533E+00	1.9028E+06	4.2017E+02	2.2010E+02	2.4409E-04	72.51	112.65	-1.74
210	-4.1226E+00	1.1948E+06	4.4958E+02	1.4156E+02	2.6544E-04	69.89	113.27	-1.73
240	1.1261E+01	3.1097E+05	2.4534E+02	2.2174E+01	3.2645E-04	67.65	113.84	-1.71
270	3.2275E+01	2.7810E+04	5.9322E+01	2.9744E+00	4.1613E-04	65.69	114.39	-1.70
300	5.3289E+01	1.9220E+03	1.1250E+01	2.3139E-01	5.1314E-04	63.95	114.90	-1.68
330	6.8673E+01	3.6024E+02	1.1250E+01	4.2966E-02	5.8880E-04	62.39	115.39	-1.66
360	7.4307E+01	2.0392E+02	1.1250E+01	2.3709E-02	6.1747E-04	60.97	115.85	-1.64

LOW TEMP CRACKING = 17.6922FT/1000FT2

THERMAL DISTRESS, FATIGUE- YEAR NO. 1

MONTH	AVE. MAX. STIF, PSI	AVE. MAX. STRAIN	FRONT CONST.	EXP. CONST.	N (FATIGUE LIFE)
1	8.8842E+01	6.0731E-04	2.0861E-04	3.1406E+00	2.6379E+06
2	4.5679E+02	5.5270E-04	1.1467E-05	3.2502E+00	4.4379E+05
3	6.6910E+03	4.6355E-04	9.8641E-08	3.4384E+00	2.8665E+04
4	9.3438E+04	3.6813E-04	9.2340E-11	3.6338E+00	2.7787E+03
5	6.5963E+05	2.9193E-04	2.8948E-11	3.7858E+00	6.9704E+02
6	1.6708E+06	2.5049E-04	5.5782E-12	3.8603E+00	4.4205E+02
7	1.7131E+06	2.5100E-04	5.3367E-12	3.8623E+00	4.2538E+02
8	7.2470E+05	2.9397E-04	2.4503E-11	3.7933E+00	6.1073E+02
9	1.2172E+05	3.7112E-04	5.7802E-11	3.6540E+00	1.9812E+03
10	1.0018E+04	4.6678E-04	4.8250E-08	3.4676E+00	1.7129E+04
11	8.7095E+02	5.5522E-04	3.6551E-08	3.2945E+00	1.9423E+05
12	2.4577E+02	6.0826E-04	3.4387E-08	3.2083E+00	7.1440E+05

LOG. STANDARD DEVIATION OF FATIGUE LIFE .250000

NO. OF MONTHS	CI-FT2/1000FT2	CI-FT/1000FT2
6	.0019	.0004
7	.0902	.0180
8	2.1397	.4279
9	6.9005	1.3801
10	9.3403	1.8681

TOTAL THERMAL CRACKING = 19.5683FT/1000FT2

YEAR NO. 2

DAY	MIN. PVT. TEMP., DEG. F	MAX. STIF, PSI	STRENGTH, PSI	MAX. STRESS, PSI	MAX. STRAIN	PEN	TRR	PI
30	6.8673E+01	3.9920E+02	1.1250E+01	4.7741E-02	5.8880E-04	59.68	116.30	-1.62
60	5.3289E+01	2.3428E+03	1.1250E+01	2.7509E-01	5.1314E-04	58.48	116.73	-1.60
90	3.2275E+01	3.8366E+04	7.1004E+01	3.9451E+00	4.1613E-04	57.38	117.15	-1.59
120	1.1261E+01	3.8099E+05	2.7882E+02	4.3617E+01	3.2645E-04	56.34	117.55	-1.57
150	-4.1226E+00	1.6505E+06	4.3399E+02	1.9366E+02	2.6544E-04	55.38	117.94	-1.55
180	-9.7533E+00	2.7423E+06	4.0114E+02	2.0117E+02	2.4409E-04	54.47	118.32	-1.53
210	-4.1226E+00	1.6809E+06	4.3171E+02	2.0149E+02	2.6544E-04	53.61	118.68	-1.51
240	1.1261E+01	3.9133E+05	2.7513E+02	4.8297E+01	3.2645E-04	52.79	119.04	-1.49
270	3.2275E+01	4.3654E+04	7.8732E+01	4.8723E+00	4.1613E-04	52.02	119.39	-1.48
300	5.3289E+01	4.0113E+03	1.5525E+01	7.9114E-01	5.1314E-04	51.28	119.73	-1.46
330	6.8673E+01	5.3109E+02	1.1250E+01	4.8272E-02	5.8880E-04	50.58	120.06	-1.44
360	7.4307E+01	3.0437E+02	1.1250E+01	2.7846E-02	6.1747E-04	49.91	120.39	-1.43

LOW TEMP CRACKING = 58.2226FT/1000FT2

THERMAL DISTRESS, FATIGUE- YEAR NO. 2

MONTH	AVE. MAX. STIF, PSI	AVE. MAX. STRAIN	FRONT CONST.	EXP. CONST.	N (FATIGUE LIFE)
1	2.6249E+02	6.0731E-04	3.0602E-04	3.2127E+00	6.6030E+05
2	1.0492E+03	5.5270E-04	2.6282E-04	3.3074E+00	1.5616E+05
3	1.3832E+04	4.6355E-04	2.7243E-08	3.4911E+00	1.1869E+04
4	1.6889E+05	3.6813E-04	3.2355E-10	3.6792E+00	1.3938E+03
5	9.8610E+05	2.9193E-04	1.4198E-11	3.8178E+00	4.4377E+02
6	2.0877E+06	2.5049E-04	3.7591E-12	3.8783E+00	3.4604E+02
7	2.0878E+06	2.5160E-04	3.7591E-12	3.8783E+00	3.4226E+02
8	9.9731E+05	2.9397E-04	1.3917E-11	3.8187E+00	4.2672E+02
9	1.7555E+05	3.7112E-04	3.0209E-11	3.6822E+00	1.2934E+03
10	1.5930E+04	4.6678E-04	2.1214E-08	3.5015E+00	9.7659E+03
11	1.4256E+03	5.5522E-04	1.5267E-06	3.3287E+00	1.0485E+05
12	3.8248E+02	6.0826E-04	1.5710E-05	3.2382E+00	4.0720E+05

LOG. STANDARD DEVIATION OF FATIGUE LIFE .250000

NO. OF MONTHS	CI-FT2/1000FT2	CI-FT/1000FT2
15	9.5955	1.9191
16	10.1240	2.0248
17	14.5822	2.9164
18	35.1012	7.0202
19	76.3115	15.2623
20	133.4524	26.6905
21	186.6858	37.3372
22	203.2223	40.6445

TOTAL THERMAL CRACKING = 98.8678FT/1000FT2

SYSTEM BEHAVIOR

Figure 10.2 shows the relationship between temperature cracking and the number of years from construction, as computed from the system. In this figure, the values of temperature cracking are those corresponding to assumed asphalt mixture properties and surrounding environmental conditions and are not necessarily typical values. However, the rate of increase of low-temperature and thermal-fatigue cracking is usually similar to what is shown; i.e., the rate of increase of low-temperature cracking is usually much less than that for thermal-fatigue cracking. Study cases performed using the developed system showed that the rate of increase of thermal-fatigue cracking is higher during the winter than the summer, as shown in Fig 10.3. Furthermore, it is important to note that the major cause of temperature cracking is either low temperature or fatigue, depending on the asphalt mixture properties and the surrounding environmental conditions.

IMPORTANT VARIABLES

One of the best available techniques for evaluating the significance of independent variables is to perform a complete sensitivity analysis, in which the interaction between the independent variables can be detected. Due to the extensive computer time required to perform such an analysis, a simple analysis that shows the importance of the individual variables without considering their interaction was performed. The dependent variable that was considered for the analysis is thermal-fatigue cracking. However, it is anticipated that the important variables for the low-temperature cracking will be the same as those for thermal-fatigue cracking, in addition to the tensile strength of the asphalt concrete mixture. Reasonable values were assigned to each of the independent variables, except that the values assigned for the fatigue constants were selected so as to result in a considerable amount of thermal-fatigue cracking in a short period of time (one year). The reason for that is to reduce the required computer time. One variable at a time was then increased by 10 percent, keeping the rest at their assigned values, and the resulting difference in thermal fatigue cracking was determined; Table 10.3 shows the result of the analysis. Figure 10.4 depicts the importance of the independent variables excluding the fatigue constants. From the figure, one may classify the independent variables into five levels in a descending order of importance as follows:

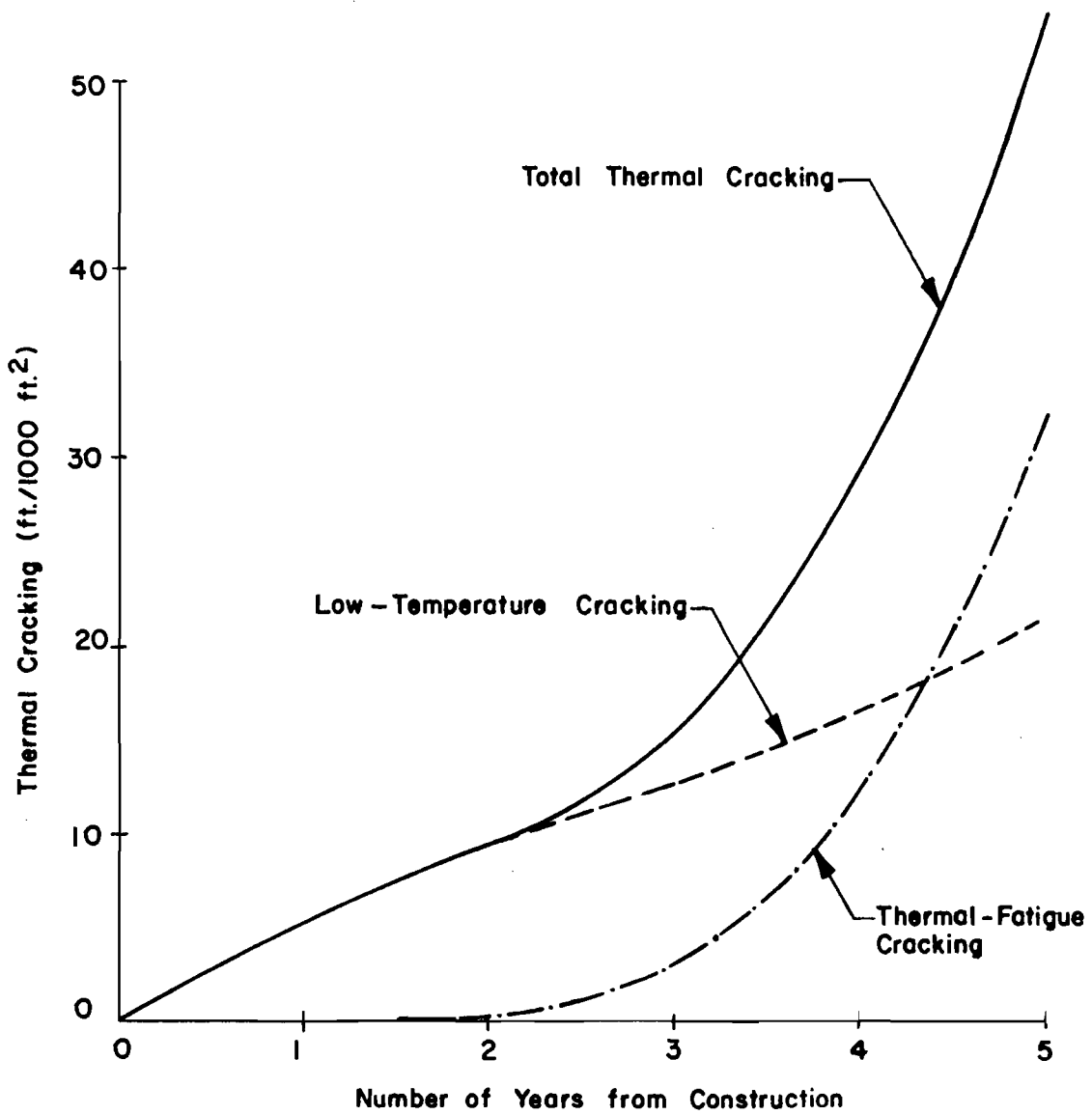


Fig 10.2. Schematic diagram showing the relationship between thermal cracking and the number of years from construction (not necessarily typical).

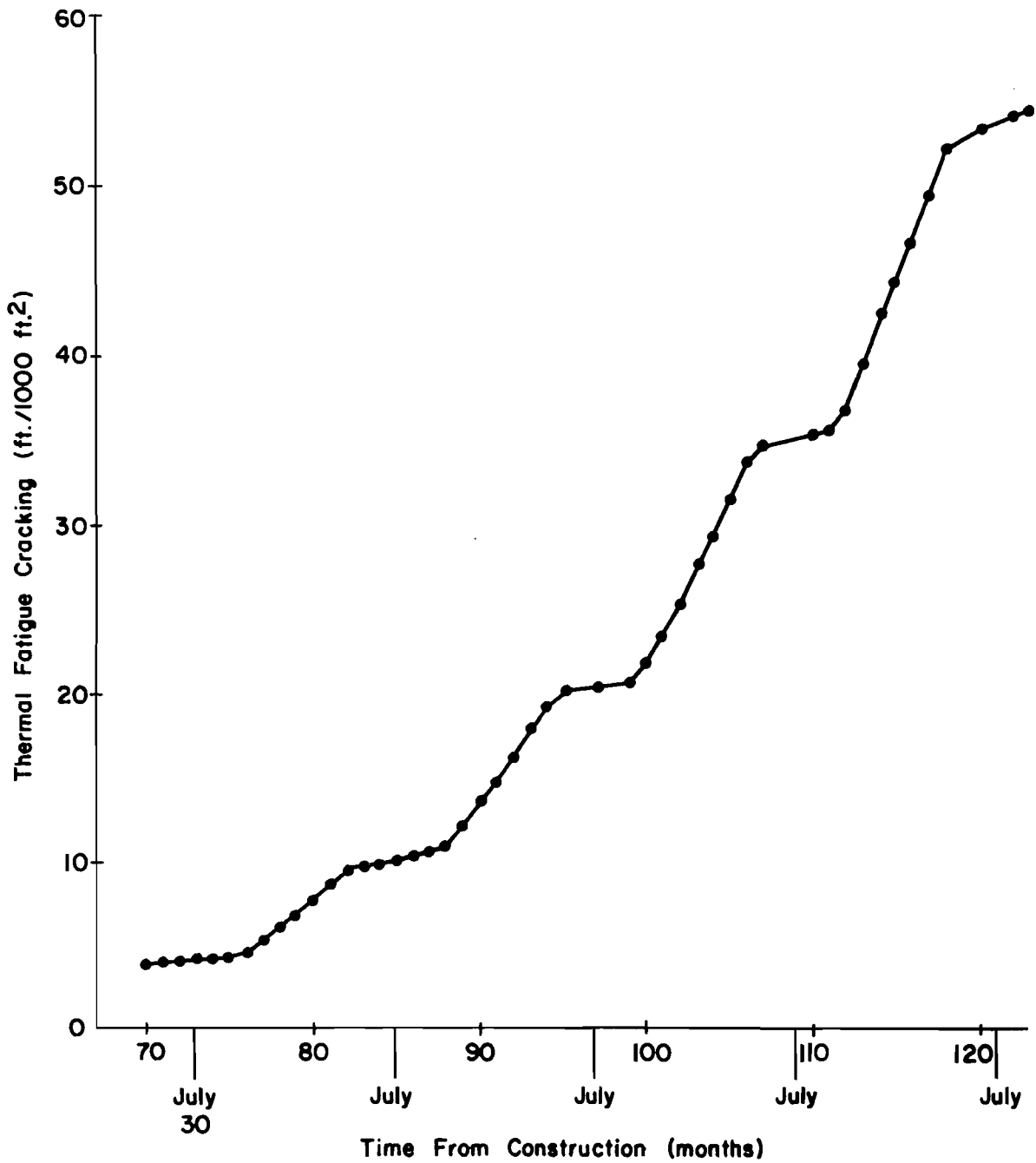


Fig 10.3. Detailed diagram showing the increase in thermal-fatigue cracking after each month from construction.

TABLE 10.3. EVALUATION OF VARIABLES IMPORTANCE FOR PREDICTING THERMAL-FATIGUE CRACKING

Independent Variable	Assigned Value	Fatigue Crack. at 10% Increase, ft/1000 ft ²	Change in * Fatigue Crack.	Percent Change	Rank
Annual average temperature, °F	50.0	65.26	- 41.90	-39.10	5
Annual temperature range, °F	70.0	124.30	17.14	15.99	12
Daily temperature range, °F	25.0	138.20	31.04	28.96	7
Annual average wind velocity, mph	8.0	105.57	- 1.59	- 1.48	16
Annual average solar radiation, L	400.0	152.65	45.49	42.45	3
July average solar radiation, L	600.0	74.13	- 33.03	-30.82	6
Original penetration, 77°F, 5 seconds**	110.0	--	--	--	-
Original softening point, °F**	110.0	--	--	--	-
TFOT (percent original penetration)	55.0	83.36	- 23.80	-22.20	8
Percent asphalt, by weight aggregate	5.0	84.14	- 23.02	-21.48	9
Aggregate specific gravity	2.5	84.14	- 23.02	-21.48	10
Asphalt specific gravity	1.0	129.54	22.38	20.88	11

(Continued)

TABLE 10.3. (Continued)

Independent Variable		Assigned Value	Fatigue Crack. at 10% Increase, ft/1000 ft ²	Change in * Fatigue Crack.	Percent Change	Rank
Percent air voids		5.0	99.99	- 7.17	- 6.69	14
$\alpha \times 10^5 / ^\circ\text{F}$		1.2	149.54	42.38	39.54	4
Low stiffness (10 psi)	A	10^{-3}	103.18	- 3.98	- 3.71	15
Fatigue constants	B	2.5	22.62	- 84.54	-78.89	2
High stiffness (5×10^6 psi)	C	5×10^{-13}	97.60	- 9.56	- 8.92	13
Fatigue constants	D	4.0	0.21	-106.95	-99.89	1
Logarithmic standard deviation of fatigue		0.25	106.36	- 0.8	- 0.74	17

* Fatigue cracking for the assigned values without 10 percent increase = $107.16 \text{ ft}/1000 \text{ ft}^2$

** Cannot be evaluated individually due to their evident interaction.

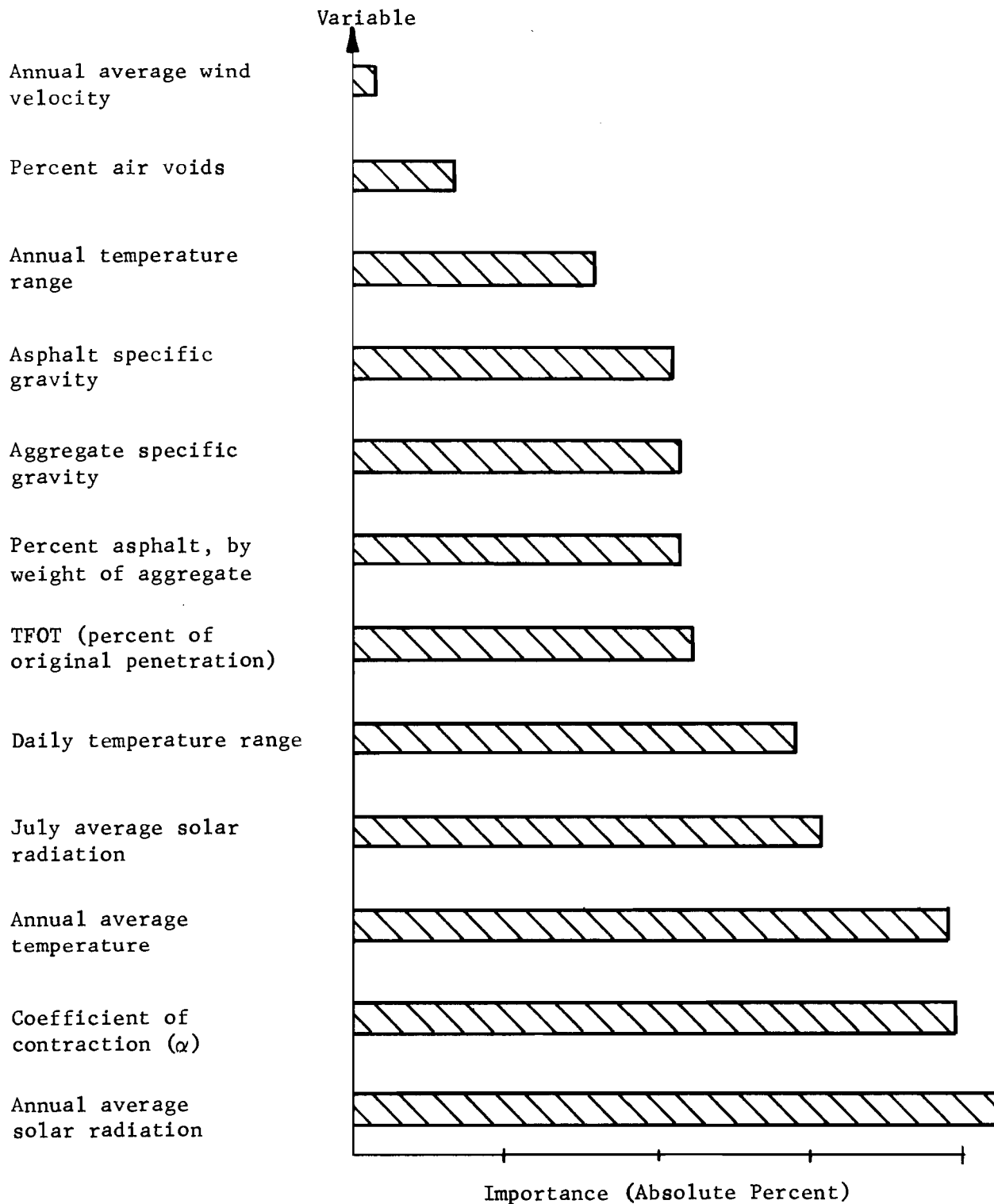


Fig 10.4. Importance of individual variables regarding their effect on thermal-fatigue cracking.

- (1) a. annual average solar radiation,
b. coefficient of thermal contraction,
c. annual average temperature.
- (2) a. July average solar radiation,
b. daily temperature range.
- (3) a. thin-film oven test, percent of original penetration,
b. percent asphalt in the mixture, by weight of aggregate,
c. aggregate specific gravity,
d. asphalt specific gravity,
e. annual temperature range.
- (4) a. percent air voids in the mixture.
- (5) a. annual average wind velocity.

Because of the evident interaction effect between the penetration and the softening point of the asphalt, the individual evaluation of their importance could be misleading. Therefore, they were omitted from the above analysis and a separate study on their influence on thermal-fatigue cracking was performed. Using the assigned values for the rest of the variables (Table 10.3), three levels were selected for both penetration and softening point and a factorial experiment was designed (Table 10.4). Figure 10.5 shows the result of the analysis, from which one may conclude the following:

- (1) The higher the penetration (the softer the asphalt), the lower the thermal-fatigue cracking.
- (2) If the penetration is held constant at the low level (100) and the softening point is allowed to change from the medium to the high level (110 to 115), the thermal-fatigue cracking decreases. If, however, the penetration is held constant at the high level (150), and the softening point is allowed to change from the medium to the high level, the thermal-fatigue cracking increases. This indicates the interaction effect between the penetration and the softening point, which can be attributed to the change of the temperature susceptibility of the asphalt.
- (3) At the low penetration level (100), the effect of the change of the softening point (105 to 115) is more significant than at the high penetration level (150).

SYSTEM VERIFICATION

A search was carried out to locate some projects in which temperature cracking was measured and reported separately from traffic load cracking.

TABLE 10.4. THERMAL-FATIGUE CRACKING AFTER 1 YEAR

Orig. Soft Point, °F	Orig. pen. at 77° F,		
	105	110	115
100	133.20	118.16	115.83
125	103.18	86.49	86.49
150	61.00	57.54	61.00

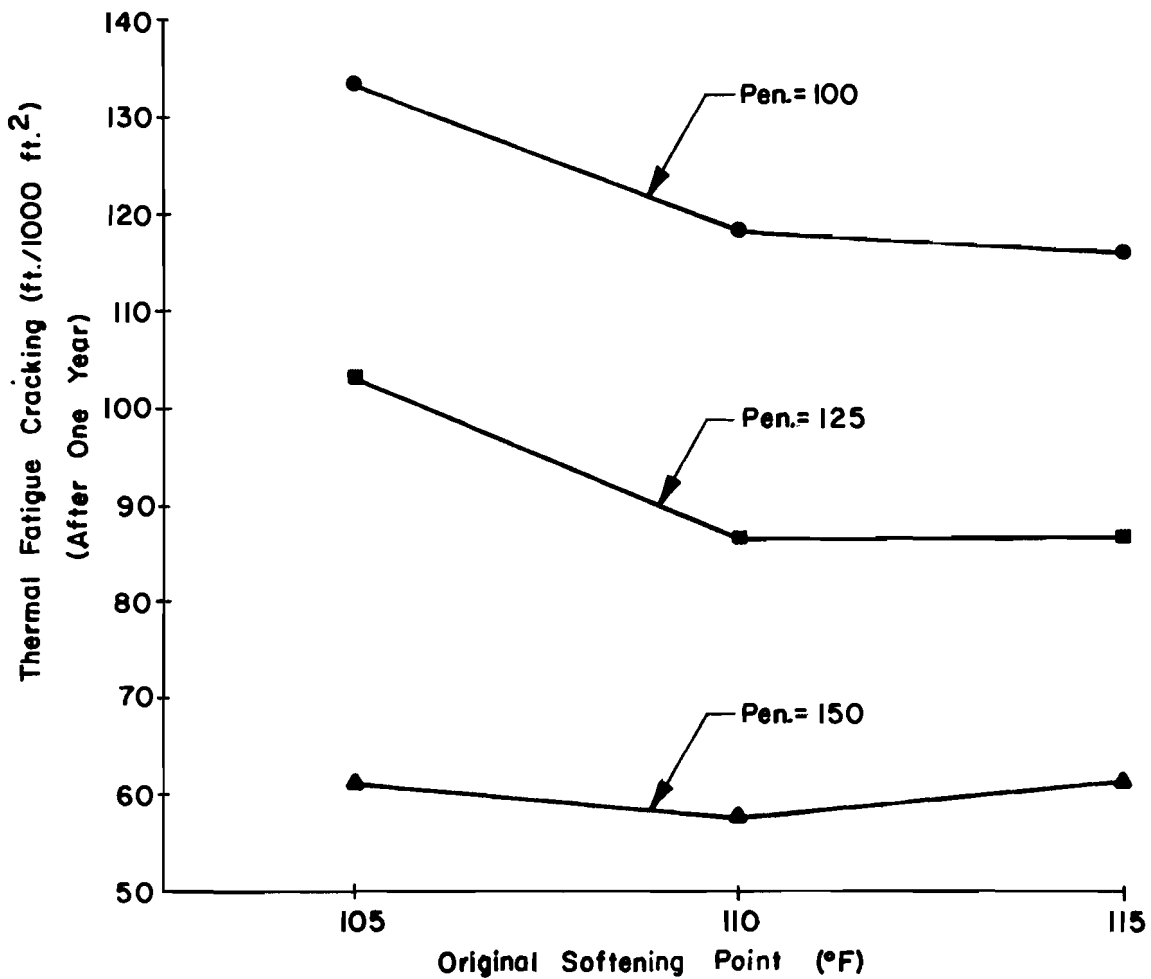


Fig 10.5. Effect of penetration and softening point on thermal-fatigue cracking.

Unfortunately, very few projects were found where such measurement was reported. Two of these projects were used to verify the system. A description of each project and the results of the analysis are presented in the next sections.

(1) Ontario Test Roads

In this project McLeod (Ref 47) made a survey of temperature cracking after the eighth, ninth, tenth, and eleventh years of service of asphalt pavements on three southwestern Ontario Test Roads, about 40 miles apart, that were constructed in 1960, all over clay loam subgrades. Each test road was six miles long and contained three 2-mile test pavements. The pavement in each 2-mile test section contained a single 85/100 penetration asphalt cement. Three 85/100 penetration asphalt cements from three different asphalt suppliers were repeated in each of the three 6-mile test roads (Fig 10.6). The properties of the asphalt from the different suppliers are given in Table 10.5. All the necessary information about the mixture properties was available except the tensile strength, which was assumed to have a maximum value of 500 psi. The environmental variables were estimated from the closest available weather station, London A. (Ref 48). The data used for the calculations are given in Appendix 6. Figures 10.7, 10.8, and 10.9 show the comparison between the measured and predicted thermal cracking for the three asphalt suppliers. Because there is not any basis upon which to differentiate between the three roads, they can be considered as replicates. However, since the fatigue constants were adjusted for Road No. 1, it would be more appropriate to compare the predicted thermal cracking with that measured in Road No. 1. In general, the agreement between the measured and predicted cracking seems to be encouraging.

(2) Ste. Anne Test Road (Refs 5, 15, 79)

The test road was constructed in 1967 for the study of transverse cracking of asphalt pavements. It is located 25 miles east of Winnipeg in the vicinity of Ste. Anne, Manitoba. The characteristics of the test road were described in Ref 79 as follows: "The road is composed of twenty-nine 400-foot pavement sections, 24 feet wide, constructed on clay and sand subgrades. The test section variables include two different types and three different grades of asphalt, two asphalt contents, two aggregate gradations, limestone and granite aggregates, and three road structure designs. The variables, shown in Table 10.6, in their interaction and combinations, were selected as being

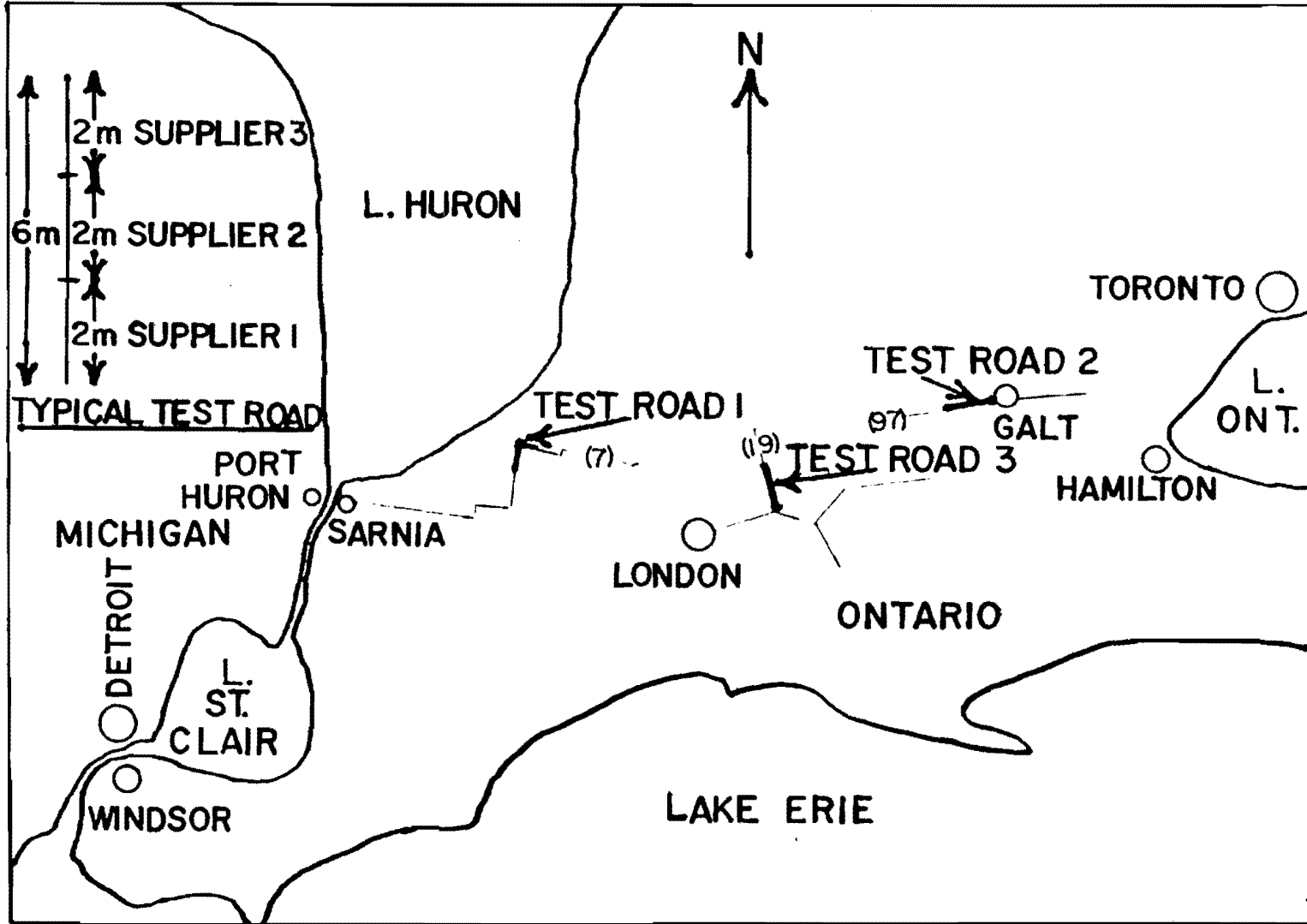


Fig 10.6. Ontario test roads (after McLeod, Ref 47).

TABLE 10.5. INSPECTION DATA ON ORIGINAL 85/100 PENETRATION ASPHALT CEMENTS USED FOR ONTARIO'S THREE 1960 TEST ROADS (Ref 47)

Supplier Number	1	2	3
Flash Point COC ^{°F}	585	525	615
Softening Point R and B ^{°F}	115	115	119
Penetration 100 gr. 5 sec 77 ^{°F}	83	96	87
200 gr. 60 sec 39.2 ^{°F}	25	36	22
200 gr. 60 sec 32 ^{°F}	22	26	19
Penetration Ratio	30.2	37.5	25.3
Ductility at 77 ^{°F} , 5 cm/min	150+	150+	128
Viscosity Centistokes at 275 ^{°F}	460	365	210
Centistokes at 210 ^{°F}	3953	2763	1472
Thin Film Oven Test			
% loss by weight	0.1	0.3	0.0
Residue			
% Original Penetration at 77 ^{°F}	67.5	60.4	61.0
Ductility at 77 ^{°F} , 5 cm/min	150+	110	115
Solubility in n-hexane			
% asphaltenes	19.7	24.7	18.8
Penetration Index (Pfeiffer and Van Doormaal)	-1.00	-0.57	-0.21
Pen-vis number	-0.19	-0.36	-1.34

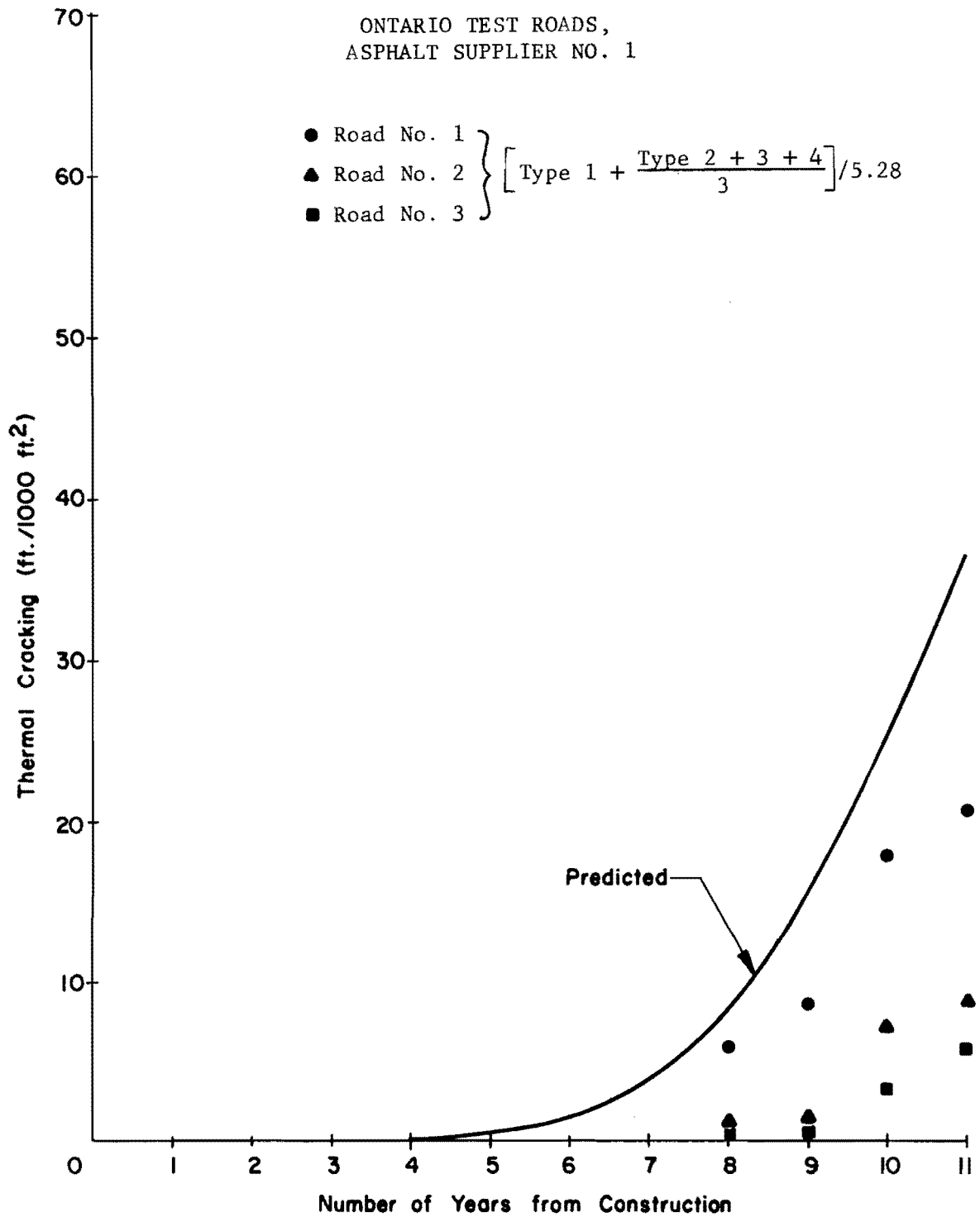


Fig 10.7. Comparison between predicted and measured thermal cracking.

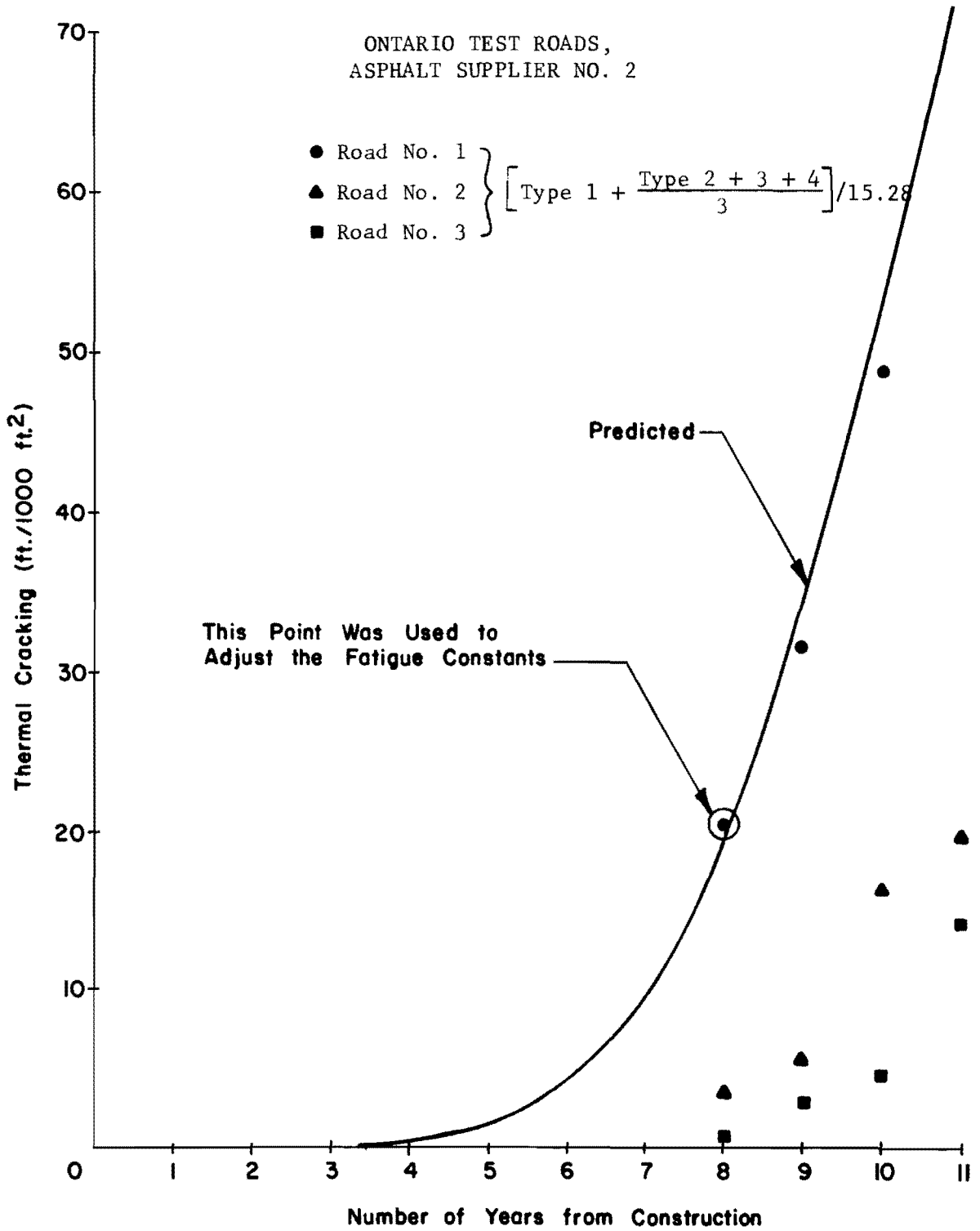


Fig 10.8. Comparison between predicted and measured thermal cracking.

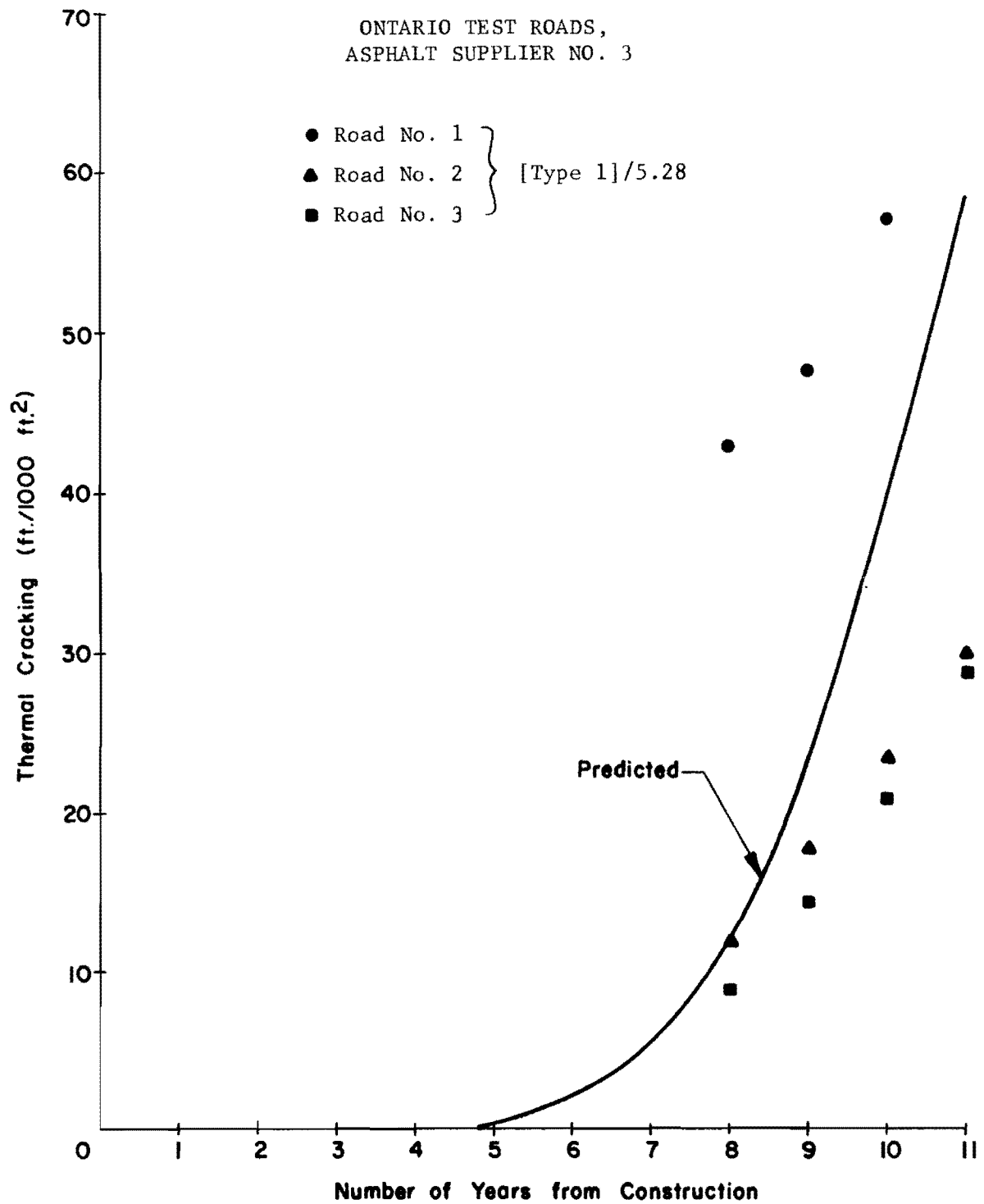


Fig 10.9. Comparison between predicted and measured thermal cracking.

TABLE 10.6. TEST ROAD DESIGN VARIABLES IDENTIFIED BY SECTION NUMBERS (Ref 79)

ROAD STRUCTURE	150-200 PENETRATION GRADE LOW VISCOSITY ASPHALT (WESTERN CANADIAN CRUDE)					150-200 PENETRATION GRADE HIGH VISCOSITY ASPHALT (WESTERN CANADIAN CRUDE)					300-400 PENETRATION GRADE LOW VISCOSITY ASPHALT (WESTERN CANADIAN CRUDE)			SC-5 ASPH. (W.C. CRUDE)	
	BELOW OPTIMUM ASPHALT CONTENT	BELOW OPTIMUM ASPHALT, CEMENT FILLER	OPTIMUM ASPHALT CONTENT	OPTIMUM ASPHALT CONTENT, CEMENT FILLER	ABOVE OPTIMUM ASPHALT CONTENT	BELOW OPTIMUM ASPHALT CONTENT	BELOW OPTIMUM ASPHALT, CEMENT FILLER	OPTIMUM ASPHALT CONTENT	OPTIMUM ASPHALT CONTENT, CEMENT FILLER	OPTIMUM ASPHALT CONTENT, 100% CRUSH IGNEOUS AGGREGATE	BELOW OPTIMUM ASPHALT CONTENT	BELOW OPTIMUM ASPHALT, CEMENT FILLER	OPTIMUM ASPHALT CONTENT	OPTIMUM ASPHALT CONTENT, CEMENT FILLER	OPTIMUM ASPHALT CONTENT
4 IN. PAVEMENT 16 IN. BASE COURSE CLAY SUBGRADE	54	55	63	53		57		62	56	51	58	59	61	60	52
4 IN. PAVEMENT 6 IN. BASE COURSE SAND SUBGRADE	74	76	67	75	77	73		66	72	78	71	70	68	69	79
10 IN. FULL DEPTH ASPHALT PAVEMENT CLAY SUBGRADE			64					65							

• All aggregates in bituminous pavement mix processed from glacial drift deposits (20% igneous, 80% limestone; 50% crush) unless otherwise indicated.

potentially important in the study of transverse pavement cracking." All the mixture properties are available in the above references, except the maximum tensile strength, which was determined for samples containing the optimum asphalt content by J. T. Christison et al (Ref 9). The fatigue constants were kept the same as for the Ontario Test Roads. The data used for the calculation are given in Appendix 6. The comparison between the measured and predicted temperature cracking are shown in Table 10.7, which indicates that the agreement is reasonable.

Discussion

The computed temperature cracking for both the Ontario Test Roads and Ste. Anne Test Road have shown the system to be reliable. The following observations were made from analyzing the results of the computations:

(1) Ontario Test Roads

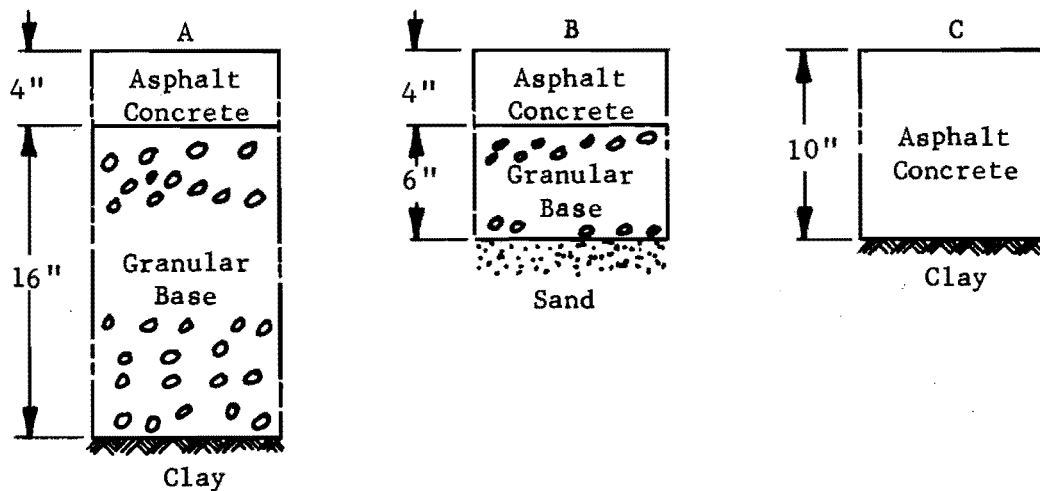
- (a) Temperature cracking was mainly thermal-fatigue cracking with a practically negligible amount of low-temperature cracking.
- (b) Sections constructed using asphalt from supplier No. 1 showed less temperature cracking than those constructed using asphalt from suppliers No. 2 and 3. The computations showed the same conclusion.
- (c) McLeod (Ref 47) explained the difference among asphalt from the various suppliers as the difference in the asphalt's temperature susceptibility. However, the analysis showed that the main difference was the percent of original penetration after the thin-film oven test. Asphalt from supplier No. 1 had the highest percentage of original penetration after the thin-film oven test. Therefore, the amount of asphalt hardening was relatively low after the mixing process, and hence the rate of increase of the temperature cracking (mainly thermal-fatigue cracking) was much lower than for asphalt from the other suppliers.
- (d) Adding the asphalt aging models (Chapter 6) to the fracture temperature concept discussed in Chapter 8, predicted temperature cracking was negligible compared to that predicted by the system. This can be explained by the fact that the temperature cracking in the Ontario Test Roads was mainly due to daily temperature cycling, which is not considered in the fracture temperature concept.

(2) Ste. Anne Test Road

- (a) Temperature cracking was a combination of thermal-fatigue and low-temperature cracking.

TABLE 10.7. COMPARISON BETWEEN MEASURED AND PREDICTED TEMPERATURE CRACKING AFTER TWO YEARS FROM CONSTRUCTION, STE. ANNE TEST ROAD

Asphalt Type	Section	Structure	Measured Crack, ft/1000 ft ² (Ref 79)	Average	Predicted Crack, ft/1000 ft ²
150/200 LVA	63	A	51.0	76.0	98.9
	67	B	154.0		
	64	C	22.9		
150/200 HVA	62	A	7.5	5.5	9.5
	66	B	5.6		
	65	C	3.3		
300/400 LVA	61	A	25.0	13.1	1.7
	68	B	1.25		



- (b) High viscosity asphalts showed much less temperature cracking than low-viscosity asphalts. The analysis reached the same conclusion. This can be explained by the observation that high-viscosity asphalts are less temperature-susceptible than low-viscosity asphalts. For instance, for the Ste. Anne Test Road, the high-viscosity asphalt had an original penetration index of -1.0, compared to -2.5 for the low-viscosity asphalt.
- (c) Different pavement structures having the same asphalt concrete mixture showed different temperature cracking. However, since the factor of pavement structure is not included in the developed system, the computed temperature cracking was compared with the average reported values of different sections with the same asphalt concrete mixture.
- (d) Without considering the aging of asphalt, predicted temperature cracking, for the low-viscosity 150/200 asphalt was found to be 0.009 ft/1000 ft² compared to a measured value of 76.0 ft/1000 ft² (Table 10.7). This observation shows the significant contribution of asphalt aging models (Chapter 6) to the developed system.

SUMMARY

A computer system for predicting temperature cracking has been developed. The system's behavior was analyzed and the important variables with respect to temperature cracking were detected. Data from Ontario Test Roads and Ste. Anne Test Road have shown the system to be reliable.

This page replaces an intentionally blank page in the original.

-- CTR Library Digitization Team

CHAPTER 11. SUMMARY, CONCLUSIONS, AND RECOMMENDATIONS

SUMMARY

A computerized system for predicting temperature cracking has been developed. The main concepts utilized in forming the system are simulation of pavement temperatures, estimation of asphalt concrete stiffness, aging of asphalts, stochastic variations, and fatigue. Temperature cracking as predicted from the developed system is the appropriate addition of two forms of cracking, which are briefly defined below:

- (1) Low-temperature cracking, which occurs when the thermal tensile stress exceeds the asphalt concrete tensile strength.
- (2) Thermal-fatigue cracking which occurs when the thermal fatigue distress, due to daily temperature cycling, exceeds the fatigue resistance of the asphalt concrete.

CONCLUSIONS

Analysis of the Ontario Test Roads and the Ste. Anne Test Road has shown the system to be reasonable and reliable. Consideration of the thermal fatigue due to daily temperature cycling, which has not previously been considered, makes the method superior to any other available technique in this field. In analyzing the system, the important weather parameters with respect to temperature cracking were found to be solar radiation and air temperature. The important asphalt concrete properties were found to be the thermal coefficient of contraction and the asphalt penetration and temperature-susceptibility. Data from the Ontario Test Roads and computations from the system showed that the percent of original penetration after the thin-film oven test can be a good guide in differentiating among the different asphalt sources whenever the rest of the asphalt properties are the same. The adoption of the system by highway agencies concerned with temperature cracking seems warranted, particularly since the system is made available in the form of a single computer program. Another factor that makes the system easy to adopt is that most of the information necessary for using the computer program needs to be collected only one

time. For example, the environmental variables for a specific area need to be collected only once. The system can be a decision-maker to accept or reject an asphalt supplier; it will also help the design engineer in designing an asphalt concrete mixture that will best fit the surrounding environmental conditions. Above all, the use of the proposed system will reduce the maintenance cost, especially for those locations that suffer from flexible pavement temperature cracking.

The acceptance of the system by highway design engineers will simply mean that all the analytical procedures are accepted, at least partially. However, all the segments of the system were put together so that any change that may develop through the advancement of asphalt concrete technology can be added without the destruction of the basic framework.

RECOMMENDATIONS

Inherent in the proposing of the adoption of the developed system by highway agencies is the further study to update any segment of the system as it becomes necessary. Although the Ontario Test Roads and Ste. Anne Test Road showed the system to be reliable, practice may show some aspects that may be missing in our current asphalt concrete pavement technology. Immediate research efforts that need to be carried out to help in updating the system are listed below:

- (1) the establishment of a regular laboratory experiment to measure the thermal coefficient of contraction of asphalt concrete mixtures,
- (2) the performance of a constant strain fatigue experiment to determine the fatigue constants of any asphalt concrete mixture as a function of its stiffness,
- (3) the consideration of the effect of different pavement structures on temperature cracking,
- (4) the addition of the reliability concept (Ref 10) to the developed system, and
- (5) more effort to reduce the computer time necessary for executing the existing version of the computer program.

Besides the independent use of the proposed system, it is recommended that it be incorporated, as a subsystem, into the available flexible pavement design systems (Refs 32 and 36). To do so, it is necessary to correlate temperature cracking and pavement performance in lieu of the present serviceability index

concept suggested by AASHO (Ref 6). At the present time, there are not enough data to develop such a correlation. However, it is hoped that these data will be available in the near future. When the preceding recommendation is accomplished, the idea of having one system that includes both traffic and environmental variables will be fulfilled.

This page replaces an intentionally blank page in the original.

-- CTR Library Digitization Team

REFERENCES

1. Anderson, K. O., B. P. Shields, and J. M. Dacyszyn, "Cracking of Asphalt Pavements Due to Thermal Effects," Proceedings, Association of Asphalt Paving Technologists, Vol 35, February 1966, p 255.
2. Barber, E. S., "Calculation of Maximum Pavement Temperatures from Weather Reports," Bulletin 168, Highway Research Board, Washington, D. C., 1957, pp 1-8.
3. Betenson, Wade B., "Rubber in Asphalt, Field and Laboratory Performance Testing," presented at the International Symposium on The Use of Rubber in Asphalt Pavements, Salt Lake City, Utah, May 1971.
4. Busby, Edward O., and Lloyd F. Rader, "Flexural Stiffness Properties of Asphalt Concrete at Low Temperatures," a paper presented at the Annual Meeting of the Association of Asphalt Paving Technologists, Cleveland, Ohio, February 1972.
5. Burgess, R. A., O. Kopvillem, and F. D. Young, "Ste. Anne Test Road - Relationships Between Predicted Fracture Temperatures and Low Temperature Field Performance," Proceedings, Association of Asphalt Paving Technologists, Vol 40, February 1971, p 148.
6. Carey, W. N., and P. E. Irick, "The Pavement Serviceability-Performance Concept," Bulletin 250, Highway Research Board, Washington, D. C., January 1960.
7. Carslaw, H. S., and J. C. Jaeger, Conduction of Heat in Solids, Oxford Press, 1947.
8. Christison, J. T., "Sawn Joints in Asphalt Pavements," Province of Manitoba Highways Department, Materials and Research Branch, prepared for presentation at the Annual Meeting of the Western Association of Canadian Highway Officials, Edmonton, Alberta, 1969.
9. Christison, J. T., D. W. Murray, and K. O. Anderson, "Stress Prediction and Low Temperature Fracture Susceptibility of Asphalt Concrete Pavements," a paper presented at the Annual Meeting of the Association of Asphalt Paving Technologists, Cleveland, Ohio, February 1972.
10. "Climatic Atlas of the United States," U. S. Department of Commerce, Environmental Science Services Administration, Environmental Data Service, June 1968.
11. Darter, M. I., B. F. McCullough, and J. L. Brown, "Reliability Concepts Applied to the Texas Flexible Pavement System - FPS," a paper presented at the 51st Annual Meeting of the Highway Research Board, Washington, D. C., January 1972, in press.

12. Darter, Michael I., "Thermal Expansion-Contraction of Asphaltic Concrete," Master's Thesis, University of Utah, June 1968.
13. Davis, T. C., and J. C. Peterson, "An Adaptation of Inverse Gas-Liquid Chromatography to Asphalt Oxidation Studies," Analytical Chemistry, Vol 38, No. 13, December 1966, pp 1938-1940.
14. Davis, T. C., J. C. Peterson, and W. E. Haines, "Inverse Gas-Liquid Chromatography - A New Approach for Studying Petroleum Asphalts," Analytical Chemistry, Vol 38, No. 2, February 1966, pp 241-243.
15. Deme, I., "Ste. Anne Test Road - Transverse Cracking of the Pavements In the Mix Trial Area of the Test Road," Manitoba Highways Internal Report 69-2, August 1969, revised and amended as Report 71-2, March 1971.
16. Draper, N. R., and H. Smith, Applied Regression Analysis, John Wiley & Sons, Inc., New York, 1966.
17. Epps, Jon A., and Carl L. Monismith, "Influence of Mixture Variables on the Direct Tensile Properties of Asphalt Concrete," Proceedings, Association of Asphalt Paving Technologists, Vol 39, February 1970, p 207.
18. "FAOV-01 Statistical Computer Program for the Analysis of Variance With Factorial Treatment Combinations," Center for Highway Research, The University of Texas at Austin, 1968.
19. Finn, F., "Factors Involved in the Design of Asphaltic Pavement Surfaces," NCHRP Report No. 39, National Cooperative Highway Research Program, Highway Research Board, Washington, D. C., 1967.
20. Finn, F. N., W. R. Hudson, B. F. McCullough, and K. Nair, "An Evaluation of Basic Material Properties Affecting Behavior and Performance of Pavement Systems," a paper presented at the 47th Annual Meeting of the Highway Research Board, Washington, D. C., January 1968.
21. Fromm, H. J., and W. A. Phang, "A Study of Transverse Cracking of Bituminous Pavements," a paper presented at the Annual Meeting of the Association of Asphalt Paving Technologists, Cleveland, Ohio, February 1972.
22. Gietz, Robert H., and Donald R. Lamb, "Age-Hardening of Asphalt Cement and Its Relationship to Lateral Cracking of Asphaltic Concrete," Proceedings, Association of Asphalt Paving Technologists, Vol 37, 1968, pp 141-159.
23. Glenny, E., "Thermal Fatigue," Metallurgical Reviews, Vol 6, No. 24, 1961, pp 387-465.
24. Gotolski, W. H., S. K. Ciesielski, and L. N. Heagy, "Progress Report on Changing Asphalt Properties of In-Service Pavements in Pennsylvania," Proceedings, Association of Asphalt Paving Technologists, Vol 33, February 1964, pp 285-319.

25. Haas, R. C. G., and T. H. Topper, "Thermal Fracture Phenomena In Bituminous Surfaces," a paper written for presentation to the Western Summer Meeting, Highway Research Board, Denver, Colorado, August 12-13, 1968.
26. Hajek, Jaroslav, "A Comprehensive System Estimation of Low-Temperature Cracking Frequency of Flexible Pavements," Master's Thesis, University of Waterloo, Waterloo, Ontario, April 1971.
27. Haugen, E. B., Probabilistic Approaches to Design, John Wiley & Sons, Inc., New York, 1968.
28. Heukelom, W., "Observations on the Rheology and Fracture of Bitumens and Asphalt Mixes," Proceedings, Association of Asphalt Paving Technologists, Vol 35, 1966, p 358.
29. Heukelom, W., and A. J. G. Klomp, "Road Design and Dynamic Loading," Proceedings, Association of Asphalt Paving Technologists, Vol 33, February 1964, pp 92-125.
30. Hicks, C. R., Fundamental Concepts in the Design of Experiments, Holt, Rinehart and Winston, Inc., New York, 1964.
31. Hills, J. F., and D. Brien, "The Fracture of Bitumens and Asphalt Mixes by Temperature Induced Stresses," Proceedings, Association of Asphalt Paving Technologists, Vol 35, February 1966, p 292.
32. Hudson, W. Ronald, B. Frank McCullough, F. H. Scrivner, and James L. Brown, "A Systems Approach Applied to Pavement Design and Research," Research Report No. 123-1, published jointly by Texas Highway Department; Texas Transportation Institute, Texas A&M University; and Center for Highway Research, The University of Texas at Austin, March 1970.
33. Hudson, W. R., F. N. Finn, B. F. McCullough, K. Nair, and B. A. Vallerga, "Systems Approach to Pavement Design," Interim Report, NCHRP Project 1-10, submitted to National Cooperative Highway Research Program, Highway Research Board, Washington, D. C., March 1968.
34. Hudson, W. R., R. K. Kher, and B. F. McCullough, "Automation in Pavement Design and Management Systems," a paper presented at the Summer Meeting of the Highway Research Board, Austin, Texas, August 1971.
35. Hveem, F. N., E. Zube, and J. Skog, "Progress Report on the Zaca-Wigmore Experimental Asphalt Test Project," Symposium on Paving Materials, American Society for Testing Materials, Special Technical Publication No. 277, 1959, pp 3-45.
36. Jain, S. P. B. F. McCullough, and W. R. Hudson, "Flexible Pavement System - Second Generation, Incorporating Fatigue and Stochastic Concepts," Research Report No. 123-10, published jointly by Texas Highway Department; Texas Transportation Institute, Texas A&M University; and Center for Highway Research, The University of Texas at Austin, December 1971.

37. Kallas, B. F., "Asphalt Pavement Temperatures," Highway Research Record No. 150, Highway Research Board, Washington, D. C., 1966, pp 1-11.
38. Kasianchuk, Donald A., "Fatigue Considerations in the Design of Asphalt Concrete Pavements," Ph.D. Dissertation, University of California at Berkeley, 1968, pp 92-136.
39. Kelly, J. E., "Cracking of Asphalt Concrete Pavements Associated With Volume Changes in Underlying Materials and Base Courses," Proceedings, Association of Asphalt Paving Technologists, Vol 35, February 1966, p 290.
40. Kenis, William J., Sr., "Progress Report on Changes in Asphaltic Concrete in Service," Bulletin 333, Highway Research Board, Washington, D. C., 1962, pp 39-65.
41. Kozlov, G. S., and D. Desai, "Performed Elastomeric Bridge Joint Sealers: Thermal Characteristics of Bridge End Movements," Highway Research Record No. 302, Highway Research Board, Washington, D. C., 1970, pp 38-49.
42. Liddle, Wallace J., George M. Jones, and Dale E. Peterson, "Use of Synthetic Rubber-in-Asphalt Pavement to Determine Mixture Behavior and Pavement Performance," Interim Report, Utah Project No. HPR 1(8), BPR Study Nos. 10 and 14, and State Study Nos. 903 and 910, Utah State Highway Department, Materials and Tests Division, December 1969.
43. Liddle, Wallace J., George M. Jones, Dale E. Peterson, and Donald C. Muir, "An Evaluation of Pavement Serviceability on Utah Highways," Interim Report 1969, Utah Project No. HPR 1(8), BPR Study No. 5, and State Study No. 912, 1969.
44. Long, Robert E., "Mix Design and Use of Black Base," paper prepared for 1970 Highway Short Course, College Station, Texas, November 17-19, 1970.
45. "Low-Temperature Pavement Cracking in Canada: The Problem and Its Treatment," Canadian Good Roads Association Ad Hoc Committee on Low Temperature Behavior of Flexible Pavements, a paper prepared for presentation to the Annual Convention, Canadian Good Roads Association, Montreal, Canada, October 1970.
46. McCullough, B. F., "A Pavement Overlay Design System Considering Wheel Loads, Temperature Changes, and Performance," Ph.D. Dissertation, University of California at Berkeley, July 1969.
47. McLeod, Norman W., "A 4-Year Survey of Low Temperature Transverse Pavement Cracking on Three Ontario Test Roads," a paper presented at the Annual Meeting of the Association of Asphalt Paving Technologists, Cleveland, Ohio, February 1972.
48. "Meteorological Observations in Canada," Monthly Records, Department of Transport, Meteorological Branch, Toronto, Ontario, January 1967 through December 1970.

49. Monismith, C. L., R. L. Alexander, and K. E. Secor, "Rheologic Behavior of Asphalt Concrete," Proceedings, Association of Asphalt Paving Technologists, Vol 35, February 1966, pp 400-450.
50. Monismith, C. L., "Asphalt Mixture Behavior in Repeated Flexure," IER Report No. TE-65-9, University of California at Berkeley, November 1965.
51. Monismith, C. L., and J. A. Epps, "Asphalt Mixture Behavior in Repeated Flexure," Report No. TE-69-6, Soil Mechanics and Bituminous Materials Research Laboratory, University of California at Berkeley, December 1969.
52. Monismith, C. L., G. A. Secor, and K. E. Secor, "Temperature Induced Stresses and Deformations in Asphalt Concrete," Proceedings, Association of Asphalt Paving Technologists, Vol 34, February 1965, p 248.
53. Moore, R. K., and T. W. Kennedy, "Tensile Behavior of Subbase Materials Under Repetitive Loading," Research Report No. 98-12, Center for Highway Research, The University of Texas at Austin, October 1971.
54. Pell, P. S., "Fatigue Characteristics of Bitumen and Bituminous Mixes," Proceedings, University of Michigan International Conference on the Structural Design of Asphalt Pavements, University of Michigan, Ann Arbor, Michigan, August 20-24, 1962, pp 310-323.
55. Pell, P. S., and P. F. McCarthy, "Amplitude Effect of Stiffness of Bitumen and Bituminous Mixes Under Dynamic Conditions," Rheologia Acta, Vol 2, No. 2, 1962.
56. Pfeiffer, J. P., and P. M. Van Doormaal, "The Rheological Properties of Asphaltic Bitumen," Journal of the Institute of Petroleum Technology, Vol 22, 1936.
57. Readshaw, E. E., "Asphalt Specifications in British Columbia for Low Temperature Performance," a paper presented at the Annual Meeting of the Association of Asphalt Paving Technologists, Cleveland, Ohio, February 1972.
58. Schmidt, R. J., "The Relationship of the Low Temperature Properties of Asphalt to the Cracking of Pavements," Proceedings, Association of Asphalt Paving Technologists, Vol 35, February 1966, p 263.
59. Scrivner, F. H., and Chester H. Michalak, "Flexible Pavement Performance Related to Deflections, Axle Applications, Temperature, and Foundation Movements," Research Report 32-13, Texas Transportation Institute, Texas A&M University, College Station, Texas, 1969.
60. Scrivner, F. H., and W. M. Moore, "An Empirical Equation for Predicting Pavement Deflections," Research Report 32-12, Texas Transportation Institute, Texas A&M University, College Station, Texas, 1968.

61. Scrivner, F. H., W. M. Moore, and G. R. Carey, "A Systems Approach to the Flexible Pavement Design Problem," Research Report 32-11, Texas Transportation Institute, Texas A&M University, College Station, Texas, 1968.
62. Simpson, W. C., R. L. Griffin, and T. K. Miles, "Correlation of the Microfilm Durability Test With Field Hardening Observed in the Zaza-Wigmore Experimental Project," Symposium on Paving Materials, American Society for Testing Materials, Special Technical Publication No. 277, 1959, pp 52-63.
63. Skog, J., "Results of Cooperative Test Series on Asphalts from the Zaza-Wigmore Experimental Project," Symposium on Paving Materials, American Society for Testing Materials, Special Technical Publication No. 277, 1959, pp 46-51.
64. Southgate, Herbert F., and Robert C. Deen, "Temperature Distribution Within Asphalt Pavements and Its Relationship to Pavement Deflection," Division of Research, Department of Highways, Commonwealth of Kentucky, Lexington, Kentucky, June 1968.
65. "Statistical Abstract of the United States," U. S. Bureau of Census, 91st Edition, Washington, D. C., 1970, p 176.
66. "STEP-01 Statistical Computer Program for Stepwise Multiple Regression," Center for Highway Research, The University of Texas at Austin, 1968.
67. Straub, A. L., H. N. Schenck, Jr., and F. E. Przybycien, "Bituminous Pavement Temperature Related to Climate," Highway Research Record No. 256, Highway Research Board, Washington, D. C., 1968, pp 53-78.
68. Strom, Oren Grant, "A Pavement Feedback Data System," Ph.D. Dissertation, The University of Texas at Austin, May 1972.
69. "The AASHO Road Test: Report 5, Pavement Research," Special Report 61E, Highway Research Board, Washington, D. C., 1962.
70. "Thermal Stresses, Factors Involved in the Design of Asphaltic Pavement Surfaces," National Cooperative Highway Research Program, Report 39, Highway Research Board, Washington, D. C., 1967, pp 35-44.
71. Tuckett, G. M., G. M. Jones, and G. Littlefield, "The Effects of Mixture Variables on Thermally Induced Stresses in Asphaltic Concrete," Proceedings, Association of Asphalt Paving Technologists, Vol 39, February 1970, p 703.
72. Vallerga, B. A., and W. J. Halstead, "Effects of Field Aging on Fundamental Properties of Paving Asphalts," presented at the 50th Annual Meeting of the Highway Research Board, Washington, D. C., January 1971.

73. Van Draat, W. E. F., and P. Sommer, "Ein Gerat zue Bestimmung der Dynamischen Elastizitattsmoduln von Asphalt," Strasse und Autobahn, Vol 35, 1966.
74. Van der Poel, C., "A General System Describing the Viscoelastic Properties of Bitumens and Its Relation to Routine Test Data," Journal of Applied Chemistry, Vol 4, May 1954.
75. Van der Poel, C., "Road Asphalt, Building Materials, Their Elasticity and Inelasticity," M. Reiner, editor, Interscience, 1954.
76. Venkatasubramnian, V., "Temperature Variations in a Cement Concrete Pavement and the Underlying Subgrade," Highway Research Record No. 60, Highway Research Board, Washington, D. C., 1963, pp 15-27.
77. Visher, Stephen Sargent, "Climatic Atlas of the United States," Howard University Press, Cambridge, Massachusetts, 1954.
78. Welborn, J. York, "Asphalt Hardening - Fact and Fallacy," Public Roads, Vol 35, No. 12, February 1970, pp 279-285.
79. Young, F. D., I. Deme, R. A. Burgess, and K. O. Kopvillem, "Ste. Anne Test Road - Construction Summary and Performance After Two Years' Service," presentation to the Canadian Technical Asphalt Association, Edmonton, November 1969.
80. Zube, E., and J. Skog, "Final Report on the Zaca-Wigmore Asphalt Test Road," a progress report presented to the Materials and Research Department of the California Division of Highways, 1959.

This page replaces an intentionally blank page in the original.

-- CTR Library Digitization Team

APPENDIX 1

TEMPERATURE PREDICTION PROGRAM LISTING AND INPUT GUIDE

This page replaces an intentionally blank page in the original.

-- CTR Library Digitization Team


```

41 FORMAT (I5,5X,5A10)
42 FORMAT (1H1,5X,*PROB. NO. *,15,5X,5A10,/)
43 FORMAT (/ ,10X,*HOUR OF DAY *,11X,*TEMP.-DEG.F*)
11 FORMAT (I2)
12 FORMAT (7F10.3)
51 FORMAT (/ ,5X,F10.0,*A.M*,10X,F10.1)
52 FORMAT (/ ,5X,F10.0,*NOON*, 9X,F10.1)
53 FORMAT (/ ,5X,F10.0,*P.M*,10X,F10.1)
54 FORMAT (/ ,5X,F10.0,*MID NIGHT*, 4X,F10.1)
14 FORMAT (5X,*AVE. AIR TEMP.==*,F10.3,5X,*DEG.F*,/,
1      5X,*TEMP.RANGE      ==*,F10.3,5X,*DEG.F  *,/,
2      5X,*WIND VELOCITY  ==*,F10.3,5X,*MPH.   *,/,
3      5X,*WATL. DENSITY  ==*,F10.3,5X,*PCI.   *,/,
4      5X,*SPEC. HEAT     ==*,F10.3,5X,*BTU.PER POUND DEG.F*,/,
5      5X,*CONDUCTIVITY   ==*,F10.3,5X,*(BTU.,HOOR,FT.,DEG.F)*,/,
6      5X,*ABSORBIVITIT   ==*,F10.3,/,
7      5X,*SOLAR RAD.     ==*,F10.3,5X,*LANGBELYS PER DAY *,/,
8      5X,*DEPTIC        ==*,F10.3,5X,*INCHES*)
      END

```

INPUT GUIDE

NTOT

I5		One card
----	--	----------

NTOT = total number of problems

The following cards have to be repeated for each problem.

NPROB		TITLE(I)	
I5	5X	5A10	One card

60

NPROB = identification problem number.

TITLE(I) = date and location of measurements.

TA TR

F10.3	F10.3	One card
-------	-------	----------

TA = average air temperature ($^{\circ}$ F)TR = temperature daily range ($^{\circ}$ F)

V	W	S	AK	B	AL	X	
F10.3	One card						

V = wind speed (mph)
W = mix density (lb/cu in)
S = specific heat (BTU per pound, $^{\circ}$ F)
AK = conductivity (BTU per square foot per hour, $^{\circ}$ F per foot)
B = absorptivity
AL = solar radiation (Langleys per day)
X = depth (inches)

This page replaces an intentionally blank page in the original.

-- CTR Library Digitization Team

APPENDIX 2

ESTIMATION OF ASPHALT CONCRETE STIFFNESS
(AFTER VAN DER POEL'S NOMOGRAPH)
PROGRAM LIST AND INPUT GUIDE

This page replaces an intentionally blank page in the original.

-- CTR Library Digitization Team

```

PROGRAM YEHTA (INPUT,OUTPUT)
DIMENSION Y(6),Z(15),FYM2(6),FYM1(6),FY0(6),FYP1(6),FYP2(6),
1FZM2(15),FZM1(15),FZ0(15),FZP1(15),FZP2(15),TEMP(50),
1E(50),EA(50),EB(50),FMIX(50)
C*****TEMP DATA POINTS ABOVE RING-AND-BALL (DEG. C)
DATA Y/40.,35.,30.,20.,10.,0.0/
C*****TEMP DATA POINTS BELOW RING-AND-BALL (DEG. C)
DATA Z/0.,-5.,-10.,-15.,-20.,-25.,-30.,-35.,-40.,-45.,-50.,-55.,
1-60.,-65.,-70./
READ 11,NTOTAL
C*****NTOTAL = TOTAL NO. OF PROBLEMS
11 FORMAT (I5)
DO 1000 I=1,NTOTAL
READ 11,NPROR
C*****NPROR = PROBLEM NO.
PRINT 12,NPROB
12 FORMAT (1H1,20(/),25X,12H PROBLEM NO ,I5)
READ 1,ITIME,NTEMP
C*****ITIME= TIME LEVEL
C*****NTEMP= NO. OF TEMP AT WHICH STIFFNESS IS NEEDED
1 FORMAT(2I5)
READ 2,(TEMP(I),I=1,NTEMP)
2 FORMAT ((5F10.1))
READ 3,PT,TPT,TRB,CV
C*****PT = PENETRATION (MULTIPLE OF 0.1 MM)
C*****TPT = PENETRATION TEMP (DEG. C)
C*****TRB = RING-AND-RAIL TEMP (DEG. C)
C*****CV = VOLUME CONCENTRATION OF MINERALS
3 FORMAT(4F10.3)
C=(ALOG10(800.)-A10G10(PT))*50./(TRB-TPT)
PI=(20.-10.*C)/(C+1.)
C*****PI = PENETRATION INDEX
IF (ITIME-2) 4,5,6
4 CALL HDSEC (PT,TPT,TRB,CV,PI,NTEMP,TEMP,Y,7)
C*****HDSEC = 1/100 SECOND
GO TO 1000
5 CALL HOUR (PT,TPT,TRB,CV,PI,NTEMP,TEMP,Y,7)
GO TO 1000
6 IF (ITIME.EQ.4) GO TO 7
CALL DYNFT (PT,TPT,TRB,CV,PI,NTEMP,TEMP,Y,7)
GO TO 1000
7 CALL HDSEC (PT,TPT,TRB,CV,PI,NTEMP,TEMP,Y,7)
CALL HOUR (PT,TPT,TRB,CV,PI,NTEMP,TEMP,Y,7)
CALL DYNFT (PT,TPT,TRB,CV,PI,NTEMP,TEMP,Y,7)
1000 CONTINUE
END

```

```

SUBROUTINE HDSEC (PT, IPT, TRB, CV, PI, NTEMP, TEMP, Y, Z)
DIMENSION Y(6), Z(15), FYM2(6), FYM1(6), FY0(6), FYP1(6), FYP2(6),
1FZM2(15), FZM1(15), FZ0(15), FZP1(15), FZP2(15), TEMP(50),
1E(50), EA(50), EB(50), EMIX(50)
DATA FYM2/1.25E3, 2.E3, 3.5E3, 1.6E4, 6.8E4, 3.E5/
C*****FYM2 = STIFFNESS AT TEMP (Y) AND PI OF -2
DATA FYM1/2.E3, 3.3E3, 5.E3, 2.E4, 7.E4, 2.5E5/
DATA FY0/3.E3, 4.8E3, 7.5E3, 2.2E4, 7.E4, 2.E5/
DATA FYP1/4.E3, 6.8E3, 9.2E3, 2.3E4, 7.E4, 1.6E5/
DATA FYP2/5.5E3, 8.E3, 1.07E4, 2.5E4, 6.E4, 1.4E5/
C*****FYP2 = STIFFNESS AT TEMP(Y) AND PI OF +2
DATA FZM2/3.E5, 8.E5, 2.E6, 7.E6, 2.E7, 5.E7, 1.4E8, 4.E8, 8.E8, 1.1E9,
11.5E9, 1.0E9, 2.05E9, 2.3E9, 2.5E9/
C*****FZM2 = STIFFNESS AT TEMP(Z) AND PI OF -2
DATA FZM1/2.5E5, 5.8E5, 1.3E6, 3.3E6, 8.5E6, 2.E7, 4.7E7, 1.E8, 2.E8,
13.5E8, 5.5E8, 9.E8, 1.3E9, 1.5E9, 2.E9/
DATA FZ0/2.E5, 4.3E5, 8.5E5, 1.8E6, 4.E6, 9.E6, 1.85E7, 4.E7, 7.E7, 1.15E8,
11.9E8, 3.3E8, 5.E8, 7.5E8, 1.E9/
DATA FZP1/1.6E5, 3.3E5, 6.E5, 1.1E6, 2.E6, 4.2E6, 7.E6, 1.6E7, 2.7E7,
14.8E7, 7.E7, 1.2E8, 1.8E8, 2.8E8, 4.6E8/
DATA FZP2/1.4E5, 2.4E5, 4.E5, 7.E5, 1.2E6, 2.E6, 3.5E6, 7.E6, 1.07E7,
11.9E7, 3.E7, 5.E7, 8.E7, 1.2E8, 1.9E8/
C*****FZP2 = STIFFNESS AT TEMP(Z) AND PI OF +2
PRINT 11
11 FORMAT (1H1,10X,*TIME OF LOADING =0.01 SEC.*)
PRINT 21
PRINT 21
21 FORMAT (25X,19H -----)
PRINT 31,PT,IPT,TRB
31 FORMAT (//,3X,13H PENETRATION=, F7.2,3X,11H PENT TEMP=, F7.2,
13X,16H TEMP RING RALL=, F7.2)
PRINT 41,PI,CV
41 FORMAT (//,5X,12H PENT INDEX=,F10.5,6X,4H CV=,F10.5)
IF(PI.GT.-2.) GO TO 1
CALL STIF (NTEMP,TEMP,TRB,Y,Z,FYM2,FZM2,E)
CALL OUTPUT (CV,NTEMP,TEMP,E,EMIX)
GO TO 100
1 IF (PI.GT.-1.) GO TO 2
CALL STIF (NTEMP,TEMP,TRB,Y,Z,FYM2,FZM2,EA)
CALL STIF (NTEMP,TEMP,TRB,Y,Z,FYM1,FZM1,EB)
DO 10 I=1,NTEMP
DL=2.0-ABS(PI)
10 E(I)=EA(I)+(EB(I)-EA(I))*ABS(DL)
C*****LINEAR INTERPOLATION
CALL OUTPUT (CV,NTEMP,TEMP,E,EMIX)
GO TO 100
2 IF (PT.GT.0.0) GO TO 3
CALL STIF (NTEMP,TEMP,TRB,Y,Z,FYM1,FZM1,EA)
CALL STIF (NTEMP,TEMP,TRB,Y,Z,FY0,FZ0,FB)
DO 20 I=1,NTEMP
DL=1.0-ABS(PI)
20 E(I)=EA(I)+(EB(I)-EA(I))*ABS(DL)
CALL OUTPUT (CV,NTEMP,TEMP,E,EMIX)
GO TO 100
3 IF (PI.GT.1.) GO TO 4
CALL STIF (NTEMP,TEMP,TRB,Y,Z,FY0,FZ0,EA)
CALL STIF (NTEMP,TEMP,TRB,Y,Z,FYP1,FZP1,EB)
DO 30 I=1,NTEMP

```

```
DL=0.0-ABS(PI)
30 E(I)=EA(I)+(EB(I)-EA(I))*ABS(DL)
   CALL OUTPUT (CV,NTEMP,TEMP,E,FMIX)
   GO TO 100
4  IF (PI.GT.2.) GO TO 5
   CALL STIF (NTEMP,TEMP,TRB,Y,Z,FYP1,FZP1,EA)
   CALL STIF (NTEMP,TEMP,TRB,Y,Z,FYP2,FZP2,EB)
   DO 40 I=1,NTEMP
   DL=1.0-ABS(PI)
40  E(I)=EA(I)+(EB(I)-EA(I))*ABS(DL)
   CALL OUTPUT (CV,NTEMP,TEMP,E,EMIX)
   GO TO 100
5  CALL STIF (NTEMP,TEMP,TRB,Y,Z,FYP2,FZP2,E)
   CALL OUTPUT (CV,NTEMP,TEMP,E,EMIX)
100 CONTINUE
   RETURN
   END
```

```

SUBROUTINE HOUR (PT,TPT,TRB,CV,PI,NTEMP,TEMP,Y,Z)
DIMENSION Y(6),Z(15),FYM2(6),FYM1(6),FY0(6),FYP1(6),FYP2(6),
IFZM2(15),FZM1(15),FZ0(15),FZP1(15),FZP2(15),TEMP(50),
IE(50),EA(50),EB(50),EMIX(50)
DATA FYM2/5.E-3,9.E-3,2.E-2,7.7E-2,2.6E-1,1.5E0/
DATA FYM1/1.E-2,1.5E-2,3.4E-2,1.E-1,3.4E-1,1.8E0/
DATA FY0/2.E-2,2.8E-2,5.E-2,1.4E-1,5.F0/
DATA FYP1/2.7E-2,4.7E-2,8.3E-2,2.E-1,7.E-1,2.9E0/
DATA FYP2/4.5E-2,7.5E-2,1.3E-1,3.E-1,1.E0,3.3E0/
DATA FZM2/1.5E0,3.4E0,1.E1,3.5E1,1.E2,5.E2,1.6E3,7.E3,4.F4,1.6E5,
17.3E5,3.7E6,1.6E7,7.E7,2.6E8/
DATA FZM1/1.8E0,3.6E0,1.F1,3.5E1,8.5E1,3.3E2,1.E3,3.7E3,1.65E4,
16.5E4,2.2E5,8.5E5,3.E6,1.2E7,4.1E7/
DATA FZ0/2.E0,4.5E0,1.E1,3.5E1,7.5E1,2.5E2,7.6E2,2.3E3,8.4E3,
13.E4,1.E5,3.2E5,9.E5,3.E6,1.E7/
DATA FZP1/2.9E0,5.E0,1.2E1,3.5E1,7.5E1,2.3E2,6.E2,1.8E3,5.F3,
11.7E4,5.F4,1.4E5,3.5E5,1.E6,3.E6/
DATA FZP2/3.3E0,6.6E0,1.5E1,3.5E1,7.5E1,2.2E2,5.F2,1.4E3,3.3E3,
11.E4,2.9E4,7.F4,1.7E5,4.1E5,1.E6/
PRINT 11
11 FORMAT (1H1,10X,* TIME OF LOADING = ONE HOUR*)
PRINT 21
PRINT 21
21 FORMAT (25X,79H -----)
PRINT 31,PT,TPT,TRB
31 FORMAT (//,3X,13H PENETRATION=, F7.2,3X,11H PENT TEMP=, F7.2,
13X,16H TEMP RING RALL=, F7.2)
PRINT 41,PI,CV
41 FORMAT (//,5X,12H PENT INDEX=,F10.5,6X,4H CV=,F10.5)
IF(PI.GT.-2.) GO TO 1
CALL STIF (NTEMP,TEMP,TRB,Y,Z,FYM2,FZM2,E)
CALL OUTPUT (CV,NTEMP,TEMP,E,EMIX)
GO TO 100
1 IF (PI.GT.-1.) GO TO 2
CALL STIF (NTEMP,TEMP,TRB,Y,Z,FYM2,FZM2,EA)
CALL STIF (NTEMP,TEMP,TRB,Y,Z,FYM1,FZM1,EB)
DO 10 I=1,NTEMP
DL=2.0-ABS(PI)
10 E(I)=EA(I)+(EB(I)-EA(I))*ABS(DL)
CALL OUTPUT (CV,NTEMP,TEMP,E,EMIX)
GO TO 100
2 IF(PI.GT.0.0) GO TO 3
CALL STIF (NTEMP,TEMP,TRB,Y,Z,FYM1,FZM1,EA)
CALL STIF (NTEMP,TEMP,TRB,Y,Z,FY0,FZ0,EB)
DO 20 I=1,NTEMP
DL=1.0-ABS(PI)
20 E(I)=EA(I)+(EB(I)-EA(I))*ABS(DL)
CALL OUTPUT (CV,NTEMP,TEMP,E,EMIX)
GO TO 100
3 IF (PI.GT.1.) GO TO 4
CALL STIF (NTEMP,TEMP,TRB,Y,Z,FY0,FZ0,EA)
CALL STIF (NTEMP,TEMP,TRB,Y,Z,FYP1,FZP1,EB)
DO 30 I=1,NTEMP
DL=0.0-ABS(PI)
30 E(I)=EA(I)+(EB(I)-EA(I))*ABS(DL)
CALL OUTPUT (CV,NTEMP,TEMP,E,EMIX)
GO TO 100
4 IF (PI.GT.2.) GO TO 5

```

```
CALL STIF (NTEMP,TEMP,TRB,Y,Z,FYP1,FZP1,EA)
CALL STIF (NTEMP,TEMP,TRB,Y,Z,FYP2,FZP2,EB)
DO 40 I=1,NTEMP
DL=1.0-ABS(PI)
40 E(I)=EA(I)+(EB(I)-EA(I))*ABS(DL)
CALL OUTPUT (CV,NTEMP,TEMP,E,EMIX)
GO TO 100
5 CALL STIF (NTEMP,TEMP,TRB,Y,Z,FYP2,FZP2,E)
CALL OUTPUT (CV,NTEMP,TEMP,E,EMIX)
100 CONTINUE
RETURN
END
```

```

SUBROUTINE DYNFT (PT,TPT,TRR,CV,PI,NTEMP,TEMP,Y,Z)
DIMENSION Y(6)*Z(15),FYM2(6),FYM1(6),FY0(6),FYP1(6),FYP2(6),
FZM2(15),FZM1(15),FZ0(15),FZP1(15),FZP2(15),TEMP(50),
IE(50),EA(50),EB(50),EMIX(50)
DATA FYM2/7.E2,1.1E3,1.85E3,9.E3,3.5E4,1.65E5/
DATA FYM1/1.1E3,1.8E3,2.7E3,1.2E4,3.3E4,1.5E5/
DATA FY0/1.8E3,2.8E3,4.F3,1.4E4,3.8E4,1.3E5/
DATA FYP1/2.5E3,3.7E3,5.E3,1.6E4,3.7E4,1.05E5/
DATA FYP2/3.5E3,5.E3,6.5E3,1.7E4,3.7E4,9.5E4/
DATA FZM2/1.65E5,4.4E5,1.2E6,3.5E6,1.E7,3.5E7,1.F8,2.5E8,6.E8,
11.E9,1.25E9,1.65E9,2.E9,2.2E9,2.5E9/
DATA FZM1/1.5E5,3.5E5,7.5E5,1.9E6,5.E6,1.4E7,3.5E7,8.E7,1.7E8,
12.8E8,5.F8,8.5E8,1.06E9,1.4E9,1.8E9,
DATA FZ0/1.3E5,2.4E5,5.E5,1.E6,2.2E6,5.E6,1.3E7,2.7E7,5.E7,9.E7,
11.5E8,2.2E8,4.E8,6.3E8,9.E8/
DATA FZP1/1.05E5,2.E5,4.E5,6.9E5,1.3E6,2.8E6,5.E6,1.E7,2.E7,3.3E7,
15.8E7,1.F8,1.5E8,2.3E8,3.6E8/
DATA FZP2/9.5E4,1.5E5,2.7E5,4.4E5,8.E5,1.5E6,3.6E6,5.E6,8.8E6,
11.5E7,2.2E7,4.E7,6.2E7,1.E8,1.6E8/
PRINT 11
11 FORMAT (1H1,25X,23H FREQUENCY=8 CYCLES/SEC)
PRINT 21
PRINT 21
21 FORMAT (25X,23H -----)
PRINT 31,PT,TPT,TRR
31 FORMAT (//,3X,13H PENETRATION=, F7.2,3X,11H PENT TEMP=, F7.2,
13X,16H TEMP RING WALL=, F7.2)
PRINT 41,PI,CV
+1 FORMAT (//,5X,12H PENT INDEX=,F10.5,6X,4H CV=,F10.5)
IF (PI.GT.-2.) GO TO 1
CALL STIF (NTEMP,TEMP,TRR,Y,Z,FYM2,FZM2,E)
CALL OUTPUT (CV,NTEMP,TEMP,E,EMIX)
GO TO 100
1 IF (PI.GT.-1.) GO TO 2
CALL STIF (NTEMP,TEMP,TRR,Y,Z,FYM2,FZM2,EA)
CALL STIF (NTEMP,TEMP,TRR,Y,Z,FYM1,FZM1,EB)
DO 10 I=1,NTEMP
DL=2.0-ABS(PI)
10 E(I)=FA(I)+(EB(I)-EA(I))*ABS(DL)
C*****LINEAR INTERPOLATION
CALL OUTPUT (CV,NTEMP,TEMP,E,EMIX)
GO TO 100
2 IF (PI.GT.0.0) GO TO 3
CALL STIF (NTEMP,TEMP,TRR,Y,Z,FYM1,FZM1,EA)
CALL STIF (NTEMP,TEMP,TRR,Y,Z,FY0,FZ0,EB)
DO 20 I=1,NTEMP
DL=1.0-ABS(PI)
20 E(I)=FA(I)+(EB(I)-EA(I))*ABS(DL)
CALL OUTPUT (CV,NTEMP,TEMP,E,EMIX)
GO TO 100
3 IF (PI.GT.1.) GO TO 4
CALL STIF (NTEMP,TEMP,TRR,Y,Z,FY0,FZ0,EA)
CALL STIF (NTEMP,TEMP,TRR,Y,Z,FYP1,FZP1,EB)
DO 30 I=1,NTEMP
DL=0.0-ABS(PI)
30 E(I)=FA(I)+(EB(I)-EA(I))*ABS(DL)
CALL OUTPUT (CV,NTEMP,TEMP,E,EMIX)
GO TO 100

```

```
4 IF (PI.GT.2.) GO TO 5
  CALL STIF (NTEMP,TEMP,TRB,Y,Z,FYP1,FZP1,EA)
  CALL STIF (NTEMP,TEMP,TRB,Y,Z,FYP2,FZP2,EB)
  DO 40 I=1,NTEMP
  DL=1.0-ABS(PI)
40 E(I)=FA(T)+(EB(T)-EA(I))*ABS(DL)
  CALL OUTPUT (CV,NTEMP,TEMP,E,EMIX)
  GO TO 100
5 CALL STIF (NTEMP,TEMP,TRB,Y,Z,FYP2,FZP2,E)
  CALL OUTPUT (CV,NTEMP,TEMP,E,EMIX)
100 CONTINUE
  RETURN
  END
```

```

SUBROUTINE STIF (NTEMP,TEMP,TRB,Y,Z,FY,FZ,F)
DIMENSION TEMP(50),Y(6),FY(6),Z(15),FZ(15),E(50),W(10),FW(10)
DO 10 K=1,NTEMP
TD=TEMP(K)-TRB
IF (TD.LT.0.0) GO TO 1
CALL LAGR (6,Y,FY,TD,S)
E(K)=S
GO TO 10
1 IF (TD.LT.-20.) GO TO 2
CALL LAGR (5,Z,FZ,TD,S)
E(K)=S
GO TO 10
2 IF (TD.LT.-40.) GO TO 3
DO 40 M=1,6
I=M+3
W(M)=Z(I)
4 Fw(M)=FZ(I)
CALL LAGR (6,W,FW,TD,S)
E(K)=S
GO TO 10
3 IF (TD.LT.-60.) GO TO 4
DO 50 M=1,6
I=M+7
W(M)=Z(I)
5 Fw(M)=FZ(I)
CALL LAGR (6,W,FW,TD,S)
E(K)=S
GO TO 10
4 DO 60 M=1,4
I=M+11
W(M)=Z(I)
6 Fw(M)=FZ(I)
CALL LAGR (4,W,FW,TD,S)
E(K)=S
10 CONTINUE
RETURN
END

```

```
SUBROUTINE LAGR (NP1,X,FX,TD,S)
DIMENSION X(15),FX(15)
S=0.0
I=1
24 C=FX(I)
J=1
22 IF (J.EQ.I) GO TO 21
C=C*((TD-X(J))/(X(I)-X(J)))
21 J=J+1
IF (J-NP1) 22,22,23
23 S=S+C
I=I+1
IF (I-NP1) 24,24,10
10 CONTINUE
RETURN
END
```

```
SUBROUTINE OUTPUT (CV,NTEMP,TEMP,E,FMIX)
DIMENSION TEMP(50),F(50),FMIX(50)
DO 10 I=1,NTEMP
E(I)=F(I)*(1.02*10.**-5)
A=(4.*10.**5)/E(I)
AN=.23*/LOG10(A)
B=1.+(2.5/AN)*(CV/(1.-CV))
E(I)=E(I)*14.216
1  EMIX(I)=F(I)*B**AN
PRINT 51
51 FORMAT (4(/),5X,12H TEMPERATURE,10X,5H SBIT,10X,5H SMIX)
PRINT 71
71 FORMAT (10X,6H DEG C,8X,6H PSI ,9X,6H PSI )
DO 20 J=1,NTEMP
PRINT 61,TEMP(J),F(J),EMIX(J)
61 FORMAT (/,10X,F5.1,5X,E12.4,5X,F12.4)
20 CONTINUE
RETURN
END
```

INPUT GUIDE

NTOTAL

15		One card
----	--	----------

NTOTAL = total number of assigned problems
(not more than 50)

FOR EACH PROBLEM

NPROB

15		One card
----	--	----------

NPROB = identification number (can be any number)

ITIME NTEMP

15	15			One card
----	----	--	--	----------

ITIME = 1 - time of loading = 0.01 seconds
 2 - time of loading = 1.0 hour
 3 - time of loading = 8 cycles per second (dynaflect)
 4 - the program will perform the calculations for all the above
 loading times

NTEMP = number of temperatures at which the stiffness is needed (up to 50)

TEMP

F10.1	F10.1	F10.1	F10.1	F10.1		5 values per card
-------	-------	-------	-------	-------	--	-------------------

TEMP = temperatures at which stiffness is needed ($^{\circ}$ C)

PT TPT TRB CV

F10.3	F10.3	F10.3	F10.3		One card
-------	-------	-------	-------	--	----------

- PT = penetration (multiples of 0.1 mm)
- TPT = temperature at which the penetration test is carried out ($^{\circ}$ C)
- TRB = softening point, ring-and-ball temperature ($^{\circ}$ C)
- CV = volume concentration of the minerals
- = $\frac{\text{volume of minerals}}{\text{volume of (minerals + bitumen)}}$

APPENDIX 3

DATA USED FOR THE PREDICTION OF THE PENETRATION AND
SOFTENING-POINT AGING MODELS

This page replaces an intentionally blank page in the original.

-- CTR Library Digitization Team

TABLE 1. DATA USED FOR THE PREDICTION OF THE PENETRATION MODEL

Penetration (Time)	Time (Month)	Original Penetration	Void %	TFOT
33.0	0.0	62.0	7.6	65.0
25.0	12.0	62.0	7.6	65.0
32.0	0.0	62.0	10.3	65.0
25.0	12.0	62.0	10.3	65.0
38.0	0.0	66.0	7.3	64.0
28.0	12.0	66.0	7.3	64.0
38.0	0.0	66.0	7.4	64.0
32.0	12.0	66.0	7.4	64.0
33.0	0.0	61.0	8.0	66.0
30.0	12.0	61.0	8.0	66.0
32.0	0.0	61.0	8.9	66.0
31.0	12.0	61.0	8.9	66.0
36.0	0.0	66.0	6.5	62.0
66.0	0.0	76.0	6.9	59.1
51.0	5.0	76.0	6.9	59.1
69.0	0.0	76.0	6.9	59.1
52.0	5.0	76.0	6.9	59.1
67.0	0.0	76.0	6.9	59.1
54.0	5.0	76.0	6.9	59.1
56.0	0.0	76.0	5.1	61.2
44.0	6.0	76.0	5.1	61.2
57.0	0.0	76.0	5.1	61.2
44.0	6.0	76.0	5.1	61.2
55.0	0.0	76.0	5.1	61.2
42.0	6.0	76.0	5.1	61.2
45.0	0.0	68.0	5.7	57.8
32.0	13.0	68.0	5.7	57.8
47.0	0.0	70.0	5.7	57.8

(Continued)

TABLE 1. (Continued)

Penetration (Time)	Time (Month)	Original Penetration	Void %	TFOT
34.0	13.0	70.0	5.7	57.8
48.0	0.0	70.0	5.7	57.8
34.0	13.0	70.0	5.7	57.8
87.5	0.0	98.5	3.85	64.5
86.5	3.0	98.5	3.85	64.5
85.5	6.0	98.5	3.85	64.5
75.5	12.0	98.5	3.85	64.5
89.0	0.0	104.0	8.5	60.5
78.0	3.0	104.0	8.5	60.5
49.0	12.0	104.0	8.5	60.5
88.0	3.0	105.0	4.0	62.8
73.5	12.0	105.0	4.0	62.8
54.5	12.0	99.5	9.8	62.3
88.5	0.0	92.5	4.45	64.9
87.5	3.0	92.5	4.45	64.9
78.0	6.0	92.5	4.45	64.9
74.0	3.0	93.5	10.1	63.1
63.5	12.0	93.5	10.1	63.1
164.0	0.0	224.0	13.6	56.3
84.0	13.0	224.0	13.6	56.3
44.0	35.0	224.0	13.6	56.3
20.0	118.0	224.0	13.6	56.3
38.0	13.0	228.0	12.2	27.7
20.0	20.0	228.0	12.2	27.7
17.0	35.0	228.0	12.2	27.7
10.0	55.0	228.0	12.2	27.7
112.0	0.0	212.0	13.05	34.7
57.0	13.0	212.0	13.05	34.7

(Continued)

TABLE 1. (Continued)

Penetration (Time)	Time (Month)	Original Penetration	Void %	TFOT
42.0	20.0	212.0	13.05	34.7
86.0	5.0	233.0	11.7	35.1
39.0	20.0	233.0	11.7	35.1
33.0	35.0	233.0	11.7	35.1
23.0	55.0	233.0	11.7	35.1
159.0	0.0	223.0	10.3	48.5
109.0	5.0	223.0	10.3	48.5
71.0	13.0	223.0	10.3	48.5
31.0	35.0	223.0	10.3	48.5
30.0	55.0	223.0	10.3	48.5
24.0	59.0	223.0	10.3	48.5
24.0	118.0	223.0	10.3	48.5
187.0	0.0	239.0	10.8	52.3
96.0	13.0	239.0	10.8	52.3
59.0	20.0	239.0	10.8	52.3
53.0	55.0	239.0	10.8	52.3
47.0	59.0	239.0	10.8	52.3
42.0	91.0	239.0	10.8	52.3
34.0	118.0	239.0	10.8	52.3

TABLE 2. DATA USED FOR THE PREDICTION OF R & B MODEL

Time (Month)	Original R & B	R & B (Time)	TFOT
0.0	123.0	137.0	65.0
12.0	123.0	142.0	65.0
24.0	123.0	146.0	65.0
0.0	123.0	139.0	65.0
12.0	123.0	140.0	65.0
24.0	123.0	146.0	65.0
0.0	124.0	135.0	64.0
12.0	124.0	143.0	64.0
24.0	124.0	145.0	64.0
0.0	124.0	136.0	64.0
12.0	124.0	141.0	64.0
24.0	124.0	144.0	64.0
0.0	125.0	136.0	66.0
12.0	125.0	138.0	66.0
24.0	125.0	145.0	66.0
0.0	125.0	136.0	66.0
12.0	125.0	138.0	66.0
24.0	125.0	146.0	66.0
0.0	124.0	135.0	62.0
24.0	124.0	145.0	62.0
0.0	100.0	106.0	56.3
13.0	100.0	116.0	56.3
35.0	100.0	125.0	56.3
118.0	100.0	142.0	56.3
13.0	99.0	138.0	27.7
20.0	99.0	148.0	27.7
35.0	99.0	151.0	27.7
55.0	99.0	161.0	27.7

(Continued)

TABLE 2. (Continued)

Time (Month)	Original R & B	R & B (Time)	TFOT
0.0	102.0	117.0	34.7
13.0	102.0	127.0	34.7
20.0	102.0	135.0	34.7
5.0	101.0	124.0	35.1
20.0	101.0	134.0	35.1
35.0	101.0	140.0	35.1
55.0	101.0	154.0	35.1
0.0	101.0	105.0	48.5
5.0	101.0	112.0	48.5
13.0	101.0	124.0	48.5
35.0	101.0	126.0	48.5
55.0	101.0	131.0	48.5
59.0	101.0	136.0	48.5
118.0	101.0	145.0	48.5
0.0	101.0	104.0	52.3
13.0	101.0	116.0	52.3
20.0	101.0	126.0	52.3
55.0	101.0	126.0	52.3
59.0	101.0	128.0	52.3
91.0	101.0	133.0	52.3
118.0	101.0	140.0	52.3

This page replaces an intentionally blank page in the original.

-- CTR Library Digitization Team

APPENDIX 4

ESTIMATION OF THERMAL STRESSES PROGRAM LIST,
INPUT GUIDE, AND EXAMPLE OUTPUT

This page replaces an intentionally blank page in the original.

-- CTR Library Digitization Team

```

PROGRAM SHAHIN(INPUT,OUTPUT)
DIMENSION T(10000)
C GIVEN THE MAXIMUM AND MINIMUM VALUES FOR A LINEAR TEMPERATURE
C DROP , ASPHALT PENETRATION AND SOFTENING POINT , ASPHALT CONERTE
C MIXTURE PROPERTIES , AND TIME OF LOADING * THE PROGRAM ESTIMATES
C ASPHALT STIFFNESS , ASPHALT CONCRETE STIFFNESS , AND ACCUMLATED
C THERMAL STRESSES RESULTING FROM TEMPERATURE DROP FOR A SPECIFIED
C NUMBER OF TEMPERATURE INTERVALS.
READ 1,NTOT
C NTOT = TOTAL NUMBER OF PROBLEMS.
1 FORMAT (I5)
DO 10 I=1,NTOT
READ 2,PT,TPTF,TRBF
C PT = PENETRATION AT 100GM.,5SEC.,DMM.
C TPTF = PENETRATION TEMPERATURE , F.
C TRBF = SOFTENING POINT , F.
2 FORMAT (6F10.6)
READ 3,PS,GS,GG,VMIX,ALPHA,VAIR
C PS = PERCENT ASPHALT BY WEIGHT OF AGGREGATE.
C GS = SPECIFIC GRAVITY OF ASPHALT.
C GG = SPECIFIC GRAVITY OF AGGREGATE.
C VMIX = DENSITY OF THE COMPATED MIXTURE , PCF.
C ALPHA = AVERAGE COEFFICIENT OF CONTRATION OF THE MIX ,F,*10**5.
C VAIR = PERCENT AIR VOIDS IN THE MIX , LEAVE BLANK IF NOT KNOWN.
ALPHA =ALPHA*(1./100000.)
C1=ALOG10(800.0)-ALOG10(PT)
TRBC=(5./9.)*(TRBF-32.)
TPTC=(5./9.)*(TPTF-32.)
C2=TRBC-TPTC
CPI=(C1/C2)*50.
PI=(20.-10.0*CPI)/(CPT+1.0)
IF(VAIR.GT.0.0) GO TO 43
WS=(PS/(100.+PS))*VMIX
WG=(100./(100.+PS))*VMIX
VS=(WS/(GS*62.4))
VG=(WG/(GG*62.4))
VAIR=(1.0-VS-VG)*100.0
43 VAIR =VAIR/100.
CC=(PS/100.0)*(GG/GS)
CV=(1.0/(1.0+CC))
IF(VAIR.(T.0.03) GO TO 11
H=VAIR*0.03
CV=CV/(1.+H)
11 CONTINUE
PRINT 3,I
3 FORMAT (1H1,20X,* PROBLEM SET NO. *,I5)
PRINT 4,PT,TPTF,TRBF,PS,GS,GG,VMIX,ALPHA
4 FORMAT ( /,9X,*GIVEN MIXTURE PROPERTIES*,//,
1 2X,*PENT. =*,F10.3,5X,*DM.,5SEC.*,/,
2 2X,*PENT. TEMP. =*,F10.3,5X,*DEG.F. *,/,
3 2X,*RING AND RAIL =*,F10.3,5X,*DEG.F. *,/,
4 2X,*PERCENT ASPH =*,F10.5,5X,*PER.AGG. *,/,
5 2X,*S.GRVITY OF ASPH.=*,F10.3,5X, /,
6 2X,*S.GRAVITY OF AGG.=*,F10.3,5X, /,
7 2X,*UNIT WT. OF MIX =*,F10.3,5X,*LR/FT3 *,/,
8 2X,*ALPHA CF MIX =*,F10.8,5X,*IN/IN /F *)
PRINT 5,PI,VAIR,CV
5 FORMAT ( /,9X,*CALCULATED MIXTURE PROPERTIES*,//,

```

```

1      2X,*PEINT. INDEX      =*,F10.3,/,
2      2X,*AIR VOIDS        =*,F10.5,/,
3      2X,*CORRECTED CV     =*,F10.5)
      READ 1,NSUB
C      NSUB = NUMBER OF SUBPROBLEMS.
      DO 20 J=1,NSUB
      PRINT 6,J
6      FORMAT(///,20X,*SUBPROBLEM NO.*,I5)
      READ 7,TO,TF,TI,N,TIL
C      TC = INITIAL TEMPERATURE , F.
C      TF = FINAL TEMPERATURE . F.
C      TI = TOTAL TIME , SEC.
C      N = NUMBER OF INTERVALS FOR CALCULATIONS.
C      TIL = TIME OF LOADING . SEC.
7      FORMAT(3F10.3,I5,F10.3)
      AN=N
      DTI=(TO-TF)/AN
      PRINT 8,TO,TF,TI,DTI
8      FORMAT( /,5X,*TEMP. AND TIME INFORMATIONS*,/,
1      2X,*INITIAL TEMP. *,F10.3,* DEG.F*,/,
2      2X,*FINAL TEMP. *,F10.3,* DEG.F*,/,
3      2X,*TOTAL TIME *,F10.3,* SEC. *,/,
4      2X,*TEMP. INTERVAL*,F8.4 ,*DEG.F.*)
      PRINT 42,TIL
42     FORMAT (2X,*LOADING TIME *,F10.3,*SEC.*)
      PRINT 9
9      FORMAT(2X,* NO. *, 3X,*SBIT- PSI  *, 3X,*SMIX- PSI  *, 3X,
1*STRESS-PSI*, 3X,*TEMP.-DEG.F*)
      SIG=0.0
      DO 30 K=1, N
      AK=K
      T(K)=TF+(TO-TF)*(1.0-AK*(DTI/(TO-TF)))
      IF(K.GT.1) GO TO 12
      T(K-1)=TO
12     TT=(T(K)+T(K-1))/2. SDT=T(K)-T(K-1)
      TC=(5./9.)*(TT-32.)
      CALL STIF (PI,CV,IRBC,TC,TIL,SBIT,SMIX)
      SIG=SIG+ALPHA*DT*SMIX
      IF(N.GT.10) GO TO 30
      PRINT 21,K,SBIT,SMIX,SIG,TT
21     FORMAT(2X,I5, 3X,E12.4, 3X,E12.4, 3X,F12.4, 3X,E12.4)
30     CONTINUE
      IF (N.LE.10) GO TO 20
      PRINT 21,N,SBIT,SMIX,SIG,TT
20     CONTINUE
10     CONTINUE
      END

```

```

SUBROUTINE STIF (PI,CV,TRBC,TC,TI,SBIT,SMIX)
  T=TC-TDHC
  SL=-1.35927-0.06743*(T)-0.90251*ALOG10(TI)+0.00038*(T**2)
1  -0.00138*(T*ALOG10(TI))+0.00161*(PI*T)
  IF (SL.>I.1.0) GO TO 1
  SL=-1.90072-0.11485*(T)-0.38423*(PI)-0.94259*(ALOG10(TI))
1  -0.00879*(T*ALOG10(TI))-0.05643*PI*ALOG10(TI)
2  -0.02915*((ALOG10(TI))**2)-0.51837*(T**2)/(10.0**3)
3  +0.00113*(PI**3)*(T)-0.01403*(PI**3)*(T**3)/(10.0**5)
1 SLL=SL*2.3025850930
  SBIT=EXP(SLL)
  X=(40000.0/SBIT)
  XN=0.83*ALOG10(X)
  SMIX=SBIT*(1.0+(2.5/XN)*(CV/(1.0-CV)))**XN
  SBIT=SBIT*14.216
  SMIX=SMIX*14.216
  RETURN
  END

```

INPUT GUIDE

NTOT

15	<u>One card</u>
----	-----------------

NTOT = total number of problems

Repeat the whole set of following cards NTOT times:

PT	TPTF	TRBF		<u>One card</u>
F10.6	F10.6	F10.6		

PT = penetration at 100 gm., 5 seconds, Dmm.

TPTF = penetration temperature, ° F

TRBF = softening point, ring and ball, ° F

PS	GS	GG	VMIX	ALPHA	VAIR		<u>One card</u>
F10.6	F10.6	F10.6	F10.6	F10.6	F10.6		

PS = percent asphalt by weight of aggregate

GS = specific gravity of asphalt

GG = specific gravity of aggregate

VMIX = density of the compacted mix, lb/ft³ALPHA = average coefficient of contraction of the mix × 10⁵

VAIR = percent air voids in the mix - leave blank if not known

NSUB

15	<u>One card</u>
----	-----------------

NSUB = number of subproblems

TO TF TI N TIL

F10.3	F10.3	F10.3	15	F10.3
-------	-------	-------	----	-------

Repeat NSUB times

TO = initial temperature, ° F

TF = final temperature, ° F

TI = total time, seconds

N = number of intervals for calculations

TIL = time of loading, seconds

PROBLEM SET NO. 1

GIVEN MIXTURE PROPERTIES

PENT. = 56.000 CM..5SEC.
 PENT. TEMP. = 77.000 DEG.F.
 RING AND BALL = 125.000 DEG.F.
 PERCENT ASPH = 6.00000 PER.AGG.
 S.GRVITY OF ASPH. = .980
 S.GRAVITY OF AGG. = 2.640
 UNIT WT. OF MIX = 144.000 LB/FT3
 ALPHA OF MIX = .00001050 IN/IN /F

CALCULATED MIXTURE PROPERTIES

PENT. INDEX = -.523
 AIR VOIDS = .03190
 CORRECTED CV = .85922

SURPROBLEM NO. 1

TEMP. AND TIME INFORMATIONS

INITIAL TEMP. 115.000 DEG.F
 FINAL TEMP. 15.000 DEG.F
 TOTAL TIME 182000.000 SEC.
 TEMP.INTERVAL 10.0000DEG.F.
 LOADING TIME 100.000SEC.

NO.	SWIT- PSI	SMIX- PSI	STRESS-PSI	TEMP.-DEG.F
1	4.2519E-02	1.2365E+02	-1.2984E-02	1.1000E+02
2	1.2152E-01	2.9214E+02	-4.3658E-02	1.0000E+02
3	3.6656E-01	7.1270E+02	-1.1849E-01	9.0000E+01
4	1.1671E+00	1.7896E+03	-3.0640E-01	8.0000E+01
5	3.9222E+00	4.6966E+03	-7.9009E-01	7.0000E+01
6	1.3912E+01	1.2093E+04	-2.0599E+00	6.0000E+01
7	5.2088E+01	3.2166E+04	-5.4373E+00	5.0000E+01
8	4.1048E+02	1.3855E+05	-1.9985E+01	4.0000E+01
9	1.1511E+03	2.7648E+05	-4.9016E+01	3.0000E+01
10	2.9971E+03	5.1952E+05	-1.0262E+02	2.0000E+01

APPENDIX 5

TEMPERATURE-CRACKING SYSTEM PROGRAM
LIST AND INPUT GUIDE

This page replaces an intentionally blank page in the original.

-- CTR Library Digitization Team

```

PROGRAM YEHIA (INPUT,OUTPUT)
C   THE PROGRAM CALCULATES THE FOLLOWING
C   1- HOURLY PAVEMENT TEMPERATURES
C   2- DAILY MAXIMUM STRAIN,STIFFNESS,AND STRESS.
C   3- LOW TEMPERATURE AND THERMAL FATIGUE CRACKING,FT/1000FT2
DIMENSION STR(400),STRAIN(400),EMIXD(400),TITLE(10),
1 AL(400),TS(16),SN(16),TSE(16),CEC(16),EEXP(20),A(20),
2 B(20),ANAVE(20,12)
READ 999,NTOT
C   NTOT = TOTAL NUMBER OF PAVEMENTS
DO 1000 INTOT=1,NTOT
READ 689,IPROB,(TITLE(I),I=1,7)
C   IPROB = IDENTIFICATION NUMBER OF THE PAVEMENT
PRINT 699,IPROB,(TITLE(I),I=1,7)
READ 35,TM
C   TM= TIME OF THERMAL LOADING,SEC.
PRINT 36,TM
PRINT 62
READ 35,ANNVE,ANR,TR
C   ANNVE = ANNUAL AVERAGE TEMPERATURE (DEG. F)
C   ANR = ANNUAL RANGE TEMPERATURE (DEG. F)
C   TR = DAILY RANGE TEMPERATURE (DEG. F)
PRINT 1,ANNVE, ANR, TR
READ 35,V,W,S,AK,BS,X
C   V = ANNUAL AVERAGE WIND VELOCITY (MPH)
C   W = MIXTURE DENSITY (LBS/CUFT)
C   S = MIXTURE SPECIFIC HEAT, BTU/LB, DEG.F
C   AK = MIXTURE CONDUCTIVITY, BTU/SQFT/HR, DEG.F/FT
C   BS= MIXTURE ABSORBTIVITY
C   X = DEPTH BELOW SURFACE FOR CALCULATION (INCHES)
READ 35,SRA,SRM
C   SRA= ANNUAL AVERAGE SOLAR RADIATION,LANGLEYS.
C   SRM= JULY AVERAGE SOLAR RADIATION,LANGLEYS.
PRINT 2,SRA,SRM,V,BS,X,AK,S,W
READ 35,OPEN,TPT,ORB,TFOT
C   OPEN=ORIGINAL PENETRATION (UMM AT 5 SECS.)
C   TPT = PENETRATION TEMPERATURE (DEG.F)
C   ORB=ORIGINAL SOFTENING POINT (DEG.F)
C   TFOT= THIN FILM OVEN TEST(PERCENT PENERATION).
PRINT 4,OPEN, TPT, ORB, TFOT
READ 35,PSG,GG,GS,PAV
C   PSG= PERCENT ASPHALT BY WEIGHT OF AGGREGATE.
C   GG= SPECIFIC GRAVITY OF AGGHEGATE.
C   GS= SPECIFIC GRAVITY OF ASPHALT .
C   PAV= PERCENT AIR VOIDS IN THE MIXTURE.
CC=(PSG/100.)*(GG/GS)
CV=1./(1.+CC)
C   CV= VOLUME CONCENTRATION OF AGGREGATE.
IF (PAV=3.) 650,650,651
651 HAV=(PAV-3.0)/100.
CV=CV/(1.+HAV)
650 CONTINUE
PRINT 5, PSG, GS, GG, PAV, CV
READ 801,NEN,CVA
C   NEN= NO. OF THERMAL COEF. OF CONTRACTION(ALPH)INPUTS.
C   CVA= COEF. OF VARIATION OF ALPH.
READ 803,(TSE(I),I=1,NEN)
C   TSE= TEMPERATURES AT WHICH ALPH IS INPUT.

```

```

      READ 803, (CEC(I),I=1,NEN)
C     CEC= CORRESPONDING ALPH*10.0**5.
      PRINT 212
      DO 213 I=1,NEN
      PRINT 214 ,TSE(I),CEC(I)
213  CONTINUE
      PRINT 421,CVA
      READ 999,ICHOSE
C     ICHOSE= STRENGTH OPTION COUNTER,WHERE
C     ICHOSE=1 ,IF MIXTURE STRENGTH AS FUNCTION OF TEMP.IS INPUT
C     ICHOSE=2 , IF MAX. MIXTURE STRENGTH IS THE ONLY INPUT.
      IF(ICHOSE-1) 230,230,231
230  READ 801 , NSN,CVT
C     NSN= NO. OF MIXTURE STRENGTH INPUTS.
C     CVT= COEF. OF VARIATION OF STRENGTH.
      READ 803 , (TS(I),I=1,NSN)
C     TS= TEMPERATURES AT WHICH STRENGTH IS INPUT,DEG.F.
      READ 803, (SN(I),I=1,NSN)
C     SN= CORRESPONDING STRENGTH ,PSI.
      PRINT 232
      DO 233 I=1,NSN
      PRINT 234,TS(I),SN(I)
233  CONTINUE
      PRINT 235,CVT
231  READ 35, TMIXMX,CVMX
C     TMIXMX= MAX. TENSILE STRENGTH OF THE MIXTURE,PSI.
C     CVMX= COEF. OF VARIATION OF MAXIMUM MIXTURE STRENGTH.
      PRINT 237,TMIXMX,CVMX
      PRINT 61
      PRINT 32
      READ 11,NUT,SIGM
C     NUT = TOTAL NUMBER OF FATIGUE INPUTS (EACH INPUT CONSISTS
C     OF STIFFNESS AND TWO CONSTANTS).
C     SIGM = LOG STANDARD DEVIATION OF FATIGUE LIFE ,ONE VALUE FOR
C     ALL THE INPUTS
      DO 310 NU=1,NUT
      READ 12,EEXP(NU),A(NU),B(NU)
C     EEXP(NU) = STIFFNESS OF THE MIXTURE
C     A(NU) = THE FRONTAL CONSTANT OF THE FATIGUE EQUATION
C     B(NU) = THE EXPONENTIAL CONSTANT OF THE FATIGUE EQUATION
      PRINT 33,EEXP(NU),A(NU),B(NU)
310  CONTINUE
      AH=1.3+0.62*V**0.75
      H=AH/AK
      AC=AK/(S*W)
      C=(0.131/AC)**0.5
      Z2=(-X)*C/12.
      Z3=H*EXP(Z2)/((H+C)**2+C**2)**0.5
      READ 999,KYEAR
C     KYEAR = DESIGN PERIOD IN YEARS
      D=0.0
      DO 300 IY=1,KYEAR
      PRINT 699,IPROB,(TITLE(I),I=1,7)
      PRINT 400,IY
      PRINT 21
      DO 10 IM=1,12
      TIME=IM+(IY-1)*12
      XTIME=1./(SQRT(TIME)+1.)

```

```

PEN=-48.258-2.561*SQRT(TIME)+OPEN*(0.1438+0.9225*XTIME)
1 -8.466*PAV*XTIME+1.363*TFOT
TRB=-4.632+3.162*SQRT(TIME)+1.58455*ORB-0.9297*TFOT
TRC=(5./9.)*(TRB-32.)
TPC=(5./9.)*(TPT-32.)
CPI=(ALOG10(800.)-ALOG10(PEN))*50./(TRC-TPC)
PI=(20.-10.*CPI)/(CPI+1.)
DC 20 IN=1*30
N=IN+30*(IM-1)
XN=N
YN=XN*(3.1415927/180.)
TA=ANNVE+(ANR/2.)*COS(YN)
AL(N)=SRA+((SRM-SRA)/0.96593)*COS(YN)
R=0.67*BS*3.69*AL(N)/(24.*AH)
STRAIN(N)=0.0
STR(N)=0.

C
C SEARCH FOR THE MAXIMUM TEMPERATURE.
K=2
CALL TE (K,Z2,Z3,R,TA,TR,T1)
51 K=K+1
CALL TE (K,Z2,Z3,R,TA,TR,T2)
IF (T2-T1) 53,110,110
110 T1=T2
GO TO 51

C
53 DT=T1-T2
TEMP=(T1+T2)/2.0
TEMC=(5./9.0)*(TEMP-32.0)
IF (TM-300.0) 111,222,111
222 CALL VAN (TEMC,TRC,CV,PI,E,EMIX) $ GO TO 333
111 CALL SHARIF (TM,TEMC,TRC,CV,PI,E,EMIX)
333 CONTINUE

C LINEAR INTERPOLATION OF THE THERMAL COEFFICIENT OF CONTRACTION.
DO 70 MS=1,NEN
IF (TEMP-TSE(MS)) 71,71,70
70 CONTINUE
71 JM=MS
JM1=MS-1
IF (CEC(JM)-CEC(JM1)) 72,73,73
72 M=JM $MM=JM1 $GO TO 74
73 M=JM1 $ MM=JM
74 TCEC=CEC(M)+(CEC(MM)-CEC(M))/ABS(TSE(JM)-TSE(JM1))*
1 ABS(TEMP-TSE(M))
TCEC =TCEC /100000.0

C
STRAIN(N)=STRAIN(N)+TCEC*DT
STR(N)=STR(N)+EMIX*TCEC*DT
T1=T2
K=K+1
IF (K-25) 52,120,120
120 K=2

C
C SEARCH FOR THE MINIMUM TEMPERATURE.
52 CALL TE (K,Z2,Z3,R,TA,TR,T2)
IF (T2-T1) 53,130,130

C
130 CONTINUE

```

```

      SA=E/14.26
      IF (ICHOSE-1) 270,270,271
270  DO 240 I=1,NSN
      IF(TEMP-TS(I)) 241,241,240
240  CONTINUE
241  KM=I
      KM1=I-1
      IF(SN(KM)-SN(KM1)) 242,243,243
242  M=KM $ MM=KM1 $ GO TO 244
243  N=KM1 $ M=KM
244  SH=SN(M)+(SN(MM)-SN(M))/ABS(TS(KM)-TS(KM1))*ABS(TEMP-TS(M))
      GO TO 1272
271  CALL STRNTH(TMIXMX,SA,SH)
1272 CONTINUE
      IF (N=180) 1140,335,1140
335  IF (JCHOSE-1) 320,320,321
321  CVT2=0.005625+CVMX**2
      CVT=SQRT(CVT2)
320  SDT=CVT*SH
      CVS2 = 0.2725+CVA**2
      CVS = SQRT(CVS2)
      SDS = CVS*STR(180)
      CALL LTC (SH,SDT,STR(180),SDS,RLTC)
1140 CONTINUE
140  EMIXD(N)=EMIX
20  CONTINUE
      PRINT 22,N,TEMP,EMIX,SH ,STR(N),STRAIN(N),PEN,TRB,PI
10  CONTINUE
      PRINT 340 ,RLTC
      CALL CRACK (NUT,A,B,EEXP,STRAIN,EMIXD,IY,SIGM,ANAVE,CIL)
      TTC=CIL+RLTC
      PRINT 420,TTC
300  CONTINUE
1000 CONTINUE
C *****
C   READ FORMAT
C
999  FORMAT (I5)
689  FORMAT (I5,5X,7A10)
35  FORMAT (6F10.3)
801  FORMAT (I5,F5.0,F10.0)
803  FORMAT (16F5.0)
11  FORMAT (I5,F10.5)
12  FORMAT (3E15.5)
C *****
C   PRINT FORMAT
C
699  FORMAT (1H1,2X,*PAV.SEC.NO.*,I5,5X,7A10)
36  FORMAT (//,5X,*TIME OF LOADING ,SEC =*,F10.3)
62  FORMAT ( // ,25X,*MONTH CODE *, /,5X,*JULY*,5X,*AUG.*,5X,*SEPT.*,
15X,*OCT.*,5X,*NOV.*,5X,*DEC.*,/,7X,*1*,7X,*2*,8X,*3*,9X,*4*,
18X,*5*,9X,*6*, /,5X,*JAN.*,5X,*FEB.*,5X,*MAR.*,5X,*APR.*,5X,
1*X,*MAY.*,5X,*JUNE*,/,7X,*7*,7X,*8*,8X,*9*,7X,*10*,7X,*11*,8X,*12*)
1  FORMAT (//,25X,*AIR TEMPERATURE *,/,
1  5X,*ANNUAL AVERAGE ,DEG.F =*,F10.3,/,
2  5X,*ANNUAL RANGE ,DEG.F =*,F10.3,/,
3  5X,*DAILY RANGE ,DEG.F =*,F10.3)
2  FORMAT (//,25X,*FACTORS AFFECTING PAV. TEMP. *,/,

```

```

1      5X,*ANNUAL AVE.SOLAR RAD. ,LANGLEYS      =*,F10.3,/,
2      5X,*JULY AVE.SOLAR RAD. ,LANGLEYS      =*,F10.3,/,
3      5X,*ANNUAL AVE.WIND VEL. ,MPH.          =*,F10.3,/,
4      5X,*SURFACE ABSORBTIVITY                =*,F10.3,/,
5      5X,*DEPTH FOR CALCULATION,IN.          =*,F10.3,/,
6      5X,*MIX. CONDUCTIVITY ,BTU-FT-HR-F.    =*,F10.3,/,
7      5X,*MIX. SPECIFIC HEAT ,BTU-LB-F.      =*,F10.3,/,
8      5X,*MIX. DENSITY ,LB/FT3              =*,F10.3)
4  FORMAT (//,25X,*ASPHALT PROPERTIES          *,/,
1      5X,*ORIG. PENETRATION ,DMM-5SEC.      =*,F10.3,/,
2      5X,*PEN. TEST TEMP. ,DEG.F            =*,F10.3,/,
3      5X,*ORIG. SOFTENING POINT,DEG.F        =*,F10.3,/,
4      5X,*THIN FILM OVEN TEST ,PCT.ORIG.PEN. =*,F10.3)
5  FORMAT (//,25X,*MIXTURE PROPERTIES          *,/,
1      5X,*PCT. ASPHALT ,BY WT.OF AGG.      =*,F10.3,/,
2      5X,*ASPH. SPECIFIC GRAV.              =*,F10.3,/,
3      5X,*AGG. SPECIFIC GRAV.              =*,F10.3,/,
4      5X,*MIX. AIR VOIDS ,PERCENT           =*,F10.3,/,
5      5X,*AGG. VOL. CONCENTRATION -CALCULATED =*,F10.3)
212  FORMAT ( 5X,*COEF. OF CONTRACTION*,5X,*TEMP(F)*,
1  5X*12H ALPH(10**5))
214  FORMAT (30X,F5.0, 9X,F10.3)
421  FORMAT ( 5X,*COEF. OF VARIATION OF ALPH  =*,F10.3)
232  FORMAT ( 5X,*MIXTURE STRENGTH * ,5X,*TEMP(F)*,
1  5X,*STRENGTH*PSI*)
234  FORMAT (30X,F5.0,9X,F10.3)
235  FORMAT ( 5X,*COEF. OF VARIATION OF ALPH  =*,F10.3)
237  FORMAT ( 5X,*MAX. TEN-STRENGTH ,PSI      =*,F10.3,/,
1      5X,*COEF. OF VARIATION OF MAX.STRENGTH. =*,F10.3)
01  FORMAT (//,25X,*INPUT FATIGUE DATA*)
32  FORMAT ( 12X,*FATIGUE CURVE*,10X,20H N=A*(1.0/STRAIN)**B,/,
1  5X,*MIX.STIF.(PSI)*, 7X,*CONST.A*,13X,*CONST.B*)
33  FORMAT ( 5X,E12.4, 7X,E12.4, 6X,E12.4)
400  FORMAT (//,30X,*YEAR NO.*,I?)
21  FORMAT (/ ,5X,*DAY*,2X,*MIN.PVT.TEMP.,DEG.F*,3X,*MAX.STIF,PSI*,4X,
1 *STRENGTH*PSI*,3X,*MAX.STRESS*PSI*,3X, *MAX.STRAIN*,5X,*PEN*,6X,
2 *TRB*,6X,*PI*)
22  FORMAT (3X,I5,4X,E12.4,7X,E12.4,4X,E12.4,4X,E12.4,4X,E12.4,
1  2X,F7.2,2X,F7.2,2X,F7.2)
340  FORMAT (/ ,10X,*LOW TEMP CRACKING = *,F10.4,*FT/1000FT2*)
420  FORMAT(//,20X,*TOTAL THERMAL CRACKING =*,F10.4,*FT/1000FT2*)
C*****
END

```

SUBROUTINE TE (J,Z2,Z3,R,TA,TR,T)

C
C
C
C
C
C

TE IS A DEVELOPED MODEL FOR THE PREDICTION OF PAVEMENT
TEMPERATURES ON HOURLY BASES.

```

TIM=J
IF (J.GT.9) GO TO 31
Z4=6.81768*(.0576*TIM+.144*Z2-.288)                                $GO TO 35
31 IF (J.GT.14) GO TO 32
Z4=-14.7534*(.02057*TIM+.075*Z2-.288)                             $GO TO 35
32 Z4=-6.94274*(.02057*TIM+.12*Z2-.288)
35 Z5=SIN(Z4)
IF (Z5) 21,22,22
21 TM=TA+.5*R
TV=.5*TR                                $GO TO 23
22 TV=0.5*TR+3.*R
TM = TA + R
23 T=TM+TV*Z3*Z5
RETURN
END

```

SUBROUTINE VAN (TEMP,TRB,CV,PI,E,EMIX)

C
C
C
C
C
C
C
C
C
C

VAN IS A COMPUTER MODEL OF VAN DER POEL NOMOGRAPH TO ESTIMATE ASPHALT STIFFNESSES UNDER THE FOLLOWING CONDITIONS:

- 1- TIME OF LOADING =1.0 HOUR;
- 2- A RANGE OF PAVEMENT TEMPERATURES OF 50.0(DEG.C) ABOVE TO 100.0(DEG.C) BELOW THE SOFTENING POINT;
- 3- A RANGE OF PENETRATION INDEX OF +2.0 TO -2.0 .

```

DIMENSION Y(6),Z(21),FYM2(6),FYM1(6),FY0(6),FYP1(6),FYP2(6),
1FZM2(21),FZM1(21),FZ0(21),FZP1(21),FZP2(21)
DATA Y/40.,35.,30.,20.,10.,0.0/
DATA Z/0.,-5.,-10.,-15.,-20.,-25.,-30.,-35.,-40.,-45.,-50.,-55.,
1-60.,-65.,-70.,-75.,-80.,-85.,-90.,-95.,-100./
DATA FYM2/5.E-3,9.E-3,2.E-2,7.7E-2,2.6E-1,1.5E0/
DATA FYM1/1.E-2,1.5E-2,3.4E-2,1.E-1,3.4E-1,1.8E0/
DATA FY0/1.E-2,2.E-2,3.E-2,1.E-1,3.E-1,1.5E0/
DATA FYP1/2.7E-2,4.7E-2,8.3E-2,2.E-1,7.E-1,2.9E0/
DATA FYP2/4.5E-2,7.5E-2,1.3E-1,3.E-1,1.E0,3.3E0/
DATA FZM2/1.5E0,3.4E0,1.E1,2.5E1,1.E2,5.E2,1.6E3,7.E3,4.E4,1.6E5,
17.3E5,3.7E6,1.6E7,7.E7,2.6E8,7.E8,1.13E9,1.55E9,2.E9,2.2E9,2.45E9/
DATA FZM1/1.8E0,3.6E0,1.E1,3.5E1,8.5E1,3.3E2,1.E3,3.7E3,1.65E4,
16.5E4,2.2E5,8.5E5,3.E6,1.2E7,4.1E7,1.E8,2.2E8,5.E8,8.5E8,1.15E9,
21.6E9/
DATA FZ0/2.E0,4.5E0,1.E1,3.5E1,7.5E1,2.5E2,7.6E2,2.3E3,8.4E3,
13.E4,1.E5,3.2E5,9.E5,3.E6,1.E7,2.4E7,6.E7,1.1E8,2.E8,4.E8,6.5E8/
DATA FZP1/2.9E0,5.E0,1.2E1,3.5E1,7.5E1,2.3E2,6.E2,1.8E3,5.E3,
11.7E4,5.E4,1.4E5,3.5E5,1.E6,3.E6,7.E6,1.6E7,3.E7,6.E7,1.03E8,
11.9E8/
DATA FZP2/3.3E0,6.6E0,1.5E1,3.5E1,7.5E1,2.2E2,5.E2,1.4E3,3.3E3,
11.E4,2.9E4,7.E4,1.7E5,4.1E5,1.E6,4.1E6,5.E6,1.E7,2.E7,3.8E7,6.6E7/
IF(PI.GT.-2.) GO TO 1
CALL STIF (TEMP,TRB,Y,Z,FYM2,FZM2,E)
CALL MIX(CV,E,EMIX)
GO TO 100
1 IF(PI.GT.-1.) GO TO 2
CALL STIF(TEMP,TRB,Y,Z,FYM2,FZM2,EA)
CALL STIF (TEMP,TRB,Y,Z,FYM1,FZM1,EB)
DL=2.-ABS(PI)
E=EA+(EB-EA)*ABS(DL)
CALL MIX(CV,E,EMIX)
GO TO 100
2 IF(PI.GT.0.0) GO TO 3
CALL STIF (TEMP,TRB,Y,Z,FYM1,FZM1,EA)
CALL STIF (TEMP,TRB,Y,Z,FY0,FZ0,EB)
DL =1.-ABS(PI)
E=EA+(EB-EA)*ABS(DL)
CALL MIX (CV,E,EMIX)
GO TO 100
3 IF(PI.GT.1.) GO TO 4
CALL STIF (TEMP,TRB,Y,Z,FY0,FZ0,EA)
CALL STIF (TEMP,TRB,Y,Z,FYP1,FZP1,EB)
DL=0.-ABS(PI)
E=EA+(EB-EA)*ABS(DL)
CALL MIX(CV,E,EMIX)
GO TO 100

```

```
4 IF (PI.GT.2.) GO TO 5
  CALL STIF (TEMP,TRB,Y,Z,FYP1,FZP1,EA)
  CALL STIF (TEMP,TRB,Y,Z,FYP2,FZP2,EB)
  DL=1.0-ABS(PI)
  E=EA+(EB-EA)*ABS(DL)
  CALL MIX (CV,E,EMIX)
  GO TO 100
5 CALL STIF (TEMP,TRB,Y,Z,FYP2,FZP2,E)
  CALL MIX (CV,E,EMIX)
100 CONTINUE
  RETURN
  END
```

SUBROUTINE STIF (TEMP,TRB,Y,Z,FY,FZ,E)

C
C
C
C
C

STIF IS A MATHEMATICAL TOOL TO LOCATE THE APPROPRIATE CURVE
OF ASPHALT STIFFNESS FOR THE GIVEN ASPHALT PROPERTIES.

```

DIMENSION Y(6),FY(6),Z(21),FZ(21),W(10),FW(10)
TD=TEMP-TRB
IF(TD.GE.40.) TD=39.999999
IF(TD.LT.0.) GO TO 1
DC 10 I=1,6
IF(TD.GT.Y(I)) GO TO 11
10 CONTINUE
11 K=I
DC 20 M=1,2
I=K-M+1
W(M)=Y(I)
FW(M)=FY(I)
20 CONTINUE
CALL LAGR (2,W,FW,TD,S)
E=S
GO TO 100
1 DO 30 J=1,21
IF(TD.GT.Z(J)) GO TO 12
30 CONTINUE
12 K=J
DC 40 L=1,2
I=K-L+1
W(L)=Z(I)
FW(L)=FZ(I)
40 CONTINUE
CALL LAGR (2,W,FW,TD,S)
E=S
100 CONTINUE
RETURN
END

```

```
SUBROUTINE LAGR (NP1,X,FX,TD,S)
```

```
C  
C  
C  
C  
C
```

```
LAGR IS A POLYNOMIAL TECHNIQUE TO INTERPOLATE THE ACTUAL ASPHALT  
STIFFNESS.
```

```
DIMENSION X(10),FX(10)
```

```
S=0.0
```

```
I=1
```

```
24 C=FX(I)
```

```
J=1
```

```
22 IF (J.EQ.I) GO TO 21
```

```
C=C*((TD-X(J))/(X(I)-X(J)))
```

```
21 J=J+1
```

```
IF (J-NP1) 22,22,23
```

```
23 S=S+C
```

```
I=I+1
```

```
IF (I-NP1) 24,24,10
```

```
10 CONTINUE
```

```
RETURN
```

```
END
```

```
SUBROUTINE MIX (CV,E,EMIX)
```

```
C  
C  
C  
C  
C  
C
```

```
MIX IS THE EQUATION THAT ESTIMATES MIXTURE STIFFNESS FROM  
THE PREDICTED ASPHALT STIFFNESS.
```

```
E=E*(1.02*10.**-5)  
A=(4.*10.**5)/E  
AN=0.83*ALOG10(A)  
B=1.+(2.5/AN)*(CV/(1.-CV))  
E=E*14.216  
EMIX=E*B**AN  
RETURN  
END
```

SUBROUTINE SHARIF (TM,TEMC,TRC,CV,PI,E,EMIX)

C
C
C
C
C

SHARIF IS REGRESSION MODELS FOR ESTIMATING ASPHALT STIFFNESS. SHARIF IS CALLED ONLY WHEN THE TIME OF THERMAL LOADING IS DIFFERENT FROM ONE HOUR.

IF (PI.LT.-2.0) PI=-2.0

IF (PI.GT.+2.0) PI =2.0

TD=TEMC-TRC

Y = -1.35927-0.06743*TD-0.90251*ALOG10(TM)+0.00038*TD**2-0.00138
1*TD*ALOG10(TM)+0.00661*PI*TD

S=10.0**Y

IF (S.LT.10.0) GO TO 1

IF (PI.LT.-1.5) PI=-1.5

Y = -1.90072-0.11485*TD-0.38423*PI-0.94259*ALOG10(TM)-0.00879*TD
1*ALOG10(TM)-0.05643*PI*ALOG10(TM)-0.02915*ALOG10(TM)**2-0.51837
2*(1.0/10.0**3)*(TD**2)+0.00113*PI**3*TD-(0.01403*PI**3*TD**3)*
3(1.0/10.0**5)

S=10.0**Y

1 CONTINUE

A=(4.0*10.0**5)/S

AN=0.83*ALOG10(A)

B=1.0+(.5/AN)*(CV/(1.0-CV))

E=S*14.216

EMIX=E*B**AN

RETURN

END

```

SUBROUTINE CRACK (NUT,A,B,EEXP,STRAIN,EMIXD,IY,SIGM,ANAVE,CIL)
C
C   CRACK IS A MODEL THAT ESTIMATES THERMAL FATIGUE CRACKING.
C
C   DIMENSION A(20),B(20),EMIXD(400),STRAIN(400),EAVE(20),SAVE(20),
*   EEXP(20),ANALPH(20),V(20),Z(1000),AA(1000),ANAVE(20,12),
*   F(20),G(20)   ,IT(1000),FF(20),GG(20)
C
C   CALCULATION OF AVERAGE STRAIN AND STIFFNESS FOR EACH MONTH
C   DC 100 I=1,12
C   ESUM=0.0
C   SSUM=0.0
C   N1=1+30*(I-1)
C   N2=30*I
C   DC 200 N=N1,N2
C   ESUM=ESUM+EMIXD(N)
C   SSUM=SSUM+STRAIN(N)
200 CONTINUE
C   EAVE(I)=ESUM/30.0
C   SAVE(I)=SSUM/30.0
100 CONTINUE
C
C   BEGIN NORMAL CURVE
C
C   BB=0.0
C   DC 10 I=1,391
C   XI=I
C   Z(I)=(391.-XI)/100.
C   Y=Z(I)+0.005
C   AA(I)=BB +0.01*EXP(-Y*Y/2.)/(2.*3.1415926)**0.5
C   BB=AA(I)
10 CONTINUE
C   J = 390
C   DO 20 I=392,780
C   Z(I) = -Z(J)
C   AA(I)=AA(I-1)+AA(J)-AA(J-1)
C   J = J-1
20 CONTINUE
C
C   END NORMAL CURVE
C
C   42 FORMAT (I5)
C   PRINT 45,IY
C   45 FORMAT (3(/),20X,*THERMAL DISTRESS,FATIGUE- YEAR NO. *,I5)
C
C   LINEAR LOGARITHMIC INTERPOLATION OF FATIGUE CONSTANTS FOR AVERAGE
C   MONTHLY VALUES OF IN SERVICE STIFFNESSES.
C   DC 400 I=1,12
C   DO 500 NU=1,NUT
C   IF(NU.EQ.1.AND.EAVE(I).LT.EEXP(1)) GO TO 111
C   IF(NU.EG.NUT.AND.EAVE(I).GT.EEXP(NU)) GO TO 222
C   IF(EAVE(I).GT.EEXP(NU)) GO TO 500
C   NUM=NU-1
C   AD=ALOG10(A(NUM))-ALOG10(A(NU))
C   IF(A(NU)-A(NUM))71,71,72
71 NUA=NU      S GC TO 73
72 NUA=NUM

```

```

73 FF(I)=ALOG10(A(NUA))+(ABS(AD)/(ALOG10(EEXP(NU))=
  1ALOG10(EEXP(NUM))))*ABS(ALOG10(EEXP(NUA))-ALOG10(EAVE(I)))
  F(I)=1.0/(10.0**(ABS(FF(I))))
C   F(I) IS THE ANTILGARITHIM OF FF(I) KNOWING THAT FF(I) IS NEGATIVE
C   -----
  BD=ALOG10(B(NUM))-ALOG10(B(NU))
  IF(B(NU)-B(NUM)) 76,76,77
76 NUB=NU    $ GO TO 78
77 NUB=NUM
78 GG(I)=ALOG10(B(NUB))+(ABS(BU)/(ALOG10(EEXP(NU))=
  1ALOG10(EEXP(NUM))))*ABS(ALOG10(EEXP(NUB))-ALOG10(EAVE(I)))
  G(I)=10.0**GG(I)
C   G(I) IS THE ANTILGARITHIM OF GG(I)
  GC TO 400
500 CONTINUE
400 CONTINUE
  PRINT 35
35 FORMAT (/ ,7X ,*MONTH* ,5X ,*AVE.MAX.STIF,PSI* ,4X ,*AVE.MAX.STRAIN* ,
  1 5X ,*FRONT CONST.* ,6X ,*EXP.CONST.* ,5X ,*N(FATIGUE LIFE)* )
  DO 600 I=1,12
  ANAVE(IY,I)=F(I)*(1.0/SAVE(I))*G(I)
  PRINT 34,I,EAVE(I),SAVE(I),F(I),G(I),ANAVE(IY,I)
34 FORMAT (5X,I5,10X,E12.4,5X,E12.4,5X,E12.4,5X,E12.4,5X,E12.4)
600 CONTINUE
  PRINT 49,SIGM
49 FORMAT (/ ,10X ,*LOGe STANDARD DEVIATION OF FATIGUE LIFE* ,F10.6)
  PRINT 36
36 FORMAT (// ,10X ,*NO.OF MONTHS* ,10X ,*CI-FT2/1000FT2* ,
  * 10X ,*CI-FT/1000FT* )
C   CALCULATION OF CRACKING INDEX USING THE MINER HYPOTHESIS CONCEPT
  L=0
  DO 700 I=1,780
  D=0.0
  DO 50 J=1,IY
  DO 800 K=1,12
  X=ANAVE(J,K)
  Y=ALOG10(X)-SIGM*Z(I)
  ANALPH(K)=10.0**Y
800 V(K)=30.0/ANALPH(K)
  DO 1000 M=1,12
  D=D+V(M)
  IF(D-1.0) 1,2,2
  1 IF(M.EQ.12) GO TO 51
1000 CONTINUE
  51 IF(J.EQ.IY) GO TO 888
  50 CONTINUE
  2 L=L+1
  IF(L-1) 3,3,4
  4 LM=L-1
  IT(L)=M+(J-1)*12
  IF(IT(LM).EQ.IT(L)) GO TO 6
  GO TO 5
  3 IT(L)=M+(J-1)*12
  5 CI=AA(I)*1000.0
  CIL=CI/5.0
  JJ=(IY-1)*12
  IF(IT(L)-JJ) 6,6,52
52 PRINT 1',IT(L),CI,CIL

```

```
17 FORMAT (10X,I5,15X,F10.4,15X,F10.4)
6 IYF=IY*12
  IF(IT(L).EQ.IYF) GO TO 999
700 CONTINUE
800 IF(L=0) 55,55 ,999
55 PRINT 56,IY
56 FORMAT (/ ,10X,*THERE IS NO THERMAL FATIGUE CRACKING IN YEAR *,I5)
  CIL = 0.0
  GO TO 999
111 PRINT 112,EAVE(I)
112 FORMAT (5X,*PLEASE INPUT MIX. STIFFNESS LESS THAN*,E12.4,*PSI*)
  GO TO 999
222 PRINT 223,EAVE(I)
223 FORMAT (5X,*PLEASE INPUT MIX. STIFFNESS GREATER THAN*,E12.4,*PSI*)
999 CONTINUE
  RETURN
  END
```

```

SUBROUTINE STRNTH (TMIXMX,SA,SH)
C
C STRNTH ESTIMATES MIXTURE TENSILE STRENGTH AS A FUNCTION OF
C ASPHALT STIFFNESS (PROVIDING THAT THE MAXIMUM TENSILE
C STRENGTH IS KNOWN)
C
  DIMENSION XR(26),SR(26),TS(16),SN(16)
  DATA XR/.025,.045,.065,.075,.085,.095,.135,.175,.22,.24,.26,
* .35,.455,.525,.575,.625,.72,.95,1.0,.99,.975,.9,.84,.82,.81,.8/
  DATA SR/.1,.2,.4,.6,.8,1.,2.,4.,6.,8.,10.,20.,40.,60.,80.,100.,
*200.,400.,600.,800.,1000.,2000.,4000.,6000.,8000.,10000./
C SR=ASPHALT CEMENT STIFFNESS IN KG/CM2
C XR=CORRESPONDING(SR) RATIO OF MIXTURE TENSILE STRENGTH TO
C MAXIMUM MIXTURE TENSILE STRENGTH.
31 IF (SA-SR(1)) 21,21,22
21 XA=XR(1)
C SA=STIFFNESS OF ASPHALT IN KG/CM2.
C XA=CORRESPONDING RATIO OF MIXTURE STRENGTH TO THE MAXIMUM
C MIXTURE STRENGTH.
  GO TO 999
22 IF (SA-SR(26)) 23,24,24
24 XA =XR(26)
  GO TO 999
23 CONTINUE
  DO 100 I=2,26
  IF (SA-SR(I)) 25,25,100
100 CONTINUE
25 IM1=I-1
  IF (XR(I)-XR(IM1)) 27,28,28
27 M=I $ MM=IM1 $ GO TO 29
28 M=IM1 $ MM=I
29 XA= XR(M) + ((XR(MM)-XR(M))/(ABS(ALOG10(SR(MM)/SR(M)))))*
1 (ABS(ALOG10(SA/SR(M))))
999 CONTINUE
  SH=XA*TMIXMX
  RETURN
  END

```

```

SUBROUTINE LTC (SH,SDT,S,SDS,RLTC)
C
C LTC PREDICTS LOW TEMPERATURE CRACKING.
C
DIMENSION Z(1000),AA(1000)
DM = SDT**2+SDS**2
DMS = SQRT(DM)
ZM = (SH-S)/DMS
IF(ZM.GT.3.9) GO TO 999
IF (ZM.LT.-3.9) GO TO 888
BB=0.0
DO 10 I=1,391
XI=I
Z(I)=(391.-XI)/100.
Y=Z(I)+0.005
AA(I)=BB +0.01*EXP(-Y*Y/2.)/(2.*3.1415926)**0.5
BB=AA(I)
IF(ZM.GE.Z(I)) GO TO 3
10 CONTINUE
J = 390
DO 20 I=392,780
Z(I) = -Z(J)
AA(I)=AA(I-1)+AA(J)-AA(J-1)
J = J-1
IF(ZM.GE.Z(I)) GO TO 3
20 CONTINUE
3 RLTC2 = AA(I)*1000.0
RLTC=RLTC2/5.0 $ GO TO 777
999 RLTC=0.0 $ GO TO 777
888 RLTC = 100.0
777 CONTINUE
RETURN
END

```

INPUT GUIDE

NTOT

(1)

I5

NTOT = total number of pavements

Repeat the following tables NTOT times:

IPROB

TITLE

(2)

I5

5X

FA10

IPROB = identification number of the pavement

TITLE = problem description

TM

(3)

F10.3

TM = time of thermal loading, seconds

ANNVE

ANR

TR

(4)

F10.3

F10.3

F10.3

ANNVE = annual average temperature ($^{\circ}$ F)ANR = annual range temperature ($^{\circ}$ F)TR = daily range temperature ($^{\circ}$ F)

V

W

S

AK

BS

X

(5)

F10.3

F10.3

F10.3

F10.3

F10.3

F10.3

V = annual average wind speed (mph)

W = mixture density (pounds per cubic foot)

S = mixture specific heat, BTU per pound, ° F
 AK = mixture conductivity, BUT per square foot per hour, ° F per foot
 X = depth below surface for calculation (inches)

SRA SRM
 (6)

F10.3	F10.3
-------	-------

SRA = annual average solar radiation, Langleys
 SRM = July average solar radiation, Langleys

OPEN TPT ORB TFOT
 (7)

F10.3	F10.3	F10.3	F10.3
-------	-------	-------	-------

OPEN = original penetration (D_{mm} at 5 seconds)
 TPT = penetration temperature (° F)
 ORB = original softening point (° F)
 TFOT = thin film oven test (percent penetration)

PSG GG GS PAV
 (8)

F10.3	F10.3	F10.3	F10.3
-------	-------	-------	-------

PSG = percent asphalt by weight of aggregate
 GG = specific gravity of aggregate
 GS = specific gravity of asphalt
 PAV = percent air voids in the mixture

NEN CVA
 (9)

I5	F5.0
----	------

NEN = number of thermal coefficients of contraction (α) inputs
 CVA = coefficient of variation of α

TSE(I), I = 1, NEN

16F5.0	
--------	--

TSE = temperatures at which α is input

CEC(I), I = 1, NEN

16F5.0	
--------	--

CEC = corresponding $\alpha \times 10.0^5$

ICHOSE

(10)

I5

ICHOSE = strength option counter, where

ICHOSE = 1, if mixture strength as function of temperature is input, and

ICHOSE = 2, if maximum mixture strength is the only input.

If ICHOSE = 1

NSN CVT

I5	F5.0	
----	------	--

NSN = number of mixture strength inputs

CVT = coefficient of variation of strength

TS(I), I = 1, NSN

16F5.0	
--------	--

TS = temperatures at which strength is input, $^{\circ}$ F

SN(I), I = 1, NSN

16F5.0	
--------	--

SN = corresponding strength, psi

If ICHOSE = 2

TMIXMX CVMX

F10.3	F10.3
-------	-------

TMIXMX = maximum tensile strength of the mixture, psi

CVMX = coefficient of variation of maximum mixture strength

NUT SIGM

(11)

I5	F10.5
----	-------

NUT = total number of fatigue inputs (each input consists of stiffness and two constants)

SIGM = logarithmic standard deviation of fatigue life, one value for all inputs

EEXP A B

E15.5	E15.5	E15.5
-------	-------	-------

Repeat NUT times

EEXP = stiffness of the mixture

A = the frontal constant of the fatigue equation

B = the exponential constant of the fatigue equation

KYEAR

(12)

I5

KYEAR = design period in years

This page replaces an intentionally blank page in the original.

-- CTR Library Digitization Team

APPENDIX 6

ONTARIO TEST ROADS AND STE. ANNE TEST ROAD DATA,
USED FOR THE VERIFICATION OF THE
TEMPERATURE-CRACKING SYSTEM

This page replaces an intentionally blank page in the original.

-- CTR Library Digitization Team

PAV.SEC.NO. 1 ASPHALT SUPPLIER NO 1 - ONTARIO

TIME OF LOADING ,SEC = 3600.000

		MONTH		CODE	
JULY	AUG.	SEPT.	OCT.	NOV.	DEC.
1	2	3	4	5	6
JAN.	FEB.	MAR.	APR.	MAY.	JUNE
7	8	9	10	11	12

AIR TEMPERATURE

ANNUAL AVERAGE	,DEG.F	=	44.820
ANNUAL RANGE	,DEG.F	=	67.400
DAILY RANGE	,DEG.F	=	18.600

FACTORS AFFECTING PAV. TEMP.

ANNUAL AVE.SOLAR RAD.	,LANGLEYS	=	314.200
JULY AVE.SOLAR RAD.	,LANGLEYS	=	538.000
ANNUAL AVE.WIND VEL.	,MPH.	=	9.475
SURFACE ABSORBTIVITY		=	.950
DEPTH FOR CALCULATION,	IN.	=	0.000
MIX. CONDUCTIVITY	,BTU-FT-HR-F.	=	.700
MIX. SPECIFIC HEAT	,BTU-LB-F.	=	.220
MIX. DENSITY	,LB/FT3	=	149.200

ASPHALT PROPERTIES

ORIG. PENETRATION	,DMM-SSEC.	=	83.000
PEN. TEST TEMP.	,DEG.F	=	77.000
ORIG. SOFTENING POINT	,DEG.F	=	115.000
THIN FILM OVEN TEST	,PCT.ORIG.PEN.	=	67.500

MIXTURE PROPERTIES

PCT. ASPHALT	,BY WT.OF AGG.	=	5.980
ASPH. SPECIFIC GRAV.		=	1.000
AGG. SPECIFIC GRAV.		=	2.652
MIX. AIR VOIDS	,PERCENT	=	3.200
AGG. VOL. CONCENTRATION	-CALCULATED	=	.861
COEF. OF CONTRACTION	TEMP (F)	ALPH(10**5)	
	-70		1.000
	0		1.200
	70		1.400
	210		1.800
COEF. OF VARIATION OF ALPH		=	.100
MAX. TEN.STRENGTH	,PSI	=	500.000
COEF. OF VARIATION OF MAX.STRENGTH		=	.200

INPUT FATIGUE DATA

FATIGUE CURVE		N=A*(1.0/STRAIN)**B	
MIX.STIF.(PSI)	CONST.A	CONST.B	
1.0000E+01	1.0000E-02	3.0000E+00	
5.0000E+06	8.0000E-13	3.9500E+00	

FAV.SEC.NO. 1 ASPHALT SUPPLIER 2 - ONTARIO

TIME OF LOADING ,SEC = 3600.000

		MONTH		CODE	
JULY	AUG.	SEPT.	CCT.	NOV.	DEC.
1	2	3	4	5	6
JAN.	FEB.	MAR.	APR.	MAY.	JUNE
7	8	9	10	11	12

		AIR TEMPERATURE	
ANNUAL AVERAGE	,DEG.F	=	44.820
ANNUAL RANGE	,DEG.F	=	67.400
DAILY RANGE	,DEG.F	=	18.600

		FACTORS AFFECTING PAV. TEMP.	
ANNUAL AVE.SOLAR RAD.	,LANGLEYS	=	314.200
JULY AVE.SOLAR RAD.	,LANGLEYS	=	538.000
ANNUAL AVE.WIND VEL.	,MPH.	=	9.475
SURFACE ABSORBTIVITY		=	.950
DEPTH FOR CALCULATION	,IN.	=	0.000
MIX. CONDUCTIVITY	,BTU-FT-HR-F.	=	.700
MIX. SPECIFIC HEAT	,BTU-LB-F.	=	.220
MIX. DENSITY	,LB/FT3	=	148.200

		ASPHALT PROPERTIES	
ORIG. PENETRATION	,DMM-5SEC.	=	96.000
PEN. TEST TEMP.	,DEG.F	=	77.000
ORIG. SOFTENING POINT	,DEG.F	=	115.700
THIN FILM OVEN TEST	,PCT.ORIG.PEN.	=	60.400

		MIXTURE PROPERTIES	
PCT. ASPHALT	,BY WT.OF AGG.	=	5.980
ASPH. SPECIFIC GRAV.		=	1.000
AGG. SPECIFIC GRAV.		=	2.627
MIX. AIR VOIDS	,PERCENT	=	2.400
AGG. VOL. CONCENTRATION	-CALCULATED	=	.864
COEF. OF CONTRACTION	TEMP(F)	ALPH(10**5)	
	-70		1.000
	0		1.200
	70		1.400
	210		1.800
CV OF ALPH		=	.100
MAX. TEN.STRENGTH	,PSI	=	500.000
COEF. OF VARIATION OF MAX.STRENGTH		=	.200

		INPUT FATIGUE DATA	
FATIGUE CURVE		N=A*(1.0/STRAIN)**B	
MIX.STIF.(PSI)	CONST.A	CONST.B	
1.0000E+01	1.0000E-02	3.0000E+00	
5.0000E+06	8.0000E-13	3.9500E+00	

PAV.SEC.NO. 1 ONTARIO TEST ROADS S3 RD3 7/17/72

TIME OF LOADING ,SEC = 3600.000

		MONTH	CODE		
JULY	AUG.	SEPT.	OCT.	NOV.	DEC.
1	2	3	4	5	6
JAN.	FEB.	MAR.	APR.	MAY.	JUNE
7	8	9	10	11	12

AIR TEMPERATURE

ANNUAL AVERAGE	,DEG.F	=	44.820
ANNUAL RANGE	,DEG.F	=	67.400
DAILY RANGE	,DEG.F	=	18.600

FACTORS AFFECTING PAV. TEMP.

ANNUAL AVE.SOLAR RAD.	,LANGLEYS	=	314.200
JULY AVE.SOLAR RAD.	,LANGLEYS	=	538.000
ANNUAL AVE.WIND VEL.	,MPH.	=	9.475
SURF. ABSORBTIVITY		=	.950
DEPTH FOR CALC.	,IN.	=	0.000
MIX. CONDUCTIVITY	,BTU-FT-HR-F.	=	.700
MIX. SPECIFIC HEAT	,BTU-LB-F.	=	.220
MIX. DENSITY	,LB/FT3	=	148.500

ASPHALT PROPERTIES

ORIG. PENETRATION	,DMM-5SEC.	=	87.000
PEN. TEST TEMP.	,DEG.F	=	77.000
ORIG. SOFTENING POINT	,DEG.F	=	119.000
THIN FILM OVEN	,PER.PEN.	=	61.000

MIXTURE PROPERTIES

PER. ASPHALT	,BY WT.OF AGG.	=	6.420
ASPH. SPECIFIC GRAV.		=	1.000
AGG. SPECIFIC GRAV.		=	2.627
MIX. AIR VOIDS	,PERCENT	=	2.200
AGG. VOL.CONC.	,CALCULATED	=	.856
COEF. OF CONTRACTION	TEMP (F)	ALPH(10**5)	
	-70		1.000
	0		1.200
	70		1.400
	210		1.800
CV OF ALPH		=	.100
MAX. TEN.STRENGTH	,PSI	=	500.000
CV OF MAX.STRENGTH		=	.200

INPUT FATIGUE DATA

FATIGUE CURVE			N=A*(1.0/STRAIN)**B
MIX.STIF.(PSI)	CONST.A		CONST.B
1.0000E+01	1.0000E-02		3.0000E+00
5.0000E+06	8.0000E-13		3.9500E+00

FAV.SEC.NO. 61 STE ANNE - 3/23/1972

TIME OF LOADING .SEC = 3600.000

		MONTH		CODE	
JULY	AUG.	SEPT.	OCT.	NOV.	DEC.
1	2	3	4	5	6
JAN.	FEB.	MAR.	APR.	MAY.	JUNE
7	8	9	10	11	12

AIR TEMPERATURE

ANNUAL AVERAGE	.DEG.F	=	36.600
ANNUAL RANGE	.DEG.F	=	80.000
DAILY RANGE	.DEG.F	=	20.900

FACTORS AFFECTING PAV. TEMP.

ANNUAL AVE.SOLAR RAD.	.LANGLEYS	=	312.000
JULY AVE.SOLAR RAD.	.LANGLEYS	=	514.000
ANNUAL AVE.WIND VEL.	.MPH.	=	11.000
SURFACE ABSORBTIVITY		=	.950
DEPTH FOR CALCULATION,IN.		=	0.000
MIX. CONDUCTIVITY	.BTU-FT-HR-F.	=	.700
MIX. SPECIFIC HEAT	.BTU-LB-F.	=	.220
MIX. DENSITY	.LB/FT3	=	146.000

ASPHALT PROPERTIES

ORIG. PENETRATION	.DMM-SSEC.	=	254.000
PEN. TEST TEMP.	.DEG.F	=	77.000
ORIG. SOFTENING POINT	.DEG.F	=	88.000
THIN FILM OVEN TEST	.PCT.ORIG.PEN.	=	44.300

MIXTURE PROPERTIES

PCT. ASPHALT	.BY WT.OF AGG.	=	5.300
ASPH. SPECIFIC GRAV.		=	1.000
AGG. SPECIFIC GRAV.		=	2.650
MIX. AIR VOIDS	.PERCENT	=	4.000
AGG. VUL. CONCENTRATION	-CALCULATED	=	.868
COEF. OF CONTRACTION	TEMP (F)	ALPH(10**5)	
	-70		1.000
	210		1.800
COEF. OF VARIATION OF ALPH		=	.100
MAX. TEN.STRENGTH	.PSI	=	550.000
COEF. OF VARIATION OF MAX.STRENGTH		=	.200

INPUT FATIGUE DATA

FATIGUE CURVE		N=A*(1.0/STRAIN)**R	
MIX.STIF.(PSI)	CONST.A	CONST.R	
1.0000E+01	1.0000E-02	3.0000E+00	
5.0000E+06	8.0000E-13	3.9500E+00	

TIME OF LOADING ,SEC = 3600.000

		MONTH CODE			
JULY	AUG.	SEPT.	OCT.	NOV.	DEC.
1	2	3	4	5	6
JAN.	FEB.	MAR.	APR.	MAY.	JUNE
7	8	9	10	11	12

AIR TEMPERATURE

ANNUAL AVERAGE ,DEG.F = 36.600
 ANNUAL RANGE ,DEG.F = 80.000
 DAILY RANGE ,DEG.F = 20.900

FACTORS AFFECTING PAV. TEMP.

ANNUAL AVE.SOLAR RAD. ,LANGLEYS = 312.000
 JULY AVE.SOLAR RAD. ,LANGLEYS = 514.000
 ANNUAL AVE.WIND VEL. ,MPH. = 11.000
 SURFACE ABSORBTIVITY = .950
 DEPTH FOR CALCULATION,IN. = 0.000
 MIX. CONDUCTIVITY ,BTU-FT-HR-F. = .700
 MIX. SPECIFIC HEAT ,BTU-LB-F. = .220
 MIX. DENSITY ,LB/FT3 = 148.000

ASPHALT PROPERTIES

ORIG. PENETRATION ,DMM-5SEC. = 159.000
 PEN. TEST TEMP. ,DEG.F = 77.000
 ORIG. SOFTENING POINT,DEG.F = 102.000
 THIN FILM OVEN TEST ,PCT.ORIG.PEN. = 47.000

MIXTURE PROPERTIES

PCT. ASPHALT ,BY WT.OF AGG. = 5.000
 ASPH. SPECIFIC GRAV. = 1.000
 AGG. SPECIFIC GRAV. = 2.650
 MIX. AIR VOIDS ,PERCENT = 5.400
 AGG. VOL. CONCENTRATION -CALCULATED = .862
 COEF. OF CONTRACTION TEMP(F) ALPH(10**5)
 -70 1.000
 210 1.800
 COEF. OF VARIATION OF ALPH = .100
 MAX. TEN.STRENGTH ,PSI = 650.000
 COEF. OF VARIATION OF MAX.STRENGTH = .200

INPUT FATIGUE DATA

FATIGUE CURVE N=A*(1.0/STRAIN)**B
 MIX.STIF.(PSI) CONST.A CONST.B
 1.0000E+01 1.0000E-02 3.0000E+00
 5.0000E+06 8.0000E-13 3.9500E+00

PAV. SEC. NO. 63 STE ANNE TEST ROAD - 3/23/1972

TIME OF LOADING ,SEC = 3600.000

MONTH CODE					
JULY	AUG.	SEPT.	OCT.	NOV.	DEC.
1	2	3	4	5	6
JAN.	FEB.	MAR.	APR.	MAY.	JUNE
7	8	9	10	11	12

AIR TEMPERATURE

ANNUAL AVERAGE ,DEG.F = 36.600
 ANNUAL RANGE ,DEG.F = 80.000
 DAILY RANGE ,DEG.F = 20.900

FACTORS AFFECTING PAV. TEMP.

ANNUAL AVE. SOLAR RAD. ,LANGLEYS = 312.000
 JULY AVE. SOLAR RAD. ,LANGLEYS = 514.000
 ANNUAL AVE. WIND VEL. ,MPH. = 11.000
 SURFACE ABSORBTIVITY = .950
 DEPTH FOR CALCULATION ,IN. = 0.000
 MIX. CONDUCTIVITY ,BTU-FT-HR-F. = .700
 MIX. SPECIFIC HEAT ,BTU-LB-F. = .220
 MIX. DENSITY ,LB/FT3 = 148.000

ASPHALT PROPERTIES

ORIG. PENETRATION ,DMM-5SEC. = 192.000
 PEN. TEST TEMP. ,DEG.F = 77.000
 ORIG. SOFTENING POINT ,DEG.F = 95.000
 THIN FILM OVEN TEST ,PCT. ORIG. PEN. = 44.100

MIXTURE PROPERTIES

PCT. ASPHALT ,BY WT. OF AGG. = 4.800
 ASPH. SPECIFIC GRAV. = 1.000
 AGG. SPECIFIC GRAV. = 2.650
 MIX. AIR VOIDS ,PERCENT = 4.900
 AGG. VOL. CONCENTRATION -CALCULATED = .871
 COEF. OF CONTRACTION TEMP (F) ALPH(10**5)
 -70 1.000
 210 1.800
 COEF. OF VARIATION OF ALPH = .100
 MAX. TEN. STRENGTH ,PSI = 450.000
 COEF. OF VARIATION OF MAX. STRENGTH = .200

INPUT FATIGUE DATA

FATIGUE CURVE N=A*(1.0/STRAIN)**B
 MIX. STIF. (PSI) CONST. A CONST. B
 1.0000E+01 1.0000E-02 3.0000E+00
 5.0000E+06 8.0000E-13 3.9500E+00

THE AUTHORS

At the time of this work, Mohamed Y. Shahin was a Research Engineer Assistant with the Center for Highway Research, where his interests were in the design analysis of flexible pavement, centering on the effect of thermal cracking on pavement performance. He is currently a Visiting Assistant Professor of Civil Engineering at Bucknell University in Lewisburg, Pennsylvania.



B. Frank McCullough is an Assistant Professor of Civil Engineering at The University of Texas at Austin. His engineering experience includes work with the Texas Highway Department and the Center for Highway Research at The University of Texas at Austin. His current research is concerned with (1) systematic pavement design and (2) the evaluation and revision of the Texas Highway Department rigid pavement design procedure. He is the author of numerous publications and a member of several professional societies.

